

Vol 16 No 1 (2012)

Vol 16 No 2 (2012)

The Malaysian Journal of Analytical Sciences Vol 16 No 1 2012

		Page
1.	ALIPHATIC HYDROCARBONS IN SURFACE SEDIMENTS FROM SOUTH CHINA SEA OFF KUCHING DIVISION, SARAWAK (Hidrokarbon Alifatik di Permukaan Enapan Laut Cina Selatan Bahagian Kuching) Hafidz B. Yusoff, Zaini B. Assim, Samsur B. Mohamad	1
2.	FORMATION AND CHARACTERIZATION OF (TI,M)Sr1212 (M= Bi, Pb, Cr) SUPERCONDUCTING CERAMICS (Penyediaan dan Pencirian Superkonduktor Seramik (TI,M)Sr1212 (M= Bi, Pb, Cr)) A. Ali Yusuf, A.K. Yahya and F. Md. Salleh	12
3.	HEAVY METAL CONCENTRATION OF SETTLED SURFACE DUST IN RESIDENTIAL BUILDING (Kepekatan Logam Berat Dalam Debu Terenap Permukaan Di Bangunan Kediaman) Nor Aimi Abdul Wahab, Fairus Muhamad Darus, Norain Isa, Siti Mariam Sumari, Nur Fatihah Muhamad Hanafi	18
4.	SYNTHESIS AND CHARACTERISATION OF MALEATED POLYPROPYLENE-LALANG FIBER/POLYPROPELYNE COMPOSITES: OPTIMISATION PREPARATION CONDITIONS AND THEIR PROPERTIES (Penyediaan dan Pencirian Komposit Polipropelena Termaleik/Gentian Lalang/Polipropilena: Keadaan Penyediaan Optimum dan Sifatnya) Sharil Fadli Mohamad Zamri, Hasratul Nadiah Mohd Rashid, Nurul' Ain Jamion and Rahmah Mohamed	24
5.	OPTIMIZATION STUDY FOR REMOVAL OF RADIUM-226 FROM RADIUM-CONTAMINATED SOIL USING HUMIC ACID (Kajian Pengoptimuman Penyingkiran Radium-226 Daripada Tanih Tercemar Radium Dengan Menggunakan Asid Humik) Esther Phillip, Muhamad Samudi Yasir, Muhamat Omar, Mohd Zaidi Ibrahim, Zalina Laili	31
6.	DETERMINATION OF BENZO[a]PYRENE IN MALAYSIAN COMMERCIALIZED COFFEE POWDER USING SOLID PHASE EXTRACTION AND GAS CHROMATOGRAPHY (Penentuan Benzo[a]pirena di dalam Serbuk Kopi di Pasaran Menggunakan Ekstraksi Fasa Pepejal dan Kromatografi Gas) Noraini Kasim, Rozita Osman, Nor'ashikin Saim, Licaberth Ismail	39
7.	A STUDY ON THE MIGRATION OF STYRENE FROM POLYSTYRENE CUPS TO DRINKS USING ONLINE SOLID-PHASE EXTRACTION LIQUID CHROMATOGRAPHY (SPE-LC) (Kajian Mengenai Migrasi Stirena daripada Cawan Polistirena kepada Minuman Menggunakan Teknik Ekstraksi Fasa Pepejal Kromatografi Cecair (SPE-LC)) Norashikin Saim, Rozita Osman, Hurin Ain Wan Abi Sabian, Mohamad Rafaie Mohamed Zubir, Nazarudin Ibrahim	49

8.	SYNTHESIS, CHARACTERISATION AND ANTIBACTERIAL STUDIES OF Cu(II) COMPLEXES THIOUREA (Sintesis, Pencirian dan Kajian Aktiviti Antibakteria Kompleks Cu(II) Tiourea) Nur Illane Mohamad Halim, Karimah Kassim, Adibatul Husna Fadzil, Bohari M. Yamin	56
9.	COPPER SUPPORTED ON FUNCTIONALISED MCM41 CONTAINING THIOUREA LIGAND AS AN CATALYST IN OXIDATION OF CYCLOHEXENE WITH HYDROGEN PEROXIDE (Sokongan Kuprum kepada MCM41 Terfungsi yang Mengandungi Ligan Tiourea Sebagai Pemangkin Terhadap Tindak Balas Pengoksidaan Sikloheksena dengan Hidrogen Peroksida) Amirah Ahmad, Hamizah Md. Rasid and Karimah Kassim	62
10.	DETERMINATION OF VITAMIN E ISOMERS IN PLASMA USING ULTRA PERFORMANCE LIQUID CHROMATOGRAPHY (Penentuan Isomer-Isomer Vitamin E di dalam Plasma Menggunakan Kromatografi Cecair Berprestasi Lampau) Shahidee Zainal Abidin, Mohammad Johari Ibahim, Mohd Hamim Rajikin and Nuraliza Abdul Satar	71
11.	SYNTHESIS AND CHARACTERISATION OF PALLADIUM(II) SCHIFF BASE COMPLEXES AND THEIR CATALYTIC ACTIVITIES FOR SUZUKI COUPLING REACTION (Sintesis dan Pencirian Palladium(II) Bes-Schiff Kompleks dan Aktiviti Sebagai Pemangkin untuk Tindak Balas Suzuki) Amalina Mohd Tajuddin, Hadariah Bahron, Karimah Kassim, Wan Nazihah Wan Ibrahim and Bohari M.Yamin	79
12.	FLUORINE-18: CURRENT APPROACH IN RADIOLABELLING AND RADIATION SAFETY ASPECTS (Fluorin-18: Pendekatan Semasa dalam Pengradiopenglabelan dan Aspek Keselamatan Sinaran) Suzilawati Muhd Sarowi, Noriah Ali and Noratikah Mat Ail	88



ALIPHATIC HYDROCARBONS IN SURFACE SEDIMENTS FROM SOUTH CHINA SEA OFF KUCHING DIVISION, SARAWAK

(Hidrokarbon Alifatik di Permukaan Enapan Laut Cina Selatan Bahagian Kuching)

Hafidz B. Yusoff¹, Zaini B. Assim^{1*}, Samsur B. Mohamad²

¹Department of Chemistry, ²Department of Aquatic Sciences, Faculty of Resource Sciences and Technology, Universiti Malaysia Sarawak, 94300 Kota Samarahan, Sarawak

*Corresponding author: zaini@frst.unimas.my

Abstract

Eighteen surface sediment samples collected from South China Sea off Kuching Division, Sarawak were analyzed for aliphatic hydrocarbons. These hydrocarbons were recovered from sediment by Soxhlet extraction method and then analyzed using gas chromatography equipped with mass spectrometer (GC/MS). Total concentrations of aliphatic hydrocarbons in surface sediments from South China Sea off Kuching division are ranged from 35.6 ug/g to 1466.1 ug/g dry weights. The sediments collected from Bako Bay, Kuching showed high concentrations of total aliphatic hydrocarbons. Several molecular indices were used to predict the predominant sources of hydrocarbons. Carbon preference index (CPI) value revealed widespread anthropogenic input in this study area (CPI= 0 to 4.1). The ratio of C_{31}/C_{19} and C_{29}/C_{31} indicated that major input of aliphatic hydrocarbon mostly transfer by lateral input to the marine environment than atmospheric movements. Generally, the concentrations of aliphatic hydrocarbons in sediment from South China Sea off Kuching division are generally higher compare to other area in the world.

Keywords: Aliphatic hydrocarbons, surface sediment, South China Sea, Soxhlet extraction, gas chromatography/mass spectrometer (GC/MS), carbon preference index (CPI)

Abstrak

Kajian telah dilakukan terhadap lapan belas enapan permukaan Laut Cina Selatan bahagian Kuching. Sampel enapan ini telah dianalisis bagi mengenalpasti kandungan hidrokarbon alifatik. Hidrokarbon alifatik daripada enapan telah diekstrak dengan menggunakan kaedah pengekstrakan Soxhlet dan dianalisis dengan menggunakan kromatografi gas/spektrometer jisim (KG/SJ). Jumlah kepekatan hidrokarbon alifatik adalah dalam julat 35.6 ug/g sehingga 1466.61 ug/g berat kering. Sampel enapan dari Teluk Bako menunjukkan kandungan hidrokarbon aliftik yang tinggi. Indek penanda hidrokarbon telah digunapakai untuk mengenalpasti sumber hidrokarbon. Indek kecenderungan karbon (IKK) menunjukkan taburan hidrokarbon antropogenik yang tinggi di kawasan kajian (IKK= 0 sehingga 4.1). NisbahC₃₁/C₁₉ dan C₂₉/C₃₁ menunjukkan kebanyakan sumber hidrokarbon alifatik dipindahkan secara lateral ke kawasan persekitaran marin. Secara umumnya, kandungan hidrokarbon alifatik di Laut China Selatan bahagian Kuching adalah tinggi berbanding dengan kawasan lain di seluruh dunia.

Kata kunci: Hidrokarbon alifatik, enapan permukaan, Laut China Selatan, pengekstrakan Soxhlet, kromatografi gasspektrometer jisim (KG-SJ), indek kecenderungan karbon (IKK)

Introduction

Kuching is one of the most urbanized and developed areas in Sarawak. The term of development usually covers the usage of well-known energy of oil. Oil includes variety of compounds and elements such as aliphatic hydrocarbons that is potential for environmental hazard for ecosystem and human life. Aliphatic hydrocarbons are ubiquitous sedimentary contaminants due to their tendency to accumulate in sediments. Sedimentary aliphatic hydrocarbons have both natural and anthropogenic sources. The anthropogenic hydrocarbons in sediment originate mainly from petroleum residues but natural hydrocarbons produce by organism such as planktons, algae and bacteria or come

Hafidz B. Yusoff et al: ALIPHATIC HYDROCARBONS IN SURFACE SEDIMENTS FROM SOUTH CHINA SEA OFF KUCHING DIVISION, SARAWAK

from terrestrial plants [1,2]. Generally, non-polluted area demonstrates hydrocarbons concentrations less than 10 ng/mg dry weight [3].

Aliphatic hydrocarbon from anthropogenic and biogenic sources can be determined using different indices. The combination of different indices will provide a better comprehension for the hydrocarbon origin. Ratio of isoprenoidpristane and phytane (Pr/Ph) can be used as molecular indices to indicate the origin of hydrocarbon in sediments. In sediments uncontaminated with oil, the Pr/Ph ratio is higher than 1 usually between 3 and 5 [4]. Carbon Preference Index (CPI) indicates the ratio of odd carbon numbers over even carbon numbers with different carbon groups. CPI is using frequently and been introduced by Farrington and Tripp in 1977 [5] and developed by other researchers [2, 6, 7].

There are two major rivers in Kuching City, namely Sarawak River and Santubong River. The areas around Sarawak River are intense with industrial activities and rapid urbanization while areas around Santubong area are intense with mangrove forest and urban area. This study were conducted in order to find the distributions and concentrations of natural and anthropogenic hydrocarbons in marine sediment from South China Sea off Kuching division and to find out the possible sources and origins of hydrocarbon in the study area.

Experimental

Sample collections

Eighteen sediment samples were collected from South China Sea off Kuching division in Mac 2009. The locations of sampling stations from S.C.S off Kuching division were shown in Figure 1. The exact positions of each sampling site as presented in Table 1 have been recorded using a Global Positioning System (GPS). The sediment samples were collected using a gravity core sampler and then sliced at 5 or 10 cm interval. However only top layers (0-5) cm was considered in this study. The sediments were then wrapped with aluminum foil and stored in cooler box during the sampling. All the sediments were then stored in cold room until further analysis.

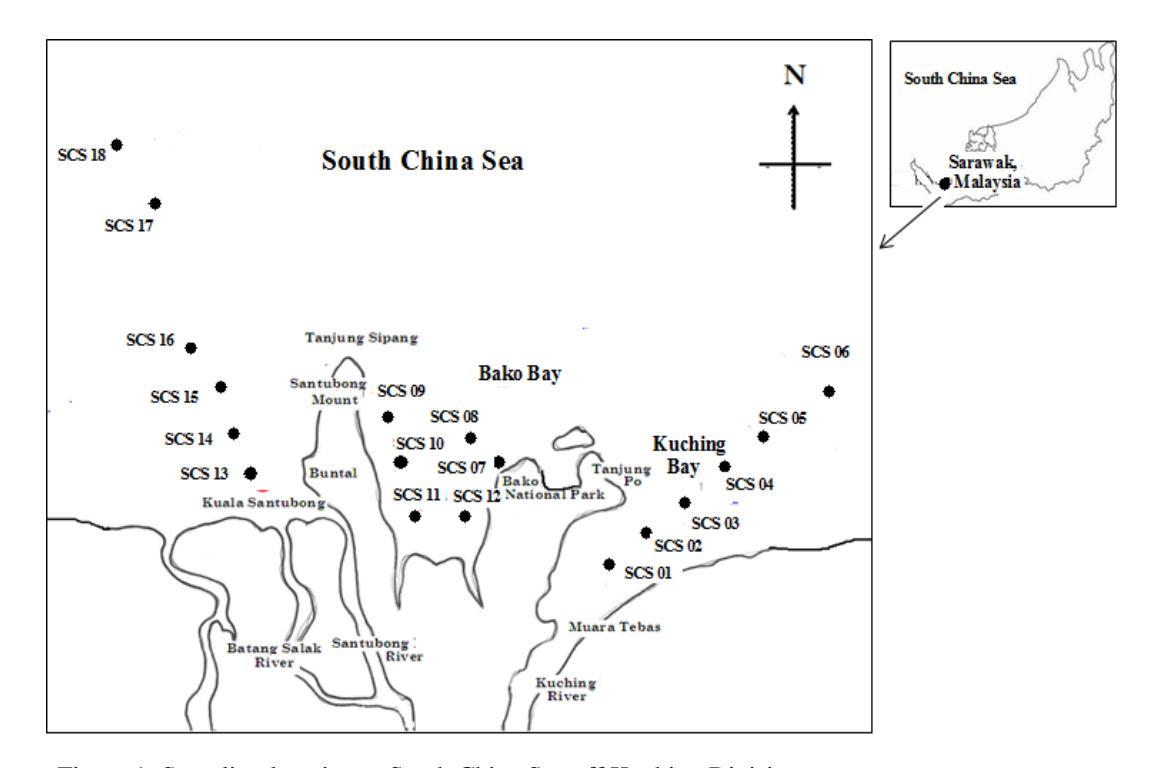


Figure 1: Sampling location at South China Sea off Kuching Division

Table 1: Sampling location at South China Sea off Kuching Division

Sampling Site	Location	Position based on GPS reading	Water Depth (m)
Station 1	Behind Chinese Cemetery at MuaraTebas	N 01° 39' 03.1"	3.5
	·	E 110° 29' 41.4"	
Station 2	Open Sea adjacent to PasirPuteh	N 01° 39'62.1"	5.0
	1	E 110° 31' 22.5"	
Station 3	Open Sea near to the Marine Department	N 01° 40'17''	7.5
	Buoy	E 110° 32' 37.8"	
Station 4	Ocean Input	N 01° 45'07.5"	10.0
	1	E 110° 41' 37.7"	
Station 5	Ocean Input	N 01° 47'10.9"	15.0
	1	E 110° 41' 56.5"	
Station 6	Ocean Input	N 01° 49'18.1"	20.0
	1	E 110° 41' 25.7"	
Station 7	Bako National Park Zone	N 01°40' 24.5"	7.5
		E 110° 14'24.6"	
Station 8	Ocean Input	N 01°44'18.2"	10.0
	r	E 110°25'39.9"	
Station 9	Ocean Input	N 01°44'42.3"	8.5
	r	E 110°24'36.5"	
Station 10	Buntal Coastal Zone	N 01°43'48.8"	12.5
		E 110°23'31.1"	
Station 11	Tabo Coastal Zone	N 01°43'47.6"	10.5
		E 110°24'44.5"	
Station 12	Bako National Park Zone	N 01°43'31.3"	12.5
		E 110°26'08.6"	
Station 13	Adjacent to Santubong Estuary	N 01° 46'147"	1.2
		E 110° 16' 691"	
Station 14	Ocean Input	N 01° 42'69"	2.5
	r	E 110° 49' 21.4"	
Station 15	Ocean Input	N 01° 47'702"	5.3
	r	E 110° 13' 684"	
Station 16	Ocean Input	N 01° 50'906"	10.2
.,	· · · r	E 110° 13' 684"	10.2
Station 17	Ocean Input	N 01° 54'626"	15.3
	· · · r	E 110° 12' 049"	10.0
Station 18	Ocean Input	N 01° 58'000"	20.5
	F 272	E 110° 30' 380"	

n.a: not available

Extraction and fractionation of geolipid

Extractions of geolipids from sediments were performed using Soxhlet extraction, 8 g sediment were placed in the extraction thimbles (30 mm x 100 mm, Whatman) and extracted with 200 ml methylene chloride for 8 hours extraction times [8]. 50 μ L of internal standard consisting of 50 ng/ μ Leicosene in DCM were spiked into the sample. Geolipid is dissolved in 5 ml n-hexane and then subject to fractionate on a chromatography column (1.1 cm X 50 cm) which are pack with 7.5 g activated silica gel (60 mesh). 40 ml hexane was used as eluting solvent.

Hafidz B. Yusoff et al: ALIPHATIC HYDROCARBONS IN SURFACE SEDIMENTS FROM SOUTH CHINA SEA OFF KUCHING DIVISION, SARAWAK

Elemental Sulfur Removal

The presence of sulfur in appreciable quantities needs to be removed due to its interferences in the accurate gravimetric determination of aliphatic hydrocarbon content of the samples in fractions 1. The elemental sulfur, S_8 was removed from fractions 1 by using the activated copper column. A bed (~3 cm high) of copper powder (~40 mesh) packed dry into a glass chromatographic column was used to treat the TAH fractions. The sample was allowed to elute slowly through the column with 25 mL dichloromethane [9].

GC-MS Analysis

Concentrations of aliphatic hydrocarbons in sediments were determined using Shimadzu Gas Chromatography/Mass Spectrometer (GC/MS) QP 2010. Chromatographic separation was achieved by a BPX-5 capillary column (29.5 m×0.25 mm i.d., 0.2 μ m film thickness) with a splitless injector and mass spectrometer detector. Helium was used as the carrier gas (0.98 ml min-1). Samples were injected in the splitless mode with an injector temperature of 250 °C. Oven temperature was programmed from 60°C to 240°C (5 min hold), at 6 °C min⁻¹, and from 240°C to 300 °C (15 min hold), at 6 °C min⁻¹ rate. The concentration of individual n-alkanes was determined by using authentic and ards of n-alkanes (C₁₁-C₃₃). Individual n-alkanes (C₁₁-T₃₃) were identified based on the retention times and mass spectra of target compounds against the authentic standards.

Results and Discussion

Aliphatic hydrocarbons in surface sediment from South China Sea off Kuching division

Quantification was carried out for individual n-alkanes in range between n- C_{11} and n- C_{33} including isoprenoid hydrocarbons, pristane and phytane. The identification of individual components in sample was based on retention time of standard, which was analyzed prior to the analysis of sediment samples. The aliphatic hydrocarbon concentrations in this study are varying between not detected to $412.2\mu g/g$ dry weights. The lowest concentrations of total aliphatic hydrocarbons (35.6 ug/g) in sediments was detected from SCS18 (open sea area) while the highest concentrations of total aliphatic hydrocarbon concentrations (1466.1ug/g) was recorded from SCS11 at Tabo coastal area. Table 2 shows the distributions of aliphatic hydrocarbons in the study area. Chromatograms can reveal many characteristic of samples. Most of the samples showed a baseline elevation or hump that cannot be resolved by capillary GC column except station 13 and 14 which located adjacent to Santubong estuary (see Figure 2, 3 and 4). This hump is due to unresolved complex mixture (UCM) which usually exists in the carbon number of 16-34 that indicates oil pollution [10]. In this study most of the UCM humps were appeared ranging from C_{16} - C_{32} (see Figure 2 and 3). It is also indicate the presence petrogenic input or biodegradation in most of the sediment samples. UCM also indicate the weathering condition of the environmental samples [11].

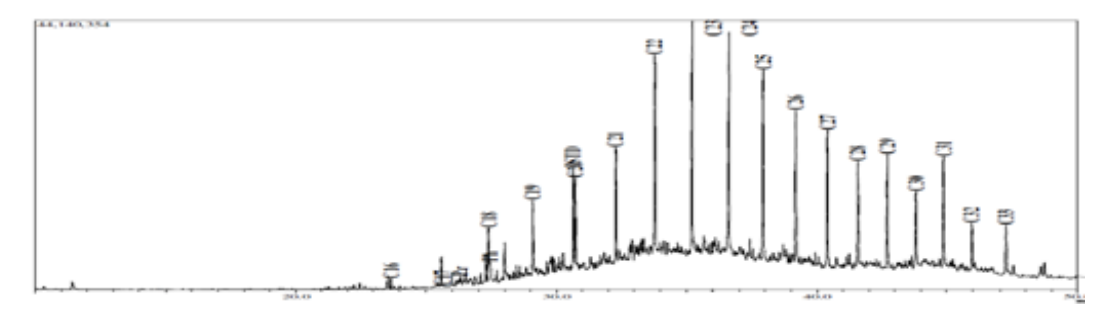


Figure 2: Gas chromatogram of aliphatic hydrocarbon from SCS 03 at Kuching Bay

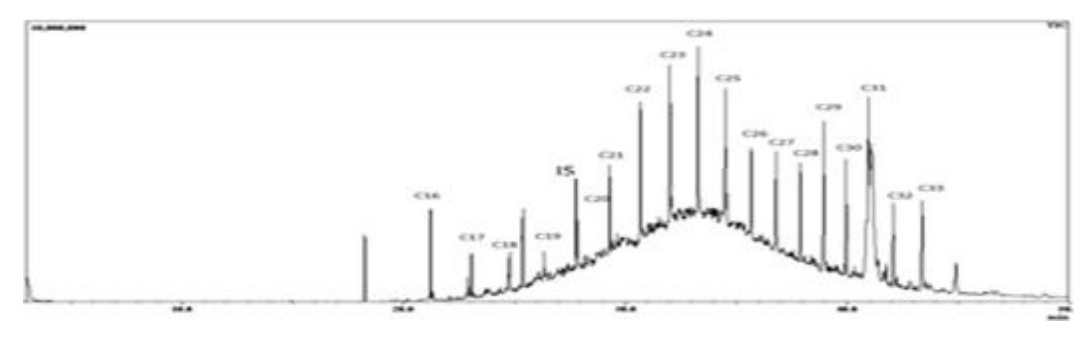


Figure 3: Gas chromatogram of aliphatic hydrocarbon from SCS 07 at Bako Bay

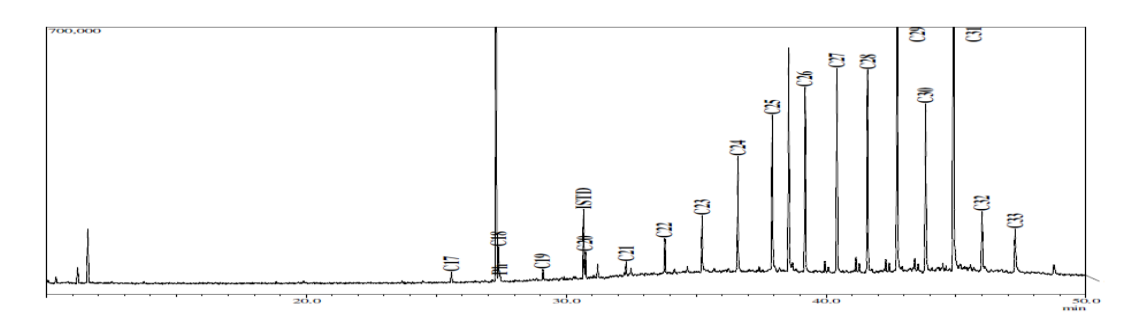


Figure 4: Gas chromatogram of aliphatic hydrocarbon frm SCS 13 adjacent to Santubong estuary

Source of Aliphatic Hydrocarbons in sediment from South China Sea off Kuching Division

Molecular biomarkers are organic compounds detected in the geosphere with structures suggesting an unambiguous link with known contemporary natural products. These specific indicator compounds which are found in extracts of geological and environmental sample can be utilized for genetic source correlations [12]. Distributions of aliphatic hydrocarbon in the samples including isoprenoids (pristane and phytane) were used to predict the source of organic matter in sediments, where there are used in terms of ratios either isoprenoid to isoprenoid or isoprenoid to n-alkanes [13]. Some of these biomarkers indices include the ratio of low molecular weight (LMW) / High molecular weight (HMW) of hydrocarbon, Carbon preference index (CPI), nC_{31}/nC_{19} , nC_{29}/nC_{23} , nC_{25}/nC_{15} , pristane/phytane and pristane/ C_{17} value. Table 3 shows the biomarkers indices for aliphatic hydrocarbons in sediments for sampling stations at South China Sea off Kuching division.

High concentration of LMW carbon indicates an anthropogenic site, while high concentration of HMW indicates a biogenic site. Thus the ratio of LMW/HMW below the unity shows natural input from marine and terrestrial biogenic sources and around and above unity for petroleum origin [14, 15]. The results from LMW/HMW ratio indicate that most of the sampling stations were dominated with LMW of hydrocarbons except station SCS01, SCS02, SCS04, SCS13 and SCS14. All samples collected from Bako Bay were dominated with LMW of aliphatic hydrocarbons and showed ratio LMW/HMW above unity. These results suggest that major inputs of aliphatic hydrocarbon in sediment from Bako Bay are from petroleum, might be from shipping activities and transportation at Bako National Park. Most of the stations located adjacent to the Santubong estuary were dominated by high molecular weight of hydrocarbons suggesting inputs of hydrocarbons in this area are from natural sources. Mangrove forest along the Santubong River might be the main sources of biogenic hydrocarbons in this area.

Hafidz B. Yusoff et al: ALIPHATIC HYDROCARBONS IN SURFACE SEDIMENTS FROM SOUTH CHINA SEA OFF KUCHING DIVISION, SARAWAK

CPI value close to one is sourced by recycled organic matters and/ or marine microorganism [7] as well as petroleum [5]. Predominant of vascular plants input to the environment usually demonstrate the CPI value from 3 to 6 [6]. In this study, the CPI value was shown that the natural input proportion is significantly lower than anthropogenic release (see Figure 5). Among stations, SCS 17 and SCS 18 which located at the open sea area showed high CPI value (3 and 4.1 respectively) indicative of predominant of natural input. The rest of the stations showed the numbers lower and around unity that represent anthropogenic inputs.

Table 2: Concentrations (ug/g) of aliphatic hydrocarbons in surface sediments from South China off Kuching Division

Carbon Numbers				Sampl	ing Sta	tions (So	CS)		
Carbon Numbers	01	02	03	04	05	06	07	08	09
C11	0.2	n.d	n.d	n.d	0.5	n.d	n.d	n.d	n.d
C12	0.8	n.d	n.d	n.d	0.1	n.d	n.d	n.d	n.d
C13	16.1	n.d	n.d	0.2	0.8	n.d	n.d	n.d	n.d
C14	11	n.d	n.d	0.1	0.5	n.d	n.d	n.d	n.d
C15	24.2	n.d	0.1	0.3	1.3	n.d	n.d	n.d	n.d
C16	10.1	3.3	0.4	0.2	3.8	10.8	1.6	n.d	4.1
C17	5.5	26.5	1.5	0.4	20.1	64.2	7.9	49.8	10.2
Pr	1.2	2	0.7	0.1	1.2	2.9	50.5	19.3	8.5
C18	4.1	39.3	2.8	0.5	21.9	75.7	51.1	87.8	8.3
Ph	4.6	21.6	2	0.4	11.9	38.6	22.9	7.1	14.3
C19	3.7	53.7	4.4	0.8	19.7	87.6	6.1	138.3	13.6
C20	3.7	28	6.3	1.2	11.8	38.9	6.4	69.1	20.8
C21	1.8	32.4	9.5	1.8	14.1	48.8	9.1	69.6	35.6
C22	3.4	55.7	15.8	3.7	20.8	68.1	10.6	110.8	72.4
C23	1.6	73.1	18.9	7.9	27.6	86.2	17.5	n.d	104.4
C24	1.7	64.5	19	8.8	21.2	114.6	18.9	140.3	116.7
C25	2.7	42.1	16.3	9.8	18.3	66.1	25.5	125.9	100.8
C26	4.4	24.9	12.8	8.6	14.2	34.9	25.9	98	83.1
C27	6.8	33.3	10.4	10.4	14	54.2	34.8	83.7	93.5
C28	9.3	29.5	8.7	8.1	9	21.1	31	77.5	79.3
C29	26.9	11.5	8.5	12.5	13.9	61.7	53.8	79.4	90.1
C30	59.7	137.3	13.1	13.1	14.4	60.5	22.1	49	47.8
C31	139	59.1	13.2	29.5	31.3	193.5	42.4	65.1	82
C32	76.2	176.2	5.9	8.5	8.6	60	16.2	37.7	34.2
C33	104	412.2	5.4	14.5	15.3	106.3	28.6	49.4	49
TAH	522	1326	176	142	316	1295	482.9	1358	1068.8

Notes;

n.d: not detected or below detection limit TAH: total aliphatic hydrocarbon

Continued Table 2

			S	Sampling	Stations	s (SCS)	1		
Carbon Numbers	10	11	12	13	14	15	16	17	18
C11	n.d	n.d	n.d	n.d	n.d	n.d	n.d	0.1	n.d
C12	n.d	n.d	n.d	n.d	n.d	n.d	n.d	n.d	n.d
C13	n.d	n.d	n.d	n.d	0.8	n.d	n.d	n.d	n.d
C14	n.d	n.d	n.d	n.d	0.8	n.d	n.d	0.3	n.d
C15	n.d	n.d	n.d	n.d	0.9	n.d	n.d	0.7	n.d
C16	2.6	n.d	5.5	n.d	0.8	1	0.9	0.9	0.6
C17	19.2	30.9	45.9	1.1	2.7	6.6	5.6	1.9	1.9
Pr	2.9	7.6	12.9	n.d	n.d	6.6	n.d	n.d	n.d
C18	11.4	12	12.6	2.7	4.8	1.6	5	3.8	3.2
Ph	7.9	15.5	12.5	0.5	0.9	1.6	1.1	0	0.4
C19	17.2	19.4	18.8	1	3.1	4.7	3.8	1.3	1.6
C20	37.6	44.7	32.1	2.6	5.4	6.7	5.8	2.8	3.5
C21	61.7	69.9	63.6	1.4	3.5	4.2	3.7	1.2	1.6
C22	106.9	113.7	114	3.4	4.6	5.4	4.4	2.3	3.1
C23	119.3	121.6	139.6	6	4.1	4.7	4	1.5	2.1
C24	116.8	115.3	168.7	20.2	4.5	6.9	4.2	2.1	2.8
C25	96.9	90.6	127.5	19.8	3.6	4.2	3.4	1.4	1.9
C26	59.2	87.7	59.9	23.9	4.3	4	3.9	1.6	1.7
C27	59.2	107.5	75.3	26.4	5.8	4.3	4.6	1.5	2.1
C28	56.8	113.3	72.1	20.2	5.3	4.2	5.7	1.4	1.8
C29	70.1	127.6	101.4	41.3	24.4	5.1	7.2	2.1	1.8
C30	36.7	79.1	57.2	48.4	8.6	6.1	12.3	2.1	2
C31	81.7	125.5	123.8	96.5	16	8.3	15.4	13.3	2.3
C32	32	69.7	44.6	13.5	4.8	4.2	8.8	1.2	0.8
C33	54.8	114.5	52.9	11	10.8	3.1	7.7	3.3	0.5
TAH	1051	1466	1340.9	339.9	120.2	93.5	107.7	46.8	35.6

Notes;

n.d: not detected or below detection limit TAH: total aliphatic hydrocarbon

Hafidz B. Yusoff et al: ALIPHATIC HYDROCARBONS IN SURFACE SEDIMENTS FROM SOUTH CHINA SEA OFF KUCHING DIVISION, SARAWAK

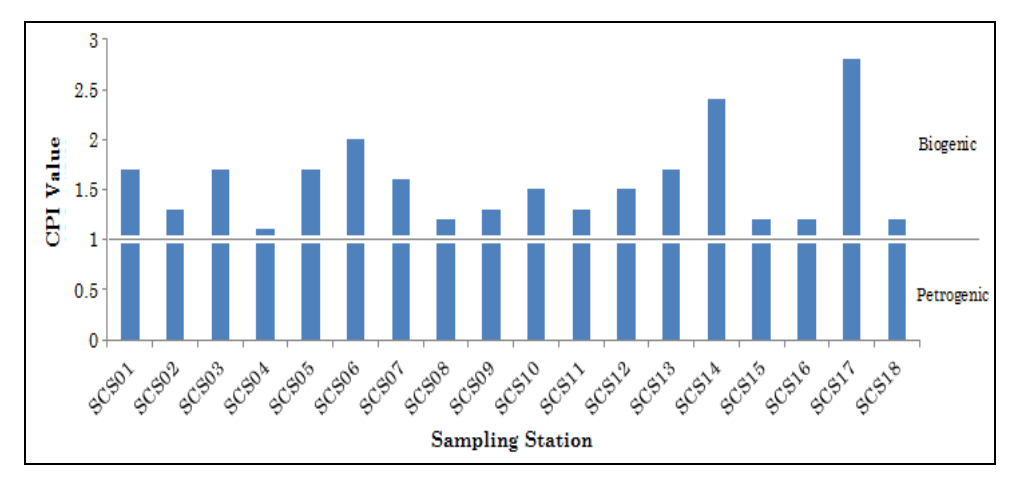


Figure 5: CPI values among stations

The carbon number of C_{31} is known to be an indication of land derived hydrocarbon while C_{19} presents the marine biogenic sources. The ratio of C_{31}/C_{19} use to identify the predominant of hydrocarbon input from land or sea basis. The value below 0.4 indicates the predominant of marine biogenic sources while number over 0.4 show land derived hydrocarbons [16]. In this study, most of the stations showed land derived hydrocarbon except station 8 which located at the open sea area adjacent to Bako Bay. The ratios C_{29}/C_{31} below than one also indicate that hydrocarbon input from land while ratio over than one indicate atmospheric cycle. Most of the sampling stations showed ratio of C_{29}/C_{31} below one indicating majority of hydrocarbon input from land. Pristane and phytane are common isoprenoids found in coastal marine sediment. They are presence in most petroleum, usually as major constituents, within a much wider range of isoprenoid alkanes. The ratio of Pr/Ph close to one indicates petroleum contamination while value greater than 1 indicating biogenic origins [4]. In this study, majority of sediment samples showed value of Pr/Ph is lower than one indicates petroleum contaminantion while 2 samples from SCS12 and SCS15 adjacent to Santubong area showed Pr/Ph value more than one indicating biogenic origin.

Table 3: Biomarkers indices for aliphatic hydrocarbons in sediments from South China Sea off Kuching Division

Ratio and		Stations (SCS)									
Index	01	02	03	04	05	06	07	08	09		
^a LMW	1093	4671	1108	449	2097	7372	254	916	592		
$^{\mathrm{b}}\mathrm{HMW}$	4210	8591	652	965	1064	5571	228	441	475		
^c LMW/HMW	0.1	0.1	1.7	0.5	2.0	1.3	1.1	2.1	1.2		
^d CPI	1.8	1.3	0.9	1.6	1.4	1.7	1.3	1.0	1.3		
enC31/nC19	37.6	1.1	3.0	35.1	1.6	2.2	7.0	0.5	6.0		
fnC29/nC31	0.2	0.2	0.6	0.4	0.4	0.3	1.3	1.2	1.1		
gnC25/nC15	0.1	n.a	111.2	35.3	13.9	n.a	n.a	n.a	n.a		
^h Pr/Ph	0.3	0.1	0.4	0.2	0.1	0.1	0.4	0.4	0.6		

Continued Table 3

Ratio and				Stat	ions (S	SCS)			
Index	10	11	12	13	14	15	16	17	18
^a LMW	659	728	813	826	444	582	459	219	712
$^{\mathrm{b}}\mathrm{HMW}$	391	737	527	2572	757	352	617	248	2760
cLMW/HMW	1.7	1.0	1.5	0.3	0.6	1.7	0.7	0.9	0.3
^d CPI	1.3	1.4	1.4	1.5	2.2	1.0	1.1	3.0	4.1
enC31/nC19	4.8	6.5	6.6	91.9	5.2	1.7	4.0	10.3	12.8
fnC29/nC31	0.9	1.0	0.8	0.4	1.5	0.6	0.5	0.2	0.8
gnC25/nC15	n.a	n.a	n.a	n.a	4.1	n.a	n.a	2.1	n.a
^h Pr/Ph	0.4	0.5	1.0	n.a	n.a	4.0	n.a	n.a	n.a

^aSum of aliphatic hydrocarbon range from C₁₁ to C₂₆;

Comparison of Aliphatic Hydrocarbons Data with Other Places

As comparison to this study, the concentration of total aliphatic hydrocarbons (TAH) for this study and other places is presented in Table 4. TAH in this study ranged from 35.6-1466.1 μ g/g dry weight.The concentrations observed in sediments from S.C.S off Kuching division (this study) are higher compare toJiaouzhou Bay, China [15], Arabian Gulf (Bahrain) [17],Black Sea (Turkey, Russia and Ukraine) [18] and Sao Sebastio, Brazil [19]. The concentrations are much lower than recorded in sediment fromPrai Strait, Penang Malaysia [2]. However, these concentrations are within the same magnitude as recorded at Patagonia, Argentina [14].

Table 4: Concentrations of total aliphatic hydrocarbons (TAH) in marine sediments from other areas

Location	Activities	TAH (μg/g dw)	References
Jiaozhou Bay, Qingdao (China)	Harbour and industrial regions	0.50 to 8.20	[15] (2006)
Arabian Gulf (Bahrain)	Oil refineries	0.67 to 4.30	[17] (2005)
Sao Sebastiao (Brazil)	Oil refineries, harbour and sewage outfalls	n.d - 28.8	[19] (2009)
Black Sea (Turkey, Russia and	Harbour, industrial regions and urban	0.10 to 3.40	[18] (2002)
Ukraine)	areas		
Patagonia, Argentina	Oil refineries and fisheries area	n.d-1304.7	[14] (2000)
Prai Strait, Penang Malaysia	Indutrial regions, urban and tourism area	421-3135	[2] (2008)
South China Sea off Kuching	Petrochemical industries, fisheries area	35.6-1466.1	This study
division	mangrove region and open sea		(2010)

Conclusion

Total concentrations of aliphatic hydrocarbons in marine sediments from South China Sea off Kuching division are varying between 35.6-1466.1 $\mu g/g$ dry weights. Concentrations of aliphatic hydrocarbons in samples sediments from Bako Bay are higher compare to other stations. The study conducted on South China Sea off Kuching division has confirmed the presence of hydrocarbon biomarkers which are emission source specific as terrestrial and oil pollution indicators. Distributions of aliphatic hydrocarbons in South China Sea off Kuching division have shown

^bSum of aliphatic hydrocarbon range from C₂₇ to C₃₃;

^cRatio of low molecular weight of aliphatic hydrocarbon over high molecular weight of aliphatic hydrocarbon;

^dCarbon Preference Index, the ratio of average Odd to Even number carbons range from C₂₅ to C₃₃;

^eRatio of C₃₁ over C₁₉;

^fRatio of C₂₉ over C₃₁;

gRatio of C₂₅ over C1₅;

^hRatio of Pristane over Phytane

Hafidz B. Yusoff et al: ALIPHATIC HYDROCARBONS IN SURFACE SEDIMENTS FROM SOUTH CHINA SEA OFF KUCHING DIVISION, SARAWAK

that majority of aliphatic hydrocarbons in sediments from Bako Bay were dominated withpetrogenic sources. These sources might be from shipping activities and transportation at Bako National Park.Most of the hydrocarbons in sediments from South China Sea off Kuching division were transferred by lateral input to the marine environment than atmospheric movements. The total concentrations of aliphatic hydrocarbons observed for marine sediment of South China Sea off Kuching division are generally higher compare to other areas in the world.

Acknowledgement

We gratefully acknowledge IRPA Grant 0802-09-0507 which supports the funding for this project. Thanks to crews of Marine Department Sarawak for helping in collecting the samples. Thanks also to UNIMAS fellowship (ZPU) for financial support to the first author. Assistance by several lab assistants in laboratories and fieldwork are kindly appreciated.

References

- 1. Doskey, P.V., 2001. Spatial variations and chronologies of aliphatic hydrocarbonsin Lake Michigan sediments. *Environmental Science and Technology*, *35*, 247-254.
- 2. Sakari, M., Zakaria, M.P., Nordin, L., Abd Rahim, M., Pourya, S.B., Sofia, A and Kuhan, C. (2008). Characterization, distributions, sources and origins of aliphatic hydrocarbons from surface sediments of Prai Strait, Penang, Malaysia: A Widespread Anthropogenic Input. *Environment Asia*, 2, 1-14.
- 3. UNEP (1995). Determination of Petroleum Hydrocarbons in sediments. *Reference Methods for Marine Pollution Studies*, 20.
- 4. Steinhauer, M.S. and Boehm, P.D. (1992). The composition and distributions of saturated and aromatic hydrocarbons in near shore sediment, river sediments, and coastal peat of the Alaskan Beaufort Sea: implications for detecting anthropogenic hydrocarbons input, *Marine Environmental Research*, 33,223-253.
- 5. Farrington, J.W. and Tripp, B.W. (1977). Hydrocarbons in Western North Atlantic surface sediments. GeochemicaCosmochemicaActa, 41, 1627-1641.
- Colombo, J.C., Pelletier, C., Brochu, C. and Khalil, M. (1989). Determinations of hydrocarbons sources using n-alkanes and polyaromatic hydrocarbon distribution indexes. Case Study: Rio de la Plata estuary, Argentina. *Environmental Science and Technology*, 23,888-894.Blumer, M.(1957). Removal of elemental sulfur from hydrocarbon fractions. *Analytical Chemistry*, 29,1039-1041.
- 7. Kennicutt, M.C., Barker, C., Brooks, J.M., DeFreitas, D.A., Zhu, G.H. (1987). Selected organic matter source indicators in the Orinoco, Nile and Changjang deltas. *Organic Geochemistry*, 11, 41-51..
- 8. Zakaria, M.P., Horinouchi, A., Tsutsumi, S., Takada, H., Tanabe, S. and Ismail, A. (2000). Oil Pollution in the straits of Malacca, Malaysia. Application of molecular marker for sources identification, *Environmental Science and Technology*, *34*,1189-1196.
- Blumer, M. (1957). Removal of elemental sulfur from hydrocarbon fractions. Analytical Chemistry, 29, 1039-1041.
- 10. Nishigima, F.N., Weber, R.R. and Bicego, M.C. (2001). Aliphatic and aromatic hydrocarbons in sediment of Santos and Canania, SP, Brazil. *Marine Pollution Bulletin*, 42, 1064-1072.
- 11. Chandru, K., Zakaria, M.P, Anita, S., Shahbazi, A., Sakari, M., Bahry, P.S., and Mohamed, C.A.R. (2008). Characterization of alkane, hopane and polycyclic aromatic hydrocarbons in tarballs collected from the East Coast of Peninsular Malaysia. *Marine Pollution Bulletin*, 56 (5), 95-962.
- 12. Simoneit, B.R.T. (1978). The organic chemistry of marine sediments. In: J.P Riley and R. Chester (Eds). *Chemical Oceanography*. Academic, New York, 2nd ed., pp. 233-311.
- 13. Hedges, J.I. and Prahl, F.G. (1993). Early diagenesis: consequences for applications of molecular markers. In: M.H. Engel and S.A. Macko (Eds). *Organic Geochemistry-Principles and Applications*. Plenum. New York, pp 237-253.
- 14. Commendatore, M.G., Esteves, J.L. and Colombo, J.C. (2000). Hydrocarbons in Coastal Sediments of Patagonia, Argentina: Levels and Probable Sources. *Marine Pollution Bulletin*, 40 (11), 989-998.
- 15. Wang, X.C., Sun S., Ma, H.Q. and Liu Y. (2006). Sources and distribution of aliphatic and polyaromatic hydrocarbons in sediments of Jiaozhou Bay, Qingdao, China. *Marine Pollution Bulletin*, 52(2),129-138.
- 16. Moldowan, J.M., Seifert, W.K., Gallegos, E.J. (1985). Relationship between petroleum composition and depositional environment of petroleum source rocks, *AAPG Bulletin*, 69, 1255-126.

- 17. Tolosa, I., De Mora, S.J., Fowler, S.W., Villeneuve, J.P., Bartocci, J. and Cattini, C. (2005). Aliphatic and aromatic hydrocarbons in marine biota and coastal sediments from the Gulf and the Gulf of Oman. *Marine Pollution Bulletin*, 50, 1619-1633.
- 18. Readman, J.W., Fillmann, G., Tolosa, I., Bartocci, J., Villeneuve, J.P., Catinni, C., Mee, L.D. (2002). Petroleum and PAH contamination of the Black Sea. *Marine Pollution Bulletin*, *44*, 48–62.
- 19. Da Silva A.M.D. and Bicego, M.C. (2009). Polycyclic aromatic hydrocarbons and petroleum biomarkers in São Sebastião. *Marine Environmental Research*, 69, 277-286.



FORMATION AND CHARACTERIZATION OF (TI,M)Sr1212 (M= Bi, Pb, Cr) SUPERCONDUCTING CERAMICS

(Penyediaan dan Pencirian Superkonduktor Seramik (Tl,M)Sr1212 (M= Bi, Pb, Cr))

A. Ali Yusuf, A.K. Yahya and F. Md. Salleh*

Faculty of Applied Sciences, Universiti Teknologi MARA, 40450 Shah Alam, Selangor

*Corresponding author: faizah163@salam.uitm.edu.my

Abstract

The derivatives of Tl1212 phase superconductors were prepared using precursors derived from coprecipitation reaction of appropriate stoichiometric metal acetates and oxalic acid based on nominal starting compositions; $Tl_{0.8}Bi_{0.2}Sr_2Ca_{0.8}Y_{0.2}Cu_2O_7$, $Tl_{0.5}Pb_{0.5}Sr_{1.8}Yb_{0.2}CaCu_2O_7$ and $Tl_{0.9}Cr_{0.1}Sr_2Ca_{0.9}Pr_{0.1}Cu_2O_7$. The oxalates precursors were calcined at 600 °C for 24 hours following which sintering were done at 870 °C for 1 hour. All three superconducting oxides showed metallic normal state properties with $T_{c\ onset}$ of around 100 °C and $T_{c\ zero}$ of between 90 –94 °C. The transport critical current density (J_c) of the samples are around 3 – 6 A/cm² while the room temperature resistivity ($\rho_{300\ K}$) values are in the range of 7 – 10 m Ω cm. Powder X-ray diffraction (XRD) patterns of all samples reveals presence of dominant 1212 phase. Scanning electron micrographs reveal fine and irregular shaped grains (<2 μ m).

Keywords: T11212 superconductor, coprecipitation method

Abstrak

Superkonduktor berfasa Tl1212 terbitan; $Tl_{0.8}Bi_{0.2}Sr_2Ca_{0.8}Y_{0.2}Cu_2O_7$, $Tl_{0.5}Pb_{0.5}Sr_{1.8}Yb_{0.2}CaCu_2O_7$ dan $Tl_{0.9}Cr_{0.1}Sr_2Ca_{0.9}Pr_{0.1}Cu_2O_7$ telah disediakan menggunakan bahan pelopor hasil tindakbalas kopemendakan antara logam asetat dan asid oksalik. Bahan pelopor oksalat dikalsin pada 600 °C selama 24 jam dan kemudian disinter pada 870 °C selama 1 jam. Kesemua superkonduktor oksida terhasil bersifat logam pada keadaan normal dan bertukarmenjadi superkonduktor pada suhu antara 90 –94 °C. Nilai ketumpatan arus (J_c) superkonduktor tersebut adalah 3 – 6 A/cm² dan kerintangan pada suhu bilik ($\rho_{300 \text{ K}}$) dalam lingkungan 7 – 10 mΩcm. Pembelauan sinar-X (XRD) menunjukkan kesemua superkonduktor mengandungi fasa 1212 yang dominan. Imej mikroskop imbasan electron (SEM) memperlihatkan zarah halus tanpa bentuk tertentu dengan saiz zarah <2 μm.

Kata kunci: Superkonduktor T11212; kaedah kopemendakan

Introduction

Single TI-O layer superconducting compounds, for example TlSr1212 and its derivatives are potential compounds for application in magnetic field. The presence of single TI-O insulating layer in the compounds structures leads to stronger coupling between adjacent Cu-O planes [1]. Substitution of rare earth elements in TlSr1212 stabilized the 1212 phase which then improved its superconducting behavior [4]. Superconductivity of around 100 K has been observed in the TlSr1212 derivatives such as (TlPb)Sr₂CaCu₂O₇ [2], (TlBi)Sr₂CaCu₂O₇ [3] and (TlCr)Sr₂CaCu₂O₇ [4] systems synthesized via the conventional solid state method.

Besides the conventional solid state method, other methods such as coprecipitation and sol-gel have been employed for the synthesis of superconducting oxides. These alternatives are mainly seeking to improve the bulk material quality and reducing particle size for further applications of the material. Coprecipitation is a solution-based procedure where simultaneous precipitation of soluble components with a precipitating agent produces fine and highly homogenized powder. Solid state synthesis using chemicals derived from coprecipitation has been reported

A.Ali Yusuf et al: FORMATION AND CHARACTERIZATION OF (TI,M)Sr1212 (M= BI, PB, CR) SUPERCONDUCTING CERAMICS

to produce high quality superconducting oxides [5,6,9]. Various reports on synthesis of superconducting BiPbSrCaCuO and YBaCuO systems via coprecipitation method can be found [5-6] but reports on the preparation of Tl-based superconducting systems via coprecipitation are sparse in literature and are limited to the preparations of non-thallium precursor materials [7]. Coprecipitated Tl-containing precursor materials are not adopted due to the high volatility of thallium oxide during heating at high temperatures. However, Bernhard [9] had successfully synthesized Tl2223 superconductors from coprecipitated Tl-containing precursors by special heating techniques. Recently, we have studied the optimum heating condition to synthesize (TlBi)Sr1212 from coprecipitated Tl-containing powders [8].

The aim of this paper is to determine the possibility of using the same heating conditions in producing other TlSr1212 derivatives, i.e. (TlPb)Sr1212 and (TlCr)Sr1212. The transport critical current density (J_c), room temperature resistivity ($\rho_{300 \text{ K}}$), powder X-ray Diffraction (XRD) and microstructure investigations using scanning electron microscope (SEM) of the samples are given and discussed.

Experimental

The coprecipitation process used was in general similar to that described earlier in Ref. [9]. Reagent-grade acetates of respective elements that make up $Tl_{0.8}Bi_{0.2}Sr_2Ca_{0.8}Y_{0.2}Cu_2O_7$ (S1) composition were dissolved in glacial acetic acid and were reacted with excess amount of oxalic acid at 50 °C under continuous stirring, yielding precipitation of mixed oxalate. The same reaction procedure was also applied in cases of $Tl_{0.5}Pb_{0.5}Sr_{1.8}Yb_{0.2}CaCu_2O_7$ (S2) and $Tl_{0.9}Cr_{0.1}Sr_2Ca_{0.9}Pr_{0.1}Cu_2O_7$ (S3) compositions. In each case, the oxalate precipitate was filtered, washed and dried overnight at 80 °C and ground to powdery state. The calcination for all samples were done at 600 °C for 20 hours in air at heating and cooling rates of 1 °C/minute. The samples were reground and pressed into pellets before they were sintered at 870 °C in flowing O_2 using a tube furnace for 60 minutes followed by furnace cooling to room temperature.

Electrical resistance (dc) measurements for all samples were carried out using the standard four-point-probe method with silver paint contacts in a Janis model CCS 350ST cryostat in conjunction with a closed cycle refrigerator from CTI cryogenics model 22. Room temperature resistivity ($\rho_{300\,\text{K}}$) was investigated using the Van der Pauw technique. The phase characterization was done by powder X-ray diffraction (XRD) using a Siemens D5000 diffractometer with Cu-K_{\alpha} source. Volume fraction of any particular phase in the samples was determined from the ratio of the highest XRD intensity peak for the phase to the total intensity peaks (highest peak only) of all phases under consideration. Transport critical current densities (J_c) were measured in zero magnetic field using electric field criterion of 1 μ Vcm⁻¹. Scanning electron micrographs were recorded using Leica S440 scanning electron microscope.

Results and Discussion

Powder X-ray diffraction patterns (Figure 1) for all samples showed presence of dominant 1212 phase and minor 1201 phase. The 1212 peaks were indexed as tetragonal unit cell with space group P4/mmm. In addition, presence of $SrCO_3$ impurity was also found in all the samples. The volume ratio of 1212 phase to 1201 phase and $SrCO_3$ impurity of all samples are tabulated in Table 1. The highest percentage of T11212 phase was observed for S1 (83 vol %) while that for S2 and S3 were 80 vol % and 70 vol %, respectively. The lowest percentage of $SrCO_3$ impurity was observed for S2. The normalized resistance versus temperature curves of all samples is shown in Fig. 2. All samples showed metallic normal state behavior and were observed to superconduct with $T_{c\ onset}$ between 100 - 103 °C and $T_{c\ zero}$ between 90 – 94 °C. $T_{c\ onset}$, $T_{c\ zero}$, resistivity (at 300K), transport critical current density (J_c) and 1212 phase :1201 phase : $SrCO_3$ impurity ratio for all samples are listed in Table 1.

Based on the XRD data and $T_{c\ onset}$ of the samples, it is clear that the 1212 phase is responsible for its observed superconductivity. The presence of 1201 phase of around 17 vol % in both TlCr1212 and TlPb1212 and 8 vol % in TlBi1212 does not affect its superconductivity as the observed $T_{c\ onset}$ of Tl1201 was reported to be below 50 K [10]. The transport critical current density values of all samples were determined to be around $1.6 - 4.3\ A/cm^2$ with the highest J_c observed for TlPb1212.

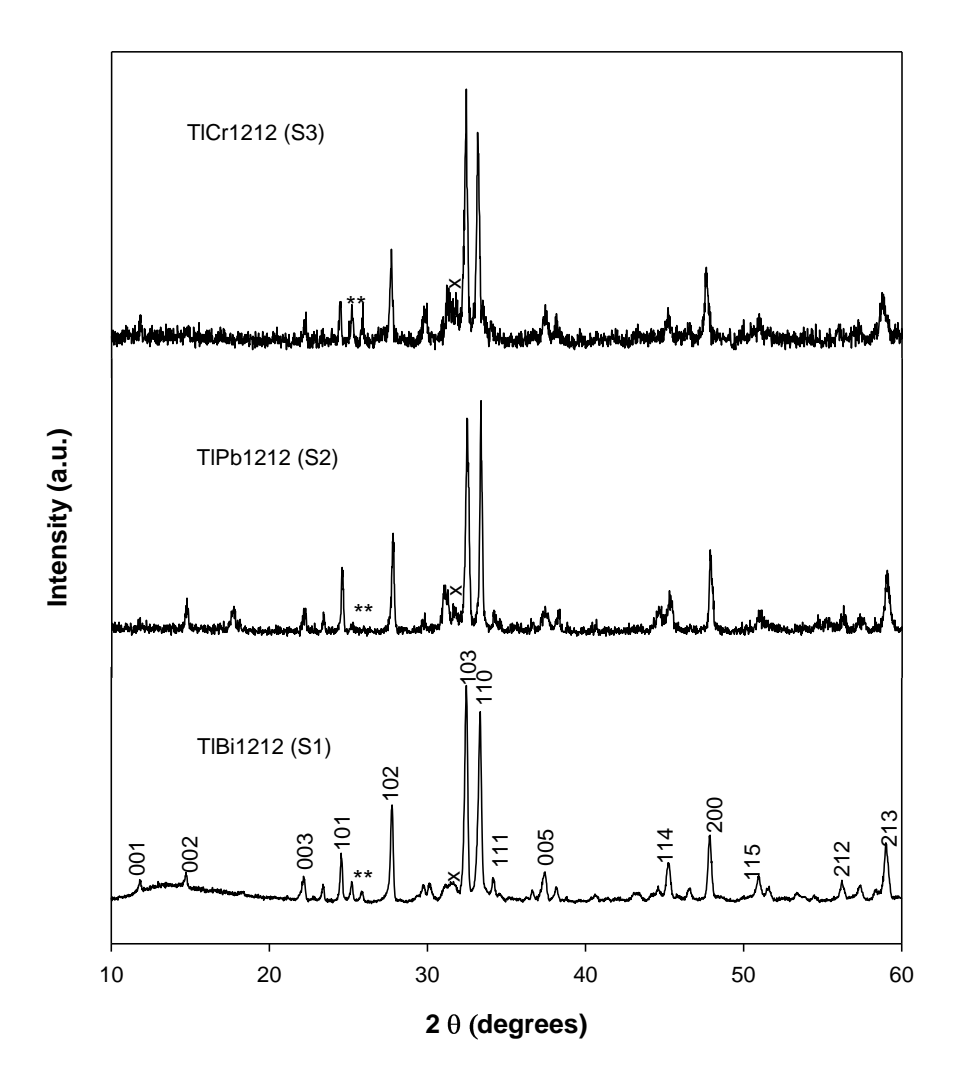


Figure 1 : Powder X-ray diffraction patterns for (Tl,M)Sr1212 (M=Cr, Pb, Bi) samples. Peaks identified as 1201 phase and SrCO₃ impurity are marked with x and *, respectively.

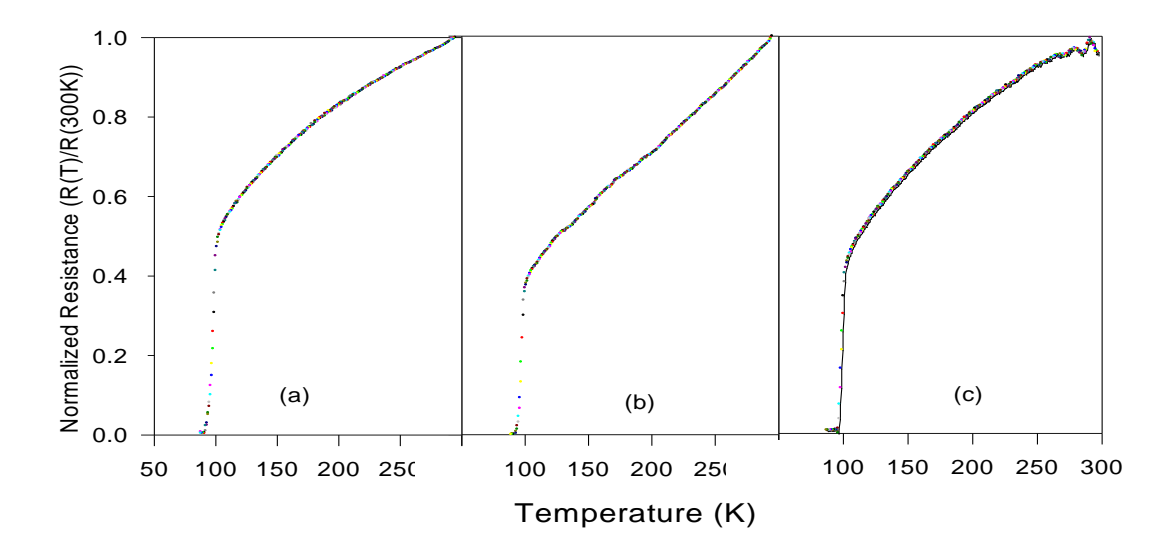


Figure 2 : Normalized resistance versus temperature curve for (Tl,M)Sr1212 (M=Cr, Pb, Bi) samples (a) (TlCr)Sr1212, (b) (TlPb)Sr1212 and (c) (TlBi)Sr1212. The vertical axes for all graphs are the same.

Table 1 : $T_{c\ onset}$, $T_{c\ zero}$, resistivity (at 300K), transport critical current density (J_c) and 1212:1201:SrCO $_3$ impurity ratio for all samples

Sample	T _{c onset} (K)	T _{c zero} (K)	Resistivity at 300 K (mΩ.cm)	J_c at 60 K (A/cm ²)	1212 :1201: SrCO ₃ impurity ratio (vol %)
TlBi1212	103	94	10	3.2	83:8:9
TlPb1212	100	91	7.7	4.3	80:17:3
TlCr1212	101	90	10	1.6	70:17:13

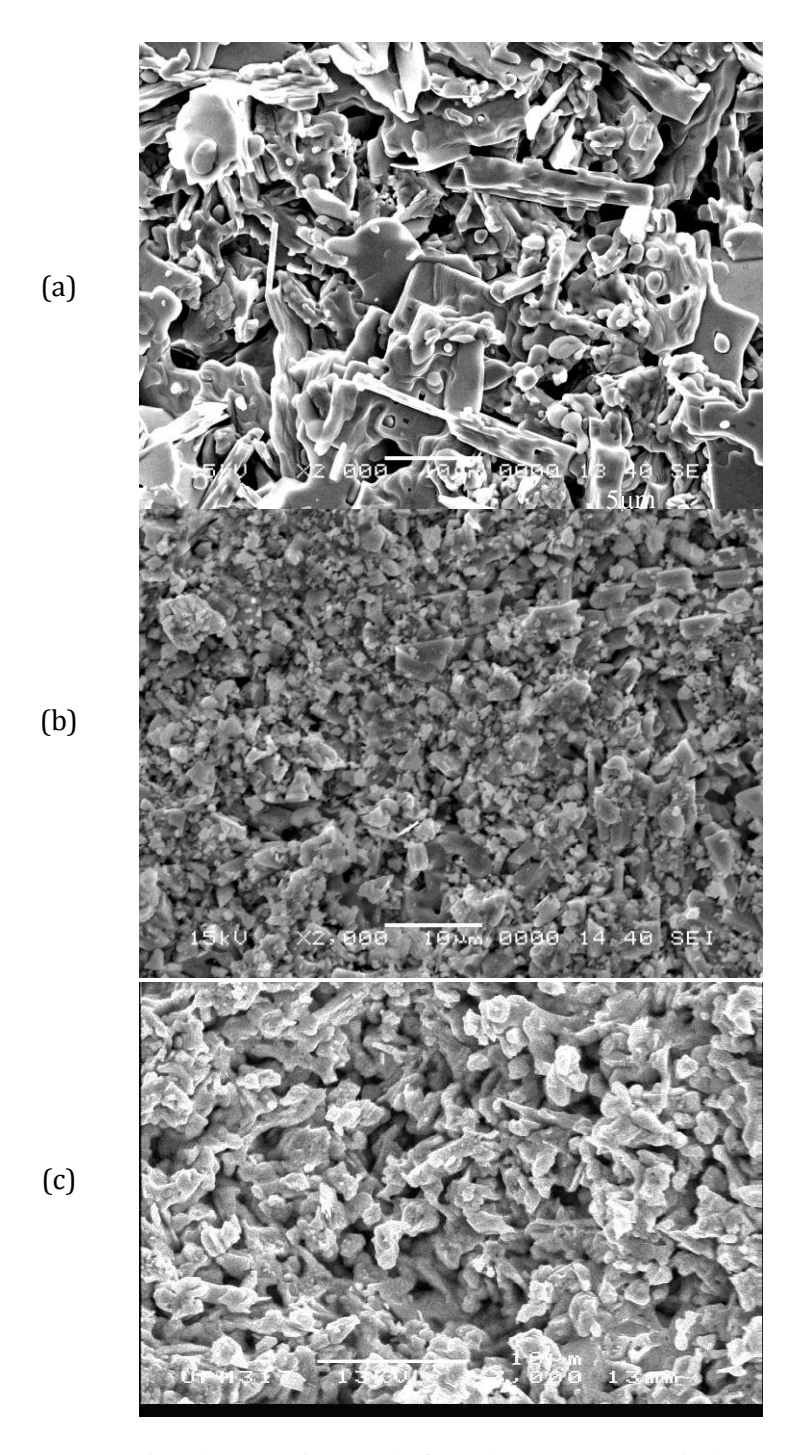


Figure 3: Scanning electron micrographs for (Tl,M)Sr1212 (M=Bi,Pb,Cr) samples (a) (TlBi)Sr1212, (b) (TlPb)Sr1212 and (c) (TlCr)Sr1212.

A.Ali Yusuf et al: FORMATION AND CHARACTERIZATION OF (TI,M)Sr1212 (M= BI, PB, CR) SUPERCONDUCTING CERAMICS

Microstructures of the fractured sections of all samples are shown by SEM micrographs in Fig. 3. The micrographs of all samples showed porous microstructure and irregularly-shaped grains. Among the samples, microstructure with the finest grain (\sim 2-4 µm) was observed for TlPb1212 while the microstructure for TlBi1212 showed the largest grain (3-10 µm). The micrograph of TlCr1212 sample showed grains of \sim 3 µm in sizes. Previous work on Tl_{0.5}Pb_{0.5}Sr_{1.8}Yb_{0.2}CaCu₂O₇ [11] and Tl_{0.9}Cr_{0.1}Sr₂Ca_{0.9}Pr_{0.1}Cu₂O₇ [12] synthesized by solid state method also showed porous microstructures.

This study shows that Tl1212 superconducting ceramics can be synthesized from coprepcipitation derived precursors. However a closer look at the amount of 1212 phase composition in TlCr1212 shows a value of 70 vol %, which is lower than the amount of 1212 phase in TlBi1212 (83 vol %) and TlPb1212 (80 vol %). In the sintering process, the 1212 phase is suggested to form at sintering conditions of 870 °C for 60 minutes. As such, the lower 1212 phase vol% in TlCr1212 indicates that the optimum sintering temperature and/or duration for TlCr1212 may be slightly different and must be further investigated. The SEM micrographs which showed different grain sizes for TlBi1212, TlPb1212 and TlCr1212 indicate the effect of chemical composition on sample microstructure. The fact that TlPb1212 sample which has the finest grain size showed the highest J_c among all samples indicates the influence of microstructure on J_c [15]. However, although TlPb1212 and TlCr1212 are less porous and possess smaller grain sizes, its transport J_c values are lower than the transport J_c values of the solid state synthesized samples [11,12]. This indicates besides microstructure, the J_c may also be influenced by other factors such as secondary phase and impurities [13]. The presence of approximately 17 vol % of Tl1201 phase in addition to SrCO₃ impurity in both TlPb1212 and TlCr1212 may act as obstacles which prevent the continuity of supercurrent path and thus, resulted in low J_c [14].

Conclusion

In conclusion, (Tl,M)Sr1212 where (M=Bi,Pb,Cr) were successfully synthesized using coprepcipitated precursor powder by sintering at 870 °C for 60 minutes. The samples showed metallic normal state behavior and superconduct with $T_{c\ onset}$ of between 100 - 103 °C and $T_{c\ zero}$ of between 90 – 94 °C. The different chemical compositions were observed to affect microstructure and 1212 phase volume fraction in the samples.

Acknowledgement

Financial support from UiTM and the Malaysian Ministry of Science, Technology and Innovation under its FRGS Grant No. 5/3/1317 are gratefully acknowledged.

References

- 1. Kim, D.H., Gray, K.E., Kampwirth, R.T., Smith, J.C., Richeson, D.S., Marks, T.J., Kang, J.H., Talvacchio, J. and Eddy, M. (1991), *Physica C* **177**, 431.
- 2. Sheng, Z.Z., Dong, C., Fei, X., Liu, Y.H., Sheng, L. and Hermann A.M. (1989), Appl. Phys. Comm. 9, 27.
- 3. Li, S. and Greenblatt, M. (1989), *Physica C* **157**, 365.
- 4. Sheng, Z.Z., Sheng, L., Fei, X. and Hermann, A.M. (1989), *Phys. Rev. B* **39**, 2918.
- 5. Gritzner, G. and Bernhard, K. (1991), *Physica C* **181**, 201-205
- 6. Padam, G.K., Raman, V., Dhingra, I. Tripathi, R.B., Rao, S.U.M., Suri, D.K., Nagpal, K.C. and Das, B.K. (1991), J. Phys. Condens. Matter 3, 4269
- 7. Salazar, K.V., Peterson, E.J., Holesinger, T.G., Bingham, B., Coulter J.Y., Sebring, R.J., Voight, J.A., Roth E.P. and Halder, P. (1995), *IEEE Trans. On Appl. Supercond.* 5, No. 2, 1494.
- 8. Md. Salleh, F., Yahya, A.K., Imad, H., and Jumali, M.H. (2005). *Physica C* **426-431**, 319
- 9. Bernhard, K and Gritzner, G. (1992), *Physica C* **196**, 259
- 10. Sheng, Z.Z. Li, Y.F. and Pederson, D.O. (1991), Solid State Comm. 80, 913 915
- 11. Abdullah, W.F., Jumali, M.H. and Yahya, A.K. (2003) J. Solid State Sci. Technol. Lett. 10 No. 2 (Supp), 73
- 12. Chen, S.K., Lau, K.T. and Abd. Shukor, R. (2002), Mat. Sci. Eng. B 90, 234
- 13. Dimos, D., Chaudhari, P. and Mannhart, J. (1990), Phys. Rev. B41, 4038
- 14. Jeong, D.Y., Kim, H.K., Kim, Y.C., Lee H.S., Tsuruta, T., Matsui, Y. and Horiuchi, S. (2000), *Physica C* **330**, 169
- 15. Kilic, A., Kilic, K. and Senoussi, S. (1998) J. Appl. Phys. 84 No. 6, 3254



HEAVY METAL CONCENTRATION OF SETTLED SURFACE DUST IN RESIDENTIAL BUILDING

(Kepekatan Logam Berat Dalam Debu Terenap Permukaan Di Bangunan Kediaman)

Nor Aimi Abdul Wahab^{1*}, Fairus Muhamad Darus¹, Norain Isa¹, Siti Mariam Sumari², Nur Fatihah Muhamad Hanafi²

¹Faculty of Applied Sciences, Universiti Teknologi MARA Cawangan Pulau Pinang, 13500 Permatang Pauh, Pulau Pinang, Malaysia ²Faculty of Applied Sciences, Universiti Teknologi MARA, 40450 Shah Alam, Selangor, Malaysia

*Corresponding author: noraimi108@ppinang.uitm.edu.my

Abstract

The concentrations of heavy metals (Cu, Ni, Pb and Zn) in settled surface dust were collected from nine residential buildings in different areas in Seberang Prai Tengah District, Pulau Pinang. The samples of settled surface dust were collected in 1 m^2 area by using a polyethylene brush and placed in the dust pan by sweeping the living room floor most accessible to the occupants. Heavy metals concentrations were determined by using inductively coupled plasma optical emission spectrometer (ICP-OES) after digestion with nitric acid and sulphuric acid. The results show that the range of heavy metals observed in residential buildings at Seberang Prai Tengah were in the range of 2.20-14.00 mg/kg, 1.50-32.70 mg/kg, 1.50-76.80 mg/kg and 14.60-54.40 mg/kg for Cu, Ni, Pb and Zn respectively. The heavy metal concentration in the investigated areas followed the order: Pb > Zn > Ni > Cu. Statistical analysis indicates significant correlation between all the possible pairs of heavy metal. The results suggest a likely common source for the heavy metal contamination, which could be traced most probably to vehicular emissions, street dust and other related activities.

Keywords: Settled surface dust, heavy metal, residential building

Abstrak

Kepekatan logam berat (Cu, Ni, Pb dan Zn) di dalam debu terenap permukaan yang diambil dari sembilan buah kediaman di lokasi berbeza di daerah Seberang Prai Tengah, Pulau Pinang. Sampel debu terenap permukaan diambil pada kawasan 1 m² menggunakan berus polietilena dan dimasukkan ke dalam penyodok debu dengan penyapu lantai pada ruang tamu yang kerap diakses oleh penghuni. Kepekatan logam berat telah dikenalpasti menggunakan spektrometer pemancaran optik gandingan plasma teraruh (ICP-OES) selepas proses pencernaan sampel dengan menggunakan asid nitrik dan asid sulfurik. Keputusan menunjukkan julat kepekatan logam berat yang diperhatikan di dalam bangunan kediaman di Seberang Prai Tengah dalam julat 2.20-14.00 mg/kg, 1.50-32.70 mg/kg, 1.50-76.80 mg/kg dan 14.60-54.40 mg/kg masing-masing untuk Cu, Ni, Pb dan Zn. Kepekatan logam berat di kawasan kajian menuruti susunan urutan: Pb > Zn > Ni > Cu. Analisis statistik menunjukkan korelasi signifikan terhadap semua pasangan logam berat. Hasil kajian mencadangkan sumber umum pencemaran logam berat yang lazim, di mana kemungkinan boleh dikesan pada pelepasan kenderaan, debu jalan dan lain-lain aktiviti yang berkaitan.

Kata kunci: Debu terenap permukaan, logam berat, rumah kediaman

Introduction

Heavy metals are among the most important pollutants in urban environment, and becoming a severe public health problem due to their acute toxicity and carcinogenicity [1]. The heavy metals are stable and persistent environmental contaminants since they cannot be degraded and destroyed. Thus any high level of heavy metals will threaten biological life. Some metals are cumulative poisons capable of being assimilated and stored in the tissues of

Nor Aimi Abdul Wahab et al: HEAVY METAL CONCENTRATION OF SETTLED SURFACE DUST IN RESIDENTIAL BUILDING

organism, causing noticeable adverse physiological effects and they may also act as cofactors in other diseases [2,3].

Humans are exposed to heavy metals via many pathways because these metals are ubiquitous in the environment, and originate from both natural and anthropogenic activities[4]. One of the important pathways of exposure to metal for humans is through dust. Dust is described as a solid matter composed of soil, antropogenic metallic constituents and natural biogenic materials [5]. Indoor and outdoor dust makes a significant contribution to heavy metal pollution in the environment. Recently, there is an increasing concern about heavy metal contamination in indoor environment since most of the people spend as much as 80 to 90% of their time indoor [6,7]. These percentages are easily exceeded mostly for children, infant and elderly.

Settled dust is present in the indoor environment as a composite of particulate matter derived from interior and exterior sources [8]. Settled surface dust often functions as a reservoir of hazardous particulate contaminants including trace metals. The metals in the dust can be accumulated in human body via direct inhalation, ingestion and dermal contact absorption, and pose potentially deleterious effects on the health of human beings. Children in particular are at higher risk compared to adults, because they engage in greater hand to mouth activity, while their neurological system is still developing and they having much higher absorption rate of heavy metal than adults [9].

The rapid growth of Seberang Perai Tengah area has created numerous environmental problems. Considerable attention has been paid to the study of metal pollution in city air, roadside dust and city soil [4-6]. However there is a lack of concern of the presence of trace metal in house dust. Therefore the present work is important in providing information on the level of heavy metal in settled surface dust in residential building in Seberang Jaya.

Experimental

Study Area

Seberang Perai Tengah is a district in Penang state of Malaysia. It covers an area of 2391 square kilometres with the population size estimated at 383,900. Seberang Perai Tengah experiences hot humid tropical climate and throughout the year, the temperatures ranges from 20 to 30 °C. The residential buildings selected for this study were located in Seberang Jaya city. Nine terrace houses were randomly selected for sample collection.

Sample collection and data analysis

The sample dust was collected in 1 m^2 area using a polyethylene brush and pan by sweeping the living room floor which was most accessible to the occupants. The indoor dust was then transferred into a resealable plastic bag, brought to the laboratory and placed in a desiccator for 24 h, sieved through a 100 μ m screen, and finally oven dried at 105° C for 24 h.

0.5 g of the fine portion of the dried samples were weighed and mixed with 6 mL of a mixture solution consisting of (HNO₃-H₂SO₄) in a ratio of 3:1 and digested using microwave digester Milestone ETHOS PLUS labstation with HPR-1000/105 high pressure segmented rotor. The samples was then made up to a volume of 50 ml in the volumetric flask with distilled water and was analyzed for Pb, Ni, Cu and Zn content by using Inductively Coupled Plasma-Optical Emission Spectroscopy (ICP-OES). The blank experiment was carried out by repeating the procedure for sample preparation without the sample. The composition of the blank solution was compared with the sample solution to identify the elemental composition of heavy metals in the dusts.

Quality control and quality assurance

In order to assess the accuracy of the results that were obtained by the methods used in this study, the blank solution were prepared and underwent the same processes and ran together with the samples in the ICP-OES. All the glassware that were use in the digestion and filtration procedures initially cleaned with soap, washed thoroughly with tap water, rinsed with distilled water and soaked in 1% HNO₃ overnight to remove any contamination by heavy metals. The glassware were then washed thoroughly with the distilled and deionized water. The samples were also left in the desiccator in order to remove the moisture. The dust samples were collected using different brush and dust pan at each sampling and kept in the sealed plastic bag to prevent contamination and to assure sample quality.

Results and Discussion

Heavy Metal Concentration

Four heavy metals (Cu, Ni, Pb and Zn) were analysed in settled surface dust from nine selected houses in Seberang Jaya. The result of heavy metal mean concentrations and their standard deviation are given in Table 1. The highest metal concentration was observed for Pb with the mean concentration of 39.48 mg/kg while the lowest metal concentration was recorded for Cu with the mean concentration of 6.84 mg/kg. The heavy metal concentration in the investigated area followed the order of Pb>Zn>Ni>Cu.

Element (mg/kg) Mean S.D Range 2.20-14.00 Cu 6.84 5.02 18.15 15.07 1.50-32.70 Ni Pb 39.48 33.27 1.50-76.80 17.60 14.60-54.40 Zn 33.78

Table 1: Mean concentration of heavy metal of house dust in Seberang Prai Tengah.

S.D = Standard Deviation

The concentration of Pb recorded was in the range of 1.50 - 76.80 mg/kg with the standard deviation of 33.27. High concentration of Pb was observed in the investigated area may be due to the house age. This may be because older homes usually have more deteriorated interior surfaces, warped windows and doors, and crevices in floors, which can trap the heavy metal particulate[10]. The enrichment of lead dust in this home maybe linked to a longer history of contamination from the former use of leaded paint, lead solder and lead pipe [10]. Pb loading rate increases significantly with house age [11]. The indoor sources such as by the presence of deteriorated or damaged paint of the old houses, carpet and furnishing may also contributed to the lead concentration in settled dust [12].

The concentration of Zn in settled dust were in the range of 14.60 - 54.40 mg/kg. The location of the houses which are closed to main road with high traffic density may have contributed to the presence of Zn in the dust. The elevated Zn content may have originated to wear and tear of vulcanised vehicle tires, and corrosion of galvanised automobile parts [13-15] . The concentration of Zn in the house dust is strongly associated with the inverse of the dustiness of the house [12]. There are a number of sources of zinc in the houses such as rubber, paints and fillers used in linoleum[16].

The concentration of Ni varies between 1.50 to 32.70 mg/kg while for Cu varies between 2.20 to 14 mg/kg. The sources of Ni and Cu in dust are believed to be from anthropogenic sources such as traffic emission and street dust. This include sources from car components, tyre abrasion, brushing, bearing metals and brake dust respectively [14,17]. One of the significant sources of indoor Cu are possibly from electric motors in vacuum cleaners and fans [18].

The results of this study suggest that the heavy metals in dust could be derived from indoor and outdoor dust. However the major influence was from outdoor sources as the selected houses in this study were ventilated with natural and mechanical (fan) ventilation system. These houses have to rely on opened windows for ventilation. The metal bearing dust particles are originated from outside, much of them from cars and some from industrial emissions, and they are atmospherically transported into the house units through the opened windows. The movement of occupants in and out from the house also contribute to the elevated level of heavy metals inside the house.

Correlation Coefficient Analysis

Pearson's correlation coefficient can be used to measure the degree of correlation between logarithms of the heavy metals data. The correlation matrix for heavy metal concentration in studied sample are summarised in Table 2. Statistical analysis indicates positive relation between all the possible pairs of heavy metal at 99% or higher confidence level. High positive correlation was found between Pb-Ni (r=0.985) and Zn-Cu (r=0.819). The result suggest that the metals originate from similar sources which may have derived from automobile emission, street dust and other related activities.

Element	Cu	Ni	Pb	Zn
Cu	1.00			
Ni	-0.909**	1.00		
Pb	-0.915**	0.985**	1.00	
Zn	0.819**	-0.852**	-0.821**	1.00

Table 2: Correlation matrix for the concentration of heavy metal

Comparison With other reported studies

Table 3 gives the comparison between metal contents values obtained in Seberang Jaya residences indoor dust with those reported in literature. The concentrations of heavy metal in settled dust in residential building in Seberang Jaya were generally lower than those in other cities. This may be due to several factors such as industrial activities, traffic density, population density, different transportation system available and also depends on the natural concentration of those particular heavy metals in the soil. The concentration of heavy metals in Sydney metropolitan were in order of Zn, Pb, Cu and Ni as reported by Chattopadhyay et al [19]. Same trend was observed for heavy metal concentration in Sonora Mexico with the highest concentration recorded for Zn followed by Pb, Cu and Ni [20].

Table 3: Heavy metal concentrations in comparison with mean from previous reported studies.

Authors	N	Ietal dete			
	Cu	Ni	Pb	Zn	Study Area
Current study	6.84	18.15	39.27	17.60	Seberang Prai Tengah
Tahir et al.,(2007) ²¹	44.00	NR	78.00	559.00	Dungun, Terengganu
Tong and Lam, (2000) ¹⁰	240.20	NR	71.50	11080.0 0	Hong Kong
Jabeen <i>et al.</i> , (2000) ²²	64.00	NR	477.00	241.00	Jalil Town, Gujranwala, Pakistan
Chattopadhyay et al., (2003) ¹⁹	147.00	27.20	389.00	657.00	Sydney
AlRajhi <i>et al.</i> , (1996) ²³	271.10	52.90	639.10	547.00	Riyadh, Saudi Arabia
Figueroa, (2006) ²⁰	24.69	4.65	44.13	478.93	Sonora, Mexico

^{**} Correlation is significant at the 0.01 level

Conclusion

The chemical analyses of settled dust in this study provide important information on the concentration level of heavy metals in residential building in Seberang Jaya. The results show the range of heavy metals observed in residential building at Seberang Prai Tengah were in the range of 2.20-14.00 mg/kg, 1.50-32.70 mg/kg, 1.50-76.80 mg/kg and 14.60-54.40 mg/kg for Cu, Ni, Pb and Zn respectively. The heavy metal concentration in the investigated area followed the order of Pb>Zn>Ni>Cu. Statistical analysis indicated positive relation between all the possible pairs of heavy metal. The results suggest a likely common source for the heavy metal contamination. The concentration of heavy metal in settled dust in Seberang Jaya were generally lower than those of other cities around the world. The amount of heavy metal in home environment may still be able to reduce by restricting the use of windows and by practising better housekeeping such as frequent wet mopping and vacuuming.

Acknowledgement

The authors would like to thank the owner of the houses for giving the opportunity and cooperation to successfully perform this study.

References

- 1. Leung, A.O.W., Duzgoren-Aydin, N.S., Cheung, K.C., Wong, M.H. (2008). Heavy Metal Concentrations of surface dust from e-waste recycling and its human health implications in southeast China. Environ.Sci. Technol. 42, 2674-2680.
- 2. Gupta, V. K., & Ali, I. (2000). Utilisation of baggase fly ash (a sugar industry waste) for the removal of copper and zinc from wastewater. Separation and purification Technology, 18, 131-140.
- 3. Nriagu, J.O. (1988) A silent epidemic of environmental metal poisoning. Environ Pollution, 50, 139-161.
- 4. Wilson, B., Pyatt, F.B., 2007. Heavy Metal dispersion, persistence and bioaccumulation around an ancient copper mine situated in Anglesey, UK. Ecotoxicology and Environmental Safety, 66, 224-231.
- 5. Ferreira-Baptista, L., De Miguel, E. (2005). Geochemistry and risk assessment of street dust in Luanda, Angola : A tropical urban environment. Atmospheric Environment. 39 4501-4512.
- Klepeis, N.E., Nelson, W.C., Ott, W.R., Robinson, J.P., Tsang, A.M., Switzer, P., Behar, J.V., Hern, S.C., and Engelmann, W.H. (2001). The National Human Activity Pattern Survey (NHAPS): a resource for assessing exposure to environmental pollutants. Journal of Exposure Analysis and Environmental Epidemiology, 11, 231-252.
- 7. Sharpe, M. (2004) Safe as houses? Indoor air pollution and health. J. Environmental Monitoring. 6, 46 49.
- 8. Butte, W., Heinzow, B. (2002). Pollutants in house dust as indicators of indoor contamination. Reviews of Environmental Contamination and Toxicology, 175, 1–46.
- 9. Cowie, C., Black, D., Fraser, I., (1997). Blood lead levels in preschool children in eastern Sydney, Australia N.Z. Journal of Public Helath 21, 755-761.
- 10. Tong, S. T. Y., Lam, K. C.(2000) Home sweet home? A case study of indoor dust contamination in Hong Kong. The Science of the Total Environment, 256, 115-123.
- 11. Lindern, I.H., Spalinger, S.M., Bero, B.N., Petrosyan V., and Braun, M.C. (2003) The influence of soil remediation on lead in house dust. The science of the Total Environment, 303;59-78.
- 12. Ferguson, J.E., Kim, N.D. (1991). Trace element in street and house dust: Source and Speciation. Sci. Total Environment, 100.125-150.
- 13. Li, X., Poon, C.S., Liu, P.S., (2001). Heavy metal contamination of urban soils and street dusts in Hong Kong. Applied Geochemistry 16: 1361–1368.
- 14. Al-Khashman, O.A., (2004). Heavy metal distribution in dust, street dust and soils from the work place in Karak Industrial Estate, Jordan. Atmospheric Environment 38: 6803–6812.
- 15. Adachi, K. and Tainosho, Y., (2004). Characterization of heavy metal particles embedded in tire dust. Environment International 30: 1009–1017.
- 16. Davies, B., Elwood, P.C., Gallacher, J., Ginnever, R.C. (1985). The relationship between heavy metals in garden soils and housedust in an old mining area of North Wales, Great Britain, Environmetal Pollution, 9, 255-266
- 17. Al-Rahji, M.A. and Seaward M.R.D. (1996). Metal level in indoor and outdoor dust in Riyadh, Saudi Arabia. Environmental International. 22: 315 324.

Nor Aimi Abdul Wahab et al: HEAVY METAL CONCENTRATION OF SETTLED SURFACE DUST IN RESIDENTIAL BUILDING

- 18. Koutrakis P., Briggs S.L.K. and Leaderer B.P. (1992) Source apportionment of indoor aerosols in Suffolk and Onondaga counties, New York. Environmental Science and Technology 26, 521-527
- 19. Chattopadhyay, G., Lin, K.C.P, and Feitz, A.J.(2003) Indoor dust metal levels in the Sydney metropolitan area. Environmental Research, 93,301-307.
- 20. Meza-Figueroa, D., De La O-Villanueva, M., and De La Parra, M.L. (2007). Heavy metal distribution in dust from elementary schools in Hermosillo, Sonora, Mexico. *Atmospheric Environment*, 41; 276-288.
- 21. Tahir, N.M., Poh, S.C., and Jaafar, M. (2007). Determination of heavy metal contents in soils and indoor dusts from nurseries in Dungun, Terengganu. The Malaysia Journal of Analytical Sciences, 11, 280-286.
- 22. Jabeen, N., Ahmad, S., Hassan, S.T. and Alam, N.M., (2000). Levels and sources of heavy metals and house dust. Radioanalytical and Nuclear Chemistry 247, 145-149
- 23. Al-Rajhi, M.A., Seaward, M.R.D. and Al- Aemer, A. S. Metals level indoor and outdoor dust in Riyadh, Saudi Arabia. Enviromental International, 22,315-324.



SYNTHESIS AND CHARACTERISATION OF MALEATED POLYPROPYLENE/*LALANG* FIBER/POLYPROPELYNE COMPOSITES: OPTIMISATION PREPARATION CONDITIONS AND THEIR PROPERTIES

(Penyediaan dan Pencirian Komposit Polipropelena Termaleik/Gentian Lalang/Polipropilena: Keadaan Penyediaan Optimum dan Sifatnya)

Sharil Fadli Mohamad Zamri^{1,2*}, Hasratul Nadiah Mohd Rashid^{1,2}, Nurul' Ain Jamion^{1,2} and Rahmah Mohamed²

¹International Education College (INTEC), UiTM Campus Section 17, 40200 Shah Alam, Selangor ²Faculty of Applied Science, Universiti Teknology MARA, 40450 Shah Alam, Selangor

*Corresponding author: sharil7240@salam.uitm.edu.my

Abstract

Polypropylene (PP) blend with natural *lalang* fiber (LF) were investigated in this study. LF was chosen in preparation of polymer composites because it is low cost, eco-friendly, abundance, renewable, biodegradable and shows excellent mechanical properties. Hence, LF has highly potential as a natural fiber filler in polymer composites. LF was prepared by drying the *lalang* leaves under the sun light and were crushed using hammer mill before they were soaked in 5% sodium hydroxide (NaOH) solution. The fiber was then washed with distilled water until neutral. LF was dried in an oven then grinded and sieved into specific sizes. LF/PP and maleated polypropylene/LF/PP (MAPP/LF/PP) composites were prepared by extrusion method using a twin-screw extruder between LF, PP and MAPP at different compositions. The LF/PP and MAPP/LF/PP composites were shaped into 3 mm sheet samples using an electric hydraulic hot press at the temperature of 180 °C. Several studies were carried out to investigate the optimum preparation conditions including the effect of size and percentage of LF, as well as the percentage of MAPP on their mechanical properties using tensile tester and izod impact tester. Meanwhile, the thermal properties of PP, 15% M size LF/PP and 1% MAPP/15% M size LF/PP composites were analyzed using thermogravimety analysis (TGA) and the characteristic of LF on the cross section of 15% M size LF/PP and 1% MAPP/15% M size LF/PP composites were investigated using a digital microscope.

Keywords: Lalang, Polypropylene, Extrusion, Maleated polypropylene, Polymer composite

Abstrak

Polipropilena (PP) diadun bersama gentian lalang semulajadi (LF) dikaji dalam kajian ini. LF dipilih dalam penyediaan polimer komposit kerana ianya rendah kos, mesra alam, tersedia dalam kuantiti yang banyak, boleh diperbaharui, boleh terhurai secara biologi dan menunjukkan sifat mekanikal yang baik. Justeru, LF mempunyai potensi yang tinggi sebagai pengisi gentian semulajadi dalam komposit polimer. LF disediakan dengan mengeringkan daun lalang di bawah cahaya matahari dan dihancurkan menggunakan penghancur tukul sebelum ia direndam di dalam larutan 5% natrium hidroksida (NaOH). Gentian tersebut kemudiannya dibasuh dengan air suling sehingga neutral. LF dikeringkan di dalam oven kemudian dikisar dan diayak kepada saiz tertentu. Komposit LF/PP dan polipropilena termaleik/LF/PP (MAPP/LF/PP) disediakan dengan kaedah pengekstrudan menggunakan pengekstrud skru-berkembar di antara LF, PP dan MAPP pada komposisi berlainan. Komposit LF/PP dan MAPP/LF/PP dibentuk kepada kepingan sempel 3 mm menggunakan hidrolik elektrik tekan panas pada suhu 180 °C. Beberapa kajian telah dijalankan untuk mengkaji keadaan penyediaan optimum termasuk kesan saiz dan peratusan LF, dan juga peratusan MAPP terhadap sifat mekanikalnya menggunakan penguji tensil dan penguji hentaman izod. Sementara itu, sifat haba PP, komposit 15% saiz M LF/PP dan 1% MAPP/15% saiz M LF/PP dianalisis menggunakan analisis termogravimetri (TGA) and ciri-ciri LF pada keratan rentas komposit 15% saiz M LF/PP dan 1% MAPP/15% saiz LF/PP disiasat menggunakan mikroskop digital.

Sharil Fadli et al: SYNTHESIS AND CHARACTERISATION OF MALEATED POLYPROPYLENE-LALANG FIBER/POLYPROPELYNE COMPOSITES: OPTIMISATION PREPARATION CONDITIONS AND THEIR PROPERTIES

Kata kunci: Lalang, Polipropilena, Pengekstrudan, Polipropilena termaleik, Polimer komposit

Introduction

Several studies were conducted by researchers to investigate the potential application of natural fibers in biodegradable polymer composites in order to minimise the dependency of artificial fillers such as fiberglass and carbon fiber for polymer composites [1-5]. The use of natural fillers in polymer composites has been reported by researchers including abaca [6], bamboo fiber [7], cotton [8] and wood fiber [9]. Natural fibers have been given a big attention due to the ability to promote several advantages over artificial fibers including greater value added, sustainability, renewability, biodegradability, non-toxicity, excellent mechanical properties and lower costs. These fibers are able to use in the preparation of natural fiber polymer composites as engineering materials especially in the automotive and construction industries [10-12].

Lalang plant or long-bladed grass (*Imperata arundinacea*) is the most abundant green short plant which grows wildly in the rain forests of tropical countries including Malaysia. The plant does not usually have any economical value and become one of the major problems to agriculture industries. This is because planters need to shed a lot of effort especially allocation of money, energy and time to control its population in order to eliminate the competition for nutrients, water and light with agro-economical plant [13].

As a natural fiber, lalang plant consists of several components including cellulose, hemicelluloses, lignin, pectins and extractives [14]. Cellulose which is the main component became one of ingredients for preparation of natural fiber polymer composites. The impurities such as hemicelluloses, lignin, pectins need to be eliminated from the natural fiber before it can be used in the preparation of natural fiber polymer composites trough a chemical treatment. The chemical treatment using NaOH hydroxide has been reported by Bessadok et al. (2003) and Bachtiar et al. (2008). The treatment will result some advantages including breaking down the bundle fibers into individual filament fibers and increasing contact area of the fiber with their matrix hence enhance the properties of the polymer composites [2;15].

Cellulose of natural fibers contains polar groups in its structure and gives a low compatibility with non-polar structure of polymeric matrices. Thus, the prepared natural fiber polymer composites show a dramatical decrease in mechanical properties of natural fiber polymer composites. Fiber surface treatments were reported to be able to improve these weaknesses [6]. Unfortunately, the modification of these natural fibers techniques such as graft copolymerization [16] and silane treatment [17] bring other implication such as high production cost, generate toxic waste and inflexible processes which may cut the potential of these fibers for a mass production scale. "In situ" surface modification via blending natural fiber with polymeric matrices with the presence of maleated polyolefin such as maleated polypropylene as MAPP and maleated polyethylene (MAPE) as the compatibiliser is able to avoid mentioned disadvantages [18].

PP is a thermoplastic has been used widely including packaging, plastic parts and various types of reusable containers of various types, loudspeakers, automotive components, and polymer banknotes [19] due to their lightweight property, inexpensive, inert against most of chemicals, high softening temperature, better thermal stability and flexible processability [20]. PP has lack of wetting characteristic against natural fiber filler. Thus, MAPP was used as compatibiliser. It has been proven that this blend is able to improve fiber—matrix bonding, resulting in improvements in the physical properties of the natural fiber polymer composites [21].

In this study, investigation to optimise the preparation conditions including the effect of size and percentage of LF, as well as the percentage of MAPP on their mechanical properties using tensile and izod impact tester were conducted. Meanwhile, the thermal stability of PP, 15% M size LF/PP and 1% MAPP/15% M size LF/PP composites were analyzed using TGA and the characteristic of LF on the cross section of 15% M size LF/PP and 1% MAPP/15% M size LF/PP composites were investigated using a digital microscope.

Materials and Methods

Materials

Lalang plants which grew wildly were collected form a rural area in Kampung Tekah Baru, Kampung Kepayang, Perak, Malaysia. Industrial grade PP was supplied from Titan (M) Sdn. Bhd. NaOH was purchased from Merck, German and MAPP was obtained from SIRIM, Shah Alam, Selangor, Malaysia.

Preparation of LF

The LF was prepared by drying the lalang leaves under the sun light then they were crushed using a hammer mill before they were soaked in 5% sodium hydroxide solution for 48 hours to remove their hemi-cellulose, lignin and pectins components. After that, LF was washed using distilled water until a solution reached pH 7 and LF was dried again in an oven at the temperature of 60 °C until it reached constant weight. Finally, the LF was grinded using domestic electrical grinder and sieved into specific of sizes.

Preparation of LF/PP and MAPP/LF/PP composites

The MAPP/LF/PP composites were prepared by extrusion method using a twin-screw extruder between LF, PP and MAPP at different compositions. The MAPP/LF/PP composites were extruded twice to improve the distribution of filler in their matrix. The LF/PP and MAPP/LF/PP composites were shaped into 3 mm sheet samples using an electric hydraulic hot press at the temperature of 180 °C.

The weight percentage of MAPP/LF/PP composites was calculated by following formula:

Results and Discussion

Table 1 shows the mechanical properties of LF/PP composites at various LF sizes prepared by extruding PP with LF at 20% of LF loading. The tensile strength of LF/PP composites are not influenced by the size of LF. The same phenomenon was observed by Ruksakulpiwat et al. [13]. Meanwhile, Young's modulus of LF/PP composites shows significant decreases with the increasing of LF size. The impact strength of LF/PP composites increased as the size of LF gets bigger. This may due to the increases of LF increasing the adhere area of PP on individual LF's filaments.

Table 1: Tensile strength, Young's modulus and impact strength of 20% LF/PP composites at various LF sizes loaded.

LF size	Tensile strength	Young's modulus	Impact strength
	(MPa)	(N/mm^2)	(kJ/m^2)
S	20.6	1434.2	10.6
M	20.5	1111.2	10.8
L	20.3	792.9	14.3

 $S\colon <1$ mm; $M\colon 1\text{--}2$ mm; $L\colon 2\text{--}3$ mm

The variation of tensile strength, Young's modulus and impact strength of LF/PP composites using M size LF as a function of percentage of LF loading is represented in Table 2. All tensile strength, Young's modulus and impact strength of LF/PP composites show the similar trends where when the percentage of LF increases, it leads to the decreasing of their mechanical properties from 0 to 10 of LF loaded. The decreases in these properties are due to the lack of affinity between the LF and PP. As a natural fiber, LF has a poor compatibility demonstrated between the fiber and the matrix. This will cause a non-homogeneous dispersion of fiber in their matrix and decreases in the mechanical properties of the polymer composites [23]. However, the results show there are no significant effects after 15% of LF has been loaded into the polymer composites.

Sharil Fadli et al: SYNTHESIS AND CHARACTERISATION OF MALEATED POLYPROPYLENE-LALANG FIBER/POLYPROPELYNE COMPOSITES: OPTIMISATION PREPARATION CONDITIONS AND THEIR PROPERTIES

Table 2: Tensile strength, Young's modulus and impact strength of M size LF/PP composites
at various percentage of LF loaded.

Percentage of LF loaded	Tensile strength (MPa)	Young's modulus (N/mm²)	Impact strength (kJ/m²)
0	31.1	1834.1	37.1
5	28.0	1586.1	13.0
10	24.1	1463.6	12.0
15	20.6	1442.1	10.0
20	20.5	1431.2	10.8
25	20.3	1449.4	10.2

The effect of MAPP as a compatibilizer for MAPP/LF/PP composites on their tensile strength, Young's modulus and impact strength are shown in Table 3. It clearly revealed that by the introduction of 1% of MAPP to the MAPP/LF/PP composites, it increases the tensile strength, Young's modulus and impact strength of the polymer composites by 18, 42 and 48%, respectively. As a natural fiber, LF naturally is hydrophilic. This will cause incompatibility between LF with hydrophobic PP and leads to a decrease in mechanical properties of the polymer composites. Good filler-matrix interface interaction is the main key for properties of polymer composites. The incorporation of MAPP in the polymer composites may improve filler-matrix adhesion strength [24]. Compatibility of the polymer composites may improve by the formation of hydrogen bond between maleic anhydride of MAPP with hydroxyl group of LF and the presence of PP segment as shown in Figure 1 [25].

Table 3: Tensile strength, Young's modulus and impact strength of MAPP/15% M size LF/PP composites at various percentage of MAPP loaded.

Percentage of MAPP	Tensile strength (MPa)	Young's modulus	Impact strength (kJ/m ²)			
loaded		(N/mm^2)				
0	20.6	1442.1	10.0			
1	24.3	2047.9	14.8			
3	23.0	1609.0	12.7			
5	21.6	1468.3	11.1			

Fig. 1: Formation of hydrogen bonding between maleic anhydride in MAPP and hydroxyl group in cellulose of LF.

Thermal stability of polymer composites has been improved by the introduction MAPP as shown in Figure 2. The figure shows that the thermal stability of 1% MAPP/15% M size LF/PP composite is in between the thermal stability of 15% M size LF/PP composite and PP. Table 4 confirms that the decomposition temperature of polymer composites measured at 5 and 50% mass loss has shifted to the higher temperature for 1% MAPP/15% M size LF/PP composite compared to 15% M size LF/PP composites. Furthermore, the different in mass loss measured at the temperature of 250 to 350 °C for 1% MAPP/15% M size LF/PP composite is lesser compared to the 15% M size LF/PP composite. MAPP improved the compatibility of the polymer composites by improving the interfacial adhesion between LF and PP. The formation of hydrogen bond in between LF and MAPP gives additional improvement toward polymer composite's properties [24-25].

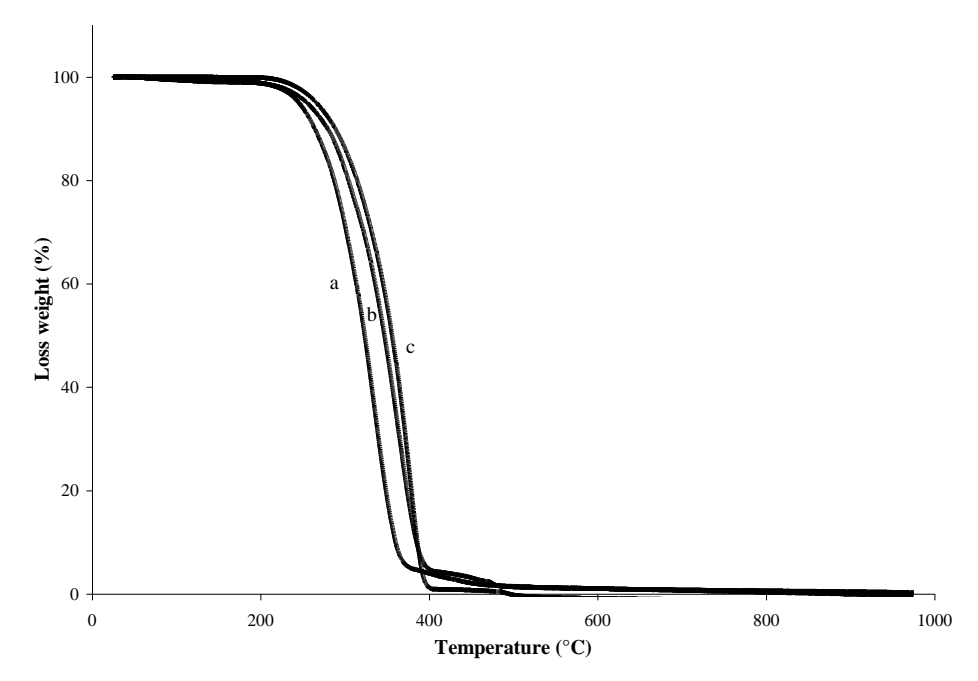


Figure 2: TG thermograms of (a) 15% M size LF/PP composite, (b) 1% MAPP/15% M size LF/PP composite and (c) PP.

	T -5 (°C)	<i>T</i> ₋50 (°C)	Different Mass Loss
			(250-350 °C) (%)
PP	266.138	356.079	41.21495
15% M size LF/PP	245.564	323.515	75.32318
1% MAPP/15% M size LF/PP	254.755	346.942	48.86728

Note: T_{-5} : Decomposition temperature at 5% loss weight, T_{-50} : Decomposition temperature at 50% loss weight

Figure 3 shows pictures of cross section samples of (a) 15% M size LF/PP and (b) 1% MAPP/15% M size LF/PP composites taken using a digital microscope. The samples were initially tested for tensile strength then the picture of the broken area resulting from the test was taken in order to investigate the relationship between pulled LF filaments with their tensile strength, Young's modulus and impact strength of the composites. The figure clearly shows that

Sharil Fadli et al: SYNTHESIS AND CHARACTERISATION OF MALEATED POLYPROPYLENE-LALANG FIBER/POLYPROPELYNE COMPOSITES: OPTIMISATION PREPARATION CONDITIONS AND THEIR PROPERTIES

the LF filament was pulled out individually resulting from the force generated from the tensile test for uncompatibilized 15% M size LF/PP. Contrary, the compatibilized 1% MAPP/15% M size LF/PP composites picture shows that the pulled out LF filaments are covered with PP as its polymeric matrix. By introduction of 1% MAPP may improve the adhering property of MAPP/LF/PP composites. This agrees with the tensile strength, Young's modulus and impact strength of MAPP/LF composites.

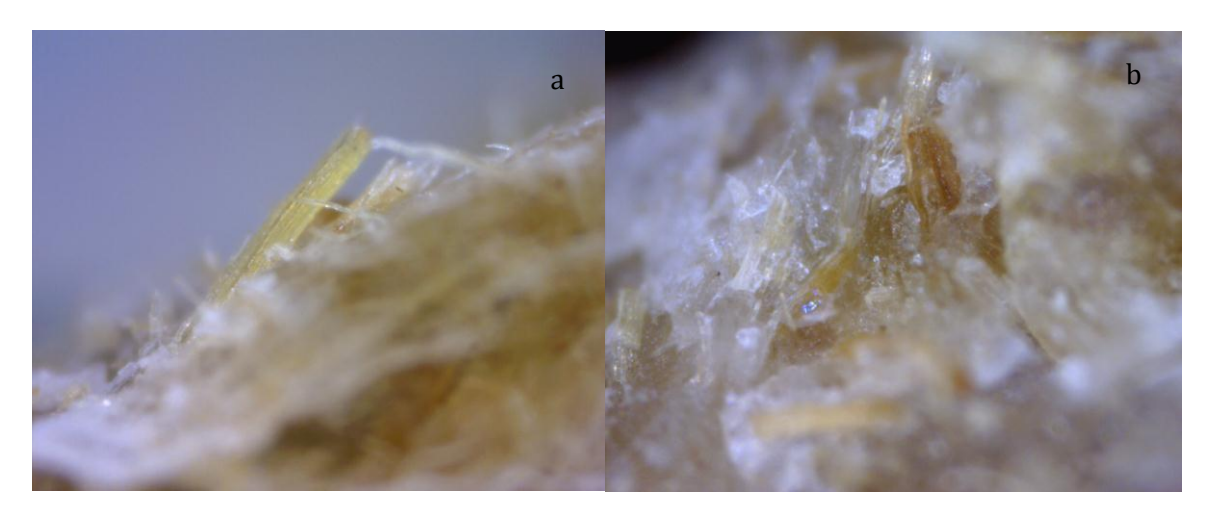


Figure 3: Digital microscopic pictures of (a) 15% M size LF/PP (b) 1% MAPP/15% M size LF/PP composites.

Conclusion

LF/PP and MAPP/LF/PP composites were successfully prepared. The mechanical properties of LF/PP composites were varied according to size and percentage LF loaded. Bad wetting characteristic between LF and PP leads to decreasing in mechanical properties of LF/PP composites. By introduction of 1% MAPP give the higher mechanical and thermal properties to MAPP/LF/PP composites. This due to ability of MAPP to improve the compatibility characteristic between LF and PP. Digital microscopic pictures of cross section samples revealed that MAPP enhanced adhering properties between LF and PP.

Acknowledgement

Authors would like to acknowledge Research Management Institute of UiTM for the financial support under Dana Kecemerlangan Grant Scheme. Authors also thanks to INTEC, UiTM and Faculty of Applied Science, UiTM for continuous supporting towards this study.

References

- 1. Paiva, M. C., I. Ammar, I., Campos, A. R., Cheikh, R. B. and Cunha, A. M. (2007) Alfa fibres: Mechanical, morphological and interfacial characterization. Composites Science and Technology 67 1132–1138.
- 2. Bessadok, A., Roudesli, S., Marais, S., Follain, N. and Lebrun, L. (2009) Alfa fibres for unsaturated polyester composites reinforcement: Effects of chemical treatments on mechanical and permeation properties. Composites: Part A 40 184–195.
- 3. Liu, W., Mohanty, A. K., Askeland, P., Drzal, L. T. and Misra, M. (2004) Influence of fiber surface treatment on properties of Indian grass fiber reinforced soy protein based biocomposites. Polymer 45 7589–7596.
- 4. Yang, H. S., Kim, H. J., Park, H. J., Lee, B. J. and Hwang, T. S. (2007) Effect of compatibilizing agents on rice-husk flour reinforced polypropylene composites. Composite Structures 77 (1) 45–55.
- 5. Wang, J., Gu, M., Songhao, B. and Ge, S. (2003) Investigation of the influence of MoS2 filler on the tribological properties of carbon fiber reinforced nylon 1010 composites. Wear 255 774–779.

- 6. Vilaseca, F., Valadez-Gonzalez, A., Herrera-Franco, P. J., Pèlach, M. A., López, J. P. and Mutjé, P. (2010) Biocomposites from abaca strands and polypropylene. Part I: Evaluation of the tensile properties. Bioresource Technology 101 387–395.
- 7. Ismail, H., Edyham, M. R., Wirjosentono, B. (2002) Bamboo fibre filled natural rubber composites: the effects of filler loading and bonding agent. Polymer Testing 21 139–144.
- 8. Bajwa, S. G, Bajwa, D. S., Holt, G., Coffelt, T. and Nakayama, F. (2011) Properties of thermoplastic composites with cotton and guayule biomass residues as fiber fillers Industrial Crops and Products 33 747–755.
- 9. Augier, L., Sperone, G., Vaca-Garcia, C. and Borredon, E. (2007) Influence of the wood fibre filler on the internal recycling of poly(vinyl chloride)-based composites. Polymer Degradation and Stability 92 1169-1176.
- 10. Bismarck, A., Baltazar-Y-Jimenez, A. and Sarlkakis, K. (2006) Green composites as Panacea? Socio-economic aspects of green materials. Environment, Development and Sustainability 8 (3) 445–463.
- 11. Wambua, P., Ivens, J. and Verpoest I. (2003) Natural fibres: can they replace glass in fibre reinforced plastics? Composites Science and Technology 63 1259–1264.
- 12. Duc, A. L., ergnes, B. and Budtova T. (2011) Polypropylene/natural fibres composites: Analysis of fibre dimensions after compounding and observations of fibre rupture by rheo-optics. Composites: Part A 42 1727–1737
- 13. Ruksakulpiwat, Y., Suppakarn, N., Sutapun, W. and Thomthong, W. (2007) Vetiver–polypropylene composites: Physical and mechanical properties. Composites: Part A 38 590–601.
- 14. Xie, Y., Hill, C. A. S., Xiao, Z., Militz, H. and Mai, C. (2010) Silane coupling agents used for natural fiber/polymer composites: A review. Composites: Part A 41 806–819.
- 15. Bachtiar, D., Sapuan, S. M and Hamdan, M. M. (2008) The effect of alkaline treatment on tensile properties of sugar palm fibre reinforced epoxy composites. Materials and Design 29 1285–1290.
- 16. Roman-Aguirre, M., Marquez-Lucero, A. and Zaragoza-Contreras E. A. (2004) Elucidating the graft copolymerization of methyl methacrylate onto wood-fiber. Carbohydrate Polymers 55 201–210.
- 17. Sgriccia, N., Hawley, M. C. and Misra, M. (2008) Characterization of natural fiber surfaces and natural fiber composites. Composites: Part A 39 1632–1637.
- Beg, M. D. H., Pickering, K. L. (2008) Mechanical performance of Kraft fiber reinforced polypropylene composites: influence of fibre length, fibre beating and hygrothermal ageing. Composites: Part A 39 1748– 1755
- 19. Liu, S. P and Liang, C. W. (2011) Preparation and mechanical properties of polypropylene / montmorillonite nanocomposites After grafted with hard/soft grafting agent. International Communications in Heat and Mass Transfer 38 434–441
- 20. Hirunpraditkoon, S and García, A. N. (2009) Kinetic study of vetiver grass powder filled polypropylene composites. Thermochimica Acta 482 30–38.
- 21. Qiu, W., Endo, T. and Hirotsu, T. (2005) A novel technique for preparing of maleic anhydride grafted polyolefins. European Polymer Journal 41 1979–1984.
- 22. Chand, N. and Dwivedi, U. K. (2006) Effect of coupling agent on abrasive wear behaviour of chopped jute fibre-reinforced polypropylene composites. Wear 261 1057–1063.
- 23. Kim, J. P., Yoon, T. H., Mun, S. P., Rhee, J. M. and Lee, J. S. (2006) Wood–polyethylene composites using ethylene–vinyl alcohol copolymer as adhesion promoter. Bioresource Technology 97 (3) 494–499.
- 24. Mohanty, S and Nayak, S. K. (2007) Dynamic and steady state viscoelastic behavior and morphology of MAPP treated PP/sisal composites. Materials Science and Engineering A 443 202–208.
- 25. Idicula, M., Boudenne, A., Umadevi, L., Ibos, L., Candau, Y and Thomas, S. (2006) Thermophysical properties of natural fibre reinforced polyester composites. Composites Science and Technology 66 2719–2725.



OPTIMIZATION STUDY FOR REMOVAL OF RADIUM-226 FROM RADIUM-CONTAMINATED SOIL USING HUMIC ACID

(Kajian Pengoptimuman Penyingkiran Radium-226 Daripada Tanih Tercemar Radium Dengan Menggunakan Asid Humik)

Esther Phillip^{1,2*}, Muhamad Samudi Yasir¹, Muhamat Omar², Mohd Zaidi Ibrahim², Zalina Laili²

¹School of Applied Physics, Faculty of Science and Technology, Universiti Kebangsaan Malaysia, 43600 UKM Bangi, Selangor Darul Ehsan, Malaysia. ² Waste and Environmental Technology Division, Malaysia Nuclear Agency, Bangi, 43000 Kajang, Selangor Darul Ehsan, Malaysia.

*Corresponding author: esther@nuclearmalaysia.gov.my

Abstract

This study discusses the various parameters involved in the removal of radium-226 from radium-contaminated soil using humic acid extracted from Malaysian peat soil. The parameters studied included the contact time, the pH and the concentration of humic acid solution and the liquid/solid ratio. The optimum removal efficiency of radium-226 was achieved after 24 hours of agitation. Further agitation did not contribute to any increase in the removal efficiency of radium-226. Meanwhile, the removal efficiency of radium-226 was optimum when the humic acid concentration was 100 ppm. The greatest removal efficiency of radium-226 was obtained using highly basic humic acid solutions of pH 10-11. Humic acid solutions of basic pH 8-9 resulted in comparable removal efficiency to humic acid solutions of pH 7. Nevertheless, acidic humic acid solutions showed the lowest removal efficiency of radium-226. For the purpose of this study, humic acid solutions of pH 7 were used throughout the study. A ratio of 20 mL humic acid solution to 1 g soil sample was found as the optimum value. Any further increment in the ratio did not contribute to the removal efficiency of radium-226.

Keywords: Radium-226, Humic Acid, Contact time, pH, Concentration, Liquid/solid ratio

Abstrak

Kajian ini membincangkan pelbagai parameter yang terlibat dalam penyingkiran radium-226 daripada tanih tercemar radium dengan menggunakan asid humik yang diekstrak daripada tanih gambut Malaysia. Parameter yang dikaji termasuk masa sentuhan, pH dan kepekatan larutan asid humik serta nisbah cecair/pepejal. Penyingkiran optimum radium-226 dicapai selepas tempoh 24 jam goncangan. Masa goncangan yang lebih lama tidak menyumbang kepada sebarang peningkatan dalam keberkesanan penyingkiran radium-226. Sementara itu, penyingkiran radium-226 adalah optimum apabila asid humik berkepekatan 100 ppm digunakan. Keberkesanan penyingkiran yang paling tinggi dicapai apabila larutan asid humik berkealkalian tinggi dalam pH 10 – 11 digunakan. Larutan asid humik beralkali dengan pH 8 – 9 menunjukkan keberkesanan penyingkiran yang sama dengan larutan asid humik berpH 7. Walaubagaimanapun, larutan asid humik yang berasid menunjukkan keberkesanan penyingkiran radium-226 yang paling rendah. Untuk tujuan kajian ini, asid humik berpH 7 digunakan sepanjang kajian. Nisbah 20 mL larutan asid humik kepada 1 g sampel tanih pula didapati sebagai nilai optimum. Sebarang pertambahan dalam nisbah larutan asid humik kepada sampel tanih tidak menyumbang kepada keberkesanan penyingkiran radium-226.

Kata kunci: Radium-226, Asid humik, Masa sentuhan, pH, Kepekatan, Nisbah cecair/pepejal

Introduction

One of the past activities that contributes to the generation of radium (Ra)-contaminated soil is luminous dial painting using radioluminescence paint that contains mixtures of radioactive and luminescent crystalline materials [1]. The radioluminescence paint used radium-226 (Ra-226) as the primary radioactive material before the discoveries of tritium (H-3) and promethium-147 (Pm-147) [2]. In Malaysia, such activity that was actively been

Esther Phillip et al: OPTIMIZATION STUDY FOR REMOVAL OF RADIUM-226 FROM RADIUM-CONTAMINATED SOIL USING HUMIC ACID

carried out since the 1960s until 1990s had left the processing sites, especially the soil being contaminated with Ra-226. Being an alpha and gamma emitter [3] with relatively long half-life of 1600 years, Ra-226 has been known to be extremely hazardous to the environment as well as human health. Therefore, removal of Ra-226 from the Racontaminated soil is vital to ensure that the hazardous effect of Ra-226 can be eliminated.

Various removal methods can be explored including the application of natural material such as humic substances extracted from soil organic matter. Humic acid (HA), the main extractable fraction of humic substances [4], has been found to interact with metal ions [5, 6] including radionuclides [7, 8]. Over the years, interaction between HA and radionuclides has been extensively studied [9, 10, 11, 12, 13, 14, 15, 16, 17, 18, 19, 20, 21]. Laili et al. [22] in particular has discussed the influence of HA on the removal of Ra from aqueous solution by adsorption of Ra ions onto coir pith. The interaction between HA and other molecules or ions is due to the presence of binding sites provided by its functional groups in particular carboxyl and phenolic groups [17, 23, 24].

As a remarkably heterogeneous ligand [17, 23] with polyelectrolytic nature [24], the interaction of HA with other molecules and ions is significantly affected by various parameters. This paper describes the various parameters involved in the removal of Ra-226 from Ra-contaminated soil using HA as removal agent. Parameters investigated include contact time, pH and concentration of HA solution and liquid/solid ratio.

Experimental

Materials

HA used was extracted from peat soil obtained from Bachok, Kelantan. Meanwhile, Ra-contaminated soil was sampled from a former compass dial painting facility site in Malaysia. The Ra-contaminated soil sample had been excavated from the site and transferred to the radioactive waste storage facility at Nuclear Malaysia since year 2000. Ra-226 standard solutions were obtained from Isotope Products Laboratories (an Eckert & Ziegler Company). Other reagents and chemicals used were of analytical grade from R&M Chemicals or Sigma Aldrich.

Extraction of HA

HA was extracted from peat soil according to the acid-base extraction method described by International Humic Substances Society (IHSS). HA stock solutions were prepared by dissolving the extracted solid HA in diluted sodium hydroxide (NaOH) solution. HA working solutions were prepared by diluting the stock solutions also in diluted NaOH.

Preparation of Ra-contaminated soil sample

The Ra-contaminated soil sample was air-dried at room temperature (27°C) in a fume hood prior to manual grinding. The ground soil sample was then sieved using a 2 mm sieve and finally stored in a sealed container for experimental purposes.

Elemental and radioactivity characterization of Ra-contaminated soil sample

Elemental composition of the Ra-contaminated soil sample was determined by neutron activation analysis (NAA) technique. Ra-226 activity concentration of the Ra-contaminated soil sample was analysed by a gamma spectrometer equipped with a CANBERRA n-type hyper-germanium detector (HPGe) (30% relative efficiency and 1.9 keV resolution at 1.33 MeV) from Oxford Instruments Inc. together with Genie 2K software for spectrum analysis.

Removal of Ra-226

The removal study was carried out in a batch method by agitating 50 mL polyethylene tubes containing 1.00 g soil sample and a measured volume of HA solutions of certain pH and concentration at a speed of 100 rpm at room temperature (27°C) for a given time. The suspensions were then centrifuged at 4000 rpm for 10 minutes. The precipitates were removed leaving the supernatants for Ra-226 analysis. The collected supernatants were sealed in 50 mL bottles and kept at room temperature (27°C) for at least 21 days before counting to allow secular equilibrium of Ra-226 with their respective decay products. Ra-226 analyses were performed using a gamma spectrometry system. For the purpose of this study, the determination of Ra-226 activity was performed based on indirect measurement of gamma ray at energy line 609 keV. The contact time ranged from a period of 2 to 96 hours (HA =

pH 7, 100 ppm, L/S = 20). Meanwhile, the pH of HA solutions investigated were in the range of 3 to 11 (contact time = 24 hours, HA = 100 ppm, L/S = 20). For the concentration experiments, five different concentrations (25, 50, 75, 100, 125 and 150 ppm) of HA solutions were chosen (contact time = 24 hours, HA = pH 7, L/S = 20). Finally, the liquid/solid ratio experiments were conducted by using 10, 20, 30 and 40 mL of HA solutions giving liquid/solid ratios of 10, 20, 30 and 40 respectively (contact time = 24 hours, HA = pH 7, 100 ppm).

Removal efficiency of Ra-226 was calculated based on the following equation;

Removal efficiency,
$$\% = \frac{\text{Ao} - \text{A}}{\text{Ao}} \times 100\%$$

A_o = Initial Ra-226 activity in Ra-contaminated soil sample, Bq

A = Final Ra-226 activity in Ra-contaminated soil sample after removal, Bq

Results and Discussion

Contact time

Contact time is a vital parameter in any desorption study of metals from soil as desorption itself is a kinetic equilibrium process [25]. Therefore, a study investigating the effect of contact time on the removal efficiency of Ra-226 from the Ra-contaminated soil sample was carried out and the results obtained are shown as semi-log plot in Figure 1. It was found that the removal efficiency of Ra-226 ranged from 4 – 24 %. Initially, increase in contact time did not affect the removal efficiency of Ra-226. Nevertheless, a progressive increase in removal efficiency of Ra-226 was observed as contact time increased to 24 hours. Further agitation however did not lead to any changes in the removal efficiency of Ra-226. The relatively long contact time required to reach maximum removal efficiency implied that Ra-226 was strongly bound to soil matrix via adsorption [26, 27, 28], precipitation and coprecipitation [29]. The fact that the adsorption of Ra is the strongest among all other alkaline earth metal [3] supported the strong binding of Ra-226 to the soil matrix. For the purpose of this study, contact time of 24 hours was selected as the optimum value.

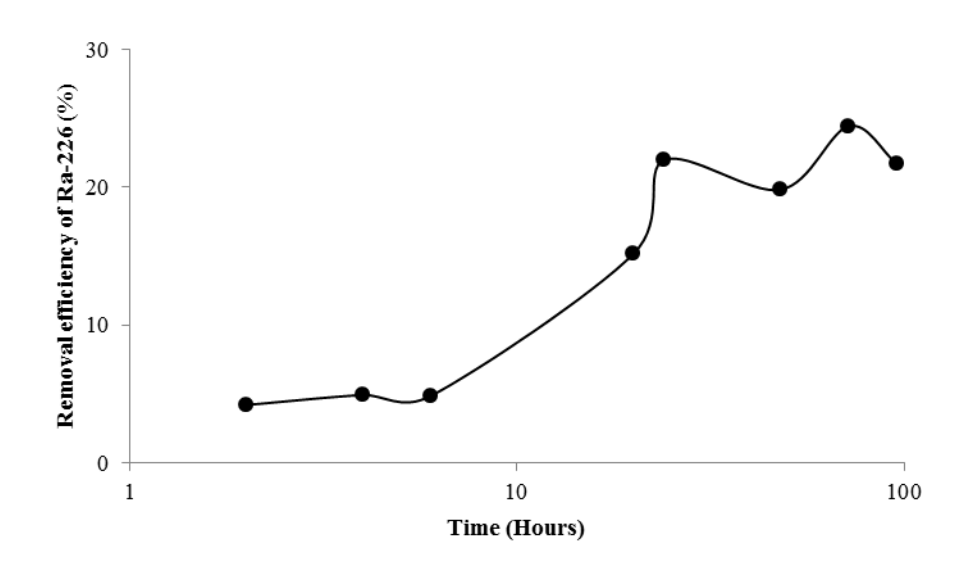


Figure 1: Effect of contact time on removal efficiency of Ra-226 from Ra-contaminated soil sample (HA = 100 ppm, pH 7, L/S = 20 mL/g)

Concentration of HA

HA solutions of different concentration were used in the removal study and the results obtained are shown in Figure 2. The removal efficiency of Ra-226 was the lowest when the concentration of HA was below 100 ppm as there was not much HA molecules present. The removal efficiency observed was almost constant with an increase of only 3 – 6 % from the condition when the HA was absent. Nevertheless, as the concentration of HA reached 100 ppm, higher removal efficiency of Ra-226 was observed. Further increase in the concentration of HA however resulted in a slight decrease in the removal efficiency of Ra-226.

The effect of different concentration of HA on the removal efficiency of Ra-226 could be explained by applying the diffusion phenomenon discussed by Wu and Nofziger [30]. According to Wu and Nofziger [30], diffusion coefficient of a solute in a dilute solution was regarded as constant. Therefore, in dilute HA solution (below 100 ppm), the diffusion coefficient of HA molecules could be considered as constant. Consequently, similar rate of transfer of HA molecules in HA solutions of different concentration (below 100 ppm) was achieved leading to less interaction between Ra-226 and HA molecules and finally resulting in the constant removal efficiency observed. Higher removal efficiency of Ra-226 achieved when HA solution of 100 ppm was used was probably due to the increase of flux from the Ra-226 – HA complexes. Nevertheless, further increase in the concentration of HA that eventually led to increase in viscosity could retard the mass transfer of Ra-226 – HA complexes thus resulting in decrease of removal efficiency of Ra-226. For the purpose of this study, 100 ppm was chosen as the optimum concentration of HA solution.

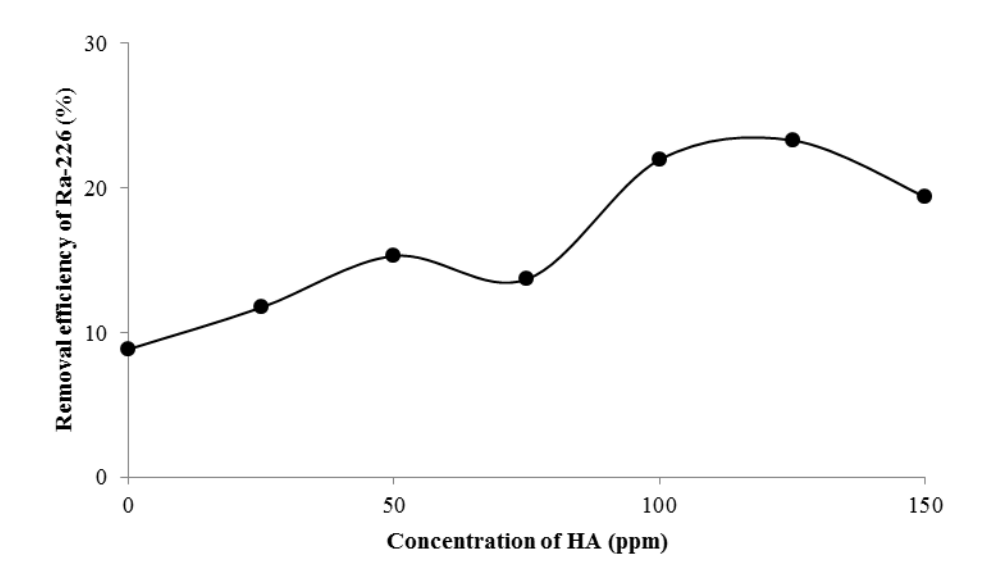


Figure 2: Effect of concentration of HA on removal efficiency of Ra-226 from Ra-contaminated soil sample (Contact time = 24 hours, pH 7, L/S = 20 mL/g)

pH of HA

Another important parameter was pH as pH could affect the retardation and mobility of metal ions and radionuclides in soil [31, 32]. Besides that, pH could also affect the removal capability of removal agent such as chelating agent to extract contaminants from soil through numerous mechanisms [25]. Interaction between metal ions and radionuclides with HA depended on pH due to the polyelectrolitic properties of HA [14, 17] and its ligand heterogeneity in terms of content of functional groups [17, 23]. Therefore, a study investigating the effect of HA

solutions of different pH on the removal efficiency of Ra-226 from the Ra-contaminated soil sample was carried out. The results obtained are shown in Figure 3.

The removal efficiency of Ra-226 using HA solutions of pH in the range 3-11 resulted in 11-44 % of Ra-226 removal. The efficiency was found to increase with the pH of HA solutions used. The increasing trend of the removal efficiency could be due to increase in the stability constants of the Ra-226 – HA complexes as the number and strength of the binding increased. Nevertheless, the removal efficiency of Ra-226 could be affected by Al that was present in the contaminated soil sample as Al could form stable complexes with HA [33].

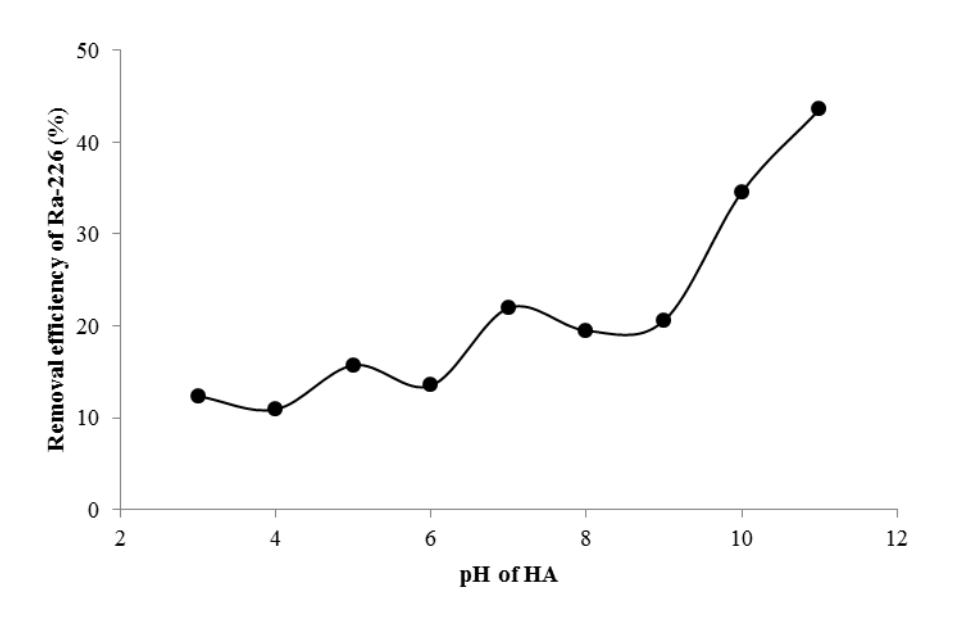


Figure 3: Effect of pH on removal efficiency of Ra-226 from Ra-contaminated soil sample (Contact time = 24 hours, HA = 100 ppm, L/S = 20 mL/g)

It was also found that the pH of the soil suspensions differed from the initial pH of the HA solutions used except for the HA solutions of pH 7, with pH tended to shift towards near neutral pH. HA increased the buffering capacity of the contaminated soil sample and permitted the soil neutral pH to stay stable. The removal efficiency of Ra-226 was the lowest when acidic HA solutions in the range 3 – 6 were used. The resulting pHs of the soil suspensions were approximately 5.0 - 6.5. Those findings could be due to less HA molecules available for binding with Ra-226 species as ionization of carboxylic functional groups of HA molecules was not favourable at pH < 7 [34]. Besides that, trapping of Ra-226 species by HA aggregates was also not favourable at this pH condition as temporary trapping of metal ions and radionuclides by HA molecules tended to occur at highly acidic condition [35]. Furthermore, the coagulation of HA molecules with Al species that was prone to occur in the pH range 4 - 7 [36] could lead to less binding of HA molecules with Ra-226 species. Increased removal efficiency of Ra-226 was observed when HA solutions of pH in the range 7 – 9 were used. The resulting pHs of the soil suspensions were around neutral thus allowed more ionization of HA molecules than at the acidic pH condition. At pH 7, the adsorption of neutral Ra-226 species namely RaSO₄⁰ and RaCO₃⁰ [37] onto Al(OH)₃ precipitates was low due to the decreasing formation of Al(OH)₃ precipitates and thus more Ra-226 species were available for binding with HA molecules. The removal efficiency of Ra-226 was high when HA solutions of pH in the range 10 - 11 were used and reached its maximum when HA solutions of pH 11 were used. The resulting pHs of the soil suspensions were found to be around 8. The greater removal efficiency in basic condition suggested the increasing importance of

Esther Phillip et al: OPTIMIZATION STUDY FOR REMOVAL OF RADIUM-226 FROM RADIUM-CONTAMINATED SOIL USING HUMIC ACID

deprotonated phenolic functional groups of HA molecules in binding with Ra-226 as pH increased. The higher removal efficiency at basic condition could also be explained by the accessibility of HA functional groups [38] as HA molecules were more open and linear due to the decrease in intra- and inter-molecular hydrogen bonding [39]. Besides that, adsorption of soil organic matter on the surface of soil mineral that decreased with pH [40] explained the decreasing adsorption of HA molecules onto soil matrix as pH increased thus allowed more mobile HA molecules for interaction with Ra-226.

For the purpose of this study, HA solutions of pH 7 were used throughout the study due to several reasons. Addition of acidic and basic reagents was not required as the prepared HA solutions were initially of neutral pH. The neutral resulting HA solutions containing removed Ra-226 did not cause any acidic or basic toxic materials emission. Besides that, the neutral resulting HA solutions also did not require any further treatment as highly acidic and basic washing solutions.

Liquid/solid ratio

Liquid/solid ratio was also another important parameter in the removal of Ra-226 from the Ra-contaminated soil sample. The results of the removal study conducted using varying liquid/solid ratios are presented in Figure 4. Different soil samples had their own requirements in terms of critical level at which almost all of their mobile metal ions could be extracted or removed; above this critical level, only slight increase in extraction or removal could be anticipated. In this study, dose was defined as moles of HA used for treating 1 g soil and the dose was directly correlated to the liquid/solid ratio if the concentration of HA was fixed. Therefore, as the liquid/solid ratio increased so did the dose. The results obtained showed that the removal efficiency of Ra-226 increased as liquid/solid ratio increased but only up to a ratio of 20 mL/g. The progressive increase in removal efficiency of Ra-226 observed at low liquid/solid ratio (below 20 mL/g) indicated that the dose of HA was less than the soil requirement. Meanwhile, further increase in the ratio higher than 20 mL/g did not result in any increment of removal. The almost constant removal of Ra-226 at liquid/solid ratio higher than 20 mL/g implied that the soil requirement had been exceeded.

For the purpose of this study, a liquid/solid ratio of 20 mL/g was chosen as optimum value.

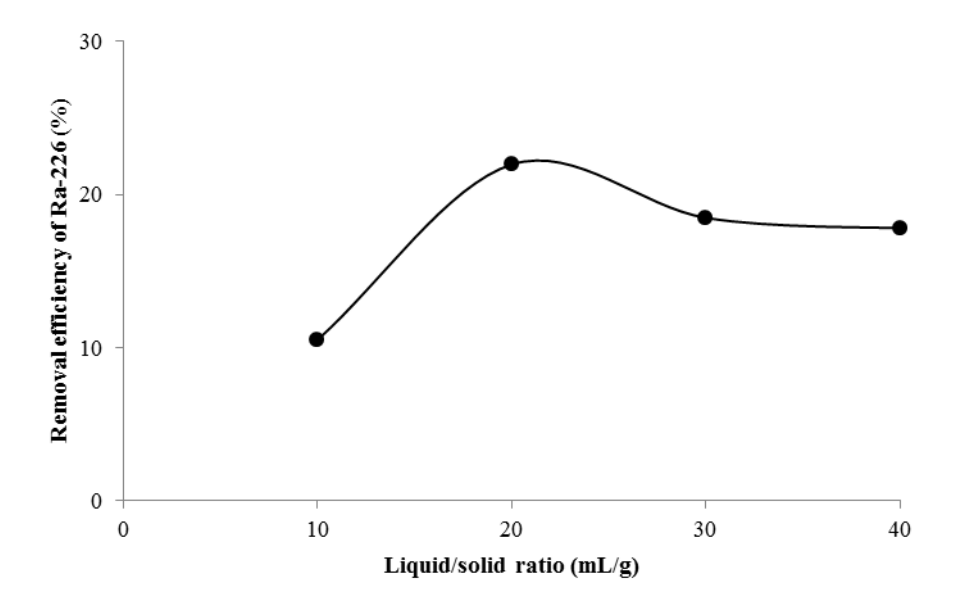


Figure 4: Effect of liquid/solid ratio on removal efficiency of Ra-226 from Ra-contaminated soil sample (24 hours, HA = pH 7, 100 ppm)

Conclusion

From this study, it was concluded that HA extracted from peat soil could be used as removal agent in removing Ra-226 from Ra-contaminated soil sample and the removal efficiency depended on parameters such as contact time, concentration of HA, pH of HA and liquid/solid ratio. The relatively long contact time of 24 hours required to reach optimum removal efficiency indicated that Ra-226 was tightly bound to soil matrix. Diffusion phenomenon was used to describe the effect of concentration of HA. HA with concentration of 100 ppm resulted in optimum removal efficiency. At lower concentration, the removal efficiency was also lower and remained constant due to constant diffusion coefficient of HA molecules in dilute HA solutions. At higher concentration, the removal efficiency trend observed was due to retardation of mass transfer of Ra-226 – HA complexes. HA solutions of highly basic pH of 10 - 11 resulted in the highest removal efficiency followed by HA solutions of pH 7 - 9. Meanwhile, HA solutions of acidic pH showed the lowest removal efficiency of Ra-226. The trend observed could be due to increasing deprotonation of HA molecules as pH increased. Nevertheless, the removal efficiency could also be affected by Al present in the contaminated soil sample. For the purpose of this study, HA solutions of pH 7 were used throughout the study. As for liquid/solid ratio, the increase in ratio did not necessarily increase the removal efficiency especially when the soil requirement had been exceeded. In this study, at optimum contact time of 24 hours using HA solutions of optimum concentration 100 ppm and pH 7 with optimum liquid/solid ratio of 20 mL/g, the resulting removal efficiency of Ra-226 obtained was recorded as 22 %.

References

- 1. Frame, P. 2007. Radioluminescent paint. http://www.orau.org/ptp/collection/radioluminescent/radioluminescentinfo.htm.
- 2. Eisenbud, M. and Gesell, T. 1997. Environmental radioactivity. From natural, industrial and military sources. UK: Academic Press.
- EPA. 2004. Understanding variation in partition coefficient, K_d, values. Volume III: Review of geochemistry and available K_d values for americium, arsenic, curium, iodine, neptunium, radium, and technetium. EPA 402-R-04-002C. Washington: Unites States Environmental Protection Agency.
- 4. Koczorowska, E., Nieloch, M. and Slawinski, J. 2002. Model radioisotope experiments on the influence of acid rain on Zn-65 binding with humic acid. Nukleonika, 47(4): 167-172.
- 5. Bowen, H.J.M., Page, E., Valente, I. and Wade, R.J. 1979. Radio-tracer methods for studying speciation in natural waters. Journal of Radioanal. Chem., 48: 9-16.
- 6. Omar, M. and Bowen, H.J.M. 1982. Separation of methyltin species from inorganic tin, and their interactions with humates in natural waters. Journal of Radioanalytical & Nuclear Chemistry, 74(1-2): 273-282.
- Marquardt, C.M. 2000. Influence of humic acids on the migration behaviour of radioactive and non-radioactive substances under conditions close to nature. Final report BMBF Project No. 02E87958. Forschungszentrum Karlsruhe GmbH, Karlsruhe.
- Moulin, V. 2005. Complexation of radionuclides with humic substances. In. Perminova, I.V., Hatfield, K. and Hertkorn, N. (eds). Use of humic substances to remediate polluted environments: From theory to practice, pp. 155-173. The Netherlands: Springer.
- 9. Ibarra, J.V., Osacar, J. and Gavilain, G.M. 1977. Ann. Quim., 77: 224-229.
- 10. Bertha, E.L. and Choppin, G.R. 1978. Interaction of humic and fulvic acids with Eu(III) and Am(III). J. Inorg. Nucl. Chem. 40(4): 655-658.
- 11. Nash, K.L. and Choppin, G.R. 1980. Interaction of humic and fulvic acids with Th(IV). J. Inorg. Nucl. Chem., 42: 1045-
- 12. Shanbhag, P.M. and Choppin, G.R. 1981. Binding of uranyl by humic acid. J. Inorg. Nucl. Chem., 43: 3369-3372.
- 13. Torres, R.A. and Choppin, G.R. 1984. Europium(III) and americium(III) stability constants with humic acids. Radiochim. Acta, 35: 143-148.
- 14. Carlsen, L. 1985. Radionuclide soil organic matter interactions. European Appl.Res.Rept. Nucl.Sci.Technol., 6: 1419–1476.
- 15. Kim, J.I. and Sekine, T. 1991. Complexation of neptunium (V) with humic acids. Radiochim. Acta, 55: 187-192.
- Maes, A., De Brabandere, J. and Cremers, A. 1991. Complexation of Eu³⁺ and Am³⁺ with humic substances. Radiochim. Acta, 52-53: 41-47.
- 17. Stevenson, F.J. 1994. Humus chemistry: Genesis, composition, reactions. 2nd ed. New York: Wiley.
- 18. Takahashi, Y., Minai, Y., Meguro, Y., Toyoda, S. and Tominaga, T. 1994. Ionic strength and pH dependence of binding constants of Am(III)- and Eu(III)- humate. J. Radioanal. Nucl. Chem., 186: 129-141.
- 19. Samadfam, M., Niitsu, Y., Sato, S. and Ohashi, H. 1996. Complexation thermodynamics of Sr(II) and humic acid. Radiochim. Acta, 73: 211-216.
- 20. Niitsu, Y., Sato, S., Ohashi, H., Sakamoto, Y., Nagao, S., Ohnuki, T. And Muraoka, S. 1997. Effects of Humic Acid on the Sorption of Neptunium(V) on Kaolinite. J. Nucl. Mater., 248: 328-332.

Esther Phillip et al: OPTIMIZATION STUDY FOR REMOVAL OF RADIUM-226 FROM RADIUM-CONTAMINATED SOIL USING HUMIC ACID

- 21. Zachara, J.M., Smith, S.C. and Resch, C.T. 1994. Influence of humic substances on Co²⁺ sorption by a subsurface mineral separate and its mineralogic components. Geochim. Cosmochim. Acta, 58: 553-566.
- 22. Laili, Z., Yasir, M.S., Omar, M., Ibrahim, M.Z. and Phillip, E. 2010. Influence of humic acids on radium adsorption by coir pith in aqueous solution. Sains Malaysiana, 39(1): 99-106.
- 23. Choppin, G.R. 1988. Humics and radionuclide migration. Radiochim. Acta, 44-45: 23-28.
- 24. Samadfam, M., Jintoku, T., Sato, S. and Ohashi, H. 1998. Effect of pH on stability constants of Sr(II)-humate complexes. Journal of Nuclear Science and Technology, 35(8): 579-583.
- 25. Zou, Z., Qiu, R., Zhang, W., Dong, H., Zhao, Z., Zhang, T., Wei, X. and Cai, X. 2009. The study of operating variables in soil washing with EDTA. Environmental Pollution, 157: 229-236.
- 26. Landa, E.R. and Reid, D.F. 1982. Sorption of radium-226 from oil-production brine by sediments and soils. Environ Geol., 5: 1-8
- 27. Benes, P. and Strejc, P. 1986. Interaction of radium with freshwater sediments and their mineral components: IV. Wastewater and riverbed sediments. Journal of Radioanalytical and Nuclear Chemistry, 99: 407-422.
- 28. ATSDR. 1990. Toxicological profile for radium. http://www.atsdr.cdc.gov/toxprofiles/tp144.pdf.
- Smith, B. and Amonette, A. 2006. The environmental transport of radium and plutonium: A review. Maryland: Institute for Energy and Environmental Research.
- Wu, J. and Nofziger, D.L. 2001. Diffusion of solute in soil media. http://soilphysics.okstate.edu/software/Diffusion/document.pdf
- 31. Reed, B.E., Carriere, P.C. and Moore, R. 1996. Flushing of a Pb(II) contaminated soil using HCl, EDTA and CaCl₂. J. Environ. Eng., 121: 48-50.
- 32. Peters, W.R. 1999. Chelant extraction of heavy metals from contaminated soil. J. Hazard Mater., 66: 151-210.
- 33. Stevenson, F.J. and Vance, G.F. 1989. Naturally occurring aluminium-organic complexes. In: Sposito, G. (ed). The Environmental Chemistry of Aluminium, pp. 117-146. Boca Raton, Florida: CRC Press, Inc.
- 34. Fukushima, M., Tanaka, S., Nakamura, H. and Ito, S. 1996. Acid-base characterization of molecular weight fractionated humic acid. Talanta, 43: 383-390.
- 35. Avena, M.J. and Wilkinson, K.J. 2002. Disaggregation kinetics of a peat humic acid: Mechanism and pH effects. Environmental Science Technology, 36: 5100-5105.
- 36. Dempsey, B.A., Ganho, R.M. and O'Melia, C.R. 1984. The coagulation of humic substances by means of aluminium salts. J. Am. Water Works Assoc., 76(141).
- 37. Baeza, A., Fernandez, M., Herbanz, M., Legarda, F., Miro, C., and Salas, A. 2006. Removing uranium and radium from a natural water. Water, Air, and Soil Pollution, 173: 57-69.
- 38. Güngör, E.B.Ö. and Bekbölet, M. 2010. Zinc release by humic and fulvic acid as influenced by pH, complexation and DOC sorption. Geoderma, 159(1-2): 131-138.
- Spark, K.M., Wells, J.D. and Johnson, B.B. 1997. The interaction of humic acid with heavy metals. Australian Journal of Soil Research, 35: 89-101.
- 40. Ganter, C. 2007. Stabilization of soil organic matter by mineral surfaces. Term Paper in Biogeochemistry and Pollutant Dynamics, M.Sc. Environmental Sciences, ETH Zürich, 1-13.



DETERMINATION OF BENZO[a]PYRENE IN MALAYSIAN COMMERCIALIZED COFFEE POWDER USING SOLID PHASE EXTRACTION AND GAS CHROMATOGRAPHY

(Penentuan Benzo[a]pirena di dalam Serbuk Kopi di Pasaran Menggunakan Ekstraksi Fasa Pepejal dan Kromatografi Gas)

Noraini Kasim*, Rozita Osman, Nor'ashikin Saim, Licaberth Ismail

Faculty of Applied Sciences, Universiti Teknologi Mara, 40450 Shah Alam, Selangor, Malaysia.

*Corresponding author: norainikasim@salam.uitm.edu.my

Abstract

Roasting is a critical process in coffee production as it enables the development of flavor and aroma. Benzo[a]pyrene (BaP) is a nondesirable product of incomplete combustion at temperatures between 300 and 600 $^{\circ}$ C and may be produced during roasting step. In this study, selected samples of roasted coffee powder were analysed for BaP. Extraction of BaP was achieved using C₁₈ solid phase extraction (SPE) prior to analysis by gas chromatography. Calibration curve prepared with concentrations ranged between 3 – 50 ppm showed good linearity with r = 0.999. The limit of detection (LOD) was 0.25 ppm and the limit of quantification (LOQ) was 0.85 ppm. Recovery of BaP obtained from spiked sample (3 ppm) was 88.7 % with RSD (n=3) of 5.4 %. Benzo[a]pyrene was detected in all samples, at level ranging from 0.14 to 0.62 ppb .

Keywords: Benzo[a]pyrene, solid phase extraction, roasting, coffee

Abstrak

Memanggang adalah proses yang kritikal di dalam penghasilan kopi kerana ia membolehkan pembentukan rasa dan aroma. Benzo[a]pirena (BaP) adalah bahan sampingan yang terhasil daripada pembakaran tidak lengkap pada suhu antara 300 dan 600° C semasa proses pemanggangan. Dalam kajian ini, BaP dalam serbuk kopi terpilih telah dianalisa. Pengekstrakan dilakukan menggunakan ekstraksi fasa pepejal C_{18} dianalisis menggunakan gas kromatografi. Graf kalibrasi yang telah disediakan menggunakan kepekatan antara 3-50 ppm menghasilkan hubungan linear dengan r=0.999. Had pengesanan (LOD) BaP adalah 0.25 ppm dan had pengesanan kuantiti (LOQ) adalah 0.85 ppm. Perolehan semula BaP daripada sampel yang telah ditambahkan dengan BaP (3 ppm) adalah 88.7 % dengan RSD (n=3) 5.4 %. Benzo[a]pyrene telah dikesan di dalam semua sampel, pada tahap diantara 0.14 sehingga 0.62 ppb .

Kata kunci: Benzo[a]pirena, ekstraksi fasa pepejal, pemanggangan, kopi

Introduction

Roasting is a critical process in coffee production as it enables the development of flavor and aroma. At the same time, roasting may lead to the formation of nondesirable compounds, such as polycyclic aromatic hydrocarbons (PAHs) [1]. Contamination of PAHs by intense thermal processing occur due to generation by direct pyrolysis of food nutrients and, also due to direct deposition of PAHs from smoke of different thermal agents [2].

Toxicological investigation showed different carcinogenic potency for various PAHs mixtures [3,4]. Very mutagenic and carcinogenic is benzo[a]pyrene and it has been accepted as a marker of carcinogenic PAHs in food and environmental samples [5]. According to existing regulations by European Commission [6], the content of BaP in some foods and baby foods should not exceed 1 ppb.

Noraini Kasim et al: DETERMINATION OF BENZO[a]PYRENE IN MALAYSIAN COMMERCIALIZED COFFEE POWDER USING SOLID PHASE EXTRACTION AND GAS CHROMATOGRAPHY

In this paper, an analytical method for the BaP determination in coffee using solid phase extraction and gas chromatography was evaluated and the amount of BaP in various coffee samples was determined.

Experimental

Chemicals

Benzo[a]pyrene standard from Sigma-Aldrich (Steinheim, Germany) had a minimum of 97% purity. A stock solution of BaP 1000 ppm was prepared by dissolving BaP in deionized water from Milli-Q. The standard solutions were prepared by conveniently diluting the stock solution with deionized water from Milli-Q. Methanol and n-hexane were purchased from Merck (Darmstadt, Germany).

Sample Preparation

Seven local coffee brands were obtained from local stores. Each coffee sample was weighed (3g to 5g) depending on the particle size. The weighed coffee was dissolved with Milli-Q water in 100 mL volumetric flask. The solution may be filtered using a glass fibre filter if necessary.

Calibration Curve

Calibration curve was in the range of 3-50 ppm from the stock solution.

Solid Phase Extraction

Solid Phase Extraction was performed using Isolute C18 (EC), 1g cartridge (Biotage Europe). The SPE cartridges were conditioned successively using 6 mL methanol and 6 mL Milli-Q water. After sample loading, cartridge was vacuum dried for 1 hour. Then, 10 mL Milli-Q water was used to wash the cartridge and vacuum dried for 30 minutes. After elution using 6 mL hexane, the collected extract was evaporated and concentrated to 1 mL under a gentle stream of nitrogen.

Chromatographic procedure

All chromatographic measurements were done on an HP 6890 gas chromatograph (Agilent Technologies, Palo Alto, CA, USA) equipped with a Flame Ionization Detector (FID). GC procedure was carried out using (a) column coated with HP-5MS 5% Phenyl methyl siloxane, capillary size $30.0 \text{m} \times 250 \mu \text{m} \times 0.25 \mu \text{m}$ nominal, from Bios Analytique (France), (b) carrier gas N₂ with 15.34 psi and 23.2 mL min⁻¹, (c) 2 μ L of sample using splitless injection, (d) temperature programming started at 90°C, then increased to 250°C (18°C min⁻¹) and ended with 310°C (15° C min⁻¹) held for 7 minutes, and (e) time retention registered approximately 13.57 min (Figure 1).

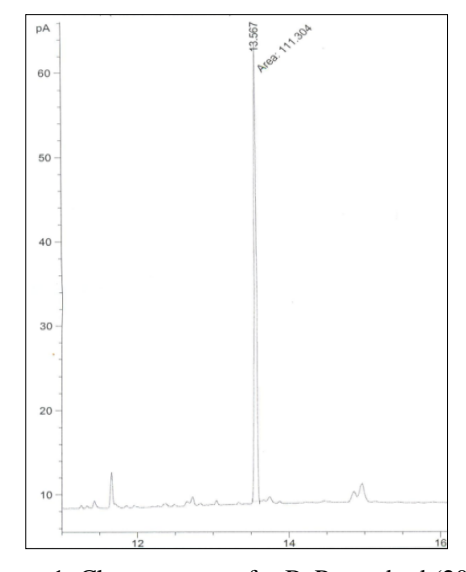


Figure 1: Chromatogram for BaP standard (20 ppm)

Results and Discussion

Method validation

For method validation, the parameters evaluated were linearity, limit of detection (LOD), limit of quantification (LOQ), % recovery and % relative standard deviation (RSD).

Linearity

The linearity of relative response (area versus concentration of standard) was evaluated. The calibration curves was evaluated in the range 3.0 - 50.0 ppm by injecting five standards in concentration range. The obtained linear regression equation for BaP standard was as follows: regression equation for the concentration of benzo[a]pyrene standard was $y = 6.2 \times 1.7$ for concentration at 3, 5, 10, 20 and 50 ppm. Good linearity with correlation coefficient of r = 0.9995 was obtained.

Limit of detection (LOD)

In this study, the LOD was estimated as the concentration that produced a peak height of three times the background noise (ratio of signal to noise = 3). The value of LOD estimated was 0.25 ppm.

Limit of quantification (LOQ)

The limit of quantification (LOQ) was calculated based on the sample concentration with a peak height of ten times the background noise (ratio of signal to noise = 10). The value for LOQ was 0.85 ppm.

Percent recovery and relative standard deviation in %

Good recovery (88.7 %) of benzo[a]pyrene from spike samples was obtained with relative standard deviation (RSD) of 5.4% using spiked samples of 3 ppm.

Analysis of coffee samples.

Figure 2 shows a chromatogram of a selected coffee extract. The amount of benzo[a]pyrene detected in coffee samples were in range of 0.14 to 0.62 ppb (Table 1). BaP detected in all samples are lower than the permissible limit (1 ppb) set by European Commission.

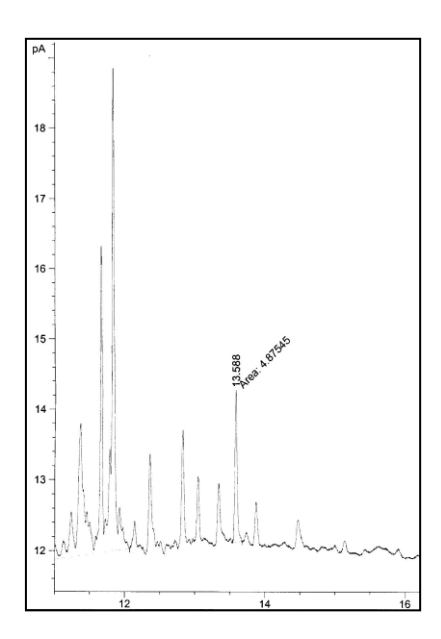


Figure 2. Chromatogram of a coffee extract

Table 1: Amount of BaP in coffee samples

Sample	Concentration of benzo[a]pyrene (ug/kg)
A	0.52 ± 0.07
В	0.29 ± 0.03
C	0.22 ± 0.01
D	0.62 ± 0.03
F	0.45 ± 0.06
G	0.14 ± 0.02
Н	0.50 ± 0.06

Conclusion

The amount of benzo[a]pyrene in all of the coffee samples analyzed is below the permissible limit set by the EU for foods and baby foods. However, since benzo[a]pyrene is considered a carcinogenic compound, monitoring the amount of this compound in a popular drink such as coffee is crucial. Thus, a simple and reliable method discussed in this study may provide a significant contribution in assessing the dietary exposure of consumers to carcinogens.

Acknowledgement

The authors would like to acknowledge the Universiti Teknologi Mara for financial support (600-RMI/ST/DANA 5/3/Dst (222/2009)).

References

- 1. Oosterveld, A., Voragen, A.G.J., Schols, H.A., 2003. Effect of roasting on the carbohytrate composition of *Coffea arabica* beans. Carbohytrates Polymers 54, 183-192.
- Santino, O., Viviana, P.C., Loredana, C., 2009. Polycyclic aromatic hydrocarbons (PAHs) in coffee brew samples: Analytical method by GC-MS, profile, levels and sources. Food and Chemical Toxicology 47, 819-826.
- 3. Collin, J.F., Brown, J.P., Alexeef, G.V., Salmon, A.G., 1998. Potency equivalency factors for some polycyclic aromatic hydrocarbons and polycyclic aromatic hydrocarbon derivatives. Regulatory Toxicology and Pharmacology, 45-54.
- 4. Delistraty, D., 1998. A critical review of the application of toxic equivalency factors to carcinogenic effects of polycyclic aromatic hydrocarbons in mammals, environmental chemistry of PAHs, PAH and related compunds. In: John, A. (Ed). The Handbook of Environmental Chemistry, vol. 3-1. Alasdair H. Neilson-Springer-Verlag, Berlin, 311-359.
- 5. Hatterman-Frey, H.A., Travis, C.C., 1991. Benzo[a]pyrene: environmental partitioning and human exposure. Toxicology and Industrial Health 7, 141-157.
- 6. Commission Regulation 2006/1881/EC European Commission , 2006. Setting maximum levels for certain contaminations in foodstuffs, Brussels.



A STUDY ON THE MIGRATION OF STYRENE FROM POLYSTYRENE CUPS TO DRINKS USING ONLINE SOLID-PHASE EXTRACTION LIQUID CHROMATOGRAPHY (SPE-LC)

(Kajian Mengenai Migrasi Stirena daripada Cawan Polistirena kepada Minuman Menggunakan Teknik Ekstraksi Fasa Pepejal Kromatografi Cecair (SPE-LC))

Norashikin Saim, Rozita Osman^{*}, Hurin Ain Wan Abi Sabian, Mohamad Rafaie Mohamed Zubir, Nazarudin Ibrahim

Faculty of Applied Sciences, Universiti Teknologi MARA, 40450, Shah Alam, Selangor

*Corresponding author: rozit471@salam.uitm.edu.my

Abstract

The migration of residual styrene from polystyrene cups to drinks has been a major concern in recent years worldwide. In this study, a three-factor response surface experimental design was used to evaluate the interactive effects of temperature (30-80 °C), pH (5-7) and contact time (35-120 min) on the migration of styrene from polystyrene cups into water. Online solid-phase extraction liquid chromatography (SPE-LC) with diode array detector (DAD) was used for the separation and detection of styrene. Initial temperature of water was found significant in increasing the rate of migration of styrene whereas the effect of contact time was less significant. In terms of interactions between the effects, the relation between temperature and pH was the most significant. The amount of styrene in water varied from 0.3 to 4.2 μ g/L with maximum migration obtained at initial water temperature of 80 °C and pH 5.

Keywords: migration of styrene, experimental design, polystyrene cups

Abstrak

Migrasi residu stirena daripada cawan polistirena ke minuman menjadi kebimbangan utama di seluruh dunia sejak kebelakangan ini. Dalam kajian ini, rekabentuk eksperimen menggunakan kaedah respon permukaan 3-faktor digunakan untuk menilai interaksi di antara suhu (30-80 °C), pH (5-7) dan tempoh sentuhan (35-120 min) ke atas migrasi stirena daripada cawan polistirena kepada air. Pengekstrakan fasa pepejal dan analisis dijalankan selari menggunakan teknik kromatografi cecair (SPE-LC) dengan alat pengesan foto diod (DAD). Suhu awal air merupakan faktor yang paling signifikan bagi peningkatan kadar migrasi stirena berbanding kesan masa sentuhan air dengan cawan polistirena. Daripada segi interaksi di antara faktor, hubungkait di antara suhu dan pH adalah paling signifikan. Amaun stirena yang dikesan di dalam air berubah daripada 0.3 ke 4.2 μg L⁻¹ dengan migrasi tertinggi didapati pada suhu 80 °C and pH 5.

Kata kunci: migrasi stirena, rekabentuk eksperimen, cawan polistirena

Introduction

Styrene monomer is one of the most widely used foods packaged contact polymers. Several adverse health effects are attributed to styrene [1,2,3,4]. Styrene is considered a possible human carcinogen by the World Health Organization International Agency for Research on Cancer. Evidence already shows that styrene causes cancer in animals. The migration of styrene monomers from polystyrene containers into foods has been extensively studied [5,6]. Previous study showed that the migration of styrene from a polystyrene cup containing cold or hot beverages has been observed to be as high as 0.025% of the total styrene for a single use [7]. Fat content, temperature, and contact time were the common parameters studied in predicting the potential exposure of consumers to styrene. Study conducted by Till et al. [8] found that increases in temperatures used in polymer processing may cause degradation and migration of polymers in food products. In this study, the effect of temperature, pH and contact

Norashikin Saim et al: A STUDY ON THE MIGRATION OF STYRENE FROM POLYSTYRENE CUPS TO DRINKS USING ONLINE SOLID-PHASE EXTRACTION LIQUID CHROMATOGRAPHY (SPE-LC)

times on migration of styrene from polystyrene cups to drinks were evaluated using an experimental design approach (Design Expert 6.0.4). This approach allows all three parameters to be investigated individually, as squared terms, and to consider two-component interaction effects. The separation of styrene achieved using an online solid-phase extraction liquid chromatography (SPE-LC) approach enabled direct injection of samples resulted in faster analysis and good reproducibility.

Experimental

Chemicals and Reagents

HPLC Grade methanol and acetonitrile were purchased from Merck (Darmstadt, Germany). Methanesulfonic acid (MSA) and styrene standard were bought from Fluka and Sigma-Aldrich (Steinheim, Germany), respectively. Ethyl acetate and ammonia solution 25% were purchased from System (ChemAR). Acetic acid was bought from R & M chemical (Essex, United Kingdom).

Preparation of styrene standard solutions

Styrene standard stock solution of 1000 mg L⁻¹ was prepared by dissolving 0.2778 ± 0.01 mL of styrene standard in methanol. The standard solution was mixed thoroughly in 250 mL volumetric flask. The quantitative analysis of styrene was achieved using a 5-point calibration curve.

Sample preparation

Polystyrene cup samples were purchased from local market. Deionized water was used and the pH was adjusted using acetic acid for acidic conditions and ammonia solution 25% for basic conditions. The initial temperature of each sample (100 mL) was adjusted and directly transferred into the polystyrene cup.

Online SPE-LC analysis

Dionex Ultimate 3000 Online SPE-LC instrument was used for styrene separation and detection. The major components of this instrument involved online SPE column, C_{16} Acclaim Polar Advantage, $5\mu m$ 120 Å (4.6 m x 50 mm), C_{18} analytical column C_{18} Acclaim Polar Advantage II, $5\mu m$ 120 Å (4.6m x 150 mm), two pumping systems, auto-sampler and photo diode array detector. The prepared styrene standards and polystyrene cup samples of large volume (3.5 mL) were loaded directly onto the system, and delivered to the SPE column for enrichment, followed by interferences washed out. Then, the SPE column is switched into the analytical column for analyte separation. The analytical column for separation is equilibrated with the second pump at the same time. The solvents system used were a mixture of ultra-purified water and 10 mM methanesulfonic acid (MSA), acetonitrile (ACN), and ethyl acetate. Table 1 shows the gradient for online SPE using the loading pump while Table 2 the gradient for separation using an analysis pump. The wavelength range used for detection of styrene by photo diode array detector in the range 214 - 282 nm, then styrene was detected at wavelength of 248 nm.

Table 1: Gradient Program for Online SPE

Time	Flow rate	Solvent A	Solvent B,	Solvent C	Curve
(min)	(mL/min)	$H_2O + 10mM MSA$, (%	ACN, (% vol.)	Ethyl Acetate, (% vol.)	
		vol.)			
0.0	1.0	95.0	5.0	0.0	
3.5	1.0	95.0	5.0	0.0	5
6.5	1.0	70.0	30.0	0.0	5
6.5	1.0	0.0	100.0	0.0	5
7.5	1.0	0.0	100.0	0.0	5
7.5	1.0	0.0	0.0	100.0	5
9.0	1.0	0.0	0.0	100.0	5

Time Flow rate Solvent A Solvent B. Solvent C Curve (mL/min) H₂O (% vol.) ACN, (% vol.) Ethyl Acetate, (% vol.) (min) 0.0 1.0 70.0 30.0 0.0 0.0 1.0 70.0 30.0 0.0 5 7 14.0 1.0 5.0 95.0 0.0 21.0 1.0 0.0 100.0 0.0 5 22.0 1.0 0.0 0.0 100.0 5 24.0 1.0 5 0.0 0.0100.0 7 24.0 1.0 0.0 100.0 0.0 0.0 0.0 7 25.0 1.0 100.0 7 27.0 1.0 70.0 30.0 0.0 28.0 1.0 70.0 30.0 0.0 7

Table 2: Gradient Program for Separation (Analytical Column)

Experimental Design Approach

The effect of three independent variables at five levels, t; contact time (t:35–120 minutes) temperature (T: 30 – 80 °C), and pH (p: 5 – 7). Each of the variables had levels set at five coded levels: $-\alpha$, -1, 0, +1, and $+\alpha$ (Table 2), requiring 20 experiments in total (Table 3). Experiments were randomised in order to minimize the effect of unexplained variability in the actual responses due to extraneous factors. The centre point was repeated 6 times to calculate the repeatability of the method [9].

Table 3: Central composite design used for the analysis of styrene in drinks

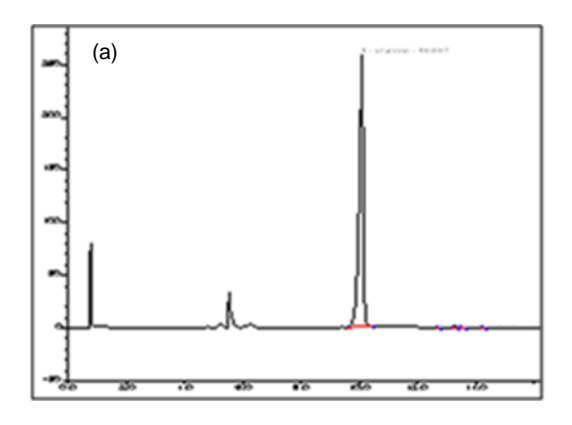
	t: contact time (min)	T: Temperature	p:pH
-α	6	13	4
- 1	35	30	5
0	78	55	6
1	120	80	7
$+\alpha$	149	97	8

Results and Discussion

Online Solid Phase Extraction-Liquid Chromatogrophy (SPE-LC) analysis

Optimization of the online SPE-LC conditions indicated that a mixture of acetonitrile, ultra-purified water, 10 mM methanesulfonic acid (MSA) and ethyl acetate were the mobile phases for conditioning the extraction column, washing the impurities, and elution of styrene. Using large volume injection of 3.5 mL, styrene in water was simultaneously concentrated and separated. Styrene was detected at wavelength of 248 nm using UV-DAD detector based on the comparison of its retention times (10.1 min) and UV-Vis absorption (Figure 1a and 1b). Calibration linearity for the determination of styrene was investigated by making replicate injections of styrene standards at four different concentrations. The calibration curve was found linear in the range of $0.01 \text{ to } 1.00 \text{ } \mu\text{g mL}^{-1}$ with correlation coefficients, r = 0.9992.

Norashikin Saim et al: A STUDY ON THE MIGRATION OF STYRENE FROM POLYSTYRENE CUPS TO DRINKS USING ONLINE SOLID-PHASE EXTRACTION LIQUID CHROMATOGRAPHY (SPE-LC)



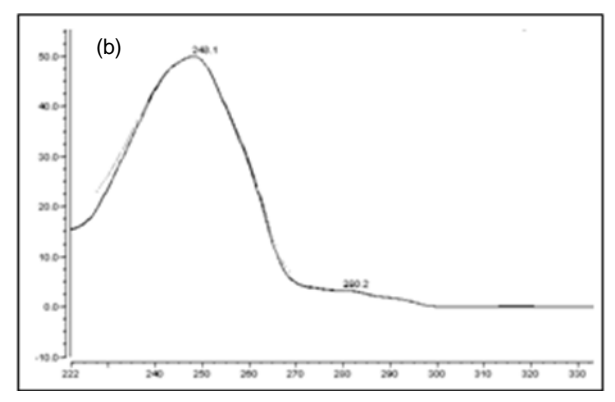


Figure 1: Chromatogram of styrene (a) and UV-Vis spectrum of styrene (b)

Experimental Design Approach

The results based on the amount of styrene recovered are tabulated in Table 3. High amount of styrene migration was observed at high initial temperature and in acidic condition. Multilinear regression was applied to the results of the central composite design (CCD). The effect of independent variables; time (t), temperature (T) and pH (p) and interactive effect (interaction between pairs of variables) on the migration of styrene were evaluated by second order (quadratic) (Table 4). The adequacy of the models were determined using model analysis, lack of fit test and coefficient of determination (\mathbb{R}^2). The significance of the equation parameters for each response variable was also assessed by F-ratio at a probability (p) of 0.05. The closer the value of \mathbb{R}^2 to unity, the better the empirical model fits the actual data. Criteria for a good fit of a model, the \mathbb{R}^2 should be at least 0.80 [10]. In this study, the \mathbb{R}^2 was 0.8923. The high value of \mathbb{R}^2 (> 0.80) indicates the adequacy of the applied quadratic model.

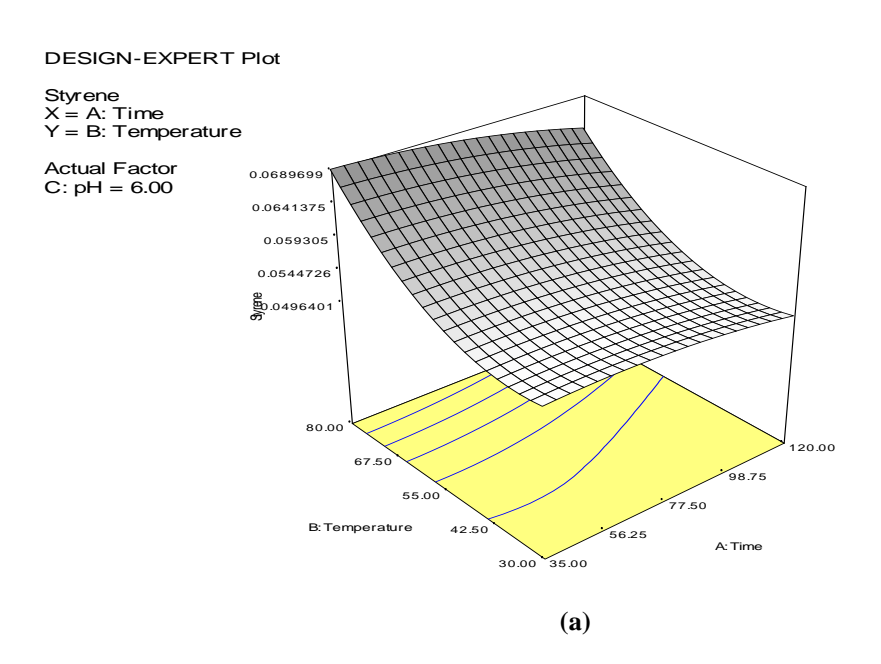
Table 4: Central Composite Design (CCD) and the amount of styrene detected

Experiment no.	Contact time	Temperature	pН	Amount of
	(min)	(°C)		Styrene (µg L ⁻¹)
1	35	30	5	2.2
2	35	80	7	3.4
3	120	80	5	3.9
4	78	55	6	2.6
5	120	30	7	2.7
6	78	55	6	2.7
7	120	30	5	2.8
8	78	55	6	2.8
9	35	80	5	4.2
10	78	55	6	3.1
11	120	80	7	3.1
12	35	30	7	1.2
13	78	97	6	3.7
14	78	55	6	0.3
15	78	55	4	2.5
16	78	55	6	2.4
17	78	13	6	2.6
18	6	55	6	2.4
19	78	55	8	2.4
20	149	55	6	2.1

Table 5: Multilinear Regression Results for analysis of styrene in drinks

Variable	p value
t	0.2177
T	0.0006
p	0.4970
t^2	0.4458
\overline{T}^2	0.0046
p^2	0.7230
tT	0.7182
tp	0.0831
Tp	0.0058

Evaluation on each factor individually, showed that the migration of styrene was strongly dependent upon initial temperature of water as shown in Table 5 (p<0.05). The results concurred with the previous studies [5,7]. The influence of other individual factors such as contact time and pH was not significant. However, based on the evaluation between two factors revealed that the interaction between initial temperature and pH gave a significant impact on the migration of styrene with the p value less than 0.05 (p=0.0058) (Table 4). Figure 1a shows that increase in initial water temperature resulted in an increased amount of styrene. The effect of the interaction between initial water temperature and pH is shown in Figure 1b. In acidic condition (pH 5), the migration of styrene increased significantly with temperature.



Norashikin Saim et al: A STUDY ON THE MIGRATION OF STYRENE FROM POLYSTYRENE CUPS TO DRINKS USING ONLINE SOLID-PHASE EXTRACTION LIQUID CHROMATOGRAPHY (SPE-LC)

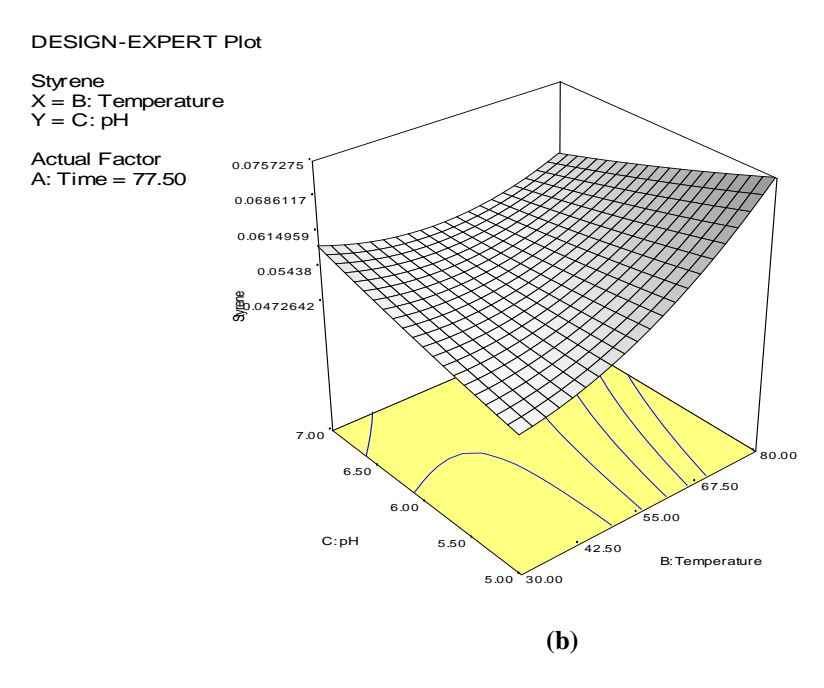


Figure 1: Contour and response surface plot (a) time against temperature, (b) temperature against pH for the migration of styrene using Central Composite Design

Conclusion

The online SPE-LC was able to determine the migration of styrene from polystyrene cups to water with minimum sample preparation as the sample concentration and separation steps were achieved on-line using two columns. Based on individual independant variable, only initial temperature was significant whereby higher migration was observed at high initial water temperature. However, using experimental design approach, the interactions between the variables were also considered. The results showed that the interaction of initial water temperature and pH was also significant and highest migration of styrene was observed at high temperature (80 °C) and in acidic condition (pH 5.0). This study showed the advantage of experimental design approach compared to conventional approach (changing one variable at a time) in studying the effect of several variables with minimal number of experiments.

Acknowledgement

The authors would like to acknowledge the financial support obtained from Ministry of Higher Education (MOHE), Malaysia for this project (Project number: 600-RMI/ST/FRGS/5.3.Fst/6/2010) and Universiti Teknologi MARA.

References

- 1. Varner, S. L., and Breder, A. (1981). C.V. Headspace sampling and gas chromatographic determination of styrene migration from food-contact polystyrene cups into beverage and food simulants. *J. Ass. Offic. Anal. Chem. Int.* 64:1122–1130.
- 2. Varner, S. L., Breder, C. V., and Fazio, T. (1983). Determination of styrene migration from food-contact polymers into margarine, using Azeotropic distillation and head space gas chromatography. *J. Ass. Offic. Anal. Chem. Int.* 66:1067–1073.
- 3. Muratak, A., Avakis, S., and Yokoyama, K. (1991). Assessment of the peripheral, central and autonomic nervous system function in styrene workers. *Am. J. Index Medicus* 20:775–784.

- 4. Cohen, T., Carlson, G., Charnley, G., Coggon, D., Delzell, E., and Graham, J. D. (2002). A comprehensive evaluation of the potential health risks associated with occupational and environmental exposure to styrene. *J. Toxicol. Env. Health B* 5:1–263.
- 5. Khaksar, M.R and Ghazi-Khansari M (2009). Determination of migration monomer styrene from GPPS (general purpose polystyrene) and HIPS (high impact polystyrene) cups to hot drinks. *Toxicology Mechanisms and Methods*; 19(3): 257–261.
- 6. Arvanitoyannis, I. S., and Bosena, L. (2004). Migration of substances from packaging materials to foods. Crit. Rev. Food Nutr. 44:63–76.
- 7. Tawfik, M.S. and Huyghebaert, A (1998). Polystyrene cups and containers: styrene migration. *Food Addit. Contam.* 15(5), 592-599.
- 8. Till, D. E., Ehntholt, D. J., Reid, R. C., Schwartz, P. S., Schwopc, A. D., Sidman, R. R., and Whelan, R. H. (1982). Migration of styrene monomer from crystal polystyrene to food and food simulating liquid. *Ind. Eng. Chem. Prod. Res. Dev.* 21:161–185.
- 9. Mirhosseini, H., Tan, C. P., Hamid, N. S. A., & Yusof, S. (2008). Optimization of the contents of Arabic gum, xanthan gum and orange oil affecting turbidity, average particle size, polydispersity index and density in orange beverage emulsion. *Food Hydrocolloids* 22, 1212-1223.
- 10. Joglekar, A. M., & May, A. T. (1987). Product excellent through design of experiments. *Cereal Foods World*, 32, 857-868.



SYNTHESIS, CHARACTERISATION AND ANTIBACTERIAL STUDIES OF Cu(II) COMPLEXES THIOUREA

(Sintesis, Pencirian dan Kajian Aktiviti Antibakteria Kompleks Cu(II) Tiourea)

Nur Illane Mohamad Halim^{1*}, Karimah Kassim¹, Adibatul Husna Fadzil¹, Bohari M. Yamin²

¹Faculty of Applied Sciences, Universiti Teknologi MARA, 40450 Shah Alam, Selangor, Malaysia ²School of Chemical Sciences and Food Technology, Faculty of Science and Technology, Universiti Kebangsaan Malaysia, 43650 UKM Bangi, Selangor, Malaysia

*Corresponding author: m.hnurillane@yahoo.com

Abstract

A series of bisthiourea ligands, 1,2-bis(N'-2-methoxybenzoylthioureido)-4-chlorobenzene (**TII**), 1,2-bis(N'-3-methoxybenzoylthioureido)-4-chlorobenzene (**TIII**) and 1,2-bis(N'-4-methoxybenzoylthioureido)-4-chlorobenzene (**TIII**) and their Cu(II) complexes have been successfully synthesised. The products have been characterised by elemental analysis (CHNS), IR spectroscopy, ${}^{1}H$ and ${}^{13}C$ Nuclear Magnetic Resonance (NMR), melting point and magnetic susceptibility determination method. The values of $\mu_{\rm eff}$ (B.M) for Cu(II) complexes in the range of 1.23-2.21 B.M reveal that the complexes are square planar geometry. The thiourea ligands along with their respective Cu(II) complexes were screened for their antibacterial activity using disc diffusion method against four strains of bacteria (*Bacillus subtillis, Pseudomonas aeruginosa, Escherichia coli and Staphylococcus aureus*). Interestingly, compound TIII, Cu(TII) and Cu(TIII) showed the activity against *Staphylococcus aureus*. The antibacterial activity of their metal complexes is higher than the ligands.

Keywords: Bisthiourea, spectroscopy, antibacterial activity

Abstrak

Siri ligan bistiourea, 1,2-bis(N'-2-metoksibenzoiltioureido)-4-klorobenzena (**TII**), 1,2-bis(N'-3- metoksibenzoiltioureido)-4-klorobenzena (**TIII**) and 1,2-bis(N'-4- metoksibenzoiltioureido)-4-klorobenzena (**TIII**) dan komplek Cu(II) telah berjaya disintesis. Sebatian dicirikan melalui analisis unsur (CHNS), spektroskopi infra merah (IR), 1 H and 13 C resonans magnet nucleus (NMR), takat lebur dan penetapan suseptibiliti magnet. Nilai $\mu_{\rm eff}$ (B.M) untuk kompleks Cu(II) berada pada julat 1.23-2.21 B.M menunjukkan bahawa kompleks ini mempunyai geometri satah persegi empat. Kajian aktiviti antibakteria telah dilakukan ke atas terbitan tiourea dan kompleksnya dengan menggunakan ujian disk resapan menentang empat strain bakteria (*Bacillus subtillis, Pseudomonas aeruginosa, Escherichia coli and Staphylococcus aureus*). Menariknya, sebatian TIII, Cu(II) dan Cu(III) menunjukkan aktiviti terhadap bacteria *Staphylococcus aureus*. Kajian aktiviti antibakteria kompleks logam adalah lebih tinggi daripada ligan.

Kata kunci: Bistiourea, spektroskopi, aktiviti antibakteria

Introduction

Thiourea ligands and their metal complexes exhibit a wide range of biological activity including anticancer [1], antimicrobial [1-3], antibacterial [4], antifungal [5], antimalarial [6] and antituberculosis [7]. There have been many researches of benzoyl-substituted thioureas and related ligands coordinated to metals where the ligand usually coordinated through S and O, giving a six membered ring system [3-5]. They are able to coordinate to arrange metal centres as neutral ligands or as anionic ligands [8,9]. As some reports demonstrated that the antibacterial activity of some compounds becomes enhanced when they are complexed with copper [4]. Only a few of aromatic diamine being reported such as 1,2-Bis[N'-(2,2-dimethylpropionyl)thioureido]cyclohexane [10], and 1,2-bis(N'-2-methoxybenzoylthioureido)-4-nitrobenzene [11].

In this study, we report herein the synthesis, characterization and antibacterial studies a sum of bisthiourea, namely, 1,2-bis(N'-2-methoxybenzoylthioureido)-4-chlorobenzene (**TI**), 1,2-bis(N'-3-methoxybenzoylthioureido)-4-chlorobenzene (**TIII**), as shown in Figure 1 and their Cu(II) complexes. Basically, there are isomers consisting of chlorobenzene as the bridging group between two substituted benzoyl chloride. The only different is the position of methoxy group. The structures of the ligands and their complexes have been characterized by elemental analysis (CHNS), IR spectroscopy, 1 H and 13 C Nuclear Magnetic Resonance (NMR), melting point and magnetic susceptibility determination method.

Figure 1: The molecular structures of the 1,2-bis(*N*'-2-methoxybenzoylthioureido)-4-chlorobenzene (**TI**), 1,2-bis(*N*'-3-methoxybenzoylthioureido)-4-chlorobenzene (**TII**) and 1,2-bis(*N*'-4-methoxybenzoylthioureido)-4-chlorobenzene (**TIII**)

Experimental

Physical measurements

Every part of reactions was performed under an ambient atmosphere and no special precautions were taken to exclude air or moisture. Chemicals and solvents were purchased from Sigma Aldrich or MERCK and used as received without further purification. Melting points were measured using BÜCHI Melting Point B-545 and magnetic susceptibility of compounds was measured on Sherwood Auto Magnetic susceptibility balance. Infrared spectra were obtained using FTIR Perkin Elmer 100 Spectrophotometer in the spectral range of 4000-350 cm⁻¹. ¹H and ¹³C NMR spectra were recorded using Bruker Avance III 300 Spectrometer at room temperature. The elemental analyses were conducted using CHNS Analyzer Flash EA 1112 series.

Synthesis of the ligands

Freshly prepared substituted benzoyl chloride (0.013 mol) was added drop wise to a stirring acetone solution (20 ml) of ammonium thiocyanate (0.013 mol). The solution mixture was stirred about 20 minutes. A solution of 4-chloro-1,2-phenylenediamine (0.0065 mol) in acetone was added and the reaction solution was heated under reflux for 3 hours. The solution was poured into a beaker containing some ice cubes. The resulting precipitate was collected by filtration, washed several times with cold ethanol/water and purified by recrystallisation from ethanol/dichloromethane mixture (1:1).

1,2-bis(*N*'-2-methoxybenzoylthioureido)-4-chlorobenzene, (*TI*): Yield 59.1%; Dark brown solid, m.p 192.7 °C. IR (KBr pellet, cm⁻¹): ν (C=O) 1668.90, ν (N-H) 3320.72, ν (C-N) 1249.18, ν (C=S) 854.76. ¹H NMR (CDCI₃- d_6 , 300.13

MHz): δ 4.06 (s, 3H, OMe); 7.02 to 8.11 (m, Ar-H); 11.19 (d, H, CONH); 12.48, 12.63 (s, H, CSNH). ¹³H NMR (CDCI₃) δ 56.50 (CH₃); 180.16, 180.65 (C=S); 164.92 (C=O); 111.77 – 157.89 (aromatic ring). *Anal.* Calc. For C₂₄H₂₁ClN₄0₄S₇: C, 54.49; H, 4.00; N, 10.59; S, 12.12. Found: C, 55.22; H, 4.89; N, 9.91; S, 8.70.

1,2-bis(N'-3-methoxybenzoylthioureido)-4-chlorobenzene (TII): Yield 64.0%; Yellowish solid, m.p 203.9 °C. IR (KBr pellet, cm⁻¹): ν (C=O) 1674.82, ν (N-H) 3322.14, ν (C-N) 1273.74, ν (C=S) 853.17. ¹H NMR (CDCI₃- d_6 , 300.13 MHz): δ 3.75 (s, 3H, OMe); 7.16 to 8.19 (m, Ar-H); 11.80 (d, H, CONH); 12.45, 12.64 (s, H, CSNH). ¹³H NMR (CDCI₃) δ 55.77 (CH₃); 180.70, 181.20 (C=S); 168.53 (C=O); 113.59 – 159.43 (aromatic ring). Anal. Calc. For $C_{24}H_{21}ClN_40_4S_2$: C, 54.49; H, 4.00; N, 10.59; S, 12.12. Found: C, 54.23; H, 4.01; N, 10.49; S, 12.16.

1,2-bis(*N'-4-methoxybenzoylthioureido*)-*4-chlorobenzene*, (*THI*): Yield 69%; Reddish brown solid, m.p 203.0 °C. IR (KBr pellet, cm⁻¹): ν (C=O) 1654.14, ν (N-H) 3286.16, ν (C-N) 1262.71, ν (C=S) 843.40. ¹H NMR (CDCI₃- d_6 , 300.13 MHz): δ 3.82 (s, 3H, OMe); 6.97-8.14 (m, Ar-H); 11.59 (d, H, CONH); 12.49, 12.69 (s, H, CSNH). ¹³H NMR (CDCI₃) δ 56.50 (CH₃); 180.86, 180.36 (C=S); 167.99 (C=O); 114.20 – 163.74 (aromatic ring). *Anal.* Calc. For C₂₄H₂₁ClN₄0₄S₂: C, 54.49; H, 4.00; N, 10.59; S, 12.12. Found: C, 55.73; H, 4.05; N, 10.50; S, 6.71.

Synthesis of [Cu(TI)]

The complexes were prepared by the template method. A solution of the copper(II) acetate (0.0005 mol) in 20 ml EtOH was added drop wise to a solution of the 1,2-bis(N'-2-methoxybenzoylthioureido)-4-chlorobenzene, (I) (0.0003 mol) in DCM (40 ml). The resulting mixture was refluxed for about 6 hours. The resulting precipitate complexes was collected, filtered, and recrystallized from ethanol/dichloromethane mixture (1:1). Yield 80%; Green solid, m.p 173.6 °C. IR (KBr pellet, cm⁻¹): ν (C=O) 1609.79, ν (N-H) 3304.34, ν (C-N) 1247.34. *Anal.* Calc. For $C_{24}H_{21}ClCuN_40_4S_2$: C, 48.64; H, 3.57; N, 9.45; S, 10.82. Found: C, 47.84; H, 3.06; N, 9.36; S, 6.24.

Synthesis of [Cu(TII)]

The complexes were prepared by the template method. A solution of the copper(II) acetate (0.0005 mol) in 20 ml EtOH was added drop wise to a solution of the 1,2-bis(N'-3-methoxybenzoylthioureido)-4-chlorobenzene, (I) (0.0003 mol) in DCM (40 ml). The resulting mixture was refluxed for about 6 hours. The resulting precipitate complexes was collected, filtered, and recrystallized from ethanol/dichloromethane mixture (1:1). Yield 93%; Dark green solid, m.p 169.0 °C. IR (KBr pellet, cm⁻¹): v(C=O) 1650.98, v(N-H) 3320.96, v(C-N) 1273.79. *Anal.* Calc. For $C_{24}H_{21}ClCuN_4O_4S_2$: $C_{24}H_{21}ClCuN_4O_4S_3$: $C_{34}H_{21}ClCuN_4O_4S_3$: $C_{34}H_{21}ClCu$

Synthesis of [Cu(TIII)]

The complexes were prepared by the template method. A solution of the copper(II) acetate (0.0005 mol) in 20 ml EtOH was added drop wise to a solution of the 1,2-bis(N'-4-methoxybenzoylthioureido)-4-chlorobenzene, (I) (0.0003 mol) in DCM (40 ml). The resulting mixture was refluxed for about 6 hours. The resulting precipitate complexes was collected, filtered, and recrystallized from ethanol/dichloromethane mixture (1:1). Yield 64%; Green solid, m.p 343.0 °C. IR (KBr pellet, cm $^{-1}$): v(C=O) 1663.98, v(N-H) 3269.62, v(C-N) 1259.10. *Anal.* Calc. For $C_{24}H_{21}ClCuN_40_4S_2$: C, 48.64; H, 3.57; N, 9.45; S, 10.82. Found: C, 45.63; H, 3.23; N, 8.78; S, 9.76.

Antibacterial screening

All of the synthesized compounds were screened for their antibacterial activity using disc diffusion method against four strains of bacteria (*Bacillus subtillis*, *Pseudomonas aeruginosa*, *Escherichia coli*, *and Staphylococcus aureus*). Streptomycin (400 µg mL⁻¹) was used as positive control and DMSO as negative control. These bacteria was cultured in nutrient broth and left for 24 hours to grow. After that, the nutrient broth was added to the sterilized medium before solidification. Then, the media with bacteria was poured into sterilized Petri dishes under aseptic condition. The thiourea ligands along with their respective Cu(II) complexes were dissolved in DMSO solvent at 10mg mL⁻¹ and were impregnated on blank disc. The impregnated disc was placed on the surface of the culture and it then incubated at 37°C for 48 hours. After incubation, the average of the inhibition zones was measured and compared with positive control. The bactericidal tests were performing in triplicate and results are shown in Table 4.

Results and Discussion

Chemical analysis

The microelemental analysis data of the product shows the relevant frequencies with the expected thioureas and their complexes (Table I). The melting point of the ligands were found between 192°C - 203°C and for the Cu(II) complexes between 169°C - 343°C.

Compound	Color	M.P (°C)	Elemental analysis data found (calculated) (%)			
	Color		C(%)	H(%)	N(%)	S(%)
TI	Dark brown	192.7	55.22 (54.49)	4.89 (4.00)	9.91 (10.59)	8.70 (12.12)
TII	Yellow	203.9	54.23 (54.49)	4.01 (4.00)	10.49 (10.59)	12.16 (12.12)
TIII	Reddish brown	203.0	55.73 (54.49)	4.05 (4.00)	10.50 (10.59)	6.71 (12.12)
Cu(TI)	Green	173.6	48.15 (49.05)	3.18 (3.60)	9.32 (9.53)	8.65 (10.91)
Cu(TII)	Dark Green	169.0	48.25 (49.05)	3.19 (3.60)	9.33 (9.53)	9.79 (10.91)
Cu(TIII)	Green	343.0	47.31 (49.05)	3.14 (3.60)	9.00 (9.53)	8.44 (10.91)

Table 1: Microelemental analysis data of the thiourea ligands and its complexes

Spectroscopic studies

The characteristic IR bands of all thiourea ligands showed the expected frequencies of $\upsilon(C=O)$, $\upsilon(N-H)$, $\upsilon(C-N)$ and $\upsilon(C=S)$ at 1654–1668 cm⁻¹, 3286-3322 cm⁻¹, 1249-1273 cm⁻¹ and 843-854 cm⁻¹, respectively. After complexation, the $\upsilon(C=O)$ band are shifted to lower frequencies suggesting coordination of the metal. The $\upsilon(C=S)$ band are expected shifted to higher frequency, but this vibration could not be assigned clearly due to appearance of broad peaks.

Peaks	TI	Cu(T1)	TII	Cu(TII)	TIII	Cu(TIII)
υ(N-H)	3320.72	3304.34	3322.14	3320.96	3286.16	3269.62
υ(C=O)	1668.90	1609.79	1674.82	1650.98	1654.14	1606.71
υ(C-N)	1249.18	1247.34	1273.73	1273.79	1262.71	1259.10
υ(C=S)	854.76	Broad	853.17	Broad	843.40	Broad

Table 2: Data of Infrared Spectroscopy

The ¹H and ¹³C NMR chemical shifts of the thiourea ligands are quite similar. ¹H NMR data demonstrate the existence of methoxy proton between 3.75-4.05 ppm and aromatic proton in the range 6.97 to 8.19 ppm. The amine protons appear dublet between 11.18 to 11.80 ppm suggesting that the ligands are not planar. There are two signals for thioamide group proton between 12.4 and 12.6 also reflex of non planarity of the ligands. The ¹³C NMR spectra show that the chemical shifts of the carbon of the CONH group around 164-168 ppm. There are also two signal of thioamide carbon chemical shifts at 180 ppm and 181 ppm.

Magnetic susceptibility determination

The effective magnetic moments of the copper(II) complexes Cu(TI), Cu(TII) and Cu(TIII) are found to be in the range of 1.23-2.21 B.M. These values correspond to the one unpaired electron. The paramagnetism of the complex agrees with the square planar geometry around the copper(II) ion.

Table 3: Magnetic data of Cu(II) complexes

omplex $\mu_{eff}(B.M)$ d^n Sugges

Complex	$\mu_{eff}(B.M)$	$d^{\rm n}$	Suggested Geometry
Cu(TI)	2.21	d^9	Square planar
Cu(TII)	1.67	d^9	Square planar
Cu(TIII)	1.23	d^9	Square planar

Antibacterial activities

The antibacterial activities of thioureas and their Cu(II) complexes were tested by the disc diffusion method and the results were showed in Table 4. According to the antibacterial studies, the efficacy of the compounds against Gram positive bacteria is higher than Gram negative bacteria. Interestingly, compound TIII, Cu(TII) and Cu(TIII) showed the activity against *Staphylococcus aureus*. The antibacterial activity of their metal complexes is higher than the ligands. Compound Cu(III) are better antibacterial agents as compared to standard drug Streptomycin.

Table 4: Antibacterial screening of thioureas and their Cu(II) complexes

Compound	Gram positive Zone of inhibit		Gram negative bacteria Zone of inhibiton (mm)		
Compound	Staphylococcus aureus	Bacillus sp.	Pseudomonas aeruginosa	Escherichia coli	
TI	-	-	-	-	
TII	-	-	-	-	
TIII	9	-	-	-	
Cu(TI)	-	-	-	-	
Cu(TII)	12	-	-	-	
Cu(TIII)	19	-	-	-	
Streptomycin	12	8	12	12	

Concentration of the positive control (Streptomycin) = $400 \mu g \text{ mL}^{-1}$

Concentration of the sample = 10 mg mL^{-1}

-: No activity

Conclusion

To conclude, bisthiourea 1,2-bis(N'-2-methoxybenzoylthioureido)-4-chlorobenzene (TI), 1,2-bis(N'-3-methoxybenzoylthioureido)-4-chlorobenzene (TII) and 1,2-bis(N'-4-methoxybenzoylthioureido)-4-chlorobenzene (TIII) and their copper(II) complexes was successfully synthesized and fully characterized by spectroscopic methods. The values of $\mu_{\rm eff}$ (B.M) calculated for Cu(II) complexes in the range of 1.23-2.21 B.M reveal that the Cu(II) complexes are square planar geometry. Compound TIII, Cu(TII) and Cu(TIII) showed the ability to inhibit *Staphylococcus aureus*. The antibacterial activity of their metal complexes is higher than the ligands.

Nur Illane et al: SYNTHESIS, CHARACTERISATION AND ANTIBACTERIAL STUDIES OF Cu(II) COMPLEXES THIOUREA

Acknowledgement

The authors would like to thank the Ministry of Higher Education Malaysia for FRGS research grant (600-RMI/SI/FRGS 5/3/Fst (47/2010)) and also MyMaster scholarship, FSG, Universiti Teknologi MARA, Universiti Kebangsaan Malaysia and International Education Center (INTEC) for providing research facilities.

References

- 1. S. Saeed, N. Rashid, P.G. Jones, M.Ali, R. Hussain. Synthesis, characterization and biological evaluation of some thiourea derivatives bearing benzothiazole moiety as potential antimicrobial and anticancer agents. *European Journal of Medicinal Chemistry*. 2010, pp. 1323-1331.
- 2. A.A. Isab, S. NAwaz, M. Saleem, M. Altaf, M. Monim-al-Mehboob, A.Ahmad, H.S. Evans. Synthesis, characterization and antimicrobial studies of mixed ligand silver(I) complexes of thioureas and triphenylphosphine. *Polyhedron*. 2010, pp. 1251-1256.
- 3. A. Saeed, U. Shaheen, A. Hameed, S.Z.H. Naqvi. Synthesis, characterization and antimicrobial studies of some new 1-(fluorobenzoyl)-3-(fluorophenyl)thioureas. *Journal of Fluorine Chemistry*. 2009, pp.1028-1034.
- 4. M.K. Rauf, I. Din, A. Badshah, M. Gielen, M. Ebishara, D.Vos, S. Ahmed. Synthesis, structural characterization and in vitro cytotoxicity and anti-bacterial activity of some copper(I) complexes with N,N'-disubstituted thioureas. *Journal of Inorganic Biochemistry*, 2009, pp.1135-1144.
- 5. R. Campo, J.J. Criado, R. Gheorghe, F.J. González, M.R. Hermosa, F. Sanz, J.L Manzano, E. Monte, E.R. Fernández. *N*-benzoyl-*N*-alkylthioureas and their complexes with Ni(II), Co(III) and Pt(II) crystal structure of 3-benzoyl-1-butyl-1-methyl-thiourea: activity against fungi and yeast. 2004.
- 6. V.R. Solomon, W. Haq, M. Smilkstein, K. Srivastava, S.K. Puri, S.B. Katti. 4-aminoquinolone derived antimalarials: Synthesis, antiplasmodial activity and heme polymerization inhibition studies. *European Journal of Medicinal Chemistry*. 2010, pp. 4990-4996.
- 7. S. Karakuş, and S. Rollas. Synthesis and antituberculosis activity of new *N*-phenyl-*N*'-[4-(5-alkyl/arylamino-1,3,4-thiadiazole-2-yl)phenyl]thioureas. I1 farmaco. 2002, pp. 577-581.
- 8. H. Arslan, N. Duran, G. Borekci, C.K. Ozer, C. Akbay. Antimicrobial activity of some thiourea derivatives and their nickel and copper complexes. *Journal of Molecules*. 2009.
- 9. A. Tadjarodi, F. Adhami, Y. Hanifehpour, M. Yazdi, Z. Moghaddamfard, G. Kickelbick. Structural characterization of a copper(II) complex containing oxidation cyclization of N-2-(4-picolyl)-N'-(4-methoxyphenyl)thiourea, new ligand of 4-picolylthiourea derivatives and the precursor molecular structure of oxidative cyclization of N-(2-pyridyl)-N'-(4-methoxyphenyl) thiourea. *Polyhedron*, 2007, pp. 4609-4618.
- 10. M.S.M. Yusof, N.A.C. Ayob, M.A. KAdir, B.M. Yamin. 1,2-Bis[N'-(2,2-dimethylpropionyl)thioureido] cyclohexane. *Acta Cryst*. 2008, E64, 937.
- 11. N.I.M. Halim, K. Kassim, A.H. Fadzil, B.M. Yamin. Synthesis, characterization and antibacterial studies of benzoylthiourea derivatives. IPCBEE, vol. 14, pp 55, 2011.



COPPER SUPPORTED ON FUNCTIONALISED MCM41 CONTAINING THIOUREA LIGAND AS AN CATALYST IN OXIDATION OF CYCLOHEXENE WITH HYDROGEN PEROXIDE

(Sokongan Kuprum kepada MCM41 Terfungsi yang Mengandungi Ligan Tiourea Sebagai Pemangkin Terhadap Tindak Balas Pengoksidaan Sikloheksena dengan Hidrogen Peroksida)

Amirah Ahmad^{1*}, Hamizah Md. Rasid¹ and Karimah Kassim²

¹Faculty of Applied Sciences, ²Institute of Science, Universiti Teknologi MARA, 40450 Shah Alam, Selangor, Malaysia

*Corresponding author: my_silberberg@yahoo.com

Abstract

MCM41 encapsulated with thiourea ligand and copper(II) acetate as catalyst for oxidation reaction is reported. First, MCM41 was modified using 3-aminopropyltriethoxysilane (APTES) and then was encapsulated with thiouracil and copper(II) acetate. The catalyst was characterized using X-Ray Diffraction (XRD), N₂ adsorption, single point BET, Fourier Transform Infrared Spectroscopy (FTIR), Field Emission Scanning Electron Microscopy (FESEM) and Elemental Analyzer. The characterization results indicated that the catalyst has an ordered hexagonal structure, a narrow pore size distribution, uniform mesopores and a high surface area. Moreover, the results also revealed that thiourea ligand and copper acetate might be encapsulated onto the pores of MCM41. Catalytic activity of the catalyst was tested in the oxidation of cyclohexene using acetonitrile as solvent and hydrogen peroxide as oxidant. The CuO₂(acac)-Thio-APS-MCM41 was proven to be a good catalyst for oxidation reaction of cyclohexene with conversion up to 96.1% after 24 h reaction and providing a high selectivity to 2-cyclohexene-1-one.

Keywords: MCM41, Thiourea Ligand, Mesoporous Material, Thiouracil

Abstrak

MCM41 yang mengandungi ligan tiourea dan kuprum(II) asetat sebagai pemangkin bagi tindak balas pengoksidaan dilaporkan. Pertama, MCM41 telah diubahsuai menggunakan 3-aminopropiltrietoksisilana (APTES) dan kemudian telah ditambah dengan tiouracil dan kuprum(II) asetat. Pemangkin dicirikan dengan menggunakan kaedah pembelauan Sinar X (XRD), penjerapan N₂, penjerapan titik tunggal BET, Spektroskopi Inframerah Transformasi Fourier (FTIR), mikroskopi electron pengimbasan pancaran medan (FESEM) dan analisis unsur. Keputusan pencirian menunjukkan bahawa pemangkin mempunya struktur heksagon, taburan liang yang kecil, liang meso yang seragam dan luas permukaan yang tinggi. Selain itu, keputusan juga mendedahkan bahawa ligan tiourea dan kuprum asetat mungkin terletak pada liang-liang MCM41. Aktiviti sebagai pemangkin telah diuji dalam tindak balas pengoksidaan sikloheksana menggunakan asetonitril sebagai pelarut dan hydrogen peroksida sebagai oksida. CuO₂(acac)-Thio-APS-MCM41 terbukti manjadi pemangkin yang bagus untuk tindak balas pengoksidaan sikloheksena dengan penukaran sehingga 96.1% selepas 24 jam tindak balas dan memilih tinggi terhadap 2-sikloheksen-1-on.

Kata kunci: MCM41, Ligan Tiourea, Bahan Meso, Tiouracil

Introduction

Oxidation process is a very important in the field of catalysis due to it significant in industrial [1, 2]. One of the focus is commercial cyclohexene oxidation to produce cylohexenol and cyclohexenone which mainly used in pharmaceuticals and fragrances [3]. However, most of the oxidation processes is low in energy efficiency and generates plenty of by-products and waste. Recently, a great demand for these products causes many researchers to find more effective catalytic processes to promote high conversion of reactant and product selectivity [4, 5]. Many of these processes utilized metal complex and porous solids as a catalyst in many reaction such as transition metal

Amirah Ahmad et al: COPPER SUPPORTED ON FUNCTIONALISED MCM41 CONTAINING THIOUREA LIGAND AS AN CATALYST IN OXIDATION OF CYCLOHEXENE WITH HYDROGEN PEROXIDE

(Cr, Mn, V, Mo, Ti, Co, etc.) doped MCM41 [6,7]. Eko Adi Prasetyanto and Sang-Eon Park, 2008, was studied catalytic oxidation of cyclohexene with hydrogen peroxide over Cu(II)-Cyclam-SBA-16 catalyst and was found that the Cu(II)-Cyclam-SBA-16 was proven to be a good catalyst for oxidation reaction of cyclohexene with conversion up to 77.8% after 13 h reaction and providing a high selectivity to cyclohexenol and 3-hydroperoxycyclohexen-1-ene [8]. Among the various solid supports, the mesoporous silica materials, MCM41 has attracted greater attention from material researchers because of the ordered pore arrangements, very narrow pore diameter, uniform mesopores and high surface area. However, pure MCM41 showed very limited catalytic activity due to the hydrophilic properties and limited application. Hence, it requires modification to introduce other features into mesoporous silicates to improve their physical properties (e.g. their hydrophobicity and adsorption characteristics) and catalytic activity such as modification of surface MCM-41 with organic functionalized groups [9], introducing metal ions to increase the active sites and by grafting a suitable ligand to become as donor ligand for transition metal ions [10]. In this research, we reported the 2-thiouracil is encapsulated onto functionalized-MCM41 as potential donor ligand for transition metal to form supported metal thiourea complex and as an efficient catalyst for oxidation of cyclohexene (Fig.1).

Fig. 1: Oxidation of cyclohexene

Experimental

Physical measurement

X-Ray diffraction (XRD) patterns of the samples were obtained by using Rigaku D/max-2500 powder diffractometer with Cu-K α source (λ = 1.5418 Å, 40 kV, 40 mA). The particle size and morphology of the samples were characterized using a Zeiss Supra 35VP Field emission scanning electron microscopy (SEM). The carbon analysis of the samples was acquired by using Flash 1100 Organic Elemental Analyzer Thermo Finnigan. The FT-IR spectra were obtained on a Perkin-Elmer Spectrum One FTIR spectrometer. N₂ adsorption isotherm and BET surface area were measured at 77K on a Micromeritics ASAP 2010 Volumetric Adsorption Analyzer.

Materials

All meterials were commercial reagent grade and obtained from Merck and Sigma-Aldrich. The starting materials were used in this research were Ludox, sodium hydroxide, cetyltrimethylammonium bromide, ammonium hydroxide, 3-aminopropyltriethoxysilane, n-Hexane, thiouracil, copper acetate monohydrate, cyclohexene, acetonitrile and hydrogen peroxide.

Synthesis of purely siliceous MCM41

The MCM41 was prepared as following molar composition below:

6 SiO₂: CTABr: 1.5 NaOH: 0.15 (NH₄)₂O: 250 H₂O

Ludox and sodium hydroxide were added in distilled water. The mixture was stirred for 2 hours as Part A. In another polypropylene bottle, cetyltrimethylammonium bromide and ammonium hydroxide were dissolved in distilled water. The mixture was heated and stirred for 1 hour as Part B. The sodium silicate solution (Part A) was added into template solution (Part B). The resulting mixture was aged overnight in an oven at 97 $^{\circ}$ C. After cooling at ambient temperature, the pH adjustment (pH = 10) of mixture was done. The precipitate was filtered, washed, dried in oven and calcined at 550 $^{\circ}$ C.

Synthesis of aminopropylated MCM41

MCM41 was added to a solution of 3-aminopropyltriethoxysilane in n-Hexane and refluxed for 6 hours. The mixture was filtered, washed and dried at room temperature.

Synthesis of thiourea ligand grafted APS-MCM41

The thiourea complex grafted APS-MCM41 was prepared as following: APS-MCM41 was added to a solution of thiouracil in n-Hexane and refluxed for 24 hours. The mixture was filtered, washed and dried under vacuum overnight.

Synthesis of CuO₂(acac)-Thio-APS-MCM41

Thio-APS-MCM41 was added into a solution of CuO₂(acac)₂ in n-Hexane and refluxed for 24 hours. The mixture was separated by filtration, washed and dried under vacuum.

Procedure for oxidation of cyclohexene with hydrogen peroxide (H_2O_2) catalyzed by $CuO_2(acac)$ -Thio-APS-MCM41

In 3 mL of acetonitrile, 0.5 mmol of cyclohexene, 1 mmol of $\rm H_2O_2$ and 0.01 g of catalyst were added in 25 ml round bottom flask equipped with magnetic stirrer. The mixture was heated at 70 °C under stirring. The reaction progress was monitored by GC. The reaction was repeated for blank experiment in the presence of oxidant and using the same experimental conditions in the absence of catalyst.

$$MCM-41 \begin{bmatrix} O \\ O \\ Si \\ OH \end{bmatrix}$$

$$OSi \\ OH \\ Si \\ OH \end{bmatrix}$$

$$OSi \\ OH \\ ICH3O)3Si(CH2)3NH2$$

$$OSi \\ OH \\ ICH3O)3Si(CH2)3NH2$$

$$OSi \\ OH \\ ICH3OH \\ ICH3OH \\ ICH2OH \\ ICH3OH \\ ICH2OH \\ ICH3OH \\ ICH2OH \\ ICH3OH \\ ICH3OH \\ ICH2OH \\ ICH3OH \\ ICH3$$

Fig. 2: Proposed structure of synthesised material

Results and Discussion

XRD Patterns

The XRD patterns of the synthesized material are shown in Figure 3A and 3B. The low angle XRD patterns show three resolved peaks that can be indexed to the (100), (110) and (200) reflections indicating the characteristics of hexagonal ordered MCM41 structure [11]. These peaks are obviously observed for the MCM41 sample (Fig. 3A (a)). High intensity of the main peak (100) shows high degree of long-range order and existence of uniform pores in the synthesized material. In the XRD pattern of CuO₂(acac)-Thio-APS-MCM41 shows the lower intensity of the (100) for the supported catalyst is attributed to filling the pore of the MCM41 due to functionalisation and

incorporation of thiourea ligand and metal. However, the mesopores structures still retain a good mesostructural order even the decreased of the long range order of the mesoporous sample. The lattice parameters, which were calculated using the d_{100} were 45.5 Å (d_{100} = 39.41 Å, 2θ = 2.24 °) and 43.9 Å (d_{100} = 38.05 Å, 2θ = 2.32) for MCM41 and CuO₂(acac)-Thio-APS-MCM41, respectively. The lattice parameter for CuO₂(acac)-Thio-APS-MCM41 decreases because of the addition of organic group, thiourea and metal results in an contraction of the hexagonal unit cell and decrease in the size of pore channels. Moreover, the addition of amino, thiourea and metal into the gel mixture will lead to some structural rearrangement. However, XRD results show that the mesopores structures still remained intact as hexagonal structure. Moreover, high angle XRD patterns shows the peak in between 2θ = 20° - 100° after addition of thiouracil and metal (Fig. 3B). The peaks at 2θ = 35.28 ° and 38.6 °, corresponding to monoclinic CuO (Fig. 3B (b)) [12].

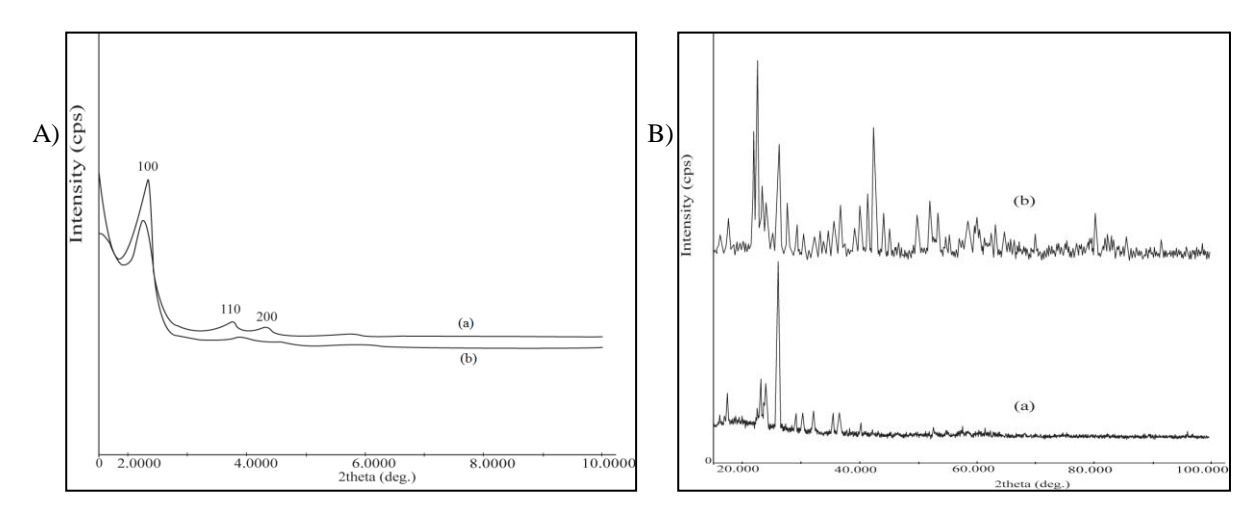


Fig. 3: (A) Low angle XRD patterns: (a) MCM41, (b) CuO₂(acac)-Thio-APS-MCM41. (B) High angle XRD patterns: (a) Thio-APS-MCM41 and (b) CuO₂(acac)-Thio-APS-MCM41.

Nitrogen adsorption

Nitrogen sorption isotherm and corresponding pore size distribution of the synthesized material is given in Figure 4. The isotherms (Fig. 3A) were of type IV which shows a typical mesoporous solid, according to IUPAC classification [13]. The MCM41 samples exhibited strong adsorption at a relative pressure in the range of $0.2 \le P/P_0 \le 0.5$. As the relative pressure increases ($P/P_0 > 0.4$), the isotherm shows inflection, where the P/P_0 position of the sharpness of the isotherm in range $0.4 \le P/P_0 \ge 0.5$ corresponds to uniformity of mesopore size [14]. However, nitrogen uptake decreases for $CuO_2(acac)$ -Thio-APS-MCM41 sample due to the presence of bulky materials inside the pores [15]. The narrow pore size distribution as seen from Fig. 3B revealed a uniform mesoporosity. The pore distribution become broader indicated the ordering of samples decreased as the content of heteroatoms increased.

Single Point BET

Table 1 displays the results of the synthesised material from the single-point BET analysis. Results show clearly that the BET surface area of MCM41 is 982.56 m²/g. It has been reported that mesoporous silica materials have surface area above 600 m²/g [16]. From the data, it can be seen that the BET surface area of APS-MCM41, Thio-APS-MCM41 and CuO₂(acac)-Thio-APS-MCM41 reduces remarkably compared to MCM41, corresponding to the various groups that were successfully grafted. The decrease in surface area suggests that mesoporous framework has turned amorphous. Once a mesoporous framework collapsed from its crystalline structure to amorphous phase, the surface area decreased significantly. Meanwhile, the pore volume of synthesized materials is significantly decreased due to the existence of high amorphous phase in Thio-APS-MCM41 and CuO₂(acac)-Thio-APS-MCM41 sample that blocked the pore structure of sample to give lower pore volume.

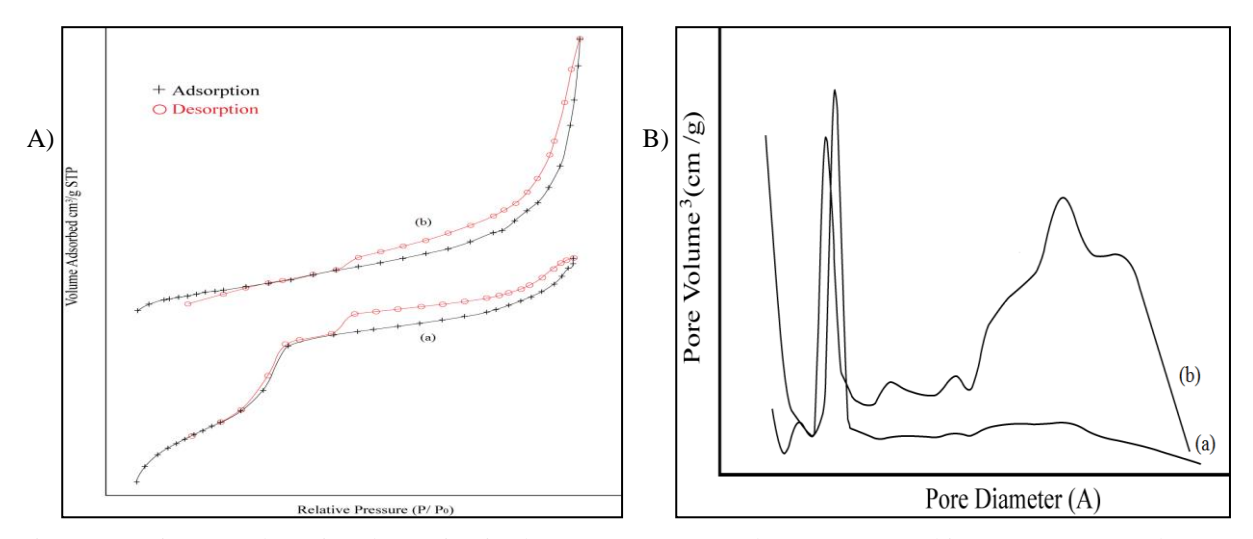


Fig. 4: (A) Nitrogen adsorption-desorption isotherms: (a) MCM41, (b) CuO₂(acac)-Thio-APS-MCM41 and (B) Pore size distributions: (a) MCM41, (b) CuO₂(acac)-Thio-APS-MCM41

Samples	BET surface area (m²/g)	Average pore diameter (Å)	Average pore volume (cm ³ /g)
MCM41	982.56	35.99	0.88
APS-MCM41	286.91	30.79	0.22
Thio-APS-MCM41	14.44	99.35	0.04
CuO ₂ (acac)-Thio-APS-MCM41	10.01	95.26	0.02

Table 1: Surface properties of synthesized materials.

FT-IR Spectra

The FT-IR spectra of synthesized material in the region of 4000 - 400 cm⁻¹ in transmission mode using pressesed KBr pellets, and shown in Fig. 5. The uncalcined MCM41 and calcined MCM41 spectra (Fig. 5A. a, b) show intense band at wavenumber 1100 and 802 cm⁻¹ which accounts for the asymmetric and symmetric stretching of the Si-O-Si bonds, respectively [17]. The bands at 970 cm⁻¹ and 460 cm⁻¹ was assigned to the stretching and bending vibrations of surface Si-O- groups respectively [18]. For calcined MCM41, the bands at 2852 cm⁻¹ and 2921 cm⁻¹ corresponding to the long chain of alkyl group of the surfactant molecules were disappeared after calcination due to removal of surfactants (Fig. 5A. b). Fig. 5A.(c) show the spectra of MCM41 after being modified with APTES with -NH₂ symmetric bending at 1553cm⁻¹ and C-N bond at 1639 cm⁻¹. Moreover, the band at 2944 cm⁻¹ corresponding to asymmetric vibration of the CH₂ groups of the propyl chain of the sylilating agent at, indicates the successful grafting of organic amine onto the surface. Figure 3B shows the spectra for thiouracil (a), Thio-APS-MCM41 (b) and CuO₂(acac)-Thio-APS-MCM41 (c). The most of the bands of thiouracil was appeared after encapsulated APS-MCM41 with thiouracil while the band of Si-O-Si also retain even after incorporation of complex. It shows that thiouracil was successfully grafted onto functionalised-MCM41. The bands at 628 cm⁻¹ and 691 cm⁻¹ represents the Cu = O vibrations [19], indicates that the CuO₂(acac)-Thio-APS-MCM41 was successfully synthesised.

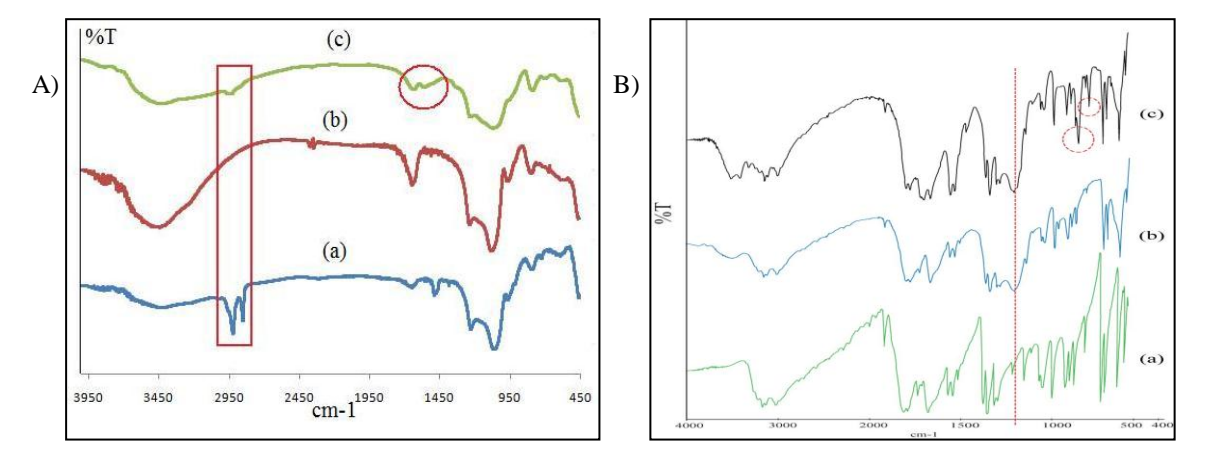


Fig. 5: (A) FT-IR spectra: (a) Uncalcined MCM41, (b) MCM41 and (c) APS-MCM41. (B) Spectra for: (a) thiouracil, (b) Thio-APS-MCM41 and (c) CuO₂(acac)-Thio-APS-MCM41.

Field Emission Scanning Electron Microscopy (FESEM)

Figure 6a and 6b display the FESEM micrograph of pure MCM41 and $CuO_2(acac)$ -Thio-APS-MCM41, respectively. The FESEM micrograph reveals that the particle morphology of both samples consists of agglomerated particles of 1 to 3 μ m in diameter. The FESEM micrograph explained the $CuO_2(acac)$ -Thio-APS-MCM41 possess the some morphology and that the solid support were structurally unchanged upon immobilization.

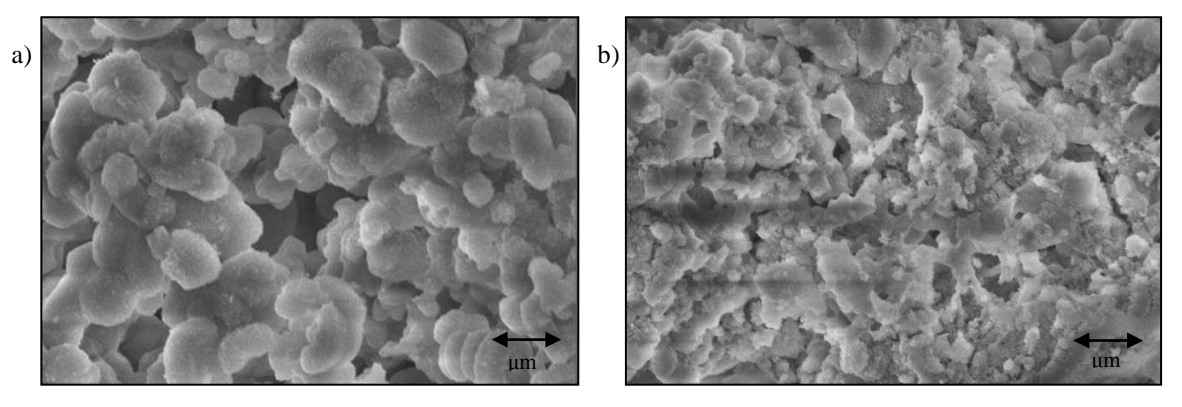


Fig. 6: Morphology of (a) MCM41 and (b) CuO₂-Thio-APS-MCM41.

Elemental Analyzer

According to elemental analysis results, the carbon contents for the Thio-APS-MCM41 and CuO2(acac) – Thio-APS-MCM41 are determined to be 23.9 and 24.4 wt.%. respectively. Considering the theoretic carbon contents of Thio-APS-MCM41 and CuO2(acac) – Thio-APS-MCM41 are 25.6 and 23.9 wt.%, indicates the composition of prepared samples close with their molecular formula.

Catalytic Performance

The catalytic activity of $CuO_2(acac)$ – Thio-APS-MCM41 was investigated for oxidation of cyclohexene with hydrogen peroxide as the oxidant. The selectivity and activity results of $CuO_2(acac)$ – Thio-APS-MCM41 catalyst on the oxidation of cyclohexene with hydrogen peroxide have been given in Table 2. As shown in the Table 2, the conversion of cyclohexene reached 50 % with 66.1% selectivity to the 2-cyclohexen-1-one after 3 h of reaction time and the other products were found to be 2-cyclohexen-1-ol, trans-1,2-cyclohexanediol and cis-1,2-cyclohexanediol.

Solvent Oxidant Time (h) Conversion (%) $\frac{\text{OH}}{\text{OH}}$ Oxidant $\frac{\text{Time}}{\text{OH}}$ Conversion $\frac{\text{OH}}{\text{OH}}$ OH $\frac{\text{OH}}{\text{OH}}$ Acetonitrile $\frac{\text{H}_2\text{O}_2}{\text{O}_2}$ 3 50 22.4 66.1 6.6 4.9

Table 2: The oxidation of cyclohexene with hydrogen peroxide.

Effect of Reaction Time

The effect of reaction time on cyclohexene conversion and product distributions at reaction temperature of 343 K is shown in Table 3. It can be seen the cyclohexene conversion steadily increased with increasing reaction time and at time 26 h, the conversion of cyclohexene in 100%.

			Product Selectivity (%)				
Reaction	Time (h)	Conversio n (%)	○H	Ċ	ОН	ОН	
1	2	52.8	16.3	73.2	6.2	4.3	
2	4	64.5	18.3	69.7	6.8	5.2	
3	8	80.8	15.4	72.7	6.6	5.4	
4	12	92.6	11.1	76.0	5.2	7.7	
5	24	96.1	7.4	80.8	5.3	6.5	
6	26	100	3.3	86.0	4.7	6.0	

Table 3: The effect of reaction time on oxidation of cyclohexane

Amirah Ahmad et al: COPPER SUPPORTED ON FUNCTIONALISED MCM41 CONTAINING THIOUREA LIGAND AS AN CATALYST IN OXIDATION OF CYCLOHEXENE WITH HYDROGEN PEROXIDE

Effect of Catalyst

The effect of catalyst was investigated by comparing the conversion and product selectivity of reaction with and without catalyst (Table 4). The results indicated that the reaction with catalyst yield more major product than without catalyst. It shows that the catalyst was increased the rate of reaction by yield more conversion and product without itself being consumed.

Table 4: The effect of catalyst on oxidation of cyclohexane

					Product S	Selectivity (%)	
Reaction	Oxidant	Time (h)	Conversion (%)	ŮH OH	Ġ	ОН	ОН
With catalyst	H_2O_2	6	73.7	17.4	70.6	6.6	5.4
Without catalyst	H_2O_2	6	70.5	33.7	56.6	-	-

Conclusion

It can be concluded that $CuO_2(acac)_2$ supported on functionalised-MCM41 containing thiourea ligand was successfully synthesised and showed a high catalytic activity in the oxidation of cyclohexene with hydrogen peroxide. The reaction was found gave high selectivity to 2-cyclohexen-1-one with conversion 96.1% after 24 h reaction.

Acknowledgement

This work has been supported by the Ministry of Science, Technology and Innovation Malaysia (MOSTI) for financial support through funding 600-RMI/ST/FRGS5/3/Fst (41/2010) and thank you very much to the Faculty of Pharmacy, UiTM and Faculty of Science, UTM for cooperation in completing this work.

References

- A.E. Shilov and G.B. Shul'pin, (1997), Activation of C-H bonds by metal complexes. Chem. Rev., 97, pp 2897-2932
- 2. L.I. Simandi, (1991), Dioxygen activation and homogeneous catalytic oxidation. *Elsevier.*, pp 57
- 3. K.F. Podraze, (1991) Organic building blocks of the chemical industry. Org. Prep. Proced. Int., 23, pp. 217
- 4. J.T. Groves, K.V. Shalyaev, J. Lee, (1999), in: K.M. Kadish (Ed.), The Porphyin Handbook. Vol. 4, Academic Press, San Diego, CA, pp 17
- 5. R.A. Sheldon, and J.K. Kochi, (2000), Metal-catalyzed oxidations of organic compounds, Academic Press, New York, 1981: G.J.T. Brink, I.W.C.E Arends, R.A. Sheldon, Science 287, pp 1636
- 6. J.H. Clark, (2001), Catalysis for green chemistry. Pure Appl. Chem. 73, pp 103-111
- 7. H. Nur, S. Ikeda and B. Ohtani*, (2000), Phase-boundary catalysis: a new approach in alkene epoxidation with hydrogen peroxide by zeolite loaded with alkylsilane-covered titanium oxide. *Chem. Comm.* pp 2235
- 8. Eko Adi Prasetyanto and Sang-Eon Park, (2008), Catalytic oxidation of cyclohexene with hydrogen peroxide over Cu(II)-Cyclam-SBA-16 catalyst. *ngew. Bull. Korean Chem. Soc.*, Vol. 29, No. 5, pp. 1033-1037.
- 9. R.S. Robert, A. Rafael, A.D. James, W.R. Thatcher, (2003), Vapor-phase silylation of MCM-41 and Ti-MCM41. *Micropor. Mesoporm Mater.*, 66: 53-67.
- T. Shahram, M. Majid, M. Valiollah, M. Iraj, and G. Kamal, (2009), Alkene epoxidation catalyzed by molybdenum supported on functionalized MCM41 containg N-S chelating Schiff base ligand. *Catal. Comm.*, 10: 853-858
- 11. S. Biz, M.L. Occelli, (1998), Synthesis and characterization of mesostructured materials. *Catal. Rev. Sci. Eng.*, 40: 329.

- 12. K.M. Parida, Dharitri Rath, S.S. Dash, (2010), Synthesis, characterization and catalytic activity of copper incorporated and immobilized mesoporous MCM-41 in the single step amination of benzene. *J. Molec. Catal. A: Chem.*, 318: 85-93.
- 13. S. Brunauer, L.S. Deming, W.S. Deming, E. Teller, (1940), On a theory of the van der waals adsorption of gases. *J. Am. Chem. Soc.*, 62 (7): 1723-1732.
- 14. H. Sepehrian, A. R. Khanchi, M. K. Rafouei and S. Waqif Husain, (2006), Non-thermal synthesis of mesoporous zirconium silicate and its characterization. *Journal of the Iran Chemical Society*, Vol 3, No. 3, pp. 253-257.
- 15. H. Yang, G. Zhang, X. Hong and Y. Zhu, (2004), Dicyano-functionalized MCM-41 anchored-palladium complexes as recoverable catalysts for Heck reaction. *J. Mol. Cat. A.*, 210: 143-8.
- 16. S. Endud, and K.L. Wong, (2007), "Mesoporous silica MCM48 molecular sieve modified with SnCl₂ in alkaline medium for selective oxidation of alcohol," *Micropor. Mesopor. Mater.*, 101, pp. 256-263.
- 17. E.M. Flanigen, H. Khatami, H.A. Szymanski, (1971), Infrared structural studies of zeolite frameworks. In: E.M. Flanigen, L.B. Sand (Eds.). *Molecular Sieve Zeolites*. ACS Adv. Chem. Ser., 101: pp 201-227.
- 18. R. Takahashi, S. Sato, T. Sodesawa, M. Kawakita, K. Ogura, (2000), High surface-area silica with controlled pore size prepared from nanocomposite of silica and citric acid. *J. Phys. Chem. B.*, 104: 12184.
- 19. L. Chmielarz, P. Kustrowski, R. Dziembaj, P. Cool. E.F. Vansant, (2006), Catalytic performance of various mesoporous silicas modified with copper or iron oxides introduced by different ways in the selective reduction of NO by ammonia. *Appl. Catal. B: Env.*, 62: 369-380.



DETERMINATION OF VITAMIN E ISOMERS IN PLASMA USING ULTRA PERFORMANCE LIQUID CHROMATOGRAPHY

(Penentuan Isomer-Isomer Vitamin E di dalam Plasma Menggunakan Kromatografi Cecair Berprestasi Lampau)

Shahidee Zainal Abidin^{2,3}, Mohammad Johari Ibahim², Mohd Hamim Rajikin¹ and Nuraliza Abdul Satar^{1*}

¹Department of Physiology, ²Institute of Medical Molecular Biotechnology, ³Centre for Pathology Diagnostic and Research Laboratories, Faculty of Medicine, Universiti Teknologi MARA, 40450 Shah Alam, Selangor, Malaysia

*Corresponding author: nuraliza064@salam.uitm.edu.my

Abstract

A rapid method for quantification of vitamin E isomers (α -, β -, γ -, δ - tocopherol and tocotrienols) was developed by using ultra performance liquid chromatography (UPLC) from human plasma. This method involved liquid-liquid extraction of plasma sample to extract the lipophilic portion for injection into UPLC system. The UPLC system was equipped with fluorescent detector (296 nm excitation, 330 nm emissions) and C18 column with 1.7 µm particle size (2.1 x 110 mm column) for particle separation. The mobile phase comprises of 1.0% of H₂O and 99.0% of methanol (HPLC grade) with flow rate adjusted at 0.4 ml min⁻¹. Peak separations were accomplished after 3.50 minutes and 5 µl treated samples were required for injection. Results obtained showed that the UPLC system was able to separate, detect and quantitate six peaks, namely α -, γ -, δ - tocopherol and tocotrienols, respectively. However, it failed to separate and quantificate both, β- tocopherol and tocotrienol due to low amount in nature. The calibration curve was linear for a concentration ranging from 1 µg ml⁻¹ – 10 µg ml⁻¹ of total vitamin E standard which $r^2 > 0.9996$ for all isomers. The within day and between day coefficients of variation were less than 10.29% (n=4) and 10.73% (n=4) for all isomers. The accuracy of isomers quantification for 1 μg ml⁻¹ (n=4) and 10 μg/ml (n=4) vitamin E stocks were 93.52% - 98.13 %. The within day and between day coefficients of variation for vitamin E standard were less than 7.59% (n=4) and 9.74% (n=4) for all isomers while for plasma sample were less than 10.29% (n=4) and 10.73% (n=4) for all isomers. The recovery rates for all isomer were ranging from 98.96 ± 7.22 and 107.50 ± 1.19 and the limit of detection was 2.53 ng. The present data suggested that this method required extremely short analysis time i.e. 2.50 min, required less samples for injection and excellent chromatographic reproducibility.

Keywords: UPLC, Tocotrienols, Tocopherol, Plasma, Vitamin E

Abstrak

Satu kaedah yang pantas bagi menentukan kandungan isomer vitamin E (α -, β -, γ -, δ - tokoferol dan tokotrienol) telah dihasilkan dengan menggunakan Kromatografi Cecair Berprestasi Lampau (UPLC) daripada sampel plasma manusia. Kaedah ini mengunakan teknik pengasingan pada fasa cecair bagi mengekstrak bahagian lipofilik yang terdapat di dalam sampel plasma untuk disuntik ke dalam sistem UPLC. Sistem UPLC dilengkapi dengan pengesan floresen (296 nm eksitasi, 330 nm emisi) dan kolum C18 yang mempunyai saiz partikel 1.7 μ m (2.1 x 110 mm kolum) bagi pengasingan kompaun. Fasa gerak terdiri dari 1.0% H₂O dan 99.0% methanol (gred HPLC) dengan kadar aliran 0.4 ml min-1. Pengasingan isomer berjaya dilakukan dalam tempoh 3.50 minit dan hanya sebanyak 5 μ l sampel diperlukan untuk disuntik ke dalam sistem. Hasil daripada keputusan yang diperolehi sebanyak enam isomer iaitu (α -, γ -, δ - tokoferol dan tokotrienol yang mampu diasingkan, dikesan dan ditentukan kandungannya oleh sistem UPLC ini. Walaubagaimanapun, ia gagal dalam pengasingan dan penentuan kandungan β - tokoferol and tokotrienol mungkin disebabkan oleh jumlahnya yang terlalu rendah. Keluk kalibrasi adalah garis lurus, dengan menggunakan kepekatan piawaian vitamin E di antara 1 μ g ml-1 – 10 μ g ml-1 bagi kesemua isomer dengan nilai r^2 > 0.9996. Pekali variasi bagi dalam tempoh sehari dan diantara hari adalah kurang dari 10.29% (n=4) dan 10.73% (n=4) bagi kesemua isomer. Ketepatan kuantifikasi isomer bagi 1 μ g ml-1 (n=4) and 10 μ g/ml (n=4) stok vitamin E adalah sebanyak 93.52% -

Shahidee et al: DETERMINATION OF VITAMIN E ISOMERS IN PLASMA USING ULTRA PERFORMANCE LIQUID CHROMATOGRAPHY

98.13%. Pekali variasi bagi dalam tempoh sehari dan diantara hari untuk piawaian vitamin E adalah kurang dari 7.59% (n=4) dan 9.74% (n=4) bagi kesemua isomer manakala sampel plasma pula adalah kurang dari 10.29% (n=4) dan 10.73% (n=4) bagi kesemua isomer. Kadar pemulihan untuk semua isomer adalah di antara 98.96 ± 7.22 dan 107.50 ±1.19 dan tahap pengesan yang dihadkan sebanyak 2.53 ng. Hasil data yang diperolehi menunjukkan bahawa kaedah ini hanya memerlukan masa analisis yang singkat iaitu selama 2.50 min sahaja, serta menggunakan jumlah sampel yang sedikit untuk suntikan dan berkeupayaan menghasilkan kromatogafi yang baik.

Kata kunci: UPLC, Tokotrienol, Tokoferol, Plasma, Vitamin E

Introduction

Vitamin E is an important source of antioxidant from food and consists of eight naturally occurring molecules [four tocopherols (Toc) and four tocotrienols (TCT)]. Molecular structure of vitamin E composed of a polar chromanol ring linked to an isopropanoid chain. The structure of TCT is different from Toc where TCT possess three double bond in its isopropanoid side chain, while Toc has a saturated hydrocarbon phytyl tail. The isomer of both Toc and TCT (α -, β -, γ - and δ -) are different with regards to the number and position of methyl groups on chromanol ring. Tocopherol and TCT are known as lipid soluble compound, being well represented in vegetable, fruits, seeds, dairy foods, nuts and oils. Biological activities of Toc and TCT are generally due to their antioxidant action, i.e. inhibiting lipid peroxidation in biological membranes by breaking free radical driven chain reactions. Tocopherols and TCT were found to possess a cholesterol-lowering property [1, 2] by down-regulating 3-hydroxy-3-methylglutaryl coenzyme A (HMG-CoA) reductase activity, which is the rate limiting enzyme in the mevalonate pathway that contributes to the synthesis of cholesterol [3, 4]. Tocopherols and TCT have been identified to show other effects such as anticancer, anticholesterolemic, antihypertensive, antioxidant, immunomodulatory and neuroprotective [5].

Several chromatographic methods were available in the literature for the determination of Toc and TCT isomers using both reversed and normal phase columns [6]. Ultra performance liquid chromatography (UPLC) is a tremendous method for quantification and characterization of vitamin E. The Acquity UPLC system consist of high-pressure fluidic modules (binary pump), efficient auto samplers characterized by fast injection cycles, low injection volumes, temperature control and high-speed detectors. Thus, the system gives UPLC a rapid, sensitive and high-resolution for separation of vitamin E. The UPLC system is equipped with special column contain bridged ethylsiloxane – silica hybrid (BEH) adsorbent, as 1.7 µm particles, which ensure a wide pH operating range [7]. The particles were created with a special design which is capable to resist high back pressure (< 15000 psi) as compared to conventional column for high performance liquid chromatography (HPLC).

Hence, the main objective for this study was to develop and validate an UPLC method for quantification of all vitamin E isomers in human plasma.

Experimental

Chemical

Methanol (grade for liquid chromatography), n-hexane and absolute ethanol were purchased from Merck Sdn Bhd. Ascorbic acid were obtained from Sigma-Aldrich. Complete natural vitamin E (E-8; α-, β-, γ-, δ- Toc and TCT) were purchased from Hovid which consist of 181.82 mg, 4.30 mg, 91.39 mg, 32.26 mg, 5.56 mg, 0.56 mg, 11.11 mg and 2.78 mg of α-, β-, γ-, δ- Toc and TCT, respectively.

Standard Solution Preparation

Vitamin E standard solution was prepared from vitamin E (E-8; Hovid) where 1 mg of the stock was accurately weighted and dissolved in methanol as a stock solution. Standard curve consist of a blank, together with a series of stock solution diluted with different concentrations i.e. 1 µg ml⁻¹, 2 µg ml⁻¹, 4 µg ml⁻¹, 6 µg ml⁻¹, 8 µg ml⁻¹ and 10 µg ml⁻¹). The standard solution were prepared daily before being analyzed using UPLC.

Sample Preparation

Blood samples were collected from healthy volunteers (man and women) and transferred into EDTA tube. The samples were centrifuged at 3000 rpm for 15 minutes. Plasma was pooled and transferred into polypropylene tube, stored at -20°C until analysis [8]. Sample analysis was done by transferring 200 µl of plasma into new polypropylene tubes containing 50 µl of 10% ascorbic acid (1 mg in 10 ml of absolute ethanol) and vortexed for

10s. The ascorbic acid was added to minimize the oxidation of target analytes. One ml of absolute ethanol was added to precipitate protein, followed by vortexing for 10 s and centrifuged at 3000 rpm for 15 min at 4°C. After that, 3 ml of n-hexane was added (for extraction of vitamins) and mixed using Shaker Orbit P4 at 500 rpm for 10 min. Then, the samples were centrifuged again at 3000 rpm for 15 min at 4°C. Supernatants (2.5 ml) were transferred into polypropylene tubes and evaporated using Vacum Concentrator (Thermo ISS110-230). Then, the residues were dissolved with 50 μ l of methanol, filtered through 0.45 μ m filter and diluted 30 times before 5 μ l of samples were injected onto the UPLC system.

Validation of Method

The method was validated by measuring the accuracy, precision, recovery and limits of detection. Accuracy of this method was determined by measuring the ability of the system to quantitate the known concentration of vitamin E standard at lower and higher concentrations. The precision of method was evaluated by determination of the value of intra-assay (within run) and inter-assay (between run) of vitamin E in standard solution and plasma sample. The reproducibility of extraction method was measured by determining the recovery of spike from plasma sample. The limit of detection or sensitivity of the florescent detector were determined by preparing vitamin E stock of different concentration over the range $0.1~\mu g~ml^{-1}-0.9~\mu g~ml^{-1}$ and the amplitude of the peak were measured.

Chromatography Condition

The chromatographic system consists of a Water Acquity ultra performance liquid chromatography (Water, Massachusetts, U.S.A) equipped with a fluorescent detector at the wavelength of 296 nm and 330 nm for excitation and emission. Particle separation were done using reversed phase C_{18} column (2.1 x 110 mm, 1.7 μ m) and the temperature of column was set at 30°C. The mobile phase was eluting isocratically with 1.0% of H_2O and 99.0% of methanol with flow rate adjusted at 0.4 ml min⁻¹. Peak separations were accomplished after 3.50 minutes and 5 μ l treated samples were required for injection. The data was collected and processed using Empower chromatographic software (Water, Massachusetts, U.S.A). All preparations were conducted in low light environment in order to minimize the photodegradation of the solution.

Results and Discussion

Peak Separation

Figure 1 presented a good six peaks separation of Toc and TCT from E-8 standard in reversed-phase UPLC on a C_{18} column and peak separations were accomplished after 3.50 minutes. The order of elution for chromatogram is α -TCT, γ -TCT, δ -TCT, δ -TCT, γ -TCT, δ -TCT, δ -TCT, δ -TCC, γ -Toc and α -Toc. The result was comparable to that reported by Xu [9]. Retention times were 1.19, 1.32, 1.44, 1.71, 1.94 and 2.12 min for α -TCT, γ -TCT, δ -TCT, δ -Toc, γ -Toc, and α -Toc, respectively. However, the system failed to detect β -TCT and β -Toc.

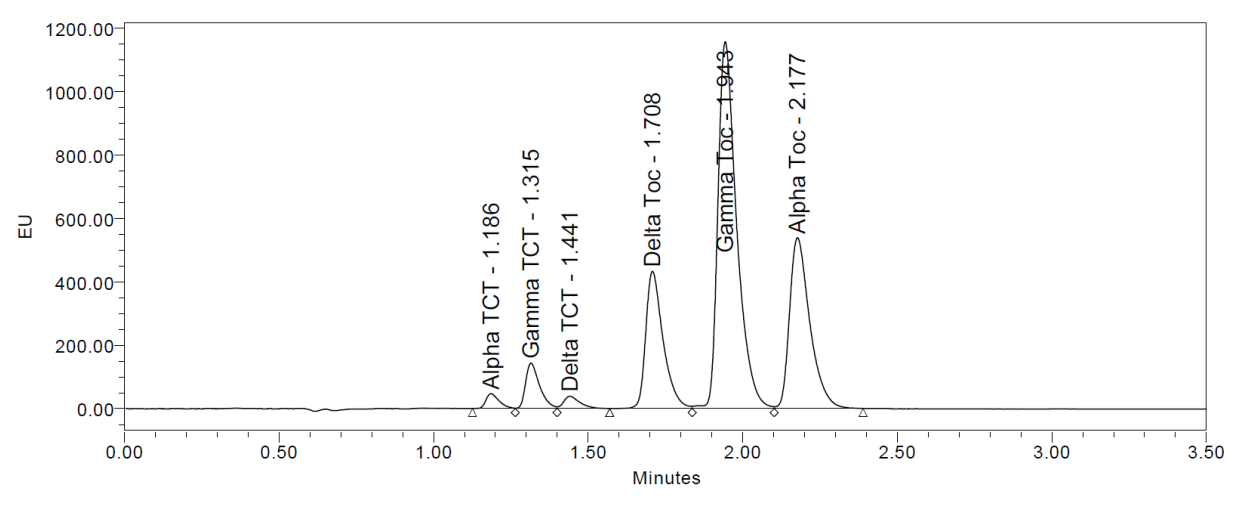


Figure 1: Chromatogram of a standard vitamin E (E-8, Hovid) retention time: α -TCT, 1.19 min; γ TCT, 1.32 min; δ -TCT, 1.44 min; δ -Toc, 1.71 min; γ -Toc, 1.94 min; and α -Toc, 2.18 min

Calibration Curve

Figure 2 showed the overlay chromatograms consisting of blank and seven different concentrations of standard solution and the retention time for each isomer appear within 5%. The calibration curve was analyzed using Empower chromatographic software and showed in Table 1. The mean linearity of the calibration curve for each isomer was 0.9996 ± 0.00019 . The r^2 value (0.9996) showed a good linearity of the analytical method.

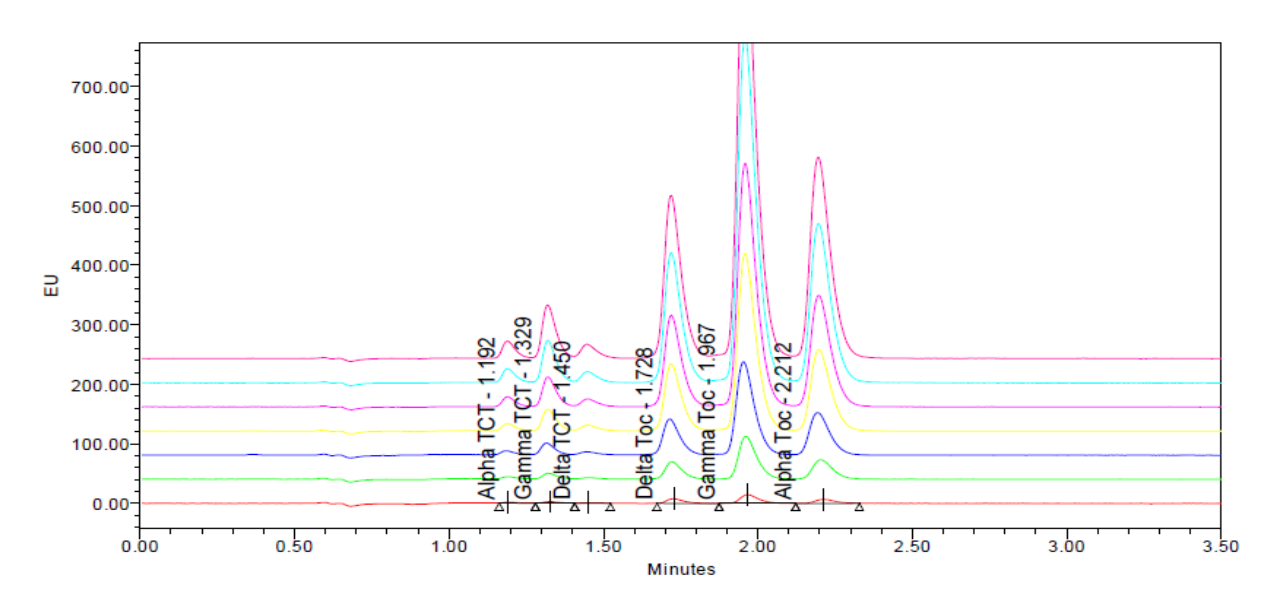
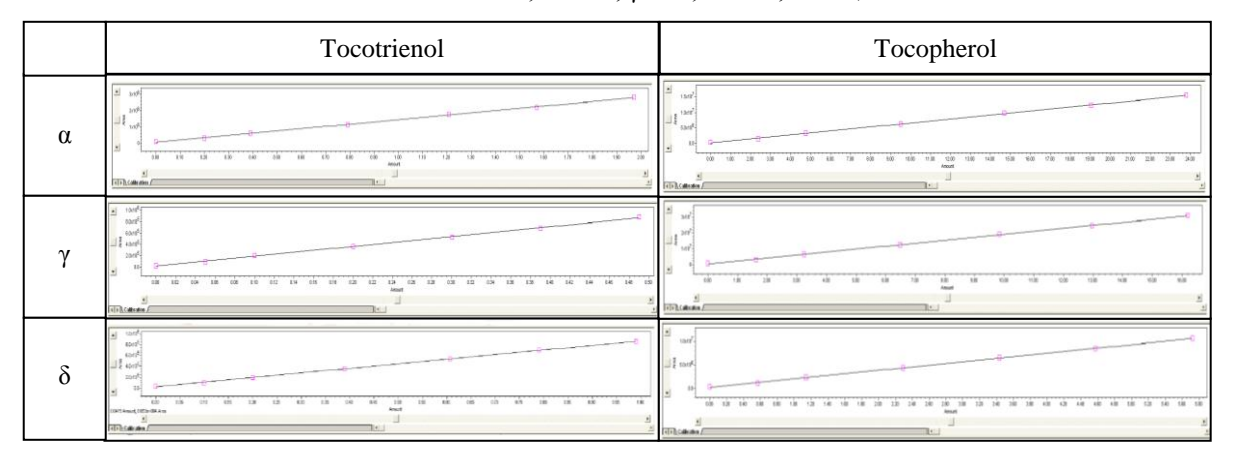


Figure 2: Overlay chromatogram of different concentrations of vitamin E isomers

Table 1: Calibration curve of standard solution: α -TCT; 0.9995, γ -TCT; 0.9997, δ -TCT; 0.9993, δ -Toc; 0.9997, γ -Toc; 0.9997, α -Toc; 0.9997



Determination of Vitamin E Isomers in Human Plasma

Figure 3 showed the chromatogram of vitamin E isomers from pooled human plasma. This system was able to detect 6 isomers, except β -TCT and β -Toc, where it is similar to results found in the determination of the isomers in vitamin E standard. The mean values of each isomer were shown in Table 2.

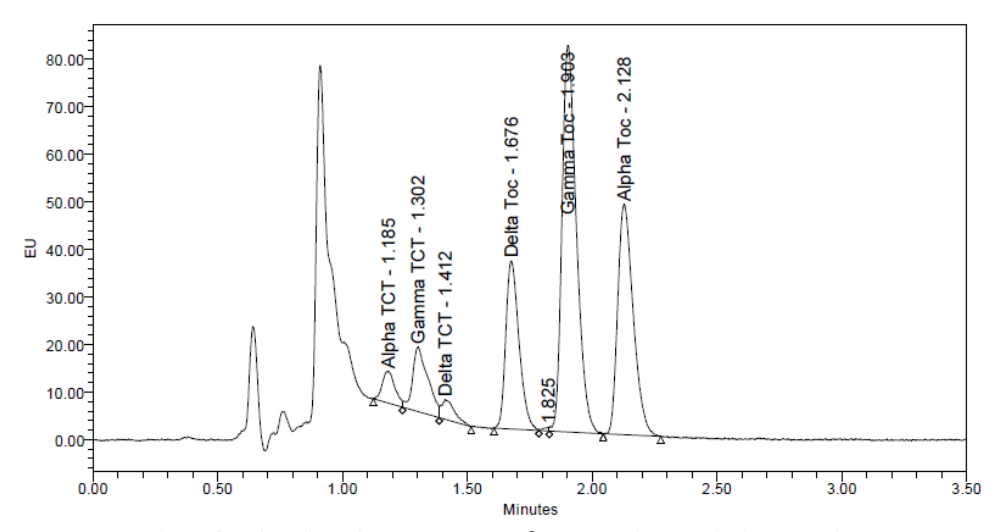


Figure 3: Separation of a vitamin E isomers (α -, γ -, δ - Toc and TCT) in human plasma on reversed phase column (C18 column with 1.7 μ m particle)

Table 2: The concentration of isomers vitamin E in pooled plasma

Isomers	Mean ± SD			n
α-TCT	0.122	±	0.008	4
γ- TCT	0.250	±	0.018	4
δ-TCT	0.051	±	0.004	4
δ-Toc	0.338	\pm	0.025	4
γ-Toc	1.015	±	0.079	4
α-Toc	3.317	±	0.232	4

Validation of Method

Table 3 showed the accuracy of this method in order to measure standard solution at 1 ug ml⁻¹ (lower concentration) and 10 ug ml⁻¹ (higher concentration). The accuracy to detect isomers at 1 ug ml⁻¹ was between 93.52 \pm 7.96 and 98.13 \pm 4.36 while 94.78 \pm 0.77 and 96.60 \pm 0.53 for 10 ug ml⁻¹. Meanwhile, for precision of the method, the coefficient variation for intra-assay and inter-assay of the isomers for standard solution were less than 7.59% (n=4) and 9.74% (n=4) for all isomers (Table 4). The coefficient value in plasma was below 10.29% and 10.54% (Table 5). The recovery for each isomer in spike pooled plasma was shown in Table 6 where it is ranging from 98.96 \pm 7.22% and 107.50 \pm 1.19%. The limit of detections showed that all detected TCT and Toc isomers can be measured at 0.1 μg ml⁻¹ except for the δ-TCT, where it can only be detected at 0.3 μg ml⁻¹. The lowest detection of UPLC was calculated by times with the percentage of δ-TCT in the solution, thus showed that the limit of detection in this study was 2.52 ng.

Shahidee et al: DETERMINATION OF VITAMIN E ISOMERS IN PLASMA USING ULTRA PERFORMANCE LIQUID CHROMATOGRAPHY

Table 3: Accuracy of 1 ug ml⁻¹ and 10 ug ml⁻¹ of isomers vitamin E determination in standard solution

Isomers	1 μg/ml				10 μg/ml				
	Me	Mean ± SD		n	Me	ean ± S	D	N	
α-TCT	93.52	<u>±</u>	7.96	4	96.11	±	0.87	4	
γ- TCT	95.59	±	4.90	4	95.39	±	1.14	4	
δ-TCT	96.05	<u>±</u>	1.09	4	95.24	±	1.81	4	
δ-Toc	98.06	±	4.39	4	96.60	±	0.53	4	
γ-Toc	98.13	±	4.36	4	95.92	±	1.28	4	
α-Toc	95.99	±	3.96	4	94.78	±	0.77	4	

Table 4: Coefficient variation of intra-assay (within run) and inter-assay (between run) of isomers vitamin E determination in standard solution

Isomers	Intra-assay				Inter-assay					
	Me	ean ± S	D	n	C.V	Mea	an ± SD		N	C.V
α-TCT	1.31	±	0.07	4	5.14	1.33	±	0.12	4	8.83
γ- TCT	2.93	±	0.22	4	7.50	3.17	±	0.19	4	6.03
δ-TCT	0.73	±	0.05	4	7.26	0.72	±	0.77	4	9.74
δ-Toc	10.00	±	0.74	4	7.43	10.00	±	0.62	4	6.24
γ-Toc	19.78	±	1.23	4	6.22	20.85	±	1.26	4	6.06
α-Toc	25.55	±	1.94	4	7.59	28.15	±	2.40	4	8.54

Table 5: Coefficient variation of intra-assay (within run) and inter-assay (between run) of isomers vitamin E determination in plasma sample

Isomers		Intra-assay					Inter-assay			
	Mo	ean ± S	D	n	C.V	Me	an ± SD		N	C.V
α-TCT	0.23	±	0.01	4	5.74	0.22	±	0.02	4	8.14
γ- TCT	0.30	±	0.03	4	10.29	0.29	±	0.02	4	5.54
δ-TCT	0.08	±	0.00	4	5.43	0.06	<u>±</u>	0.01	4	10.54
δ-Toc	0.53	±	0.04	4	7.62	0.54	±	0.05	4	9.55
γ-Toc	1.20	±	0.11	4	9.38	1.12	±	0.10	4	8.99
α-Toc	4.04	±	0.25	4	6.26	3.80	±	0.33	4	8.80

Table 6: Mean recovery of all isomers vitamin E in human plasma

Sample	Recovery (% mean ± SD)					
Isomer	TCT	Toc				
α	107.50 ± 1.19	100.79 ± 3.31				
γ	99.21 ± 5.04	98.96 ± 7.22				
δ	103.00 ± 7.02	101.63 ± 6.79				

Ultra performance liquid chromatography (UPLC) system that was used in this study for sample separation using column packed with 1.7 μ m provide a superior resolution, increase in speed of analysis, improve in sensitivity of detection and resist to the higher back pressure (<15000 psi). The UPLC also uses very low mobile-phase flow rates

(0.4 ml min⁻¹), which is more economically important in processing large samples. Methanol was used in mobile phase and all the stationary phases because it was found to improve the retention and separation of the compounds [10].

The β -TCT and β -Toc were not able to be detected in this study using E-8 as a standard, since a reversed-phased column that was used cannot separate β -TCT with γ -Toc [11]. Other studies also speculated that the two isomers were commonly reported together as the sum of β - and γ - Toc [12, 13]. In addition, the separation process using reversed-phase column is difficult to separate β -, γ - and δ - Toc due to the position of the methyl group on the aromatic ring [8]. Another probability on failure to separate and quantitate β -TCT and β -Toc is due to its very low amount in vitamin E.

In addition, in normal-phase HPLC on a silica column, seven peaks of Toc and TCT was eluted and there are α -TCT, β - TCT, γ -TCT, δ -Toc, α -Toc, γ -Toc and δ -Toc [9]. The normal-phase diol column gave reproducible and consistent separations of all the Toc and TCT (α -, β -, γ -, δ - Toc and TCT) as compared to reversed-phase column which is lack of separation [14]. Tocotrienol was eluted first compared to the Toc because of the chemical structure, i.e. the tocols with unsaturated side chain have shorter retention time than those with saturated side chain. In addition, the substituents on the chromanol ring also affect the retention times of tocotrienol and tocopherol, where this effect only seen in reversed-phase column rather than normal-phase column [9].

The precision of the assay was evaluated by determining the intra- and inter-assay coefficient of variation (CV) of the vitamin E concentration in the standard solution and the plasma sample. The standard solution and the sample plasma were analyzed four times daily (intra-assay) for five days (inter-assay). Results from the intra-assay and inter-assay analysis shown, that this method are precise and reliable, except for the inter-assay analysis of δ -TCT. This result might be due to very low concentration of δ -TCT in plasma sample. The results obtained from these analytical analyses were presented in Table 4 and 5. The result was considered acceptable with the CV values obtained were not exceeding 10%.

The accuracy study was done by preparing two different concentrations of standard solution (1 µg ml⁻¹ and 10 µg ml⁻¹) and was evaluated for 4 samples which were prepared individually. The accuracy was calculated as mean and associated standard deviation which was presented in Table 3. The mean accuracy obtained, expressed as percentage, ranges between 93.52 - 98.13 % for all isomers.

The results of recovery were presented in Table 6, based on the difference between the total amount determined in the spiked samples and the amount observed in the non-spiked samples. All analyses were carried out four times. The mean recoveries were in the range between 99 - 108% with a trend of full recovery and of good reproducibility. This range is within the acceptable recovery limits (90 - 110%).

The limit detection of this analysis was assessed for all the vitamin E isomers in the range of concentration of $0.1 - 0.9 \,\mu g \, ml^{-1}$. The results indicated that the detector has sufficient sensitivity for the method where it provides a good margin for the identification at the lowest concentration of vitamin E.

Conclusion

In summary, UPLC has been proved to be an effective technique for analyzing Toc and TCT in plasma samples. The analysis required shorter time to complete (2.50 min), which is two to three time faster as compared to currently reported HPLC methods [13,15]. This system which used 1.7-µm particles provides significantly more resolution while reducing run times and improves sensitivity for the analyses of plasma sample.

The condition of chromatography must be selected to allow complete baseline separation and able to quantitate all the vitamin E isomers. This method was validated by linearity, precision, accuracy, recovery and limits of detection and quantification. This method is low in cost where the liquid-liquid extraction sample preparation allows fast quantitation of the vitamin E constituents from various samples.

In conclusion, analytical performance of the method used in this study is satisfactory.

Shahidee et al: DETERMINATION OF VITAMIN E ISOMERS IN PLASMA USING ULTRA PERFORMANCE LIQUID CHROMATOGRAPHY

Acknowledgement

Authors acknowledge the facilities provided by Centre for Pathology Diagnostic and Research Laboratories (CPDRL), Faculty of Medicine Universiti Teknologi MARA. The research was funded by Fundamental Research Grant Scheme (600-RMI/ST/FRGS 5/3/Fst (15/2009)).

References

- 1. Qureshi AA, Karpen CW, Nor RM, Qureshi N, Papasian CJ, Morrison DC and Folts JD (2011). Tocotrienol-Induced Inhibition of Platelet Thrombus Formation and Platelet Aggretation in Stenosed Canine Coronary Arteries. *Lipid in Health and Disease*, 10:58, 1-13.
- 2. Tan B (2005). Appropriate Spectrum Vitamin E and New Perspectives on Desmethyl Tocopherols and Tocotrienols. *The Journal of the American Nutraceutical Association*, 8:1, 35-42.
- 3. Llacuna L, Fernández A, Von Montfort C, Matías N, Martínez L, Caballero F, Antoni Rimola, Montserrat Elena, Morales A, Fernández-Checa JC and García-Ruiz C (2011). Targeting Cholesterol at Different Levels in the Mevalonate Pathway Protects Fatty Liver against Ischemia–Reperfusion Injury. *Journal of Hepatology*, 54, 1002–1010
- 4. Pearce BC, Parker RA and Deason ME (1992). Hypocholesterolemic Activity of Synthetic and Natural Tocotrienols. *Journal of Medicine Chemistry*, *35*:20, 3595–3606.
- 5. Schauss AG (2009). Tocotrienols: A Review. In Watson RR and Preedy VR, Tocotrienols Vitamin E Beyond Tocopherols. *CRC Press Taylor & Francis Group*. 3-12.
- 6. Abidi S. (2000). Chromatographic Analysis of Tocol-Derived Lipid Antioxidants. *Journal of Chromatography A*, 881:1-2, 197-216.
- Citová I, Havlíková L, Urbánek L, Solichová D, Nováková L and Solich P (2007). Comparison of a Novel Ultra-Performance Liquid Chromatographic Method for Determination of Retinol and α-Tocopherol in Human Serum with Conventional HPLC using Monolithic and Particulate Columns. *Anal Bioanal Chem*, 388:3, 675–681.
- 8. Paliakov EM, Crow BS, Bishop MJ, Norton D, George J and Bralley JA (2009). Rapid Quantitative Determination of Fat-Soluble Vitamins and Coenzyme Q-10 in Human Serum by Reversed Phase Ultra-High Pressure Liquid Chromatography with UV Detection. *Journal of Chromatography B*, 877:1-2, 89-94.
- 9. Xu Z (2002). Analysis of Tocopherols and Tocotrienols. In Wrolstad RE, Current Protocols in Food Analytical Chemistry. *John Wiley & Sons Inc.* D1.5.1-D1.5.12.
- 10. Fountain KJ, Grumbach ES, Xu J, Messina CJ and Diehl MD (2008). Application of Novel Ethylene Bridged Hybrid Particles for Hydrophilic Interaction Chromatography. *Milford: Water Corporation*.



SYNTHESIS AND CHARACTERISATION OF PALLADIUM(II) SCHIFF BASE COMPLEXES AND THEIR CATALYTIC ACTIVITIES FOR SUZUKI COUPLING REACTION

(Sintesis dan Pencirian Palladium(II) Bes-Schiff Kompleks dan Aktiviti Sebagai Pemangkin untuk Tindak Balas Suzuki)

Amalina Mohd Tajuddin¹, Hadariah Bahron^{1*}, Karimah Kassim¹, Wan Nazihah Wan Ibrahim¹ and Bohari M.Yamin²

¹Faculty of Applied Sciences, Universiti Teknologi MARA, 40450 Shah Alam, Selangor, Malaysia ²School of Chemical Sciences and Food Technology, Faculty of Science & Technology, Universiti Kebangsaan Malaysia, 43600 UKM Bangi, Selangor, Malaysia

*Corresponding author: hadariah@salam.uitm.edu.my

Abstract

The syntheses, physico-chemical and spectroscopic characterization of salicylaldimine-type Schiff-base ligands (Hapbam, HapFbam) and their novel mononuclear Pd(II) complexes (HapbamPd, HapFbamPd) are reported herein. The compounds were characterized by elemental analysis, FT-IR, ¹H NMR as well as magnetic susceptibility measurements. X-ray crystallography investigation of HapbamPd revealed that the Schiff bases behave as singly charged bidentate ligands, coordinating to the palladium centre in the ratio of ligand:metal of 2:1. The geometry of the palladium centre was a perfect square planar. The catalytic potential of the Pd(II) complexes for Suzuki coupling reaction were investigated and monitored using GC. It was observed that both Pd(II) complexes displayed properties of good catalysts for the reaction, indicated by more than 90% conversion of the starting materials to the biphenyl product after 12 hours of reaction time at 100°C in inert conditions. The catalytic activity was compared with that of commercially available palladium(II) acetate.

Keywords: Schiff base, Palladium(II), Suzuki reaction

Abstrak

Sintesis, fizik-kimia dan pencirian spektroskopi ligands-bes Schiff salicylaldimine jenis (Hapbam, HapFbam) dan novel mononuklear mereka Pd(II) kompleks (HapbamPd, HapFbamPd) dilaporkan di sini. Sebatian dicirikan oleh unsur analisis, FT-IR, ¹H NMR serta ukuran kerentanan magnet. Potensi sebagai pemangkin Pd(II) kompleks bagi tindak balas gandingan Suzuki disiasat dan dipantau menggunakan GC. Diperhatikan bahawa kedua-dua Pd(II) kompleks dipaparkan hartanah pemangkin yang baik untuk tindak balas yang ditunjukkan oleh lebih daripada 90%. Penukaran bahan permulaan untuk produk terpoliklorin selepas 12 jam masa tindak balas pada 100°C dalam keadaan lengai. Aktiviti pemangkin dibandingkan dengan palladium(II) asetat yang boleh didapati secara komersial.

Kata kunci: bes-Schiff, Palladium(II), tindak balas Suzuki

Introduction

Schiff bases are an important class of ligands in coordination chemistry and have studied extensively [1] as they are selective and sensitive toward various metal ions. Metal complexes of Schiff bases have found diverse applications in addition to interesting structural chemistry. Metal complexes containing Schiff-base ligands also have shown attractive properties such as antibacterial behaviour, exhibit interesting magnetic properties and catalytic oxidation [2].

Palladium is a versatile metal for homogeneous and heterogeneous catalysis [3,4]. A large number of carbon-carbon bond forming reactions such as the Heck and Suzuki coupling are facilitated by catalysis with palladium compounds. During the past 10 years, there has been considerable interest in the development of new phosphorus free palladium catalysts for higher activity, stability and substrate tolerance that allow reactions to be carried out under milder reaction conditions.

This paper aims to report the synthesis and characterization bidentate Schiff base ligands and their novel palladium(II) complexes and also their catalytic activities for Suzuki coupling reaction, as shown in Figure 1.

Experimental

All the chemicals and solvents received from commercial suppliers were used as received. Carbon, hydrogen and nitrogen analyses were carried out on Thermo Finnigan Flash EA 2000 Elemental Analyser. The melting points were determined using Buchii-B454. IR spectra were obtained as potassium bromide (KBr) pellets using a Perkin-Elmer model 1750X FTIR spectrophotometer. ¹H NMR spectra were recorded on a Bruker Varian-300MHz spectrometer with chemical shifts given in ppm from the internal TMS or centre line of CDCl₃. Magnetic measurements were carried out using the Guoy method with Hg[(Co(SCN)₄] as calibrant on Sherwood Auto Magnetic Susceptibility Balance. Molar conductance of the palladium(II) complexes were determined in CHCl₃ (~10⁻³ M) at room temperature using a Mettler Toledo Inlab 730 conductivity meter. A single-crystal x-ray diffraction investigation was carried out on Bruker SMART APEX CCD area-detector diffractometer.

Figure 1: Synthesis scheme of the Schiff base ligands and their Pd(II) complexes

Synthesis of Ligands

(a) Synthesis of Hapbam

An ethanoic solution of 2-hydroxyacetophenone (50 mmol, 6.8126 g) was heated to boiling. Benzylamine (50 mmol, 5.3662 g) was also boiled in ethanol (10 mL). The two hot solutions were mixed in a round-bottomed flask to give a bright yellow solution. The mixture was heated under reflux for one hour. More yellow solid was appeared when the solution was allowed to cool slowly to room temperature. The solid was filtered off, washed with ice-cold ethanol and air-dried at room temperature with 76.3% yield.

(b) Synthesis of HapFbam

An ethanoic solution of 2-hydroxyacetophenone (50 mmol, 6.8112 g) was heated to boiling. 4-fluorobenzylamine (50 mmol, 6.2647 g) was also boiled in ethanol (10 mL). The two hot solutions were mixed in a round-bottomed flask to give a bright yellow solution. Upon cooling, bright yellow solid was appeared without heated under reflux. The solid was filtered off, washed with ice-cold ethanol and air-dried at room temperature with 82.7% yield.

Synthesis of Complexes

(a) Synthesis of HapbamPd

The ligand, Hapbam, (5 mmol, 1.1271 g) was dissolved in hot ethanol (20 mL) in a round-bottomed flask. Palladium(II) acetate (2.5 mmol, 0.5618 g) was dissolved separately in hot ethanol (40 mL) and added into the flask containing the ligand solution. The mixture was stirred and refluxed for 5 hours upon which green solid was formed. It was isolated by gravity filtration, washed with ice-cold ethanol and air dried at room temperature. The solid product was recrystallized from chloroform yielding yellow crystals with 87.8% yield.

(b) Synthesis of HapFbamPd

The ligand, HapFbam, (2 mmol, 0.4877 g) was dissolved in acetonitrile (30 mL) in a round-bottomed flask. Palladium(II) acetate (1 mmol, 0.2251 g) was dissolved separately in acetonitrile (20 mL) and added into the flask containing the ligand solution. The mixture was stirred and refluxed 5 hours upon which turmeric yellow solid was formed. It was isolated by gravity filtration, washed with ice-cold acetonitrile and air dried at room temperature with 48.5% yield.

General Procedure for The Suzuki Coupling Reaction

The general procedure was as followed: iodobenzene (1 mmol, 0.2 g), phenylboronic acid (0.2 mmol, 0.24 g), triethylamine (2.4 mmol, 0.24 g), Et₃N, palladium(II) Schiff base (1 mmol%) (HapbamPd, HapFbamPd) and solvent DMA (10 mL) were mixed together in Radley's 12-placed reaction carousel and refluxed (100°C) whilst being purged with nitrogen. The reaction was monitored regularly using GC.

Figure 2: Suzuki reaction catalyzed by Pd catalysts

Results and Discussion

Elemental Analysis

The analytical data of the compounds are presented in Table 1 and are in good agreement with the theoretical values.

Ligand/Complex	Empirical Formula	Colour	Melting Point (°C)	Eleme	ntal Analys (found)	sis (%)	$\Lambda_{ m M}^{\;\;a}$
				С	Н	N	<u> </u>
Hapbam	$C_{15}H_{15}NO$	Yellow	120-122	79.97	6.71	6.22	-
-				(79.42)	(6.36)	(6.15)	
HapbamPd	$C_{30}H_{28}N_2O_2Pd$	Moss green	248-257	63.82	4.59	5.32	0.00
				(64.58)	(4.97)	(4.94)	
HapFbam	$C_{15}H_{14}FNO$	Yellow	140-142	74.06	5.80	5.76	-
_				(73.65)	(5.46)	(5.78)	
HapFbamPd	$C_{30}H_{26}F_2N_2O_2Pd$	Turmeric	235-237	60.97	4.43	4.74	0.00
-		yellow		(60.81)	(4.49)	(4.66)	

Table 1: Analytical data for the Hap-ligands series and their complexes

Based on the elemental analysis results, the structures of the ligands and palladium(II) complexes were indicated to be as those predicted (Figure 1). The melting points of the parent ligands were typically lower than those of the complexes.

FTIR Spectroscopy

Infrared spectra of ligands and complexes are presented in Figure 3 and 4 while the data of the compounds are presented in Table 2. The strong bands around 1619-1586 cm⁻¹ are assignable to v(C=N) while the v(Pd-O) and v(Pd-N) bands in Pd(II) complexes appeared in the regions of 700-500 cm⁻¹ and 440-500 cm⁻¹, respectively. The IR frequencies are in agreement with those previously reported [5]. Comparing the v(C=N) and v(C-O) values for Hapbam/HapbamPd and HapFbam/HapFbamPd, it was observed generally that the peaks experienced a redshift i.e. shifted to a lower frequency upon complexation to Pd(II). The shifting indicated that both the N and O donor atoms in the ligands were involved in the chelation to the metal centre. The nature of this interaction is such that it reduces the electron density on the C=N and C-N moieties as shown by the reduction of the frequency implying the reducing strength of the C=N and C-N bonds. It is also observed that the C-OH peaks in both the ligands disappeared upon complexation with Pd that indicated the participation of the phenolic oxygen on bonding with the metal centre. The phenolic protons were replaced by the Pd²⁺ cations forming an ionic bond of O-Pd.

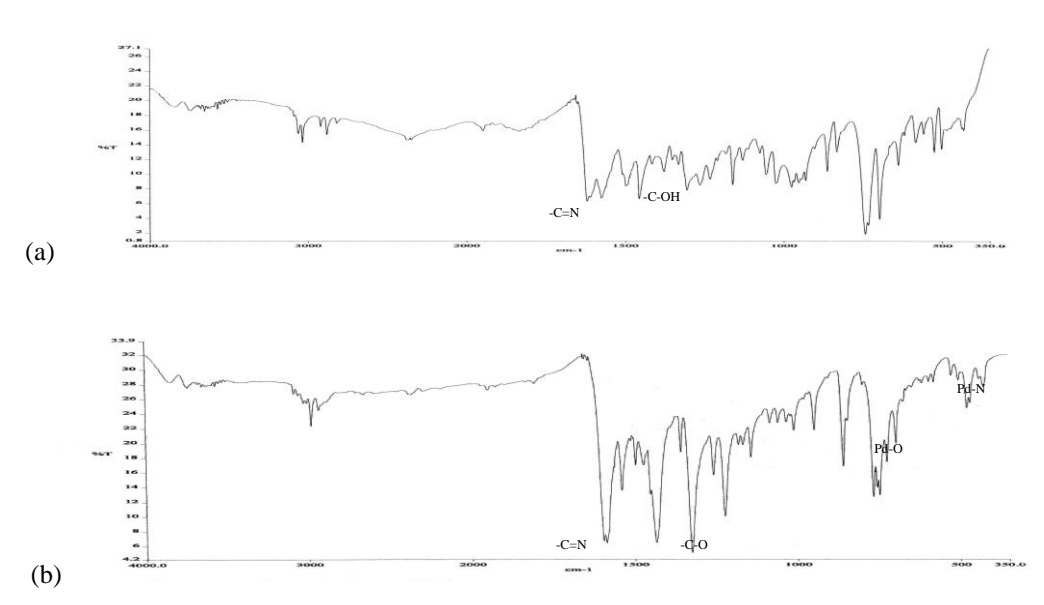
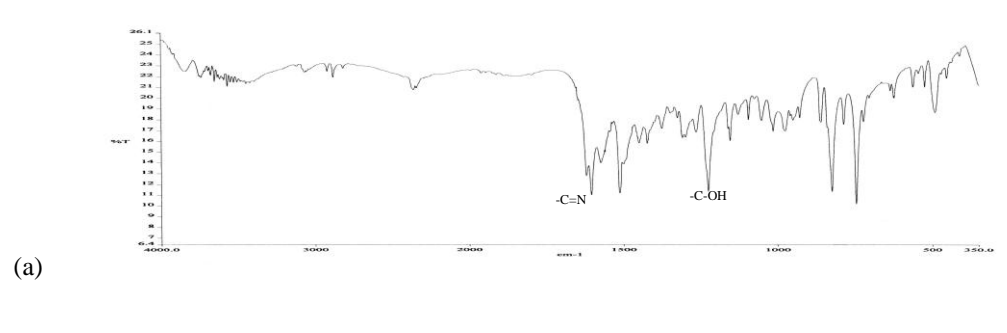


Figure 3: Infrared spectra of (a) Hapbam and (b) HapbamPd



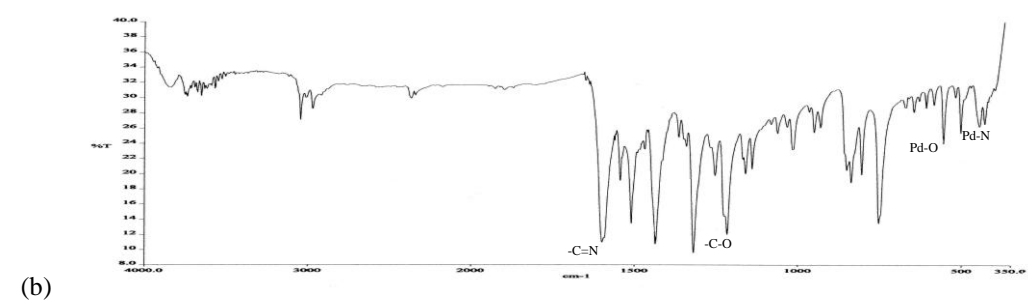


Figure 4: Infrared spectra of (a) HapFbam and (b) HapFbamPd

Table 2: Infrared spectra data for ligands and palladium(II) complexes

Ligand/Complex		Frequency (cm ⁻¹)						
	C=N	C-N	-CH	С-ОН	Pd-O	Pd-N		
Hapbam	1619 (s)	1376 (w)	2878 (w)	1304 (w)	-	-		
HapbamPd	1586 (s)	1355 (w)	2977 (w)	-	695 (w)	476 (w)		
HapFbam	1604 (s)	1310 (w)	2879 (w)	1226 (s)	-	-		
HapFbamPd	1598 (s)	1319 (s)	2969 (w)	-	556 (w)	446 (w)		

Nuclear Magnetic Resonance (NMR) Spectroscopy

The ¹H NMR data and spectra of Hapbam and HapFbam are presented in Table 3 and Figure 5 and 6, respectively. The OH peaks in Hapbam and HapFbam that were expected to appear in the downfield region (10-14 ppm) [6] of the spectra were not observed as the labile phenolic ¹H may have undergone a rapid exchange with the deuterium in the solvent. The presence of the methyl groups attached to the C=N was confirmed by the singlet appearing at 2.41 ppm. The ¹H of methylene and aromatic moieties were observed in 4.75-4.80 and 6.76-7.57 ppm, respectively.

Table 3: Significant	1H NMP	enactral	data fo	r ligande
Table 5. Significant	LIMINI LI	specual	uata 10	n nganus

Ligand/Complex	Assignment (ppm)						
	H-C-aromatic ^(m)	-CH ₂ ^(s)	$H_3C-C=N^{(s)}$	C-OH ^(s)			
Hapbam	6.76-7.56	4.80	2.41	N.D.			
HapFbam	6.81-7.57	4.75	2.41	N.D.			

s, singlet; m, multiplet; N.D., Not Detected

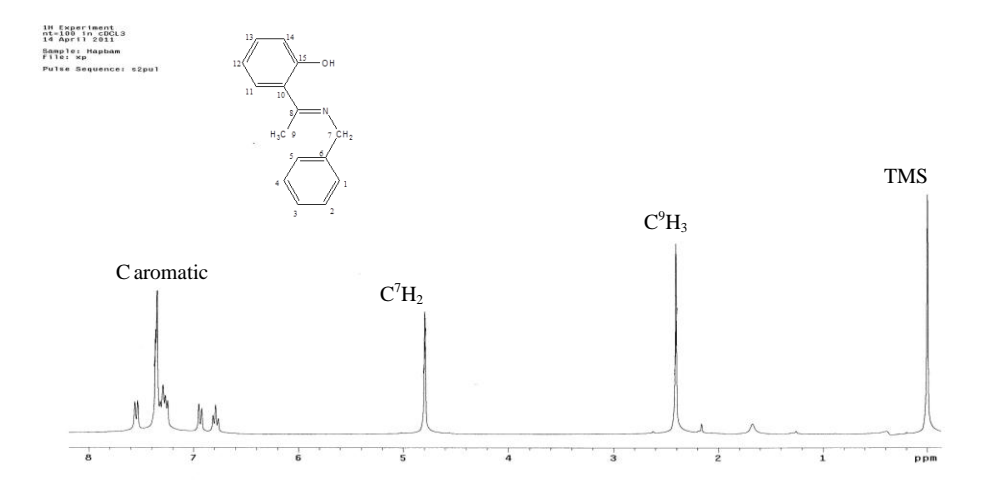


Figure 5: ¹H NMR spectrum of Hapbam

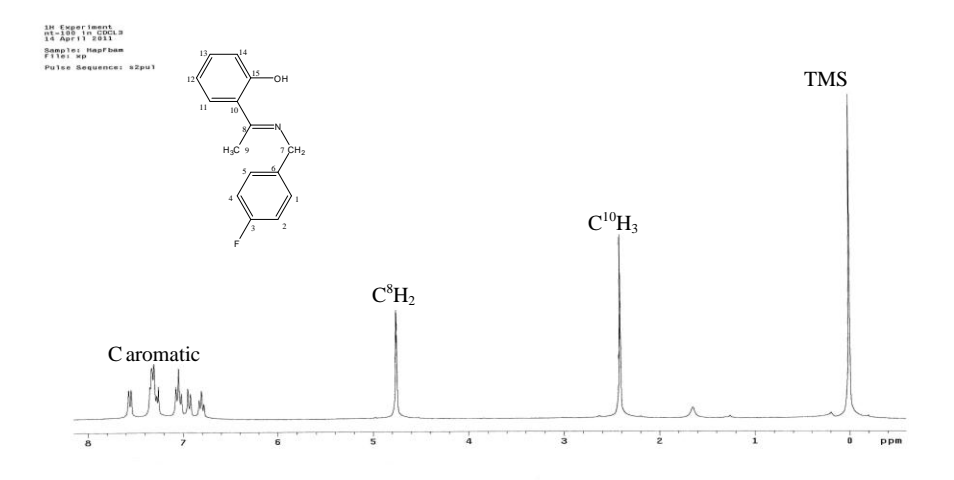


Figure 6: ¹H NMR spectrum of Hapbam

Molar Conductance and Magnetic Moment

The molar conductance values for the synthesized complexes were determined using $1x10^{-3}M$ CHCl₃ solutions, as shown in Table 1. Molar conductivity measurements conducted on the palladium(II) complexes revealed the non-conductivity nature of the solution at room temperature indicating the absence of any electrolytes [7]. These values show that there are no ions existing in the outer sphere coordination of the complexes. As expected, the magnetic susceptibility measurements showed diamagnetic behaviour reflected in the zero effective magnetic moment, $\mu_{eff} = 0$, in all of the complexes consistent with the 0 unpaired electrons of Pd(II) d^8 species having square planar geometry [8].

Single x-ray Crystallography

Structure of HapbamPd is shown in Figure 7 and selected bond lengths and angles are listed in Table 4.

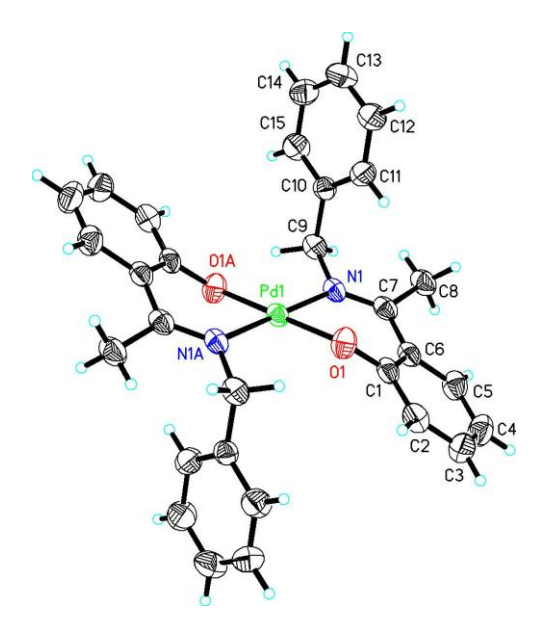


Figure 7: ORTEP diagram of HapbamPd with 50% probability ellipsoids [9]

Table 4: Bond lengths [A] and angles [°]	around Pd atom in HapbamPd
--	----------------------------

Atom1 - Atom2	Bond Length (Å)	Atom1 - Atom2	Bond Angle (°)
Pd1-O1	1.981 (2)	O1—Pd1—O1 ⁱ	180.00 (8)
Pd1-O1 ⁱ	1.981 (2)	O1—Pd1—N1	90.97 (10)
Pd1-N1	2.039 (2)	O1 ⁱ —Pd1—N1	89.03 (10)
Pd1-N1 ⁱ	2.039(2)	O1—Pd1—N1 ⁱ	90.97 (10)
		O1 ⁱ —Pd1—N1 ⁱ	89.03 (10)
		N1—Pd1—N1 ⁱ	180.00 (11)
		C1—O1—Pd1	120.0 (2)

The palladium atom lies on an inversion center and is coordinated to two ligand molecules through the oxygen and nitrogen atoms in a bidentate manner to form a perfect square planar geometry. The Pd1—O and Pd1—N bond lengths of 1.981 (2) and 2.039 (2)Å, respectively, in a square planar geometry are typical of square planar Pd(II) of Schiff bases. The dihedral angle between the benzene rings is 76.5 (2)°.

Catalytic Studies

The palladium complexes that have been prepared in this study were tested as catalysts in the Suzuki reactions of iodobenzene with phenylboronic acid in the presence of triethylamine (Et_3N) as base in N,N-dimethylacetamide at 100° C.

Triethylamine was chosen as a base due its capability to give the highest conversion compared to other bases. The reaction was monitored by measuring the % conversion of the aryl iodide starting material using gas chromatography [10]. The results are summarized in the Table 5. Phenylboronic acid was found to couple smoothly with iodobenzene providing excellent yields that were more than 90% after a 12-hour reaction. All these data indicate that the palladium complexes may be utilized as catalysts in the Suzuki reaction.

Table 5: Activities of palladium catalyst on Suzuki reaction between iodobenzene and phenylboronic acid

Catalyst	% Conversion After 12 hours
HapbamPd	94
HapFbamPd	99
$\overline{Pd}(OAc)_2$	96

Conclusion

Two ligands and their palladium(II) complexes have been successfully synthesized as confirmed by the characterization via various physico-spectral techniques. X-ray crystallography investigation of HapbamPd revealed that the Schiff bases behave as singly charged bidentate ligands, coordinating to the palladium centre in the ratio of ligand:metal of 2:1. The geometry of the palladium centre was a perfect square planar. The coordination occur through the azomethine nitrogen and phenyl oxygen, indicated by the redshift of the ν (C=N) and appearance ν (C-O) upon complexation. It was observed that both Pd(II) complexes displayed properties of good catalysts for the reaction, indicated by more than 90% conversion of the starting materials to the biphenyl product after 12 hours of reaction time at 100° C in inert conditions.

Acknowledgement

Thanks are gratefully extended to the Ministry of Higher Education of Malaysia, Universiti Teknologi MARA and Universiti Kebangsaan Malaysia for the research grants no: 600-RMI/ST/FRGS 5/3/Fst(7/2009) and UKM-OUP-BTT-28/2007.

References

- 1. He, Y., and Cai, C., (2010). Polymer-supported macrocyclic Schiff base palladium complex: An efficient and reusable catalyst for Suzuki cross-coupling reaction under ambient condition. *Catalysis Communications*, 12, 678-683.
- 2. Nayak, S., Gamez, P., Kozlevc`ar, B., Pevec, A., Roubeau, O., Dehnen, S., and Reedijk, J., (2011). Coordination compounds from the planar tridentate Schiff-base ligand 2-methoxy-6-((quinolin-8-ylimino)methyl)phenol (mqmpH) with several transition metal ions: Use of [FeIII(mqmp)(CH₃OH)Cl₂] in the catalytic oxidation of alkanes and alkenes. *Polyhedron*, 29, 2291–2296.
- 3. Cui, J., Zhang M., and Zhang, Y., (2010). Amino-salicylaldimine-palladium(II) complexes: New and efficient catalysts for Suzuki and Heck reactions. *Inorganic Chemistry Communications*, 1, 81-85.
- 4. Dhara, K., Sarkar K., Srimani D., Saha, S.K., Chattopadhyaye P., and Bhaumik, A., (2010). A new functionalized mesoporous matrix supported Pd(II)-Schiff base complex; an efficient catalyst for the Suzuki-Miyaura coupling reaction. *Dalton Transactions*, 39, 6395–6402.
- 5. Ben-saber A.M., Maihub A.A., Hudere S.S., and El-ajaily M.M., (2005). Complexation behavior of Schiff base toward transition metal ions. *Microchemical Journal*, *81*, 191-194.
- 6. Soliman, A.A., and Linert, W., (1999). Investigation on New Metal Chelates of 3-methoxy -salicylidene-2-aminothiphenol Schiff base. *Thermochimica Acta*, *338*, 67-75.

- 7. Raman, N., Raja, Y.P., and Kulandaisory, A., (2001). Synthesis and characterisation of Cu(II), Ni(II), Mn(II), Zn(II) and VO(II) Schiff base complexes derived from *o*-phenylenediamine and acetoacetanilide. *Journal of Chemical Sciences*, 113, 183-189.
- 8. Aslantas, M., Kendi, E., Demir, N., Sabik, A.E., Tümer, M., and Kertmen, M., (2009). Synthesis, spectroscopic, structural characterization, electrochemical and antimicrobial activity studies of the Schiff base ligand and its transition metal complexes. *Spectrochimica Acta Part A*, 74, 617-624.
- 9. Mohd Tajuddin, A., Bahron, H., Wan Ibrahim, W.N., and Yamin, B.M., (2010). Bis{2-[1-(benzylimino)ethyl]phenolato}-palladium(II). *Acta Crystallographic*, E66, m1100.
- 10. Brayton, D.F., Larkin, T.M., Vicic, D.A., and Navarro, O., (2009). Synthesis of a bis(phenoxyketimine) palladium(II) complex and its activity in the Suzuki-Miyaura reaction. *Journal of Organometallic Chemistry*, 694, 3008-3011.



FLUORINE-18: CURRENT APPROACH IN RADIOLABELLING AND RADIATION SAFETY ASPECTS

(Fluorin-18: Pendekatan Semasa dalam Pengradiopenglabelan dan Aspek Keselamatan Sinaran)

Suzilawati Muhd Sarowi¹*, Noriah Ali¹ and Noratikah Mat Ail²

¹Radiation Safety Division, Malaysian Nuclear Agency, 43000 Kajang, Selangor, Malaysia. ²Nuclear Medicine Department, Ground Floor, Putrajaya Hospital,Precinct 7, 62250 Putrajaya, Malaysia.

*Corresponding author: suzie@nuclearmalaysia.gov.my

Abstract

Positron Emission Tomography (PET) imaging has currently become an important technique to study physiological, biochemical and pharmacological functions in humans. The radiopharmaceuticals or tracers for the PET scan incorporating the positron emitting radioisotopes such as Fluorine-18, Carbon-11, Nitrogen-13 and Oxygen-15. A Fluorine -18 (¹⁸F) is oftenly used in development of radiopharmaceuticals due to its favourable physical and nuclear characteristics. By far, the most common radiopharmaceutical used in PET imaging is 2-[¹⁸F]-fluoro-2-deoxy-D-glucose, or [¹⁸F]FDG. There are several approaches in radiolabelling using ¹⁸F and the disadvantage is the time consuming multi-step reactions. Therefore, there is a need to make the radiolabelling prosess more speedy. Once working with radionuclide, the radiation safety is concerned and must be addressed. This paper will discuss on the current approach in the ¹⁸F radiolabelling using "click reaction" based on paper review and a practical aspects of radiation safety. The advantages of this system are cheap, does not require an inert atmosphere, can be performed in the presence of water and eliminates the need for a base. As a result, the radiolabelling prosess can be performed in shorter time and a good yield.

Keywords: Fluorine-18, click reaction and radiation safety

Abstrak

Pengimejan Tomografi Pancaran Positron (PET) kini telah menjadi satu teknik penting untuk mengkaji fungsi fisiologi, biokimia dan farmakologi pada manusia. Radiofarmaseutikal atau pengesan untuk imbasan PET menggabungkan radioisotop pemancar positron seperti Fluorin-18, Karbon-11, Nitrogen-13 dan Oksigen-15. Fluorine -18 (¹⁸F) kerap digunakan dalam pembangunan radiofarmaseutikal ini disebabkan oleh ciri-ciri fizikal dan nuklearnya yang menggalakkan. Setakat ini, radiofarmaseutikal yang paling biasa digunakan dalam pengimejan PET ialah 2 - [18F]-fluoro-2-deoxy D-glukosa, atau [¹⁸F] FDG. Terdapat beberapa pendekatan dalam radiopenglabelan menggunakan ¹⁸F dan kelemahannya ialah melibatkan pelbagai langkah tindakbalas yang memakan masa. Oleh itu, terdapat keperluan untuk membuat proses radiopenglabelan yang lebih cepat. Apabila bekerja dengan radionuklid, keselamatan sinaran dititikberatkan dan mesti ditangani. Kertas kerja ini akan membincangkan pendekatan semasa dalam radiopenglabelan ¹⁸F menggunakan "tindak balas klik" berdasarkan kajian semula kertas kerja dan aspek-aspek praktikal keselamatan sinaran. Kelebihan sistem ini adalah ia murah, tidak memerlukan atmosfera yang lengai, boleh dibuat dengan kehadiran air dan tanpa keperluan asas. Keputusannnya, proses radiopenglabelan boleh dilakukan dalam masa yang lebih singkat dan hasil yang baik.

Kata kunci: Fluorin-18, tindak balas klik dan keselamatan sinaran

Introduction

Positron Emission Tomography (PET) imaging has become an important technique to study physiological, biochemical and pharmacological functions in humans. It is a non-invasive imaging technique that can measure the concentration of the tracer in tissues accurately due to its high sensitivity and high spatial resolution.[1,2] The radiopharmaceuticals or tracers for the PET scan incorporating the positron emitting radioisotopes such as Fluorine-

Suzilawati et al: FLUORINE-18: CURRENT APPROACH IN RADIOLABELLING AND RADIATION SAFETY ASPECTS

18, Carbon-11, Nitrogen-13 and Oxygen-15. But, a Fluorine -18 (¹⁸F) is oftenly used for radiolabelling due to its favourable physical and nuclear characteristics [3].

The most common radiopharmaceutical used in PET imaging is 2-[¹⁸F]-fluoro-2-deoxy-D-glucose, or [¹⁸F]FDG. However, its specificity in cellular dynamics in regards to energy requirements has limited its use in molecular imaging. [4] Therefore, there is a need for new PET radiopharmaceuticals other than [¹⁸F]FDG as there are still many biological aspects of cancer that cannot be measured by [¹⁸F]FDG alone.[5] To date, several approaches in radiolabelling using ¹⁸F were developed. But the disadvantage is the time consuming multi-step reactions which is need for improvement to make the radiolabelling proses more speedy. Table 1 shows some of the different approaches for labelling biomolecules with ¹⁸F.

Recently, a click chemistry which uses fewer chemical reactions and milder conditions to generate labelled substrates compared to other current methods is discovered.[6] The click reaction is high yielding and easy to perform using readily available reagents and starting materials. It is also tolerant to water, and the subsequent work-up and product isolation are straight-forward.[7,8] A variety of Cu(I) sources have been used in the Huisgen cycloaddition reaction including CuI salts such as copper iodide [9] and copper bromide [10] however, this type of reaction needs a large of excess of copper and ligand to work efficiently.[11] The use of metallic copper has also been employed, however, the reaction with copper turnings took a long time to form the desired triazole in good yield [12].

The most common click reactions is using an in situ reduction of a Cu(II) salt system to produce Cu(I), such as Cu(II) sulfate with sodium ascorbate as reducing agent. The click reaction forms a 1,2,3-triazole via the Cu(I) catalyzed 1,3-cycloaddition of azides and terminal alkynes (Fig.1). The advantages of this system is it is cheap, does not require an inert atmosphere, can be performed in the presence of water and eliminates the need for a base.[12,13] Marik and Sutcliff (2006) were demonstrated that peptides could be efficiently labelled with [18F]alkynes in high yield, under mild conditions, and with rapid preparation times of 30 min.[14] The first sugar analog successfully labelled via click chemistry was also demonstrated by Korean.[15] This paper described how 4-[18F]fluoro-1-butyne was successfully synthesized for labelling of biomolecules.

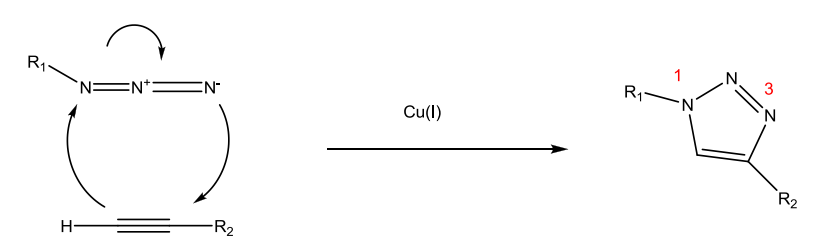


Fig. 1: The 'click reaction' of an azide and terminal alkyne to give a 1,2,3-triazole.(Adapted from ref.16)

Table 1: Different	approaches for	labelling	biomolecules	with ¹⁸ F.	(Adapted from	ref.17, 18	()
I dole 1. Dillerelli	approactics for	Idocining	Didilioloculos	WILLI I .	(1 luapicu II om	101.1/, 10	, ,

Method	¹⁸ F labelling agent	Preparation	Radiochemical
		time (min)	yield (%)
Acylation	4-Nitrophenyl-2-[¹⁸ F]fluoropropionate [NPFP]	90	60
	N-Succinimidyl-4 [¹⁸ F]fluorobenzoate [SFB]	35-100	25-60
Imidation	3- [¹⁸ F]Fluoro-5-nitrobenzimidate	45	20-23
Alkylation	4- [18F]Fluorophenacyl bromide	75	28-40
Click reaction	[¹⁸ F]fluoroalkynes	10-15	36-81

Once working with radionuclide, the radiation safety is concerned and must be addressed. Fluorine-18 has physical half-life of 109.8 min. The principle radiations of ¹⁸F are 511-keV annihilation photons (1.94 per decay) and 640-keV (Emax) positron (0.97 per decay). It can be exposed to human by ingestion, inhalation, puncture, wound and skin contamination absorption. Thus, As Low As Reasonable Achievable (ALARA) guideline should be followed.

Materials and Methods

Chemicals and solvents were obtained from Sigma – Aldrich Chemical Company and used without further purification. All reactions were performed in standard glassware. Fluorine-18 was produced on a Cyclotron via the ¹⁸O(p, n)¹⁸F nuclear reaction. A fluorination reactions were carried out in the presence of potassium carbonate and the amino polyether Kryptofix_{2,2,2} in acetonitrile under nitrogen.

Firstly, the non-radiolabelled for standard on High Purification Liquid Chromatography (HPLC) was obtained. Next, radiolabelled the material which radiofluorination was carried out prior to the click chemistry. The scheme of the radiolabelling of targetted material using click reaction was shown in (Fig.2).

Fig.2: Radiolabelling of biomolecule using click reaction.

Butynyl tosylate (5) (refer scheme 1 in Results and Discussion) was synthesized as in literature.[15] The product was purified using flash column chromatography (4:1 hexane-ethyl acetate). The terminal fluoroalkyne (1) was prepared by nucleophilic substitution of the corresponding tosylate, (5) with [18 F]fluoride. The [18 F]fluoride anion was produced by the 18 O(p,n) 18 F nuclear reaction in the cyclotron machine. A solution of Kryptofix (K₂₂₂) and potassium carbonate, K₂CO₃ were added to the [18 F]fluoride vial. The solvent was evaporated under a stream of nitrogen at 100°C with a reducing vacuum. This azeotropic drying was repeated twice by further addition of anhydrous acetonitrile. The precursor, butynyl tosylate (5) was dissolved in CH₃CN and added to the dried K_{2,2,2}.K₂CO₃.K¹⁸F complex. The reaction was heated for 10-20 min and the volatile product, 4-[18 F]fluoro-1-butyne (bp 45 °C) distilled and transfered into another vial for use in the click reaction.

In term of radiation safety, dosimetry should always be monitored. This can be performed by wearing radiation dosimetry monitoring badges [body & ring] whenever handling ¹⁸F.[21] The labeling work should be done behind a shielding and the activity of ¹⁸F also should always monitored. General precautions include the personal protection equipment such as glove, safety glass and lab coat.

Results and Discussion

1. A route to obtain the cold standard for HPLC

Scheme 1: A route to obtain the cold standard for HPLC

No.	Reagents	Conditions	Yield (%)
a	Cu(II) sulfate,	room temperature,	84
	sodium ascorbate,	2 hours	
	tert- butanol, water		
b	Diethylaminosulfur trifluoride,	0 °C,	68
	Dichloromethane	30 minute	

Table 2: The result of reaction in scheme 1(Adapted from ref.15)

2. A route to label the target material

$$= \underbrace{\begin{array}{c} -OH \\ 4 \end{array}} \xrightarrow{a} = \underbrace{\begin{array}{c} -OTs \\ 5 \end{array}} \xrightarrow{b} = \underbrace{\begin{array}{c} -18F \\ 1 \end{array}} \xrightarrow{R-N_3} \underbrace{\begin{array}{c} N=N \\ R-N_3 \end{array}} \xrightarrow{18F}$$

Scheme 2: A route to label the target material.

No. Reagents Conditions Yield (%) p-toluenesulfonyl chloride, 0 °C. 72 a Triethylamine, Dichloromethane 3 hours K[¹⁸F]fluoride/Kryptofix₂₂₂ complex, 100 °C, Not determined as through b Acetonitrile. 10-20 minutes distillation process Cu(I) Iodide, sodium ascorbate, 2,6-90 °C, c lutidine/DIEA 10 minutes

Table 2: The result of reaction in scheme 1(Adapted from ref.14,15)

The click reaction is recent method in radiolabelling field. First of all, the non-radiolabelled standard was synthesized (Scheme 1). To obtain this standard, the fluorination was carried out using diethylaminosulfur trifluoride (DAST), a common fluorinating agent for the conversion of aliphatic alcohol into alkyl fluorides.[19] The cold standard product (7) (non radiolabelled) is necessary to be used in authenticating the ¹⁸F radiolabelled derivative and in developing HPLC conditions for radiolabelling and purification.

The labeling of (2) began with radiofluorination of the tosylated precursor (5) to give $4-[^{18}F]$ -fluoro-1-butyne (1) via nucleophilic substitution (Scheme 2). To a dried $K[^{18}F]$ -fluoride/Kryptofix₂₂₂ complex, the tosylated alkyne (5) in acetonitrile was added and the reaction facilitated by heating, after which distillation was used to obtain the desired

compound. The next step was click reaction of (1) with the molecule (2) (scheme 2). Marik et. al and Kim et. al used acetonitrile for the click reaction during the radiofluorination instead of tert butanol (m.p. $23-26^{\circ}C$), as the latter would freeze during the distillation at $-50^{\circ}C$.

It was mention earlier that the most common click reactions is use an in situ reduction of a Cu(II) salt system to produce Cu(I), such as Cu(II) sulfate with sodium ascorbate as reducing agent (Scheme 1). But, in the click reaction to incorporate the [¹⁸F]fluoroalkyne (1) with molecule (2), the optimisation of catalytic system using Cu(I) with the presence of nitrogen base (2,6-lutidine, DIEA) showed a better result (Scheme 2). Sodium ascorbate was required to prevent oxidation of Cu(I) to Cu(II) by atmospheric oxygen (Scheme 2). The reagents were combined and the reaction stirred for 10 min after which, the reaction mixture containing the desired radiolabelled product (3) was filtered to remove any precipitate. The reaction mixture was then directly injected onto a HPLC column and the product (3) was collected. An aliquot from this fraction was co-injected with the cold fluorine standard (7) which was confirming the presence of the radiolabelled target (3)[14, 15] The biomolecule was successfully labelled with ¹⁸F via click chemistry.

Above all, occupational radiation exposure is concerned. The dose limit for radiation workers is 20 mSv/year. By reinforcing the ALARA concepts; time, distance and shielding, it will minimize radiation exposure to the occupational worker. Radiation dose is directly related to the time exposure. Accordingly, the time of handling the ¹⁸F must be done as fast as posible. These study, 10 min of labelling time seems as the quick method and complies with the ALARA concepts. In the literature, 1.61 in. of lead are required to shield the 511-keV photons of ¹⁸F effectively.[20] The rate of exposure will be considerably reduced according to the inverse square law. Therefore, if possible, include the use of long-handled tongs while handling the ¹⁸F. An operational survey meter present in the work area and turned on whenever ¹⁸F is handled, the activity of the radiation source also always measured, so that any external exposure issues will be immediately apparent and hence quickly addressed.[21]

Conclusion

PET imaging of tumours is important because it is a non-invasive functional imaging modality which can provide information not only about the location of the disease but also about how the target area (organ) is functioning. These group, Marik et.al (2006) and Kim et.al (2008) have described the development of a new method for radiolabelling various biomolecule (sugar and peptide) for use in PET imaging through the utilisation of click chemistry. Their work resulted in the labelling of biomolecules via click chemistry is more easy and fast (10 min) compared to other methods as described in Table 1. The radiochemical yield was reported as very good which is 98%.[14] This method is promising to be used in the development of PET radiopharmaceuticals. For the safety purposes, ALARA concepts must be applied to reduce an occupational radiation exposure.

Acknowledgement

Malaysian Nuclear Agency in collaboration with Ministry of Health on setting up the National Cyclotron Facility in Putrajaya Hospital.

References

- 1. Comar D(ed). Positron emission tomography for drug development and evaluation. 1995: Kluwer Academic Publishers, Boston.
- 2. Dijkgraaf I, Boerman OC, Oyen WJG, Corstens FHM, Gotthardt M. (2007) Development and application of peptide-based radiopharmaceuticals. *Anti-Cancer Agents in Medicinal Chemistry*. 7: 543-551.
- 3. Welch MJ, Redvanly CS. Handbook of radiopharmaceuticals, radiochemistry and applications. 2003: John Wiley & Sons Ltd., England.
- 4. Mercer JR. (2007) Molecular imaging agents for clinical positron emission tomography in oncology other than fluorodeoxy glucose (FDG): applications, limitations and potential. *Journal of Pharmacy and Pharmaceutical Sciences*. 10: 180-202.
- 5. Nanni C, Rubello D, Al-Nahlas A, Fanti S. (2006) Clinical PET in oncology: not only FDG. *Nuclear Medicine Communications*. 27: 685-688.
- 6. Schirrmacher R, Wangler C, Schirrmacher E. (2007) Recent developments and trends in 18F-radiochemistry: syntheses and applications. *Mini Review in Organic Chemistry*. 4: 317 329.

Suzilawati et al: FLUORINE-18: CURRENT APPROACH IN RADIOLABELLING AND RADIATION SAFETY ASPECTS

- 7. Kolb HC, Finn MG, Sharpless KB. (2001) Click chemistry: diverse chemical function from a few good reactions. *Angewandte Chemie International Edition*. 40: 2004-2021.
- 8. Kolb HC, Sharpless KB. (2003) The growing impact of click chemistry on drug discovery. *Drug Discovery Today*. 8: 1128-1136.
- 9. Tornoe CW, Christensen C, Meldal M. (2002) Peptidotriazoles on solid phase: [1,2,3]-triazoles by regiospecific copper(I)-catalyzed 1,3-dipolar cycloadditions of terminal alkynes to azides. *Journal of Organic Chemistry*. 67: 3057-3064.
- 10. Van Kasteren SI, Kramer HB, Jensen HH, Campbell SJ, Kirkpatrick J, Oldham NJ, Anthony DC, Davis BG. (2007) Expanding the diversity of chemical protein modification allows post-translational mimicry. *Nature*. 446: 1105-1109.
- 11. Hong V, Presolski SI, Ma C, Finn MG. (2009) Analysis and optimization of copper-catalyzed azide–alkyne cycloaddition for bioconjugation. *Angewandte Chemie International Edition*. 48: 9879-9883.
- 12. Bock VD, Hiemstra H, Maarseveen JH. (2006) Cu^I- catalyzed alkyne-azide "click" cycloaddition from a mechanistic and synthetic perspective. *European Journal Organic Chemistry*. 1: 51-68.
- 13. Hein CD, Liu XM, Wang D. (2008) Click chemistry, a powerful tool for pharmaceutical sciences. *Pharmaceutical Research*. 25: 2216-2230.
- 14. Marik J, Sutcliffe JL. (2006) Click for PET: rapid prepation of [18F]fluoropeptides using CuI catalyzed 1,3-dipolar cycloaddition. *Tetrahedron Letters*. 47: 6681-6684.
- 15. Kim DH, Choe YS, Jung KH, Lee KH, Choi JY, Choi Y, Kim BT. (2008) A ¹⁸F-labelled glucose analog: synthesis using a click labeling method and in vitro evaluation. *Archives of Pharmacal Research*. 31: 587-593.
- 16. Evans RA. (2007) The rise of azide-alkyne 1,3-dipolar 'click' cycloaddition and its application to polymer science and surface modification. *Australian Journal Chemistry*, 60: 384-395.
- 17. Okarvi SM. (2001) Recent progress in fluorine-18 labelled peptide radiopharmaceuticals. *European Journal Nuclear Medicine*. 28: 929-938.
- 18. Glaser M, Robins EG. (2009) 'Click labelling' in PET radiochemistry. *Journal of Labelled Compounds and Radiopharmaceuticals*. 52: 407-414.
- 19. Gree D, Gree R. (2007) A new strategy for the synthesis of optically active benzylic fluorides and corresponding five-membered heteroaromatic analogues. *Tetrahedron Letters*. 48: 5435-5438.
- 20. Bixler A, Springer G, Lovas R. (1999) Practical aspects of radiation safety for using fluorine-18. *Journal Nuclear Medicine Technology*. 27: 14-16.
- 21. www.nchps.org. Nuclide safety data sheet fluorine-18.

The Malaysian Journal of Analytical Sciences Vol 16 No 2 2012

4	EFFECTS OF DUVCTOO CHEMICAL COTL DEODEDTIES ON THE ADCOUNT ON AND	Page
1.	EFFECTS OF PHYSICO-CHEMICAL SOIL PROPERTIES ON THE ADSORPTION AND TRANSPORT OF ¹³⁷ Cs IN RENGAM AND SELANGOR SOIL SERIES (Kesan Sifat Fizikokimia Terhadap Penyerapan dan Pengangkutan ¹³⁷ Cs Dalam Tanah Siri Rengam dan Selangor) Zidan Mohamed M. Houmani, Amran Ab.Majid, Shahidan Radiman, Zaharudin Ahmad	94
2.	SYNTHESIS, STRUCTURAL, ANTIBACTERIAL AND SPECTRAL STUDIES OF Co(II) COMPLEXES WITH SALICYLALDEHYDE AND p-CHLORO-BENZALDEHYDE 4-PHENYLTHIOSEMICARBAZONE (Sintesis, Penstrukturan, Antibakteria dan Analisis Spektrum Sebatian Kompleks Co(II) dengan Salisilaldehid dan p-klorobenzaldehid 4-feniltiosemikarbazon) Nur Nadia Dzulkifli, Yang Farina, Ibrahim Baba and Nazlina Ibrahim	103
3.	SYNTHESIS AND CATALYTIC ACTIVITY OF N,N'-BIS-(a-METHYLSALICYLIDENE)-PROPANE-1,3-DIAMINEPALLADIUM(II) AND ITS 4-METHYL DERIVATIVES IN HECK CARBON-CARBON COUPLING REACTION (Sintesis dan Aktiviti Pemangkinan N,N'-Bis-(a-Metilsalisilidina-Propan-1,3-Diamina-palladium(II) dan Terbitan 4-Metil dalam Tindak Balas Gandingan Karbon-Karbon Heck) Siti Kamilah Che Soh, Mustaffa Shamsuddin, Bohari M. Yamin	110
4.	UPTAKE OF HEAVY METAL IONS BY CHELATING ION-EXCHANGE RESIN DERIVED FROM P-HYDROXYBENZOIC ACID-FORMALDEHYDE-RESORCINOL: SYNTHESIS, CHARACTERIZATION AND SORPTIONDYNAMICS (Pengambilan Ion Logam Berat oleh Resin Penukar Ion Terbitan Asid p-Hidroksibenzoik-Formaldehid-Resorsinol: Sintesis, Pencirian dan Dinamik Erapan) Riddhish R. Bhatt, Bhavna A. Shah and Ajay V. Shah	117
5.	DETERMINATION OF ORGANIC AND INORGANIC MERCURY SPECIES IN SUNGAI KINTA, PERAK BY REVERSED-PHASE HIGH PERFORMANCE LIQUID CHROMATOGRAPHY (HPLC) ON-LINE COUPLED WITH ICP-MS (Penentuan Kandungan Spesis Raksa Organik dan Bukan Organik di Sungai Kinta, Perak Melalui Kaedah HPLC-ICP-MS) Norshidah Baharuddin, Norashikin Saim, Rozita Osman, Sharifuddin Md. Zain, Hafizan Juahir, Siti Rafzah Saari	134
6.	STABILITY OF THE ABSORBED DOSE TO WATER CALIBRATION COEFFICIENT, ND,w FOR THERAPY LEVEL IONIZATION CHAMBERS BELONGING TO LOCAL RADIOTHERAPY CENTRES: ANALYSIS OF RESULTS OBTAINED DURING 2004 -2010 (Kestabilan Pekali Kalibrasi Dos Terserap Terhadap Air, ND,w Untuk Kebuk Pengionan Tahap Terapi Kepunyaan Pusat Radioterapi Tempatan: Analisis Keputusan Yang Diperoleh Sepanjang 2004-2010) S. B. Samat, W. Priharti, S. S. Chong, T. Kadni and M.T. Dolah	142

7.	EFFECTS OF VARIOUS PARAMETERS ON IN-HOUSE COCKTAIL DEVELOPED FOR THE MEASUREMENT OF GROSS ALPHA AND BETA IN AQUEOUS ENVIRONMENTAL SAMPLES USING LIQUID SCINTILATION COUNTING TECHNIQUE (Kesan Pelbagai Parameter Ke Atas Koktil yang Dibangunkan Sendiri bagi Pengukuran Gros Alfa dan Beta Di Dalam Sampel Air Persekitaran Menggunakan Teknik Pembilang Sintilasi Cecair) Zaini Hamzah, Masitah Alias, Ahmad Saat, Abdul Kadir Ishak and Zaharudin Ahmad	148
8.	SORPTION COEFFICIENTS OF ¹³⁷ Cs ONTO VARIOUS MALAYSIAN SOIL SERIES (Pekali Serapan ¹³⁷ Cs ke atas Pelbagai Siri Tanih Malaysia) Zidan Mohamed M.Houmani, Amran Ab.Majid, Shahidan Radiman, Zaharudin Ahmad	157
9.	SEASONAL INFLUENCE ON WATER QUALITY STATUS OF TEMENGGOR LAKE, PERAK (Pengaruh Musim Terhadap Kualiti Air Tasik Temenggor, Perak) Wan Mohd Afiq Wan Mohd Khalik and Md. Pauzi Abdullah	163
10.	ANALISIS KROMATOGRAFI GAS x KROMATOGRAFI GAS-SPEKTROMETRI JISIM MASA-PENERBANGAN MINYAK PATI <i>GLOBBA PATENS VAR. PATENS</i> (Analysis of Gas Chromatography x Gas Chromatography-Time-of-Flight Mass Spectrometry of Essential Oils from <i>Globba patens var. patens</i>) A. Masila, W.A. Yaacob, I. Nazlina	172
11.	SPECTROPHOTOMETRIC DETERMINATION OF ORGANOPHOSPHATE INSECTICIDE (CHLORPYRIFOS) BASED ON DIAZOTISATION WITH ANTHRANILIC ACID (Penentuan Spektrofotometri Racun Serangga Organofosfat (Chlorpyrifos) Berdasarkan Pendiazoan dengan Asid Antranilik) N.V.S.Venugopal, B.Sumalatha, Srinivasa Rao Bonthula and G.Veeribabu	180
12.	RADIOLOGICAL IMPACT OF DRINKS INTAKES OF NATURALLY OCCURRING RADIONUCLIDES ON ADULTS OF CENTRAL ZONE OF MALAYSIA (Impak Radiologi Radionuklid Tabii dalam Air Minuman ke atas Orang Dewasa di Kawasan Tengah Semenanjung Malaysia) A.A. Tawalbeh, S.B. Samat, M.S. Yasir, M.Omar	187
13.	DEVELOPMENT OF A METHOD FOR THE SPECIATION OF MERCURY IN ENVIRONMENTAL SAMPLE ANALYSIS (Pembangunan Kaedah Bagi Analisis Penspesian Merkuri Dalam Sampel Sekitaran) M. M. Rahman, M. Awang, A. M. Yusof, A. K. H. Wood, S. Hamzah and A. Shamsiah	194



EFFECTS OF PHYSICO-CHEMICAL SOIL PROPERTIES ON THE ADSORPTION AND TRANSPORT OF $^{137}\mathrm{Cs}$ IN RENGAM AND SELANGOR SOIL SERIES

(Kesan Sifat Fizikokimia Terhadap Penyerapan dan Pengangkutan ¹³⁷Cs Dalam Tanah Siri Rengam dan Selangor)

Zidan Mohamed M. Houmani¹, Amran Ab.Majid¹, Shahidan Radiman¹ Zaharudin Ahmad²

¹Faculty of Science and Technology, Universiti Kebangsaan Malaysia, 43600 UKM Bangi, Selangor, Malaysia. ²Nuclear Malaysia , 43000 Bangi, Selangor D.E, Malaysia

*Corresponding author: houmani67@yahoo.com

Abstract

In this study, the adsorption of 137 Cs in soil samples were quantified using the distribution coefficient (K_d -value). The distribution coefficients (K_d) of 137 Cs in Rengam and Selangor soil series were determined by a batch technique. The Malaysian soil series (Rengam and Selangor soil series) were collected systematically at three different depths (0-20 cm, 20-40 cm and 40-60 cm) at two different sites in Malaysia. The batch K_d tests were used with deionized water that was spiked with 137 Cs tracer to the soil sample and the activities of 137 Cs in the supernatant solution were measured by a low background but high efficiency well-type HPGe detector. Several physicochemical soil properties were also characterised for each soil type. Pearson's correlation and stepwise multiple regression models were applied at 0.05 level of significance throughout all analysis to determine the relationships and influences between distribution coefficients (K_d -value) of 137 Cs with physicochemical soil properties of each soil type. The calculated K_d -value for Rengam and Selangor soil series at several depth were determined to be in the range of 202 to 1739 ml.g- 1 and 3389 to 5919 ml.g- 1 respectively. The results indicate that the stepwise multiple regression model incorporating pH and porosity influence the K_d -value of 137 Cs in Rengam Soil Series and exhibits an R^2 equal to 0.922 indicating that 92.2% of total variation has been explained by the regression model. The regression model also reveals that cation exchange capacity, bulk density, porosity and free manganese oxide (Mn²⁺) have influence on the K_d -values of 137 Cs in Selangor soil series and exhibits an R^2 equal to 0.997 indicating 99.7 % of total variation. Therefore, the sorption coefficients in relation to the environmental factors including physicochemical properties can be used to predict and design the radionuclide transport and safety assessment models.

Keywords: K_d -value, ¹³⁷Cs, physicochemical soil properties

Abstrak

Dalam kajian ini, penyerapan ¹³⁷Cs dalam sampel tanih telah dikuantitikan dengan menggunakan Kaedah Pekali Taburan (Nilai K_d). Pekali Taburan (K_d) ¹³⁷Cs bagi siri tanih Rengam dan Selangor telah ditentukan menggunakan teknik kelompok. Siri tanih Rengam dan Selangor telah dikumpulkan secara sistematik pada tiga kedalaman yang berbeza (0-20 cm, 20-40 cm dan 40-60 cm) di dua lokasi yang berlainan di Malaysia. Nilai K_d ditentukan menggunakan air ternyahion yang ditambahdengan penyurih ¹³⁷Cs kepda sampel tanih. Aktiviti ¹³⁷Cs di dalam larutan supernatant dibilang menggunakan pengesan HPGe yang mempunyai latar beakang yang rendah tetapi kecekapan yang tinggi. Beberapa sifat fisikokimia tanih juga telah dicirikan bagi setiap jenis tanih. Korelasi Pearson dan Model Regresi Berganda Berperingkat turut digunakan pada tahap signifikan 0.05 untuk keseluruhan analisis bagi menentukan hubungan dan pengaruh antara pekali taburan (nilai K_d) ¹³⁷Cs dengan sifat fisikokimia bagi setiap jenis tanih. Nilai K_d yang telah dikira untuk masing-masing siri tanihRengam dan Selangor dicatatkan dalam julat 202 hingga 1739 ml g⁻¹ dan 3389 hingga 5919 ml g⁻¹. Keputusan menunjukkan bahawa model regresi berganda berperingkat menggabungkan pH dan keliangan mempengaruhi nilai K_d ¹³⁷Cs bagi tanih siri Rengam dan mempamerkan *R*² bersamaan dengan 0.922 yang mana menunjukkan 92.2 % dari jumlah variasi telah diterangkan oleh model regresi. Model regresi juga menunjukkan bahawa kapasiti

Zidan Mohamed M. Houmani et al: EFFECTS OF PHYSICO-CHEMICAL SOIL PROPERTIES ON THE ADSORPTION AND TRANSPORT OF ¹³⁷Cs IN RENGAM AND SELANGOR SOIL SERIES

pertukaran kation, ketumpatan pukal, keliangan dan mangan oksida bebas (Mn^{2+}) dapat mempengaruhi nilai K_d ¹³⁷Cs dalam tanih siri Selangor dan mempamerkan R^2 bersamaan 0.997 yang menunjukkan bahawa 99.7 % daripada jumlah variasi. Maka kajian ini mendapati pekali penyerapan yang berkaitan dengan faktor sekitaran termasuklah sifat fisikokimia boleh digunakan untuk meramal dan merekabentuk pengangkutan radionuklid dan model penilaian keselamatan.

Kata kunci: Nilai K_d, ¹³⁷Cs, sifat fizikokimia tanah

Introduction

Cs is one of the important radionuclides for several reasons: it shows the almost unlimited solubility in the inventory of radioactive waste is significant [1]. A radioisotopes of cesium, ¹³⁷Cs is relatively resistant and provides important problems radioecologically [2]. The main sources of soil contamination are global fallout of ¹³⁷Cs from the atmosphere as a result of atmospheric testing of nuclear weapons, surface and underground nuclear explosions and accidental releases from nuclear facilities. In addition to these main sources of ¹³⁷Cs soil contamination, there have been few cases of local contamination which could increase the radiation dose to the population in surrounding areas[3]. In addition, because of its chemical similarity to K, Cs is easily assimilated by terrestrial and aquatic organisms [1]. The study of sorption of pollutants in soil is of great interest in terms of ecological and agricultural. It is known that ion exchange reactions occur mainly between Cs ions and clay minerals. The bioavailability of Cs⁺ in natural systems depends largely on the adsorption properties of the solid phase [4].Radionuclides present in soil have the potential to be released or leached to the groundwater. In order to understand the way in which radioactive contamination may be transferred from soil to plants, animals and finally to man, it is useful to have a basic knowledge on both the physical and chemical properties of soils and the mechanisms by which radionuclides are passed from the soils to the food chain or the means that lead to the contamination of water supplies [5]. The primary objective of the present study is to determine the effects of physico-chemical soil properties on adsorption of 137Cs in Rengam and Selangor soil series. Such study could assist future environmental study such as environmental radiological impact assessments (RIA) in the future. One of the important factors that needs to be considered in RIA is the possible release or leaching of radionuclides into ground water.

The Rengam Series is a member of the Rengam Family which is a fine, kaolinitic, isohyperthermic, red-yellow Tipik Lutualemkuts. It typifies this family which is developed over coarse grained acid igneous rocks [6]. The Selangor soil series is clay dominated, often derived from Entisols. This clay is typically found near the surface of marine alluvial plains typical of the west coast of peninsular Malaysia that have for many years been drained for the cultivation of crops [6]. The complex sorption interaction can be expressed as a distribution coefficient (K_d), which is the ratio of the amount of the radionuclide sorbed by the solid (g g⁻¹) divided by the concentration in the equilibrium solution (g ml⁻¹). The K_d -value is commonly used as a means of assessing the mobility of radionuclides in the environment and for comparing adsorption data obtained from different sources [7]. The parameter known as (K_d -value) is defined as the ratio of the concentration of the radionuclide bound to soil to the concentration in the pore water. The value of K_d depends on the type of radionuclides, physico-chemical soil properties and mineralogy of the soil, The K_d -value of the radionuclides needs to be determined in order to estimate the transport or leaching potential used to assess associated risks.

Materials and Methods

Soil sampling and preparation

The studied soil were Rengam and Selangor series, Typic Kandiudult and Typic Endoaquepts, respectively [6]. Undisturbed soil samples were taken from the designated sampling stations shown in Figure 1. First, the detritus (grass and litter) at each sampling station were cleared from the ground surface and the soil was dug with a spade. Soil samples were collected from depths of 0-20 cm, 20-40 cm and 40-60 cm. About 500 g soil samples were collected from each depth. The samples were sealed in plastic bags and taken to the laboratory for further analysis. In the laboratory, the samples were air dried at room temperature, disaggregated using a wooden mortar and pestle and sieved through a 2 mm mesh for further use and analysis. In addition, soil cores (7.6 cm diameter and 4 cm long) were also taken from each depth for bulk density determination.

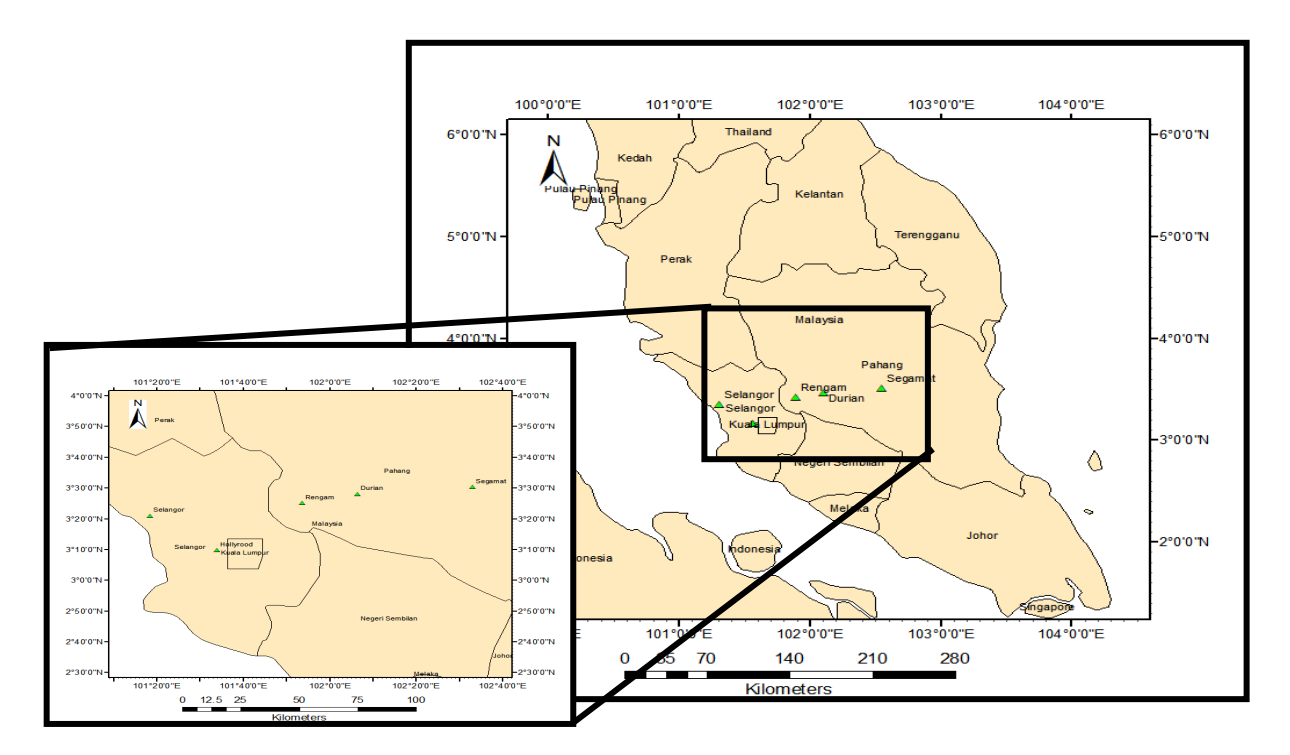


Figure 1. Location of soil sampling stations of Rengam and Selangor soil series

Determination of physico-chemical soil properties and soil clay mineralogy

Triplicate sieved soil samples from each of three depths were used for determination of the following physicochemical soil parameters: bulk density, porosity and soil particle size distribution. Porosity was calculated as the difference between the soil particle density and bulk density, while particle size distribution was determined by the Pipette method, together with dry sieving [8]. The texture of the soils was obtained by plotting their percentages of sand, silt and clay and categorized using the triangular texture map. Soil bulk densities (g/cm³) were derived by dividing the mass of the dried soil cores by their volumes [9].

The pH was measured using a pre calibrated lab-top pH meter equipped with a glass electrode in an aqueous suspension of 10 g of dry soil and 25 ml of distilled water (1:2.5,w/w), shaken for 30 minutes in a conical flask [10]. Exchangeable acid ions (Al^{3+} and H^{+}) were measured in 1.0 M KCl extract by titration. Exchangeable base cations were measured in 1.0 M ammonium acetate extract by Flame Atomic Absorption Spectrophotometer (FAAS, model Perkin Elmer 3300) and cation exchange capacity (CEC) was obtained by summation of the acid and base cations. The base saturation was calculated by the equation [sum cations / CEC] \times 100]. The extractable free Fe- and Mnoxides contents were determined by the dithionite-citrate method [11]. Sulphate contents were measured on a sediment water extract [1 g :10 mL] after two hours of shaking and filtration using the barium sulphate turbidometric procedure [12]. The specific surface area was determined by the ethylene glycol monoethyl ether (EGME) method [13]. Organic carbon was estimated using the Walkley and Black method and organic matter (OM) was calculated by multiplying the values of organic carbon by 1.72 [14].

For identification of clay minerals in the bulk soil samples, X-ray diffraction (XRD) analysis was performed using a Siemens D500 powder X-ray diffractometer using CuKα radiation, and operated at 40 kV and 30 mA. The oriented specimens were scanned from 3 to 35 degrees 2θ. All samples were prepared for both qualitative and quantitative determination by X-ray diffraction analysis according to the general procedure of Moore and Reynolds [15]. About 1g of soil was placed into 10-ml measuring cylinder. About 5 ml of distilled water was then added in to it and was mixed thoroughly using a glass rod. After 15-20 minutes, the upper solution was then pipetted (using an

eyedropper) and placed slowly on the clean glass slide so that the liquid covered the entire surface of the slide. It was assumed, according to Stoke's Law, that the solution that was sampled contained the clay particles of less than $2 \mu m$. The slide was dried at the room temperature. High drying temperature was not used to avoid any damage to poorly crystallised clay minerals in soils. Several treatments have been undertaken to verify the clay minerals in the soil.

Laboratory sorption experiments

The sorption of 137 Cs on Rengam and Selangor soil series were studied by batch technique using at least three replicates. The solution-soil ratio was maintained as 20:1 throughout the experiments in accordance with ASTM D4319-93 [16]. Twenty 20 ml of 1788.570 Bq ml $^{-1}$ 137 Cs was spiked into deionised water. The spiked solutions were mixed with 1.0 ± 0.1 g of the soil in 50-cm 3 polyethylene centrifuge tubes with screw caps and septum sealed. Suspensions were initially preconditioned, using deionised water with on 137 Cs spike by shaking for 24 h at 23 ± 2 0 C using an end-over-end shaker. The mixture was shaken for 7 days to achieve the equilibrium of 137 Cs adsorption, the solution phase was separated by centrifugation at 3000 rpm, and the supernatant was filtered though a 0.45- μ m micropore filter. The 5ml aliquots of the filtered supernatant were placed in small glass vials. The activity concentration measurements of 137 Cs in the vials was performed with a Canberra p-type HPGe well detector (GCW 2523) with active volume of 155 cm 3 , a relative photopeak efficiency of 25%, and a resolutions at the 1332 keV energy of 60 Co of 2.3 keV (FWHM).

 $K_{\rm d}$ (ml g⁻¹) was then calculated using equation 1:

$$K_d(ml/g) = \frac{(C_i - C_f)}{C_f} \cdot \frac{V}{M}$$
 (1)

where C_i (Bq ml⁻¹) is initial activity of the radiotracer in the aqueous phase, C_f (Bq ml⁻¹) is activity of radiotracer in the final supernatant, V is solution volume (20 ml), and M is soil dry weight (1.0 ± 0.01 g).

Treatment of the raw counting data was performed with the GENIE 2000 program. The activity (cps) of the ¹³⁷Cs photopeak (661.6 keV) was determined. Based on the background and blank counts, the minimum detectable activity (MDA) for this geometry was derived using Currie's Method formula [17]:

$$MDA = \frac{\sigma\sqrt{B}}{\varepsilon PTW} (Bq.kg^{-1}), \tag{2}$$

where, σ is statistical coverage factor (= 1.645) (P \leq 0.05), B is background radiation of the radionuclide of interest, ε is counting efficiency of the detector, P is absolute transition probability of γ -decay, W is dried sample weight in g, and T is counting time in seconds. The MDA for ¹³⁷Cs determined was 2.087 Bq kg⁻¹.

Data analysis

In the data analysis, the soil's physical and chemical properties were considered as independent factors while the observed adsorption of 137 Cs was considered as the one dependent factor. The coefficient of correlations and stepwise multiple regressions were calculated to determine the independent factors which were significantly controlled with the dependent factor. The statistical significance was considered at significant level 0.05 ($\alpha = 0.05$). Therefore, we considered that the regression models and coefficients correlations of the 5% or less chance of error (p ≤ 0.05). Data analysis was performed using the statistical software Statistical Package for Social Sciences (SPSS) Ver.15.0. Assuming that the data were normally distributed, significant differences were considered at $p \leq 0.05$. Pearson's correlation and a stepwise multiple linear regression technique was used to derive the relationship and influences between physico-chemical soil properties and distribution coefficients (K_d -value).

Results and Discussion

The results of K_{d-} experiments on two Malaysian soil types are shown in Table 1 and Figure 1. The range of K_{d-} Cs values of these Malaysian soil series were determined to be between 202 ml g⁻¹ to 1739 ml g⁻¹ and 3389 ml g⁻¹ to 5919 ml g⁻¹ for Rengam and Selangor soil series, respectively. The results also showed that the K_{d-} value of ¹³⁷Cs dependeds on the depths of soil. The results showed that the K_{d-} value of ¹³⁷Cs is higher as the depth of soil increased for Rengam soil series. However, for the Selangor soil series, the K_{d-} Cs-value was found to decrease as the soil depth increased. The remarkable difference in K_{d} values of the Rengam and Selangor soil series can be attributed to be influenced by number of factors including soil texture, pH, porosity etc (Table 2 and 3).

Table 1. Me	an of distribution coefficients (K_d -	value) for ¹³⁷ Cs in Rengam and Selangor soil series
ha (am)	Donoom	Colongon

Depths (cm)	Rengam		Selangor	
·	Range	Mean value K_d -value	Range	Mean value K_d -value
		in (ml g^{-1}) ± $S.D^*$		in (ml g ⁻¹) \pm S.D*
0-20	202 - 210	206 ± 4	5001 - 5919	5345 ± 499
20-40	326 - 367	341 ± 22	4608 - 5375	5099 ± 426
40-60	1676 - 1739	1716 ± 35	3389 – 3636	3526 ± 125

*S.D: Standard deviation

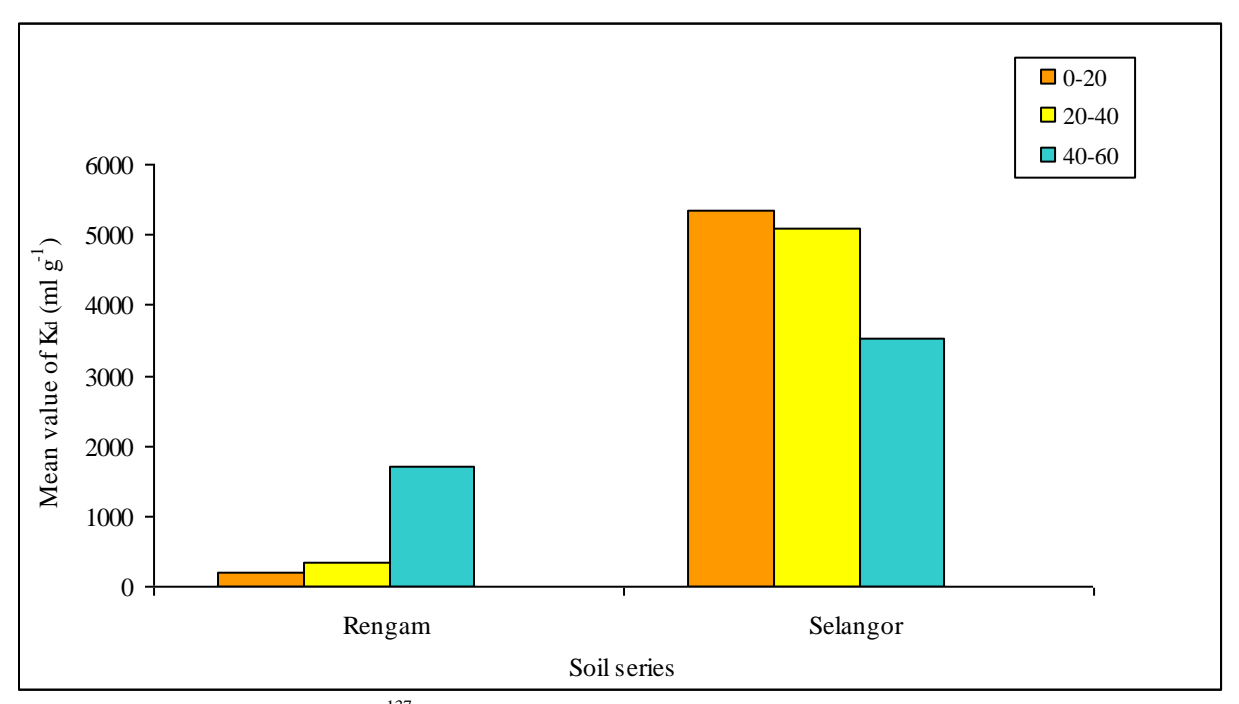


Figure 2. ¹³⁷Cs adsorption onto Rengam and Selangor soils series

Zidan Mohamed M. Houmani et al: EFFECTS OF PHYSICO-CHEMICAL SOIL PROPERTIES ON THE ADSORPTION AND TRANSPORT OF ¹³⁷Cs IN RENGAM AND SELANGOR SOIL SERIES

Table 2. Physico-chemical and mineralogical characteristics of Rengam soil series

Rengam soil series					
Parameter	Unit -		Depths (cm)		
	- Cilit	0-20	20-40	40-60	
Bulk density	(g/cm^3)	0.98 ± 0.02	1.06 ± 0.02	1.10 ± 0.03	
Porosity*	(%)	60.28±0.49	59.58±0.91	57.37±0.44	
Sand	(%)	57±0.58	50±0.6	48±1	
Silt	(%)	16±0.58	13±1.2	12±1.15	
Clay	(%)	27±1	37±0.6	40 ± 0.58	
Soil texture		Sandy clay loam	Sandy clay	Sandy clay	
Specific surface area	(m^2/g)	77.2±7	88.1±9.5	94.1±0.9	
pH (H ₂ O)		4.10 ± 0.08	4.06 ± 0.06	4.10 ± 0.08	
Total organic carbone	(%)	1.89 ± 0.20	0.65 ± 0.06	0.45 ± 0.13	
Organic matter	(%)	5.59 ± 0.59	1.93 ± 0.17	1.33±0.38	
Cation exchange capacity	meq / 100 g soil	5.62±0.15	6.00±0.57	5.99 ± 0.79	
Cation exchange capacity of clay	CEC / 100 g clay	20.85 ± 0.95	16.36 ± 1.54	15.12 ± 2.20	
Base Saturation	(%)	13.00 ± 2.65	7.67 ± 2.08	5.33 ± 0.58	
Free Iron oxide (Fe ³⁺)	$\mu \mathrm{g.g^{-1}}$	5021.1±481.5	5696.4±486.7	6094.4±611.4	
Free Manganese oxide (Mn ²⁺)	$\mu \mathrm{g.g^{ ext{-}1}}$	142.1±28.3	121.6±43.8	120.2±62.8	
Sulphate (SO ₄ ²⁻)	$\mu \mathrm{g.g}^{\text{-1}}$	35 ± 0	47.5 ± 2.5	22.5 ± 2.5	
Main cay mineral type (in order of predominance)		Kaolinite	Illite	Montmorillonite	

 $^{^*\}overline{Porosity}$ calculated based on soil particle density of 2.65 g $/cm^3$ and soil bulk density value; meq: milli-equivalents.

Table 3. Physico-chemical and mineralogical characteristics of Selangor soil series

Selangor soil series					
Parameter	Unit		Depths (cm)		
rarameter	Unit	0-20	20-40	40-60	
Bulk density	(g/cm^3)	0.98 ± 0.02	1.07 ± 0.06	1.05 ± 0.04	
Porosity*	(%)	60.39 ± 0.74	57.87 ± 0.57	58.16 ± 2.84	
Sand	(%)	12 ± 2.08	10 ± 1.53	8 ± 0.58	
Silt	(%)	23 ± 2.65	16 ± 2.89	16 ± 1.73	
Clay	(%)	65 ± 4.51	74 ± 1.53	76 ± 2.08	
Soil texture		Clayey	Clayey	Clayey	
Specific surface area	(m^2/g)	101.8 ± 3.1	113.7 ± 14.6	121.3 ± 3.2	
pH (H ₂ O)		3.70 ± 0.17	3.49 ± 0.03	3.41 ± 0.07	

Total organic carbone	(%)	4.26 ± 0.10	2.70 ± 0.10	1.93 ± 0.29
Organic matter	(%)	12.65 ± 0.29	8.00 ± 0.30	5.73 ± 0.87
Cation exchange capacity	meq / 100 g soil	8.79 ± 0.31	8.71 ± 0.15	5.55 ± 0.87
Cation exchange capacity of clay	CEC / 100 g clay	15.65 ± 2.07	11.83 ± 0.11	7.27 ± 1.06
Base Saturation	(%)	32.33 ± 1.23	15.67 ± 2.08	21.67 ± 3.79
Free Iron oxide (Fe ³⁺)	$\mu g.g^{-1}$	2647.3 ± 277.0	2815.6 ± 292.5	3315.4 ± 365.7
Free Manganese oxide (Mn ²⁺)	$\mu \mathrm{g.g^{-1}}$	196.0 ± 24.9	227.3 ± 24.9	169.6 ± 11.1
Sulphate (SO ₄ ²⁻)	$\mu \mathrm{g.g}^{\text{-1}}$	145 ± 5	247.5 ± 7.5	92.5 ± 7.5
Main cay mineral type (in order of predominance)		Kaolinite	Illite	Montmorillonite

^{*}Porosity calculated based on soil particle density of 2.65 g/cm³ and soil bulk density value; meq: milli-equivalents.

Table 4 reports the regression result between K_d -value of ¹³⁷Cs of Rengam soil series and physico-chemical soil parameters. The final ¹³⁷Cs K_d model uses two independent variables, porosity and pH and exhibits an R^2 equal to 0.922 indicating that 92.2% of total variation has been explained by the regression model. The final regression model is:

$$K_{\rm d}$$
-value of ¹³⁷Cs = 16377.562 - 485.848 × porosity + 3200.708 × pH (3)

Base on the objective of this study, correlation analysis was followed by stepwise multiple regression analysis in order to verify the correlation. From the final equation model described above, the porosity is a negative influencing parameter on K_d -Cs-value and pH has positive influence on K_d -Cs-value in Rengam soil series. One of largely influencing parameter related to porosity is a factor of particle (grain) size. Statistical data reveals that there is a negative relationship between porosity with clay and porosity with bulk density. Clay soils exhibit a variety of micropores and macropores which may hold water contents and control the filtration rates. [18]. The Cs sorption is related to the pH of the soil because of its nature of charge density at specific value. The equation A determines the pH factor as a significant parameter to evaluate the sorption. It is reported that the maximum Cs sorption was observed at higher pH, when the negative charge density on the surface of absorbents was highest [19]. Therefore, The pH influence found agreed with the findings reported by Kami-Ishikawa et al. for the clayey nature of soils. As the acidic conditions are concerned, the availability of cations may create competition with other cations for the available sorption sites [20].

Table 4 presents the regression model between physic chemical soil properties and K_d -value of ¹³⁷Cs of Selangor soil series. The final ¹³⁷Cs K_d model was established using four independent variables including cation exchange capacity, bulk density, porosity and free manganese oxide (Mn²⁺) which exhibits an R^2 equal to 0.997 indicating 99.7 % of total variation as mentioned in equation B. The final regression model is:

$$K_{\rm d}$$
-value of ¹³⁷Cs = -9203.798 + 393.586 × CEC + 4219.826 × B.D + 90.337 × porosity + 5.013 × Mn (4)

where CEC is cation exchange capacity, B.D is bulk density.

Table 4. Regression summary for K_d -value of ¹³⁷Cs of Rengam and Selangor soil series respectively

Dhygiaa ahamiaal yawiahla	Regression parameters			
Physico-chemical variable	Regression coefficient	t-statistic	<i>p</i> -value	
Model 1			-	
Constant	16377.56			
Porosity	- 485.85	-8.29	0.001	
$pH(H_2O)$	3200.71	2.58	0.042	
Model 2				
Constant	-9203.798			
Cation exchange capacity(CEC)	393.586	16.43	0.001	
Bulk density (B D)	4219.826	4.79	0.009	
Porosity	90.337	5.81	0.004	
Free manganese oxide (Mn ²⁺)	5.013	3.09	0.036	

It can be concluded from the final equation model described as Eq 4, the cation exchange capacity, bulk density, porosity and free manganese oxide (Mn^{2+}) have positive effect on K_d -Cs-value in Selangor soil series. It is fact that the cation exchange capacity influence on the adsorption of ¹³⁷Cs due to its ion exchange characteristics. The CEC value strongly depends on the clay content and thus the relationship between the K_d -value and CEC will be similar to but weaker than that for the K_d value and the clay content [21]. The bulk density and porosity have influence on the adsorption of ¹³⁷Cs due to their relation with the permeability of the contents to perform sorption. The small pore size and high density may not allow the contents for migration to create the negative influence and vice versa. The free manganese oxide (Mn^{2+}) influence positively on the adsorption of ¹³⁷Cs due to its ability to adsorb the Cs. It may provide the binding sites for the incorporation of Cs to migrate through the channels in the soil. Hasany and Chaudhary (1984) have reported the adsorption of ¹³⁷Cs on MnO^2 under different conditions of physical parameters [22].

Conclusion

The study results suggest that Cs- K_d was affected by several soil properties, such as pH, porosity in Rengam soil series and bulk density, cation exchange capacity and free manganese oxide (Mn^{2+}) in Selangor soil series. The study signified that the Rengam and Selangor soil series have good sorption for ^{137}Cs radionuclide. The distribution and migration of Cs in the soil depends in particular on its physicochemical properties and the movement of soil water with associated contents. The transport of the Cs in the soil is determined by the amount of absorbed Cs and other soil properties including texture, porosity and organic contaminants. The adsorption properties have also relation with the type and composition of the clay mineral content of the soil. This study has revealed some trends of sorption in relation to the nature of soil texture and other physicochemical properties and the data could be used in radionuclide transport and safety assessment models.

Acknowledgement

The authors would like to thank Mr. Yii from the Malaysian Nuclear Agency for his invaluable guidance and assistance during the experimental work of ¹³⁷Cs measurements by the well-type HPGe detector, We are also grateful to Dr. Sahibin Abd. Rahim from the School of Environmental and Natural Resource Sciences, FST, UKM, for his advice on the physico-chemical properties of Selangor soil series.

References

- 1. Poinssot, C., Baeyens, B., &Bradbury, M. H. (1999). Experimental and modelling studies of caesium sorption on illite. *Geochimica et Cosmochimica Acta* 63 (19-20):3217-3227.
- 2. Staunton, S., & Roubaud, M. (1997). Adsorption of 137Cs on montmorillonite and illite: Effect of charge compensating cation, ionic strength, concentration of Cs, K and fulvic acid. *Clays and clay minerals* 45 (2):251-260.
- 3. Nabyvanets, Y. B., Gesell, T. F., Jen, M. H., &Chang, W. P. (2001). Distribution of ¹³⁷Cs in soil along Ta-han river valley in Tau-Yuan County in Taiwan. *Journal of Environmental Radioactivity* 54 (3):391-400.
- 4. Atun, G., & Kilislioglu, A. (2003). Adsorption behavior of cesium on montmorillonite-type clay in the presence of potassium ions. *Journal of Radioanalytical and Nuclear Chemistry* 258 (3):605-611.
- 5. Eisenbud, M. (1973). Environmental radioactivity. 2nd ed, Environmental sciences. New York,: Academic Press.
- 6. Paramananthan, S. (2000). Soils of Malaysia. Their Characteristics and Identification. Vol. 1. Academy of Sciences Malaysia, Kuala Lumpur.
- Sheppard, M. I., & Thibault, D. H. (1990). Default soil solid/partition coefficients, K_d s, for four major soil types: A compendium. *Health Physics* 59 (4):471-482.
- 8. Day, P. R. (1965). Particle fractionation and particle-size analysis. In *Methods of soil analysis, Part 1* edited by Black, C. A., Evans, D. D., White, J. L., Ensminger, L. E. &Clark, F. E. Madison: American socity of Agronomy.
- 9. Blake, G. R. (1965). Particle density, Bulk density. In *Methods of soil analysis*, edited by Black, C., Evans, D. D., Ensminger, L. E., White, J. L. &Clark, F. E. Madison: American Society of Agronomy.
- 10. Metson, A. J. (1956). *Methods of chemical analysis for soil survey samples*. Vol. 12. Wellington: Dept. of Scientific Industrial, Research.
- 11. Carter, M. R. (1993). Soil sampling and methods of analysis. Boca Raton: Lewis Publishers.
- 12. HACH. (1996). Spectrophotometer Instrument Manual. For use with the software Ver. 3. Loveland Colorado: HACH Company.
- 13. Wan Zuhairi, W. Y. Access (2006). *SSA based on EGME method* 2006 [cited 27/11/2006 2006]. Available from http://pkukmweb.ukm.my/~zuhairi/Pengajaran/intranet/e-library/Soil lab/Specific surface area.pdf.
- 14. Walkley, A., & Black, I. A. (1934). An examination of the Degtjareff method for determining organic carbon in soils: Effect of variations in digestion conditions and of inorganic soil constituents. *Soil Science* 63:251-263.
- 15. Moore, D. M., & Reynolds, R. C. (1997). *X-Ray Diffraction and the Identification and Analysis of Clay Minerals*, 2nd ed. New York: Oxford University Press.
- 16. ASTM. (1984). Standard Test Method for Distribution Ratios by the Short-Term Batch Method. In *Annual Book of ASTM Standards*: American Society for Testing and Materials.
- 17. Currie, L. A. (1968). Limits for qualitative detection and quantitative determination *Anal Chem* 40:586-593.
- 18. Munshower, F. F. (1994). Practical handbook of disturbed land revegetation. Florida: Lewis.
- 19. Giannakopoulou, F., Haidouti, C., Chronopoulou, A., &Gasparatos, D. (2007). Sorption behavior of cesium on various soils under different pH levels. *Journal of Hazardous materials* 149 (3):553-556.
- 20. Kamei-Ishikawa, N., Uchida, S., &Tagami, K. (2008). Distribution coefficients for ⁸⁵Sr and ¹³⁷Cs in Japanese agricultural soils and their correlations with soil properties. *Journal of Radioanalytical and Nuclear Chemistry* 277 (2):433-439.
- 21. Shenber, M. A., & Eriksson, Å. (1993). Sorption behaviour of caesium in various soils. *Journal of Environmental Radioactivity* 19 (1):41-51.
- 22. Hasany, S., & Chaudhary, M. (1984). Adsorption behaviour of microamounts of cesium on manganese dioxide. *Journal of Radioanalytical and Nuclear Chemistry* 84 (2):247-256.



SYNTHESIS, STRUCTURAL, ANTIBACTERIAL AND SPECTRAL STUDIES OF Co(II) COMPLEXES WITH SALICYLALDEHYDE AND p-CHLORO-BENZALDEHYDE 4-PHENYLTHIOSEMICARBAZONE

(Sintesis, Penstrukturan, Antibakteria dan Analisis Spektrum Sebatian Kompleks Co(II) dengan Salisilaldehid dan *p*-klorobenzaldehid 4-feniltiosemikarbazon)

Nur Nadia Dzulkifli¹, Yang Farina^{1*}, Ibrahim Baba¹ and Nazlina Ibrahim²

¹School Of Chemical Sciences and Food Technology, ²School Of Biosciences and Biotechnology, Faculty of Science and Technology, Universiti Kebangsaan Malaysia, Bangi, Selangor

*Corresponding author: farina@ukm.my

Abstract

The Co(II) complexes derived from salicylaldehyde 4-phenylthiosemicarbazone; SaOHtsc, p-chlorobenzaldehyde 4-phenylthiosemicarbazone; ph-HClbtsc is reported and characterized based on elemental analysis, IR, magnetic susceptibility measurement, 1 H and 13 C NMR spectra. The Co(II) complexes have the molecular formula CoL $_{2}$ where the ligand corresponding to SaOHtsc and ph-HClbtsc. The elemental analysis for the ligands and complexes were in a good agreement with the theoretical values. The ligands coordinate to metal ions in different ways which is through mononegative bidentate or dinegative tridentate. The magnetic susceptibility measurements showed that the CoL $_{2}$ complexes with ligand SaOHtsc are diamagnetic thus making this complexes suitable for NMR studies. The signals at the 10.04 ppm were assigned to N^{2} H in the 1 H-NMR spectra of the free ligands was absent in the spectra of the complexes due to the deprotonation of the N^{2} H and coordination to the metal centres. The absence of the band in IR spectrum which is assigned to $v(N^{2}$ -H) in the spectra of CoL $_{2}$ complexes is due to the deprotonation of the ligands upon complexation through azomethine nitrogen and thionic sulphur atom to metal ion. The thiosemicarbazones and its Co(II) complexes showed moderate inhibitory against bacteria *Bacillus Subtilis, Staphylococcus Epidermis, Escherichia Coli* and *Proteus Mirabilis* in 10 μ g/disc.

Keywords: Thiosemicarbazone, Co(II), antibacterial

Abstrak

Sebatian kompleks Co(II) diterbitkan daripada salisilaldehid 4-feniltiosemikarbazon, SaOHtsc, dan *p*-klorobenzaldehid 4-feniltiosemikarbazon, ph-HCltsc telah dilaporkan serta dilakukan pencirian melalui analisis unsur, IR, ukuran kebolehrentangan magnet momen, ¹H dan ¹³C RMN. Sebatian kompleks tersebut mempunyai formula molekul CoL₂ di mana ligan mewakili SaOHtsc dan ph-HClbtsc. Analisis unsur bagi sebatian ligan dan kompleks mematuhi nilai teori. Sebatian ligan berkoordinat dengan ion logam melalui pelbagai cara iaitu sama ada mononegatif monodentat atau dinegatif tridentat. Pengukuran kebolehrentangan magnet momen menunjukkan bahawa sebatian kompleks CoL₂ dengan ligan SaOHtsc adalah diamagnet di mana sesuai untuk pencirian RMN. Puncak pada 10.04 ppm mewakili N²H dalam spektrum ¹H-RMN bagi ligan bebas di mana puncak tersebut tidak muncul dalam spketrum sebatian kompleks disebabkan nyahprotonan N²H dan pengkoordinatan dengan logam pusat. Ketiadaan jalur serapan v(N²H) dalam spektrum IR bagi sebatian kompleks, CoL₂ merujuk kepada nyahprotonan ligan semasa berlaku pengkoordinatan melalui azometina N dan tionik S dengan logam pusat. Sebatian ligan tiosemikarbazon dan kompleks Co(II) menunjukkan sifat sederhana rencatan menentang bakteria *Bacillus Subtilis, Staphylococcus Epidermis, Escherichia Coli* dan *Proteus Mirabilis* dalam 10 μg / cakera.

Kata kunci: Tiosemikarbazon, Co(II), antibakteria

Nur Nadia Dzulkifli et al: SYNTHESIS, STRUCTURAL, ANTIBACTERIAL AND SPECTRAL STUDIES OF Co(II) COMPLEXES WITH SALICYLALDEHYDE AND p-CHLORO-BENZALDEHYDE 4-PHENYLTHIOSEMICARBAZONE

Introduction

Thiosemicarbazones also known as Schiff or soft bases are widely applied in analytical determination by using complex formation reactions. Most Schiff bases are chemically unstable and showed tendency to be involved in various equilibria such as tautomerism, hydrolysis or formation of ionized species [3]. Thiosemicarbazones can behave as mononegative or neutral bidentate ligands to coordinate with Co(II) through sulfur azomethine and the hydrazinic nitrogen atoms which is known as N, S- donor ligands. They can exist as thione-thiol tautomer and can bind to a metal centre in the neutral or the anionic forms act as monodentate, bidentate or bridge ligands [8]. The 4-phenylthiosemicarbazone derivatives is an interesting compound because of their ability to form highly stable and intense coloured complexes with metal ion [1]. A wide range of biological activities of heterocyclic thiosemicarbazones species has become a great interesting field including antibacterial, antifungal, antitumor and antiviral [5]. Sometimes, the biological activity of the ligands is enhanced or only takes place when the presence of metal ions. Bingol and Atalay 2006 [1] also said that determination of Co(II) in natural water is of considerable interest because it is important for living species in the forms complexes with vitamin B12.

Experimental

Material and instrumentation

All chemicals and solvents used for synthesis were of reagent grade and used without further purification. Melting points were taken on a melting point apparatus. IR spectra were recorded on a Perkin Elmer GX spectrophotometer between 400-4000 cm⁻¹ by using KBr pellet while ≥ 400 cm⁻¹ using polyethylene. The micro-elemental analysis data was obtained on a Model Fison EA 1108 Analyzer, NMR data also obtained from 600MHz FT-NMR Cryoprobe and the molar magnetic susceptibilities were measured on powdered samples using the Gouy balance.

Synthesis of the ligands

Salicylaldehyde 4-phenylthiosemicarbazone, SaOHtsc, L^1

The synthesis of SaOHtsc ligand involved condensation between ethanolic solution of salicylaldehyde (0.001 mol, 0.122 g) was slowly added dropwise into an ethanolic solution of 4-phenylthiosemicarbazide (0.001 mol, 0.167 g) were stirred for 2 hour at 60-70 °C. After that, the solution of mixture was filtered and cooled at room temperature. After 3 days later, the yellow precipitate was formed and collected by filtration, washed with cold ethanol and dried overnight in a dessicator. Yield: 82 %. Analyses: Calculated: C, 61.97; H, 4.83; N, 15.49; S, 11.82 %. Found: C, 62.60; H, 4.86; N, 16.93; S, 12.07 %. IR v_{max} cm⁻¹: 1620 (C=N), 1079 (N-N), 1152 (C=S), 3308 (N-H), 1033 (C-N). ¹H NMR (DMSO) (δ , ppm): 10.04 (N²H, 1H, s), 11.70 (N¹H, 1H, s), 6.83-8.04 (aromatic, 9H, m), 8.48 (aliphatic, 1H, s). ¹³C NMR (DMSO) (δ , ppm): 140.81 (C=N), 176.23 (C=S), 116.53-139.53 (aromatic).

p-chlorobenzaldehyde 4-phenylthiosemicarbazone, ph-HClbtsc, L^2

The synthesis of ph-HClbtsc ligand involved condensation between ethanolic solution of p-chlorobenzaldehyde (0.001 mol, 0.141 g) was slowly added dropwise into an ethanolic solution of 4-phenylthiosemicarbazide (0.001 mol, 0.167 g). Yield:79 %. Analyses: Calculated: C, 58.03; H, 4.17; N, 14.50; S, 12.23 %. Found: C, 57.95; H, 4.11; N, 15.87; S, 11.51. IR v_{max} cm⁻¹: 1597 (C=N), 1086 (N-N), 1199 (C=S), 3311 (N-H), 1013 (C-N). ¹H NMR (DMSO) (δ , ppm): 10.16 (N²H, 1H, s), 11.84 (N¹H, 1H, s), 7.20-7.96 (aromatic, 9H, m), 8.14 (aliphatic, 1H, s). ¹³C NMR (DMSO) (δ , ppm): 141.94 (C=N), 176.63 (C=S), 125.89-139.51 (aromatic).

Synthesis of complexes

The complexes were prepared by mixing with ratio 2:1 of ligand and metal salt in refluxing ethanolic solution for 3h.

Co(II) salicylaldehyde 4-phenylthiosemicarbazone, CoSaOHtsc (1)

 $C_{28}H_{24}N_6O_2S_2Co$. Yield:65 %. Analyses: Calculated: C, 56.17; H, 4.04; N, 14.04; S, 10.72 %. Found: C, 55.95; H, 3.69; N, 14.07; S, 9.06. IR ν_{max} cm⁻¹: 1596 (C=N), 1081 (N-N), 650 (C-S), 3357 (N1H), 1250 (C-N), 500 (Co-N), 352 (Co-S).

Co(II) p-chlorobenzaldehyde 4-phenylthiosemicarbazone, Coph-HClbtsc (2)

 $C_{28}H_{22}N_6S_2Cl_2Co$. Yield:68 %. Analyses: Calculated: C, 52.83; H, 3.48; N, 13.21; S, 10.08 %. Found: C, 51.63; H, 3.43; N, 13.13; S, 9.46 %. IR v_{max} cm⁻¹: 1594 (C=N), 1093 (N-N), 661 (C-S), 3386 (N¹-H), 1251 (C-N), 536 (Co-N), 353 (Co-S). 1H NMR (DMSO) (δ , ppm): 9.51(N¹H, 1H, s), 6.65-7.71 (aromatic, 9H, m), 8.74 (aliphatic, 1H, s). ¹³C NMR (DMSO) (δ , ppm): 171.21 (C=N), 158.12 (C-S), 116.34-141.47 (aromatic)

Figure 1. Salicylaldehyde 4-phenylthiosemicarbazone, SaOHtsc, L¹

Figure 2. p-chlorobenzaldehyde 4-phenylthiosemicarbazone, ph-HClbtsc, L²

Figure 3. Co(II) salicylaldehyde 4-phenylthiosemicarbazone, CoSaOHtsc (1)

Figure 4. Co(II) p-chlorobenzaldehyde 4-phenylthiosemicarbazone, Coph-HClbtsc (2)

Antibacterial and antifungi test

The ligands and the complexes were tested for antibacterial and antifungi activities. The test organisms chosen for antibacterial activity were two Gram positive and two Gram negative while for antifungi activity were only one fungi species. The screening property was done by the disc diffusion method. The bacterial cultures were maintained in nutrient agar slants and fungi in potato dextrose. The diameter of inhibition zone resulting with DMSO for both antibacterial and antifungi activities was measured and compared with standard values.

Bacteria Gram(+)	Bacteria Gram(-)	Fungi
i. B. Subtilis ii S. Epidermis	i. E. Coli ii. P. Mirabilis	i. Candida Albican

Results and Discussion

Infrared spectra

Selected vibration bands of ligands and its metal complexes are given in Table 1 and Table 2.

Table 1. IR spectral assignments for ligands

Molecular formula		waver	number	(cm ⁻¹)	
	C=N	N-N	C=S	N-H	C-N
SaOHtsc, L ¹	1620	1079	1152	3308	1033
ph-HClbtsc, L ²	1597	1086	1199	3311	1013

Table 2. IR spectral assignments for cobalt(II) complexes

Compounds	wavenumber (cm ⁻¹)						
	C=N	N-N	C-S	N¹-H	C-N	M-N	M-S
CoSaOHtsc (1)	1596	1081	650	3357	1250	500	352
Coph-HClbtsc (2)	1594	1093	661	3386	1251	536	353

In principle, Qing et al. 2006 [6] said that the ligands can exhibit thione-thiol tautomerism, since it contains a thioamide -NH-C=S functional group. The vibration of v(S-H) band at 2600-2800 cm⁻¹ is absence from the IR spectral of the ligands but the vibrations of $v(N^2H)$ band at 3308 and 3311 cm⁻¹ where corresponding ligands \mathbf{L}^1 and \mathbf{L}^2 are present indicated that in the solid state the ligands remain as the thione tautomer. In the complexes spectral, the vibration of $v(N^2H)$ band in the ligands spectral disappears which indicates the deprotonation of the $-N^2H$ proton and coordination of azomethine nitrogen atom to the central metal ion, Co(II). The bands appearing at 1152 and 1199 cm⁻¹ which assigned to the v(C=S) band for the ligands \mathbf{L}^1 and \mathbf{L}^2 are absent in the spectral of the complexes. While the vibration band of v(C-S) are appeared at 650 and 661 cm⁻¹ in the spectral of the complexes which confirmed the coordination occur through the sulfur atom to the metal ion. For the ligand \mathbf{L}^1 , the broad band of v(OH) overlapping with $v(N^2H)$ at 3308 cm⁻¹. The vibration band of v(OH) deprotonated and coordinate to the central metal ion through oxygen atom. The coordination between azomethine nitrogen, thiolate sulfur and oxygen atom from the ligand \mathbf{L}^1 to the Co(II) ion can be approved by the presence of bands at 500, 352 and 466 cm⁻¹ which the ligand act as dinegative tridentate. Whereas for the ligand \mathbf{L}^2 , the coordination between azomethine N and thiolate S atoms to the Co(II) ion can be approved by the presence of bands at 536 and 353 cm⁻¹ where the ligand act as mononegative bidentate.

¹H and ¹³C NMR

Table 3. Selected chemical shifts of ligands and its metal complexes for ¹H NMR.

Compounds	Chemical shift, δ (ppm)				
	N(2)H	N(1)H	Aromatic	Aliphatic (C-H)	
SaOHtsc, L ¹	10.04,	11.70,	6.83-8.04,	8.48, 1H (s)	
	1H (s)	1H (s)	9H (m)		
ph-HClbtsc, L ²	10.16,	11.84,	7.20-7.96,	8.14, 1H (s)	
	1H(s)	1H (s)	9H (m)		
Coph-HClbtsc (1)	-	9.51,	6.65-7.71,	8.74, 1H (s)	
•		1H (s)	9H (m)		

Table 4. Selected chemical shifts of ligands and its metal complexes for ¹³C NMR.

Compound	Chemical shift, δ (ppm)				
	C=N	C=S	C-S	Aromatic	
SaOHtsc, L ¹	140.81	176.23	-	116.53-139.53	
ph-HClbtsc, \mathbf{L}^2	141.94	176.63	-	125.89-139.51	
Coph-HClbtsc, (2)	171.21	-	158.12	116.34-141.47	

The 1 H and 13 C NMR spectra of all the ligands and complexes have been taken in DMSO- d_6 . The ligands does not show any peak attributable to S-H proton in the 1 H NMR spectra but the spectra show the signal of $v(N^{2}H)$ at 10.04-10.16 ppm which indicates that the ligand exist as thione tautomer. Aromatic protons appear as a multiplet at 6.83-8.04 ppm and 7.20-7.96 ppm which is assigned for the ligands L^{1} and L^{2} . The diamagnetic Co(II) complex (2) is soluble in DMSO- d_6 , thus when the spectral data are compared with the free ligands, several differences can be observed. The peak corresponding to the proton N^{2} H is absent in the spectrum of complex which is evidence of the deprotonation of the ligand and coordination between azomethine N with metal centre. The chemical shift for aliphatic hydrogen, C-H in spectrum complex (1) shifted downfield to be compared with its ligand where the signal appeared to be at 8.74 ppm. This happens due to the influenced of coordination between azomethine N with Co(II) [7]. The proton OH in the spectrum of ligand L^{1} at 10.01 ppm is absent in spectrum of complex (1) which is the evidence of deprotonation of OH and coordination between O phenolic with metal centre [4]. The chemical shift for C=S in the spectral of ligands L^{1} and L^{2} appeared at the lowest downfield which is at the range 176.23 and 176.63 ppm. The phenomenon happens due to the influence of electronegativity of N and S atoms that attached it. The peak of C=S is absent in the spectrum of ligand L^{1} but the peak of C-S appear at the range 158.12 ppm in spectrum of complex (1) which is the evidence that coordination occur between thiolate S with Co(II).

Antibacterial properties

The antibacterial properties of the ligands and complexes were determined by the standard "disc diffusion' method. The bacteria were growth in nutrient agar slants. The compounds to be tested were dissolved in DMSO and soaked in filter paper disc No.3. The disc incubated at 28°C for 28 h. The diameter clearing zone around the disc was measured which the diameter indicated the inhibitory activity of the compound on the bacteria. The results of antibacterial studies were given in Table 5 and 6.

Table 5. Diameter clearing zone around the disc for bacteria G(+).

Compound	B. Subtilis (cm)	S. Epidermis (cm)
Standard (Tobramycin)	1.7	1.7
SaOHtsc, L ¹	0.6	1.0
ph-HClbtsc, L^2	0.7	0.6
CoSaOHtsc, (1)	1.0	0.7
Coph-HClbtsc, (2)	0.7	1.8

Table 6. Diameter clearing zone around the disc for bacteria G(-)

Compound	E. Coli (cm)	P. Mirabilis (cm)
Standard (Tobramycin)	1.2	1.5
SaOHtsc, L ¹	0.7	0.7
ph-HClbtsc, \mathbf{L}^2	0.7	0.7
CoSaOHtsc, (1)	0.6	0.6
Coph-HClbtsc, (2)	0.7	0.6

From the Table 5 and 6, the ligands and Co(II) complexes are found to be moderate active against bacteria. While the compound (1) was very active against *S. Epidermis sp.* The compound have electron withdrawing group which will increase the activity of antibacterial. The velocity of compound to diffuse into membrane cell was depends on the density of electron in the compound. The faster the compound to diffuse into membrane cell, more active antibacterial activity of the compound [2].

Conclusion

The coordination ability of the thiosemicarbazone derivatives as mononegative and dinegative bidentate through thiolate sulfur, azomethinic nitrogen and phenolic oxygen has been proved in complexation reaction with Co(II) and characterization with elemental analysis, NMR and IR spectroscopy. The biological behaviour revealed that most of the ligands are moderate active as antibacterial activity. While the complex (2) are very active as antibacterial against *S. Epidermis* sp due to presence of withdrawing group in the complex structure.

Acknowledgement

The authors thank to Faculty of Science and Technology, Universiti Kebangsaan Malaysia for the provision of laboratory facilities and technical assistance. The authors also gratefully acknowledge the research grant from UKM-GUP-NBT-08-27-112 and UKM-ST-06-FRGS112-2009 and scholarship from the National Science Fellowship (NSF).

References

- 1. Bingol, H & Atalay. T. 2006. Study of Kinetics of Complexation Reaction of Co²⁺ with 2-benzoylpyridine-4-phenyl-3-thiosemicarbazone and Kinetic-spectrophotometric Determination of Cobalt. Acta *Phys. -Chim. Sin* 22(12): 1484-1488.
- 2. Hania, M. M. 2009. Synthesis and Antibacterial Activity of Some Transition Metal Complexes of Oxime, Semicarbazone and Phenylhydrazone. *E-Journal of Chemistry* **6(S1)**: S508-S514.
- 3. Ibrahim, M. N & Sharif, S. E. A. 2007. Synthesis, Characterization and Use of Schiff Bases as Fluorimetric Analytical Reagents. *E-Journal of Chemistry* 4(4): 531-535.
- Kannan. S., Sivagamasundari. M., Ramesh. R & Yu Liu. 2008. Ruthenium(II) carbonyl complexes of dehydroacetic acid thiosemicarbazone: Synthesis, structure, light emission and biological activity. Journal of Organometallic Chemistry 693:2251–2257.
- 5. Kizilcikli, I., Kurt, Y. D., Akkurt, B., Genel, A. Y., Birteksöz, S., Ötük, G & Ülküseven, B. 2007. Antimicrobial Activity of a Series of Thiosemicarbazones and Their ZnII and PdII Complexes. Folia Microbiol. 52 (1):15–25.
- 6. Qing, Y., Hua, D. J., Gang, Z. L., Qing, Z. X., Dong, B. H & Hong, L. 2006. Structure studies of Ni(II) complexes with picolinaldehyde N-oxide thiosemicarbazone. *Journal of Molecular Structure* **794**:71–76.

- 7. Sau, D. K., Butcher, R. J., Chaudhuri, S & Saha, N. 2004. Synthesis and spectroscopic characterization of new cobalt(III) complexes with 5- methyl-3-formyl pyrazole 3-hexamethyleneiminyl thiosemicarbazone (HMPz3Hex): X-ray crystallographic identification of HMPz3Hex and [Co(MPz3Hex)₂]Br.H₂O with evidence for unusual rotation about the azomethine double bond of the ligand on complexation with cobalt(III). *Polyhedron* 23:5–14.
- 8. Vinuelas-Zahínos, E., Luna-Giles, F., Torres-García, P & Fernandez-Calderon, M. C. 2011. Co(III), Ni(II), Zn(II) and Cd(II) complexes with 2-acetyl-2-thiazoline thiosemicarbazone: Synthesis, characterization, X-ray structures and antibacterial activity. *European Journal of Medicinal Chemistry* **46**: 150-159.



SYNTHESIS AND CATALYTIC ACTIVITY OF N,N'-*BIS*-(α-METHYLSALICYLIDENE)-PROPANE-1,3-DIAMINEPALLADIUM(II) AND ITS 4-METHYL DERIVATIVES IN HECK CARBON-CARBON COUPLING REACTION

(Sintesis dan Aktiviti Pemangkinan N,N'-*Bis*-(α-Metilsalisilidina-Propan-1,3-Diamina-palladium(II) dan Terbitan 4-Metil dalam Tindak Balas Gandingan Karbon-Karbon Heck)

Siti Kamilah Che Soh^{1,2}, Mustaffa Shamsuddin¹*, Bohari M. Yamin³

¹Department of Chemistry, Faculty of Science, Universiti Teknologi Malaysia, 81310 Skudai, Johor, Malaysia. ²Department of Chemical Sciences, Faculty of Science and Technology, Universiti Malaysia Terengganu, 21030 Kuala Terengganu, Terengganu, Malaysia. ³School of Chemical Sciences and Food Technology, Faculty of Science & Technology, Universiti Kebangsaan Malaysia, 43650 Bangi, Selangor, Malaysia.

*Corresponding author: mustaffa@kimia.fs.utm.my

Abstract

Carbon-carbon bond formation is an important step in organic synthesis. Palladium(II) complexes have been widely used as catalyst in the transition metal catalysed bond formation. This paper reports the synthesis, characterization and catalytic performance of two palladium(II)-Schiff base complexes obtained from the condensation of 2'-hydroxyacetophenone and its 4'-methyl derivative with 1,3-diaminopropane followed by complexation with palladium(II) acetate, Pd(OAc)₂. Ligands and complexes were characterized by NMR and FTIR spectroscopic methods as well as X-ray crystallographic analysis and CHN elemental analyses. The ligands acted as N,N,O,O tetradentate, coordinating to the palladium atom through both its imine nitrogens and phenolic oxygens. The efficiency of these palladium complexes were evaluated as catalysts in the Heck reaction of 4'-bromoacetophenone with methyl acrylate in the presence of sodium hydrogen carbonate as base in N,N-dimethylacetamide as solvent at reflux temperature 120 °C. The activities of the catalysts were monitored by GC-FID. Both catalysts gave 100% conversion after 12 hours. The product of the reactions is 3-(4-Acetylphenyl)-acrylic acid methyl ester.

Keywords: Palladium, Schiff base, Heck reaction

Abstrak

Pembentukan ikatan karbon-karbon merupakan langkah penting dalam sintesis organik. Kompleks palladium(II) telah digunakan secara meluas sebagai mangkin dalam logam peralihan yang memangkinkan pembentukan ikatan. Kajian ini melaporkan hasil sintesis, pencirian dan prestasi pemangkinan bagi dua kompleks palladium(II)-bes Schiff yang telah dihasilkan daripada tindak balas kondensasi 2'-hidroksiasetofenon dan terbitan 4'-metil dengan 1,3-diaminopropan, diikuti oleh pengkompleksan dengan palladium(II) asetat, Pd(OAc)₂. Ligan dan kompleks ini dicirikan dengan kaedah spektroskopi RMN dan IM, diikuti oleh analisis kristalografi sinar-X dan analisis unsur CHN. Ligan ini berfungsi sebagai ligan tetradentat N,N,O,O dan terkoordinat kepada atom palladium melalui kedua-dua atom nitrogen imina dan kedua-dua atom oksigen fenolik. Kecekapan kompleks palladium ini dinilai sebagai mangkin dalam tindakbalas Heck antara 4'-bromoasetofenon dan metil akrilat dalam N,N-dimetilasetamida dengan kehadiran bes sodium hidrogen karbonat pada suhu refluks 120 °C. Aktiviti pemangkinan ini dipantau menggunakan GC-FID. Kedua-dua mangkin ini memberikan penukaran 4-bromoasetofenon 100% selepas 12 jam tindakbalas. Hasil daripada tindak balas ini adalah 3-(4-asetilfenil)-akrilik-asid metal ester.

Siti Kamilah Che Soh et al: SYNTHESIS AND CATALYTIC ACTIVITY OF N,N'-BIS-(α-METHYL-SALICYLIDENE)-PROPANE-1,3-DIAMINEPALLADIUM(II) AND ITS 4-

METHYL DERIVATIVES IN HECK CARBON-CARBON COUPLING REACTION

Kata kunci: Palladium, bes Schiff, tindak balas Heck

Introduction

The Heck coupling reaction, a versatile, powerful and efficient tool for construction of new C-C bonds in organic synthesis has become one of the best methods for fine chemical production [1]. It is referred to as the palladiumcatalyzed of aryl halides with alkenes derivatives. Since it was put forward mainly by Mizoroki and Heck et al. in the late 1970s, more and more chemicals especially the cinnamate derivatives and the medicine intermediates have been synthesized through this process [2,3].

In particular, palladium complexes associated with phosphine ligands which stabilize palladium species serve as highly active systems for carbon-carbon bonds formation [4]. However, these ligands are undesirable in industry due to the toxicity, high price and water and air sensitivity [5]

To date, many efforts have been made to search for more phosphine-free ligands for Heck catalytic reaction [6]. In this present work, the Schiff base ligands have been chosen for this purpose. The palladium(II)-Schiff base complexes have been widely studied due to the versatility of their steric and electronic properties, which can be fine-tuned by choosing the amine precursors and ring substituents [7]. N,O-bidentate and N₂O₂-tetradentate ligands possess many advantages such as facile approach, readily adjusted ancillary ligands, and tunable steric and electronic coordination environments on the metal centre [8] Due to these properties, the N₂O₂-tetradentate ligands and their transition metal complexes often act as catalysts.

In our attempt to evaluate a phosphine free conditions of Heck coupling reaction, the Schiff bases derived from the condensation between 1,3-diaminopropane with 2'-hydroxyacetophenone and its 4'-methyl derivative have been chosen. In this present work, the performance of the corresponding palladium(II) complexes as catalysts have been evaluated in the Heck reactions of 4'-bromoacetophenone and methyl acrylate. The reactions were carried out in N,N-dimethylacetamide as a solvent in the presence of sodium hydrogen carbonate as base at 120 °C.

Materials and Methods

All glasswares were dried overnight in an oven. Commercial grade solvents were distilled according to normal procedures and dried over molecular sieves (Å) before used. All reagents were purchased either from Aldrich, Merck or Fluka and were used without further purification. All reactions were carried out in an inert atmosphere of dry nitrogen.

The melting point of the solid products was determined using an Electrothermal Digital Melting Point Apparatus and were uncorrected. Infrared spectra were recorded as KBr pellets on a Perkin Elmer Spectrum One FTIR spectrometer in the range of 4000-400 cm⁻¹. NMR spectra were recorded in CDCl₃ on a Bruker Avance 400MHz spectrometer. The chemical shifts are reported in ppm using tetramethylsilane (TMS) as internal standard. Elemental analysis was performed on a Thermo Finnigan CE 125 CHN analyzer. The single crystal X-ray crystallographic measurements were performed on a Bruker AXS Ltd, Siemens SMART APEX 4K CCD model using graphite-monochromated Mo-K α radiation ($\lambda = 0.71073$ Å). The structures were solved by direct methods and all calculations were carried out with the aid of the SHEXTL software package [9]. Gas Chromatography (GC) analyses were carried out on a Hewlett-Packard 6890H gas chromatograph equipped with a 30 m x 250 µm x 0.25 μm nominal capillary column (UTRA-1.0.05, 100% dimethylpolysiloxane) and Flame Ionization Detector (FID). The microliter samples were injected at 50 °C. The temperature increment was at 15 °C per minute and the final temperature was 300 °C.

Synthesis of N,N,O,O Ligands

Figure 1. Synthesis of N,N,O,O-tetradentate ligands

N,N'-bis(α -methylsalicylidene)-propane-1,3-diamine (1a)

Stoichiometric amount of 1,3-diaminopropane (5.0mmol) with two equivalents of 2-hydroxyacetophenone are mixed together in 10 mL anhydrous ethanol (Figure 1). The resulting mixture was refluxed under N_2 atmosphere for 5 h after which a yellow solid had precipitated out. This was separated by vacuum filtration, washed with cold ethanol and dried in vacuum. Yield 80%. m.p. = 95-96°C. Calc. for $C_{19}H_{22}N_2O_2$: C, 73.52; H, 7.14; N, 9.03%. Found: C, 75.31; H, 7.28; N, 9.55%. IR (KBr) v_{max} cm⁻¹: 3445 (OH), 1614 (C=N), 1161 (C-O). ¹H-NMR (CDCl₃), δ_{H} : 12.28 (s, 2H, OH), 7.54-7.52 (dd, 2H, J=8.2 Hz Ar-H), 7.32-7.28 (t, 2H, J=8.0 Hz, Ar-H), 6.95-6.92 (dd, 2H, J=8.2 Hz, Ar-H), 6.81-6.77 (t. 2H, J=8.0 Hz, Ar-H), 3.78-3.74 (t, 4H, N-CH₂), 2.37 (s, 6H, CH₃) and 2.29-2.20 (m, 2H, CH₂). ¹³C-NMR (CDCl₃), δ_{C} : 172.36 (CC=N), 164.09 (C-OH), 132.59, 128.02, 119.17, 118.76, 117.05 (arom. C), 46.46 (N-CH₂), 30.82 (CCH₂) and 14.53 (CCH₃).

N,N'-bis(4-methyl- α -methylsalicylidene)-propane-1,3-diamine (1b)

The 4-methyl analogue was prepared in 85% yield in a similar manner to the method described for **1a**. Suitable crystal for **1b** was obtained by slow evaporation of acetone solvent. m.p. = $111-112^{\circ}$ C. Calc. for $C_{21}H_{26}N_{2}O_{2}$: C, 74.52; H, 7.74; N, 8.28 %. Found: C, 73.81; H, 7.37; N, 8.31%. IR (KBr) v_{max} cm⁻¹: 3436 (OH), 1611 (C=N), 1154 (C-O). ¹H-NMR (CDCl₃), δ_{H} : 12.30 (s, 2H, OH), 7.40-7.38 (d, 2H, J=8.0 Hz, Ar-H), 6.74 (s, 2H, Ar-H), 6.60-6.58 (d, 2H, J=8.0 Hz, Ar-H), 3.74-3.71 (t, 4H, N-CH₂), 2.33-2.31 (d, 6H, CH₃), 2.26-2.20 (m, 2H, CH₂) and 1.82 (s, 6H, CH₃). ¹³C-NMR (CDCl₃), δ_{C} : 172.06 (CC=N), 164.63 (C-OH), 143.50, 127.88, 119.11, 118.17, 116.67 (arom. C), 46.11 (NCH₂), 30.80 (CCH₂), 21.57 (N=CCH₃) and 14.38 (CCH₃).

Synthesis of Palladium(II)-Schiff base Complexes

Figure 2. Synthesis of palladium(II)-Schiff base complexes

N,N'-bis(α -methylsalicylidene)-propane-1,3-diaminepalladium(II) (2a)

The ligand 1a (0.5 mmol) dissolved in 10 mL acetonitrile was added to a solution of palladium(II) acetate (0.5 mmol) in 10 mL acetonitrile in a three necked round bottom flask (Figure 2). The mixture was refluxed under N_2 atmosphere for 5 hours after which it was filtered and evaporated to low volume. The required palladium complex 2a was obtained as brown needles. This was filtered off and dried in vacuum. Yield 77.44%. m.p. = 335-336°C.

Calc. for $C_{19}H_{20}N_2O_2Pd$: C, 55.02; H, 4.86; N, 6.75%. Found: C, 54.76; H, 4.77; N, 6.79%. IR (KBr) v_{max} cm⁻¹: 1597 (C=N), 1141 (C-O). ¹H-NMR (CDCl₃), δ_H : 7.31-7.28 (dd, 2H, J=8.0 Hz, Ar-H), 7.18-7.14 (t, 2H, J=8.0 Hz, Ar-H), 7.07-7.06 (d, 2H, J=8.0 Hz, Ar-H), 6.56-6.52 (t, 2H, J=8.0 Hz, Ar-H), 3.35-3.33 (t, 4H, N-CH₂), 2.78-2.76 (m, 2H, CH₂), 2.35 (s. 6H, CH₃). ¹³C-NMR (CDCl₃), δ_C : 169.18 (CC=N), 166.50 (C-OH), 133.44, 129.94, 127.02, 121.84, 114.83 (arom. C), 53.43 (NCH₂), 32.14 (CCH₂), 19.83 (CCH₃).

N.N'-bis(4-methoxysalicylidene)-2,2-dimethylpropane-1,3-diaminepalladium(II) (2b)

The corresponding palladium complex **2b** was prepared and isolated as green solid in 75.25% yield after treating palladium(II) acetate with one mole equivalent of ligand **1b** in a similar manner to the method described for **2a**. m.p. = 341-343°C. Calc. for $C_{21}H_{24}N_2O_2Pd$: C, 56.96; H, 5.46; N, 6.33%. Found: C, 56.64; H, 5.42; N, 6.61%. IR (KBr) v_{max} cm⁻¹: 1607 (C=N), 1165 (C-O). ¹H-NMR (CDCl₃), δ_{H} : 7.20-7.18 (d, 2H, J=8.0 Hz, Ar-H), 6.90 (s, 2H, Ar-H), 6.37-6.35 (d, 2H, J=8.0 Hz, Ar-H), 3.34-3.32 (t, 4H, N-CH₂), 2.76-2.74 (m, 2H, CH₂), 2.33 (s, 6H, CH₃) and 2.22 (s, 6H, CH₃). ¹³C-NMR (CDCl₃), δ_{C} : 168.76 (CC=N), 166.48 (C-OH), 144.25, 129.73, 124.48, 121.80, 116.47 (arom. C), 53.28 (NCH₂), 32.18 (CCH₂), 21.39 (N=CCH₃) and 19.62 (CCH₃).

Catalytic Study

4-bromoacetophenone (1 mmol; 0.20 g), methyl acrylate (3 mmol; 0.3 mL), sodium hydrogen carbonate (2.4 molar equiv.), palladium complex 2a (1 mol %; 0.01 mmol) and N,N-dimethylacetamide solvent (2.5 mL) were mixed together in a Radley's 12-placed reaction carousel whilst purging with nitrogen (Figure 3). The reaction carousel was then heated to 120 °C with the temperature carefully controlled by a contact thermometer (\pm 1 °C) for 3, 6 and 12 h. The conversion of reaction was monitored by GC-FID. The Heck reaction was repeated by using complex 2b as catalyst.

Figure 3. Heck reaction catalyzed by Pd(II) catalysts

Results and Discussion

The Schiff base ligands, N,N'-bis(α -methylsalicylidene)-propane-1,3-diamine (1a) and N,N'-bis(4-methyl- α -methylsalicylidene)-propane-1,3-diamine (1b) were obtained as a yellow solid in high yield through condensation reaction between 1,3-diaminopropane with 2-hydroxyacetophenone and the 4-methyl derivative respectively. These Schiff bases were fully characterised. Elemental analytical, IR, IR and IR NMR data are in the Experimental section. The synthesis of the palladium(II) complexes are outlined as in Figure 2. Microanalytical data for the ligands and the palladium complexes are consistent with the calculated empirical formula values.

The IR spectrum of the Schiff bases 1a and 1b showed the appearance of a very strong azomethine v(C=N) stretching bands at 1615 and 1611 cm⁻¹ respectively. These values are consistent with other similar imine compounds [10]. Besides that, the absorption bands for v (-NH₂) stretching mode from 1,3-diaminopropane and v (C=O) stretching mode from 2-hydroxyacetophenone and its 4-methyl derivative have totally disappeared, demonstrating that ligands 1a and 1b have been successfully synthesized.

Meanwhile, the IR spectrum of the palladium(II) complexes 2a and 2b exhibit the strong and sharp v(C=N) stretching band at 1597 and 1607 cm⁻¹ respectively. The slight displacement of the v(C=N) from 1615 and 1611 cm⁻¹ in the free ligands to 1597 and 1607 cm⁻¹ in the complexes respectively suggested the coordination of the azomethine nitrogen atom to the palladium metal. This results show that the contribution of C=N stretching have been reduced as the nitrogen atoms are involved in bond formation with the metal ion. Besides, the broad O-H

bands at 3245 and 3421 cm⁻¹ in the ligands **1a** and **1b** respectively are absent in the IR spectrum of the complexes, suggesting the coordination of phenolic oxygen atom to the metal centre.

In the 1H NMR spectrum, the signal of the acidic OH proton for ${\bf 1a}$ and ${\bf 1b}$ appeared as single resonance at low field at $\delta 12.28$ ppm and $\delta 12.30$ ppm respectively. These signals have totally disappeared in the 1H spectra for the complexes, further indicating the coordination of oxygen atoms to the palladium metal due to the participation of OH group in chelating to metal ion through proton displacement [11]. Meanwhile, the ^{13}C NMR spectral data showed the displacement to low field of the imine carbon (C=N) resonance from $\delta 172.36$ ppm for ${\bf 1a}$ and $\delta 172.03$ ppm for ${\bf 1b}$ in the free ligand to the $\delta 169.18$ ppm and $\delta 168.76$ ppm respectively in the complexes due to the coordination of azomethine nitrogen atom to the palladium metal.

Single X-ray Crystallography

Suitable crystals of ligand **1b** for X-ray diffraction analysis were successfully grown by slow evaporation from a solution of acetone at room temperature. The structure is shown in Figure 4. The selected bond lengths and angles are listed in Table 1.

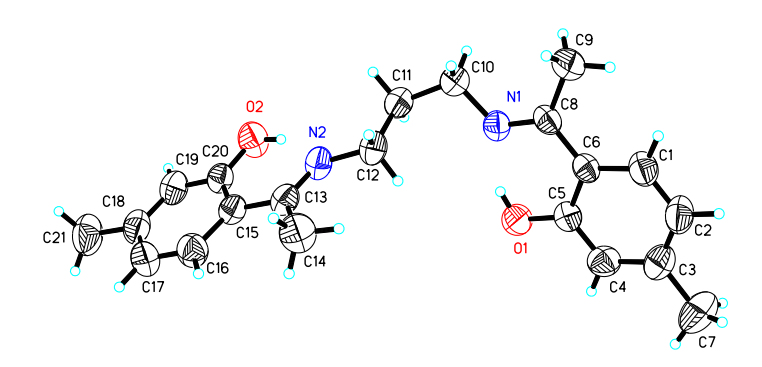


Figure 4. The ORTEP drawing of ligand 1b

TC 1.1. 1 (C . 1	1	1 1 1 1 1 1	1 (0)	for ligand 1b
I anie i s	Selected nond	IANGTH (A	1 and nond	angles (*)	i tor maana in

Bond	Dist.
N(1)-C(8)	1.286(3)
N(2)-C(13)	1.284(3)
O(1)-C(5)	1.339(3)
O(2)-C(20)	1.343(3)
Angle	(°)
C(5)-O(1)-H(1B)	105(3)
C(20)-O(2)-H(2B)	107(2)
N(1)-C(8)-C(6)	117.6(2)
N(2)-C(13)-C(15)	117.3(2)

The bond lengths and angles of the compound is in agreement with the analogues of N,N'-bis-(5-methylmethylsalicylidene)-2,2-dimethylpropane-1,3-diamine [12]. From analysis showed that bond lengths of azomethine C8=N1, 1.286(3) Å and C13=N2, 1.284(3) Å in the molecule are in normal range and consistent with other similar imine compounds [13].

Catalytic Studies

The palladium complexes **2a** and **2b** were applied to the Heck reaction (Figure 3) of methyl acrylate with 4-bromoacetophenone in N,N-dimethylacetamide at 120°C for 12h, using sodium hydrogen carbonate as base. Catalytic reactions were performed under an atmosphere of nitrogen. Catalytic loading was kept to 1.0 mol%, so as to give an expected turnover number of 100 if 100% conversion was achieved. The reaction was monitored by % conversion of the starting material, 4-bromoacetophenone, using GC-FID. A control experiment was also performed for comparison. The results are summarized in Table 2. The catalytic data obtained indicate that these palladium(II) complexes efficiently catalyse the Heck reaction of 4-bromoacetophenone with methyl acrylate, giving more than 90% conversion after 6h. The effect of temperature, solvent, base and amount of catalyst on the catalytic properties of the palladium(II) complexes is currently in progress.

Table 2. Heck reaction of 4-bromoacetophenone with methyl acrylate catalysed by palladium complexes **2a** and **2b**

Cotolyst		% Conversion	
Catalyst	AFTER 3H	After 6h	After 12h
Complex 2a	59.65	97.07	100
Complex 2b	64.90	97.76	100
Without catalyst	3.89	7.09	13.7

Conclusion

In summary, we have synthesised and characterised two chelated palladium(II) complexes with Schiff bases obtained from the condensation reaction between 1,3-Diaminopropane and 2-hydroxyacetophenone or 2-hydroxy-4-methoxyacetophenone. These complexes efficiently catalyse the Heck reaction of 4'-Bromo- acetophenone with methyl acrylate. The influence of temperature, solvent, bases and catalyst loading on the catalytic performance on the Heck or other palladium catalysed carbon-carbon coupling reactions is currently been investigated.

Acknowledgement

We would like to acknowledge the financial support provided by the Ministry of Higher Education, Malaysia through the FRGS Vote No. 78323. S.K.C.S wishes to thank Universiti Malaysia Terengganu for a scholarship and study leave, Universiti Teknologi Malaysia and Universiti Kebangsaan Malaysia for providing research facilities

References

- 1. Keles, M., Keles, T. and Serindag, O. (2008). Palladium complexes with bis(diphenylphosphino methyl)amino ligands and their application as catalysts for Heck reaction. Transition Met Chem. 33, 717-720.
- 2. Hartung, C. G., Köhler, K. and Beller, M. (1999). Highly Selective Palladium-Catalyzed Heck Reactions of Aryl Bromides with Cycloalkenes. *Org Lett.* 1, 709-711.
- 3. Blaser, H. U., Indolse, A., Schnyder, A., Steiner, H. and Stder, M. (2001). Supported Palladium Catalysts for Fine Chemicals Synthesis. *J. Mol. Catal: A. Chem.* 173,3-18.
- 4. Kayan, C., Biricikkk, N. and Aydemir, M. (2011). Aminophosphine ligands: Synthesis, Coordination Chemistry and Activity of Their Palladium(II) Complexes in Heck and Suzuki Cross-coupling Reactions. Transition Met Chem. 36, 513-520.
- 5. He, Y. and Cai, C. (2011). Polymer-Supported Macrocyclic Schiff Base Palladium Complex as an Efficient Catalyst for the Heck Reaction. Appl. Organomatal. Chem. 25, 799-803.
- 6. Lu, J. M., Ma, H., Li, S. S., Ma, D. and Shao, L. X. (2010). 2,2'-Diamino-6,6'-Dimethylbiphenyl as an Efficient Ligand in the Palladium-Catalyzed Suzuki-Miyaura and Mizoroki-Heck Reactions. Tetrahedron. 66, 5185-5189.
- Basak, S., Sen, S., Mitra, S., Marschner, C. and Sheldrick, W. S. (2008). Square Planar Complexesof Cu(II) and Ni(II) with N₂O Donor Set of Two Schiff Base Ligands: Synthesis and Structural Aspects. Struct Chem. 19, 115-121

- 8. Wang, M., Zhu, H., Jin, K., Dai, D. and Sun, L. (2003). Ethylene Oligomerization by Salen-Type Zirconium Complexes to Low-Carbon Linear α-Olefins. *J. Catal.* 220, 392-398
- 9. Sheldrick, G. M. (2008). A Short History of SHELX. Acta Cryst. A64, 112-122.
- 10. Montazerozohori, M., Habibi, H. M., Hajjati, A., Mokhtari, R., Yamane, Y. and Suzuki, T. (2009). 2,2'-[(E,E)-1,1'-(2,2-Dimethylpropane-1,3-diyldinitrilo)diethyllidene]diphenol. *Acta Cryst*. E65, o1662-o1663.
- 11. Soliman, A. A. and Linert, W. (1999). Investigations on New Transition Metal Chelates of the 3-Methoxy-Salicylidene-2-Aminothiophenol Schiff Base. *Thermochimica acta*. 338, 67-75.
- 12. Ibrahim, W. N. W., Shamsuddin, M. and Yamin, B. M. (2007). N,N'-bis-(5-Methyl-Methylsalicylidene)-2,2-Dimethylpropane-1,3-Diamine Palladium(II): Catalyst for Heck Reaction. *Malaysian. J. Anal. Sci.* 11, 98-104.
- 13. Shamsuddin, M., Nur, A. M. M. and Yamin, B. M. (2005). N-[2-(Diphenylphosphanyl)benzylidene]-4-methylaniline. *Acta Cryst*. E61, o2263-o2264.



(Pengambilan Ion Logam Berat oleh Resin Penukar Ion Terbitan Asid p-Hidroksibenzoik-Formaldehid-Resorsinol: Sintesis, Pencirian dan Dinamik Erapan)

Riddhish R. Bhatt¹, Bhavna A. Shah^{1*} and Ajay V. Shah²

¹Department of Chemistry, Veer Narmad South Gujarat University, Surat-7, Guj., India. ²Department of Chemistry, Polytechnic, Vidhyabharti Trust, Umrakh, Bardoli, Guj., India

*Corresponding author: rrbhatt_chem@yahoo.com

Abstract

Chelating ion-exchange resin (pHFR) has been synthesized by condensing p-hydroxybenzoic acid with formaldehyde employing resorcinol as cross linking agent at 80 ± 5 °C using DMF as a solvent. The resin was characterized by elemental analysis, FTIR, 1 H-NMR and XRD. The thermal analysis (TGA, DTA and DTG) was done at the heating rate of 10 °C/min in N₂ atmosphere. The morphology of the resin was studied by optical photographs and scanning electron micrographs (SEM) at different magnifications. The physico-chemical properties have been studied. The uptake behaviour of various metal ions viz. Ni(II), Cu(II), Zn(II), Cd(II) and Pb(II) towards pHFR resin have been studied depending on contact time, pH, metal ion concentration and temperature. The maximum uptake capacity for Ni(II), Cu(II), Zn(II), Cd(II) and Pb(II) are found 1.310, 2.304, 1.690, 1.591 and 2.020 mmol/g respectively. The selectivity order is: Cu(II)>Pb(II)>Zn(II)>Cd(II)>Ni(II). The intra-particle diffusion rate constant (K_{si}) and external diffusion rate constant (K_s) are calculated by Saphn-Schlunder and Weber-Morris models respectively. Equilibrium adsorption data were analyzed by Langmuir and Freundlich equations. The adsorption process follows first order kinetics and specific rate constant K_r was obtained by the application of Lagergan equation. Thermodynamic parameters viz. ΔG° , ΔS° and ΔH° have also been calculated for the metal-resin systems.

Keywords: Chelating resin, thermal study, SEM, Thermodynamics, optical photograph, kinetics

Abstrak

Satu resin penukar ion kelat (pHFR) telah disintesis melalui kondensasi asid p-hidroksibenzoik dengan formaldehid menggunakan resorsinol sebagai agen taut silang pada suhu 80 ± 5 °C dan DMF sebagai pelarut. Resin ini telah diciri menggunakan analisis unsur, FTIR, ¹H-NMR dan XRD. Analisis terma (TGA, DTA dan DTG) telah dilakukan pada kadar pemanasan 10° C/min dalam atmosfera N_2 . Morfologi resin telah dikaji menggunakan fotograf optik dan mikrograf electron imbasan (SEM) pada pelbagai pembesaran. Sifat fiziko-kimia telah juga dikaji. Perlakuan pengambilan pelbagai ion logam seperti Ni(II), Cu(II), Zn(II), Cd(II) dan Pb(II) terhadap resin pHFR telah dikaji pada pelbagai masa sentuhan, pH, kepekatan ion logam dan suhu. Muatan maksimum pengambilan bagi Ni(II), Cu(II), Zn(II), Cd(II) dan Pb(II), masing-masing ialah 1.310, 2.304, 1.690, 1.591dan 2.020 mmol/g. Tertib selektiviti ialah : Cu(II)>Pb(II)>Zn(II)>Cd(II)>Ni(II). Pemalar resapan intra-zarah (K_{id}) dan pemalar kadar resapan luaran (K_s) dikira menggunakan model Saphn-Schlunder dan Weber-Morris. Data jerapan keseimbangan dianalisis berdasarkan persamaan Langmuir dan Freundlich. Proses jerapan didapati mengikut kinetik tertib satu dan pemalar kadar tentu K_r didapati melalui persamaan Langmuir dan Freundlich. Proses jerapan didapati mengikut kinetik tertib satu dan pemalar kadar tentu K_r didapati melalui persamaan Langmuir dan Freundlich. Proses jerapan didapati mengikut kinetik tertib satu dan pemalar kadar tentu K_r didapati melalui persamaan Langmuir dan Freundlich. Proses jerapan didapati mengikut kinetik tertib satu dan pemalar kadar tentu K_r didapati melalui persamaan Langmuir dan Freundlich. Proses jerapan didapati mengikut kinetik tertib satu dan pemalar kadar tentu K_r didapati melalui persamaan Langmuir dan Freundlich.

Kata kunci: Resin kelat, kajian terma, SEM, termodinamik, fotograf optik, kinetik

Introduction

Removal, separation and enrichment of trace metals in aqueous solutions play an important role for the analysis of wastewaters, industrial and geological samples. Many separation techniques such as solvent extraction and ion-exchange chromatography have been applied for this purpose. Ion exchange is a popular method owing to its applicability to both pre-concentration and separation. The ion-exchange resin from salicylic acid and formaldehyde was derived by DeGeiso et al [1] in 1962. They have studied the ion exchange capacity and selectivity of salicylic acid-formaldehyde copolymer with Fe³⁺, UO₂²⁺ ions as a function of pH. Patel et al [2, 3] have prepared the terpolymer of salicylic acid/p-hydroxy benzoic acid and thiourea with trioxane in the presence of acid catalyst with different molar proportions of monomers. Shah et al have been synthesized chelating resin from o-substituted benzoic acid and studied its ion-exchange properties [4]. The micro-wave assisted synthesized phenolic-formaldehyde polymers were prepared and their ion exchange properties towards the heavy metal ions were studied using a static batch equilibrium technique at 25 °C as a function of contact time, pH and concentration [5]. The sorption capacity of salicylic acid-formaldehyde condensate towards Al(III), Cu(II), Ni(II), Zn(II) and Co(II) were studied. The resin was found selective for Cu(II) ion with highest exchange capacity of 0.7 mmol/g [6].

Kapadia et al [7-9] prepared ion exchange resins from various phenolic derivatives like salicylic acid, gallic acid, β-resorcylic acid, anthranilic acid, 8-hydroxyquinoline and hydroquinone using DMF as a solvent. They have studied their anion as well as cation exchange properties towards various metal ions. Mubarak and coworkers [10] have studied the chelation behavior of the phenolic-formaldehyde polymers towards the trivalent lanthanide metal ions such as La³⁺, Nd³⁺, Sm³⁺, Gd³⁺ and Tb³⁺ by a static batch equilibrium technique at 25 °C as a function of contact time, pH and concentration. Samal et al [11] prepared resins from the diazonium salt of aniline with phenol/resorcinol coupled with formaldehyde in alkaline medium. They have studied the uptake behavior of alkali and alkaline earth metal ions by the resin. The optimum conditions for effective separation of Cu²⁺ from UO₂²⁺ were also determined.

Recently, in 2006, Burgeson et al [12] evaluated resorcinol-formaldehyde resin for cesium removal and cesium elution characteristics. A new spherical form of resorcinol-formaldehyde resin [13] was also tested for efficiency of cesium removal from the complex mixture of radioisotopic liquid wastes. Resin from salicylic acid and formaldehyde with resorcinol [14] in DMF media has also been prepared and studied for its chelation ion-exchange properties. Shah et a [15] synthesized ion-exchange resin from anthranilic acid and formaldehyde with resorcinol in DMF media. They have separated transition and post transition metal ions from synthetic binary mixtures using tartaric acid as eluting agent.

So far no resin based on p-hydroxy benzoic acid-formaldehyde-resorcinol in DMF media has been reported with its morphology and thermal characteristics along with its kinetic and thermodynamic parameters. As industrial effluents are often rich in transition and post transition metal ions, removal and recovery of these metals is an important task for industries. In this paper, synthesis, characterization and different physico-chemical and chelation properties of the resin are reported along with its thermal and morphological studies. Various diffusion models and isotherm equations were employed to analyze the sorption data.

Materials and Methods

Materials and Reagents

Analytical grade chemicals such as p-Hydroxybenzoic acid (Ranbaxy fine chemicals S.A.S. Nagar), formaldehyde (37%) (Qualigens fine chemicals, Mumbai) and catechole (SRL Mumbai, extra pure) used as received without further purification. Solutions of acids and alkalies were prepared by dissolving appropriate amount of the particular compound in double distilled water and standardized by the literature methods [16]. Stock solution of metal salts under study were prepared by dissolving appropriate amount of metal acetates in double distilled water and standardized by EDTA titration [16]. Stock solution of EDTA (0.1M) was prepared and standardized against a solution of MgSO₄ using Ereochrome Black T (EBT) indicator. Buffer of acetic acid/sodium acetate (pH 3.0-6.0) was used for the batch experiments carried out to study uptake behaviour of metal ions. Mureoxide indicator was used for the estimation of Ni(II), Ereochrome Black T was used for Zn(II), Xylenol orange was used for Cd(II) and Pb(II), Fastsulphon Black F was used for Cu(II) estimation [16]. Glasswares were cleaned by overnight soaking in nitric acid (1:1) followed by multiple rinsing with water. All the other reagents used were of analytical grade and

were used as such. Double distilled and deionized water was used throughout the research work. All pH measurements were carried out with digital pH meter (Elico CL-44) equipped with a combine glass/calomel electrode.

Resin Synthesis

p-Hydroxybenzoic acid (13.5 g, 0.1 mole) was taken in 250 ml round bottom flask and dissolve in DMF solvent (20 ml) to give clear solution. A solution of resorcinol (11 g, 0.1 mole) in 10 ml DMF was added to above solution and stirred for two hours. Formaldehyde (0.3 mole as 37%) was added and stirred for an hour. Then mixture was refluxed on a water bath at 80 ± 5 °C for 2-3 h with constant stirring during which the mixture gelled to a soft mass, which was dark brown in colour. A gel was separated from the reaction vessel and cured in an oven at 80-90 °C for 12 h. As carboxylic acid group normally get decomposed above 100 °C, the resin was cured below 90 °C. The resulting resin was washed with DMF to remove monomer impurities and finally with deionised water. After complete washing cycle, the yield of the resin was found to be 63 % (13.7 g). This purified and dry resin sample was finely ground and passed through 20 mesh screen and then 50 mesh screen to get uniform particle size (20 to 50 mesh). This sieved resin was again washed with water, air dried at room temperature and stored in polyethylene bottle. The solubility test of resin in different solvents was performed at room temperature and pressure with intermittent shaking. It was found non-melting and insoluble in almost all common organic solvents like acetone, ethanol, benzene, DMF, chloroform etc and also in acids and alkalies of higher strength (up to 6 M). But the resin exhibits poor solubility in DMSO-d₆ solvent. This sieved resin was characterized using different instrumental techniques and was used for all the experiments during the research period. The resin obtained from pHydroxybenzoic acid-fromaldehyde-resorcinol is abbreviated as pHFR (Scheme-I).

The particle size was measured by Malvern particle size Analyzer (Mastersizer-2000). The elemental analysis was carried out on Elemental Analyser (Carlo Erba, model 1160). Infra-Red spectra of the synthesized resin sample had been scanned in KBr pallets on FTIR Spectrophotometer (Shimadzu model-8201PC). The ¹H-NMR spectra was scaned in DMSO-d6 solvent on NMR Specrometer (Bruker DPX-200) at 200 MHz with a seep time of 10 min. at room temperature. The x-ray diffraction analysis (XRD) was performed by advanced Diffractometer (Bruker AXE D8). The thermograms (TGA, DTG and DTA) of the present resin sample were taken on TG/TGA instrument (Perkin Elmer Pyris Damond) at constant heating rate of 10 °C/min. in N₂ atmosphere. The surface analysis was done using an optical photograph (Olympus SZX12) and scanning electron microscope (Philips XL30) at different magnifications.

To convert the resin sample in H⁺ form, resin sample having uniform particle size (20-50 mesh) was equilibrated with 1M HCl solution for 24 h and washed with deionized water till it was free from chloride by testing with silver nitrate solution. This H⁺ form of resin was used for further studies. The batch equilibrium method was adopted to study the ion-exchange properties. The surface area of the resin was calculated using the following equation:

$$A_{s} = \frac{G \text{ Nav } \phi 10^{-20}}{M \text{ Mw}}$$
 (1)

where, A_s is the resin surface area in m^2/g , G is the amount of methylene blue adsorbed (g), N_{AV} is the Avogadro's number (6.023 x 10^{23} mol⁻¹), ϕ is the methylene blue molecular cross section (197.2 °A), Mw the molecular weight of methylene blue (373.9 g.mol⁻¹) and M is the mass of the resin (g).

The surface area of pHFR is found to be 143.2 m²/g.

The sorption properties such as effect of pH, contact time, metal ion concentration, temperature, and distribution coefficient (K_d) for different metal ions as a function of pH and concentration of tartaric acid were studied according to literature methods [17, 18].

Scheme-I. Route of synthsis of pHFR resin.

Batch sorption experiments

To study the effect of important parameters like pH, contact time and metal ion concentration on uptake of various metal ions, batch experiments were conducted at room temperature (30 ± 2 °C). To study the effect of pH on the metal ion uptake, it is necessary to buffer the resin and the solutions used. Different sets of accurately weighed (0.250 ± 0.001 g) dry resin having uniform particle size (20-50 mesh) were equilibrated with buffer in different stoppered bottles for 24 h, so that resin attained desired pH value. After 24 h buffer solutions were decanted and 50 ml of 0.2 M metal ion solutions of varying pH from 3-6 were added. Metal ion solutions were equilibrated at room temperature (30 ± 2 °C) for 24 h with intermittent shaking. After 24 h solutions were filtered with 0.02 µm membrane to separate the resin and solution. The pH of the filtrate was measured and it was found that pH remain stable throughout the experiment (\pm 0.2). From the filtrate unadsorbed metal ions were estimated by complexometric titration with 0.1 M EDTA solution using appropriate indicator. To study the effect of contact time on sorption of metal ions, H⁺ form of accurately weighed (0.250 \pm 0.001 g) dry resin samples were taken in different glass stoppered bottles and equilibrated with buffer solutions of optimum pH value (pH of highest exchange) for 24 h. For Ni(II) and Pb(II) pH was maintained 5.0, for Cu(II) and Cd(II) pH audjusted to 5.5 and for Zn(II) ph was adjusted to 6.0. After decanting buffer solution, 50 ml (0.2 M) metal ion solution of the same pH was added. The

amounts of unadsorbed metal ions were determined by complexometric titration at fixed time intervals. To study the effect of metal ion concentration on uptake of different metal ions by the resin, the resin was equilibrated with acetate buffer at desired pH values (pH value of highest exchange) for 24 h and then buffer solutions were decanted. The accurately weighed $(0.250 \pm 0.001~g)$ dry resin were equilibrated with metal ion solutions (50 ml) of varying molar concentration i.e. 0.05~M, 0.1~M, 0.15~M, 0.20~M, 0.25~M and 0.30~M at the same pH value at room temperature for 15 h with intermittent shaking. After 15 h metal ion solutions were filtered and unchelated metal ions were estimated. The study the effect of temperature was performed at fixed metal ion concentration (0.15~M) for fixed resin loading $(0.250 \pm 0.001~g)$ and initial pH (different optimum pH for dofferent metal ions) at four different temperatures i.e. 20, 30, 40 and $50~^{\circ}C$.

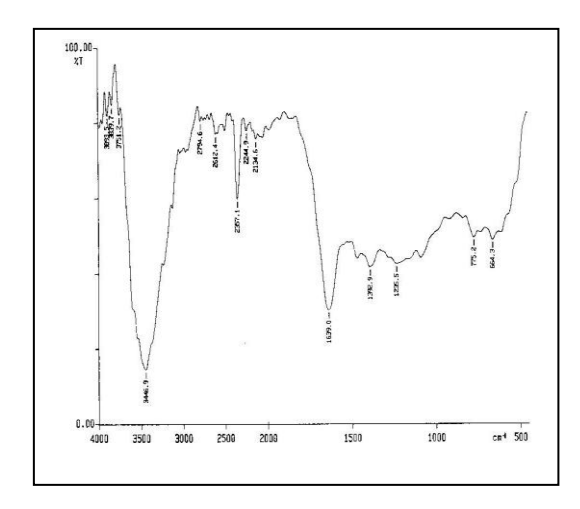
Results and Discussion

Elemental analysis

The %C, %H and %N were calculated from the general formula ($C_{14}H_{11}O_7$) of the repeating unit of the assumed structure (scheme-I) of the resin. The value obtain are 64.15% (64.85%) and 3.91% (4.11%) for %C and %H respectively. The results of the elemental analysis are good agreement with calculated values of %C, %H and %N. The values of elemental analysis confirm the proposed structure of the resin presented in scheme-I.

Spectral characterization of resin (FTIR, ¹H-NMR, XRD)

The FTIR spectrum of pHFR resin is exhibited in Figure 1. The strong band at 3446.9 cm⁻¹ is due to the $\upsilon(\text{O-H})$ stretching of phenolic group. The presence of medium band at 2983 cm⁻¹ is due to the $\upsilon(\text{C-H})$ stretching of methylene group [15, 19]. The presence of broad band at 2612.4 cm⁻¹ is due to $\upsilon(\text{C-OH})$ stretching of carboxylic group. The medium strong band at 1639.0 cm⁻¹ can be assigned to $\upsilon(\text{C=O})$ stretching of aromatic acid group. The weak band at 1410 cm⁻¹ is due to $\delta(\text{C-H})$ deformation of methylene group [20]. The weak medium band at 1392.9 cm⁻¹ can be assigned to $\delta(\text{C-O-H})$ bending of aromatic –OH group. The band at 1235.5 cm⁻¹ can be assigned to the aromatic $\delta(\text{O-H})$ bending of phenol. The medium band at 775.2 cm⁻¹, is due to the $\delta(\text{C-H})$ bending of 1,2,3,4-tetra substituted benzene ring [21]. The medium band at 664.3 cm⁻¹, is due to the $\delta(\text{C-H})$ bending of poly ethylene – (CH₂)-bridges.



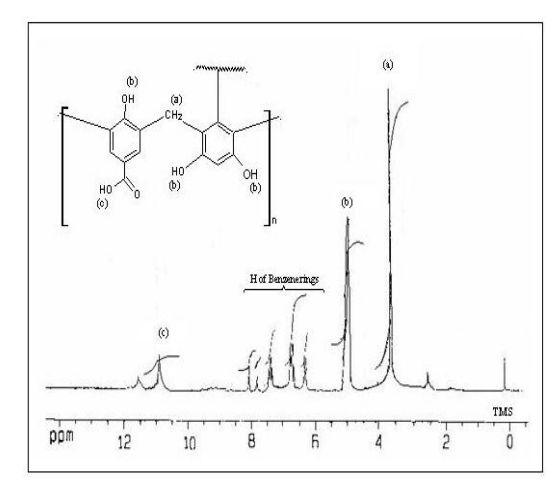


Fig. 1. FTIR spectrum of pHFR

Fig. 2. ¹H-NMR spectrum of pHFR

The ¹H-NMR spectra of synthesized resin (pHFR) is shown in Figure 2. The peak observed at 10.9 ppm is due to the H of carboxylic acid group (Ar-COOH). The peaks observed at 6.2 ppm to 8.12 ppm are due to the H of benzene ring. The peak observed at 3.86 ppm is due to the 2H of methylene group (Ar-CH₂-Ar) [19]. The sharp singlet peak at 5.2 ppm is due to the H of phenolic (–OH) group.

The XRD pattern of the compound provides information whether the compound is crystalline or amorphous or crystalline and amorphous region co-exist in he same compound [21]. The XRD pattern of pHFR is shown in Figure 3. No sharp peaks are observed in the difractogram of the resin. The pHFR resin exhibits irregular pattern, which is a characteristic of the amorphous compound [21, 22]. Phenol-formaldehyde resin [23] also exhibited similar XRD pattern, which confirms the amorphous nature of the pHFR resin.

Thermal analysis (TGA, DTG, DTA)

The examination of the result of the thermograms (TGA, DTG and DTA) (Fig 4) reveals that resin sample undergoes degradation in two steps like salicylic acid-formaldehyde-resorcinol [14]. In the beginning of TGA curve, weight loss of 8.2 % was observed at 57 to 142 °C, this may be due to the loss of surface water which is loosly bound and evolved slowly. The maximum rate of weight loss was at 113 °C, which is observed in DTG curve. This is further confirmed from the DTA curve, which shows endothermic moisture loss at 113 °C. The second step decomposition of polymeric material starts at 400 °C which extends upto 800 °C involving 66 % (2.58 mg) weight loss. The DTG curve reveals that at 492 °C the rate of weight loss is highest. The first step DTA curve of pHFR exhibits broad endotherm at 112 °C with enthalpy 542 mJ/mg while in second step the exothermic peak observed at 493 °C with enthalpy -398 mJ/mg. The thermal degradation of the resin may be due to the random cleavage of polymeric resin affording simpler degradation products [3, 23]. It is very difficult to draw any conclusion from the magnitude of the thermal activation because the decomposition mechanism is expected to be very difficult [24]. The typical observations from the TGA are that the thermal degradation is steep and almost no left over residue is seen and similar observation was reported for salicylic acid-formaldehyde-resorcinol resin [14] and anthranilic acid-formaldehyde-resorcinol [15].

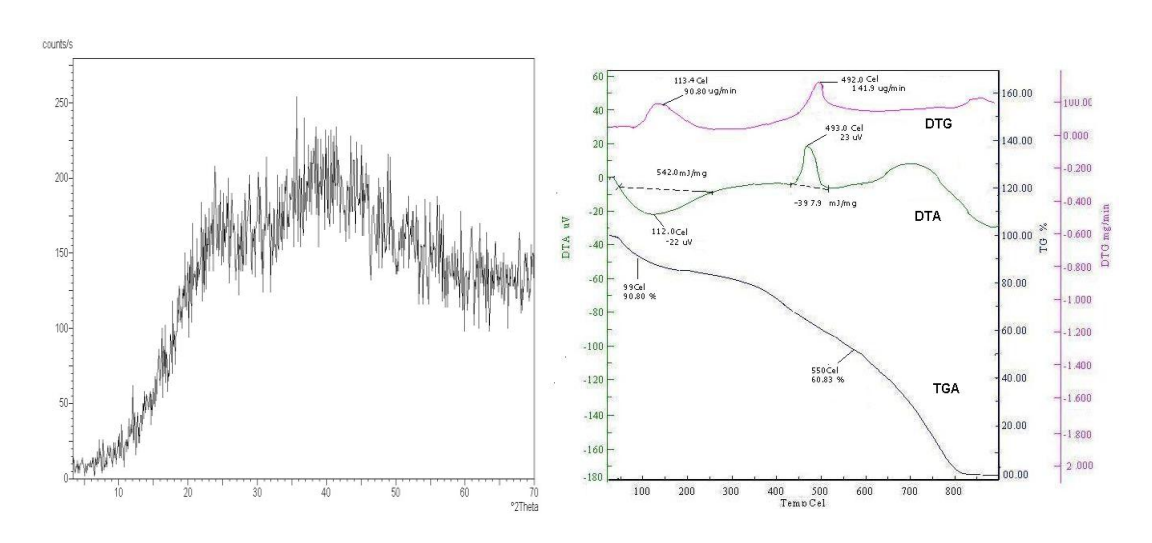


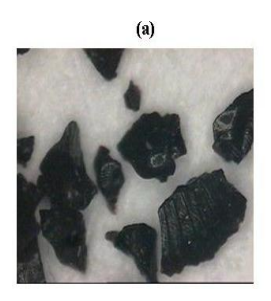
Fig. 3. XRD pattern of pHFR

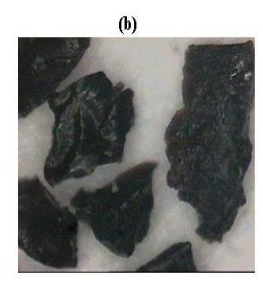
Fig. 4. TGA, DTG and DTA of pHFR resin at heating rate of 10 $^{\circ}$ C/min. in N_2 atmosphere

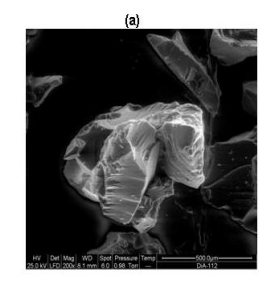
Surface Analysis (Optical and SEM photographs)

Surface analysis has been found to be of great use in understanding the surface features of the material. The morphology of the reported resin sample was investigated by optical photographs and scanning electron micrographs to characterize particle shape, size and surface morphology which are shown in Figure 5 and 6 respectively. Several observations were made of the resin before the micrographs (optical and SEM) were taken to ensure that the photographed regions were representative of the overall resin sample [12]. The optical and SEM photographs were taken at different magnifications, here in the present communication optical photograph of 110X (Fig. 5a) and 290X (Fig. 5b) magnifications and SEM photograph of 200X (Fig. 6a) and 500X (Fig. 6b)

magnifications have been presented. The white bar at the bottom of the SEM micrographs represents the scale. Resin appeared dark brown with rough surface in optical photograph. From the SEM photographs it is observed that the resin exhibits angular edges with regular fringes. The fringes represent the transition material between crystalline and amorphous phases [15, 21]. The morphology of the resin shows a fringed micelle model of the crystalline-amorphous structure, similar observation was obtained for salicylic acid-formaldehyde-resorcinol resin [14].







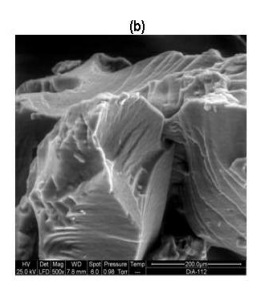


Fig. 5. Optical photographs of pHFR (a)110X (b) 290X magnifications

Fig. 6. SEM photographs of pHFR
(a) 200X (b) 500X magnifications

Sorption dynamic studies

Effect of pH on exchange capacity

The removal of metal ions from aqueous solution by sorption is highly dependent on pH of the solution that affects the surface charge of the sorbent [3]. Chelating ligand forms complexes with various metal ions at specific pH conditions [4]. Therefore, the effect of variation in pH on chelating ability of the resin has been studied. The results are presented as exchange capacity against pH for different metal ions in Figure 7. The results show that adsorption of metal ions were increased with increase in pH upto a certain value and thereafter decreased. From the nature of the trend observed indicates that the cation exchange behaviour of this resin is similar to weak acid cation exchangers [1, 14]. Because in weak acid cation ion exchanger, exchange capacity is pH dependent [17]. The maximum adsorption for Ni(II) and Pb(II) took place at pH 5, for Cu(II) and Cd(II) it was at pH 5.5 and for Zn(II) it was at pH 6. The selectivity order for metal ions is Cu(II) > Pb(II) > Zn(II) > Cd(II) > Ni(II).

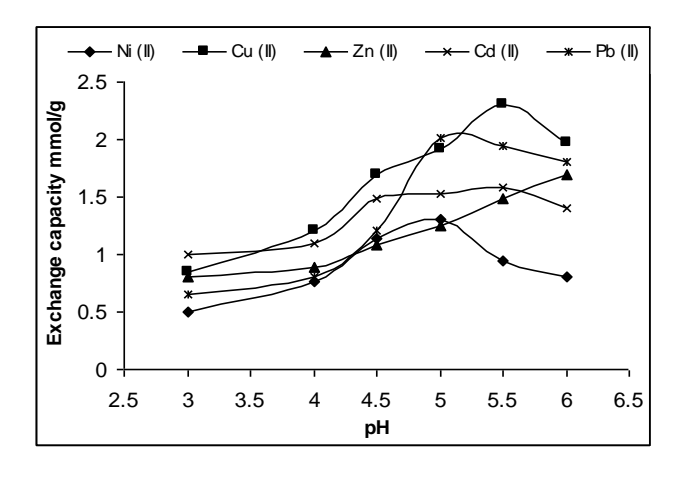


Fig. 7. The metal uptake capacity of Ni(II), Cu(II), Zn(II), Cd(II) and Pb(II) on pHFR resin as a function of pH [initial metal ion conc. = 0.2 M, amount of resin = 0.250 g, vol. of metal ion solution = 50 ml, temp.= 30 ± 1 °C]

An increase in pH increases the negatively charged nature of the sorbent surface. This leads to an increase in the electrostatic attraction between positively charged metal ions and negatively charged sorbent and results in increase in the adsorption of metal ions. The decrease in the removal of metal ions at lower pH is due to the higher concentration of H⁺ ions present in the reaction mixture which compete with the metal ions for the sorption sites on the sorbent surface. Meanwhile the observed decrease in sorption at higher pH is due to the formation of insoluble hydroxy complexes of the metal ions [25]. Therefore, pH 5 is taken as the optimum pH for Ni(II) and Pb(II), pH 5.5 is considered optimum pH for Cu(II) and Cd(II), pH 6 is considered optimum pH for Zn(II). The further sorption experiments were carried out at these different pH conditions for different metal ions.

Rate of exchange for metal ions

The exchange of metal ions on resin exhibits the time dependant phenomenon. The rate of exchange for different metal ions is illustrated in Figure 8. The rate of metal ion adsorption of the resin was determine to ascertain the shortest time period for which equilibrium could be carried out [3]. The graph shows that the time required for 50 % exchange ($t_{1/2}$) for zinc(II) and lead(II) is about 55 min., for cadmium(II) and nickel(II) is 2.5 h, for copper(II) is 48 min. respectively. The fast rate of exchange in the beginning can be explained on the basis of law of mass action [6]. The faster rate of exchange facilitates column chromatographic separation. Kinetics of metal ion exchange mainly depends on the various physical properties like particle size distribution, pore size, physical core structure and diffusion of counter ion [14, 15].

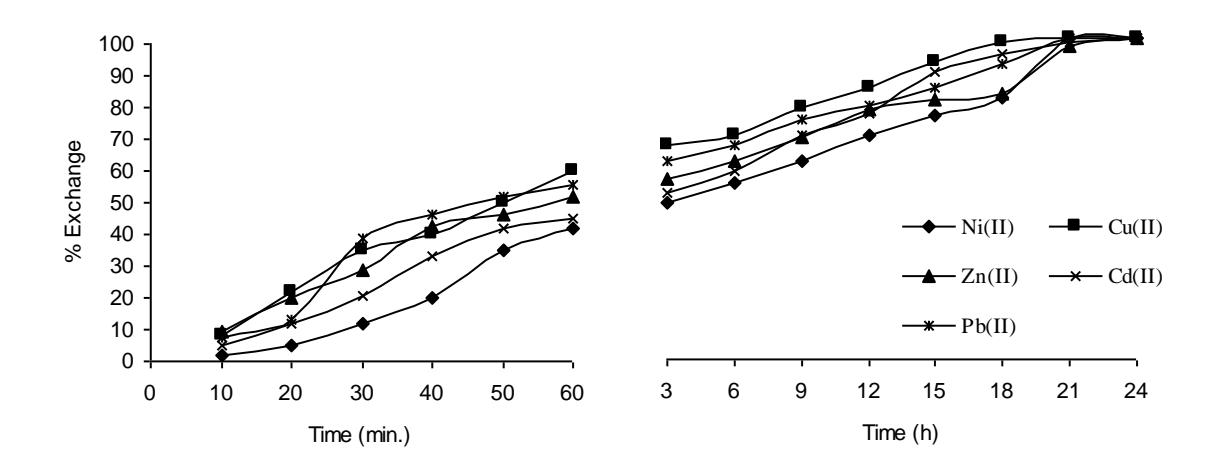


Fig. 8. Rate of metal ion exchange on pHFR resin

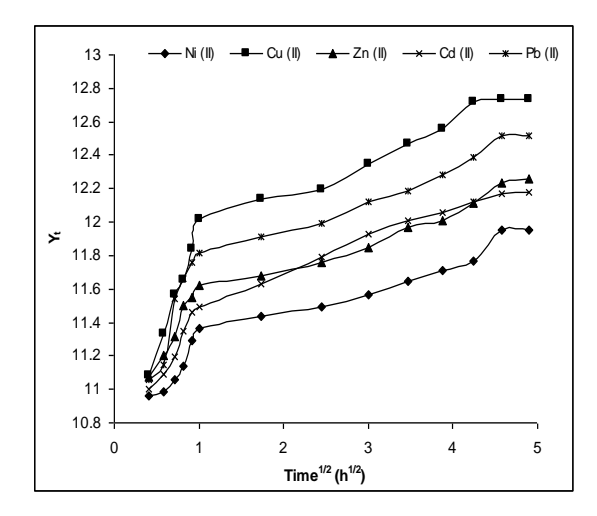
Time dependence of the fraction of metal uptake on resin

Time dependence is determined by politting the fraction of adsorption, Y_t against the retention time, $t^{1/2}$. The Y_t is define as[27]:

$$Y_t = C_o - C_t / C_o - C_e$$
 (2)

where, C_o denotes the initial concentration of metal ions, C_t is the concentration of metal ions at time 't' and C_e is the equilibrium concentration.

The rate of fraction of adsorption Y_t expressed as square root of time is estimated from the three staged curve illustrated in Figure 9. The initial steep sloped portion is attributed to the transfer of metal ions from the bulk of the solution to the boundary film of the adsorbent and later to its surface. The second stage corresponds to the transfer of the metal ions from the surface to the intraparticular active sites of the resin. This stage is slow and the rate determining step of the reaction. The final stage shows the completion of sorption reaching equilibrium [26]. At equilibrium there is a definite distribution of the solute particle between the solution and the resin particle. Karthikeyan et al [27] reported similar observation while studying the adsorption of reactive dye and Zn (II) ion respectively over chitosan.



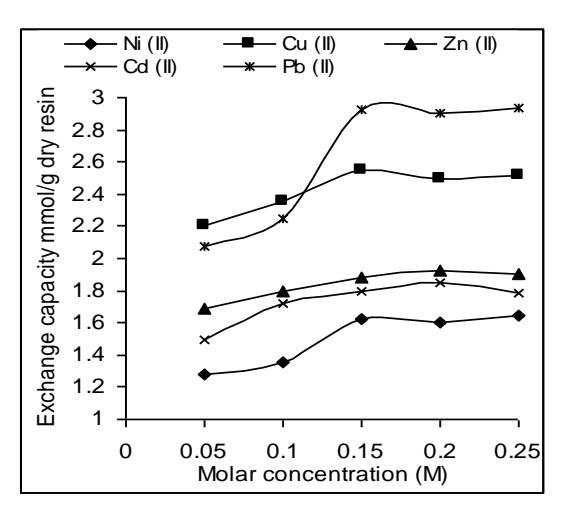


Fig. 9. Time dependence of the fraction of adsorption of metal ions on pHFR resin

Fig. 10. The metal uptake capacity of pHFR resin as a function of metal ion concentration

Effect of metal ion concentration on exchange capacity

The examination of data presented in Figure 10 reveals that the amount of adsorbed metal ion increases with the increase in concentration of metal ions in solution until a maximum value, and will remain constant upon further increase in metal ion concentration. At lower concentration of metal ions the number of metal ions available in solution is less as compared to the available sites on the sorbent [28]. However, at higher concentration the available sites of sorption remain same whereas more metal ions are available for sorption and subsequently the sorption becomes almost constant thereafter [14, 15]. Therefore 0.15 M is consider as optimum concentration and used for all further experiments.

Effect of temperature and thermodynamic parameters

The effect of temperature on the adsorption of various metal ions on pHFR resin was also studied using the optimizing conditions. The temperature was varied from 20 to 50 °C. It was observed that the adsorption of metal ions increase with the increase in temperature (Table 1). This is due to the endothermic ion-exchange reaction of divalent cation [20]. The working of an ion-exchange depends on metal ion concentration and temperature. The surface energy of the pHFR resin increases with temperature. Similar results have also been reported for the adsorption of Ni(II), Cu(II), Zn(II),Cd(II) and Pb(II) with Dowex 50 [20] and Amberlite IR 120 [29].

Table 1. The metal uptake capacity of pHFR resin as a function of temperature

Table 2. Thermodynamic parameters for metal ion adsorption on pHFR resin.

Metal	Exchange capacity at various temperature (mmol/g)				
IOIIS	293 K	303 K	313 K	323 K	
Ni(II)	1.37	1.41	1.46	1.49	
Cu(II)	1.28	1.35	1.44	1.47	
Zn(II)	1.78	1.80	1.84	1.87	
Cd(II)	1.56	1.59	1.63	1.68	
Pb(II)	2.21	2.27	2.31	2.35	

Metal	Temp	ΔG^{o}	ΔH°	ΔS^{o}	
ions	K	kJ mol ⁻¹	kJ mol ⁻¹	J K ⁻¹ mol ⁻¹	
	293	-2.588			
	303	-2.591			
Ni	313	-2.607	7.021	19.56	
	323	-2.615			
	293	-4.803			
	303	-4.812			
Cu	313	-4.835	4.794	10.57	
	323	-4.853			
	293	-3.845			
	303	-3.892			
Zn	313	-3.911	4.819	11.97	
	323	-3.923			
	293	-3.701			
	303	-3.722			
Cd	313	-3.735	5.135	13.39	
	323	-3.739			
	293	-4.371			
	303	-4.391			
Pb	313	-4.406	7.113	18.23	
	323	-4.409			

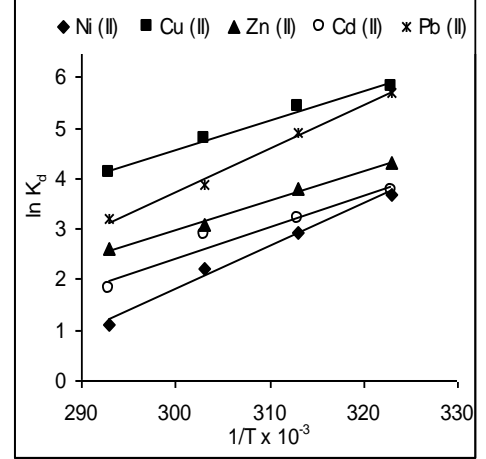


Fig. 11. Van't Hoff plot for the adsorption of metal ions on pHFR resin

The values of ΔH^o , ΔS^o and ΔG^o were also calculated from the slope and intercept of the Vant' Hoff plot of the adsorption of metal ions on pHFR resin, i.e. the linear variation of lnK_d with reciprocal temperature 1/T (Fig. 11) using the following relation:

$$\ln K_{\rm d} = \frac{\Delta S^{O}}{R} - \frac{\Delta H^{O}}{RT} \tag{3}$$

where K_d is the distribution coefficient (cm³/g), ΔS^o is the entropy change for the process, ΔH^o is the enthalpy change for the process.

The free energy of the adsorption and ΔG^{o} was calculated using the following Van't Hoff equation (4):

$$\Delta G^{o} = -RT \ln K_{d} \tag{4}$$

The thermodynamic parameters for the adsorption of various metal ions on pHFR resin are given in Table 2. The value of ΔH^o is positive which indicates an endithermic adsorption process and it is likely that the chelation mechanism dominates [30]. The entropy (ΔS^o) is positive corresponding to an increase in degree of freedom of the system due to release of two hydrogen ions for the divalent metal ions under study [31]. The negative value of ΔG^o indicate the feasibility of the process and also the spontaneity of the adsorption process. The amount of metal ions adsorbed at equilibrium must increase with increasing temperature, because ΔG^o decrease with the rise in temperature of the solution [27].

Sorption Isotherms

Equilibrium is described by usual isotherm equations such as Langmuir and Freundlich isotherms. A preliminary screening of the corresponding equations has shown that Langmuir and Freundlich models best fit the experimental data and the following equations are used for the modeling of results.

Langmuir model:
$$(C_e/Q_e) = (1/Q^o b) + (C_e/Q^o)$$
 (5)

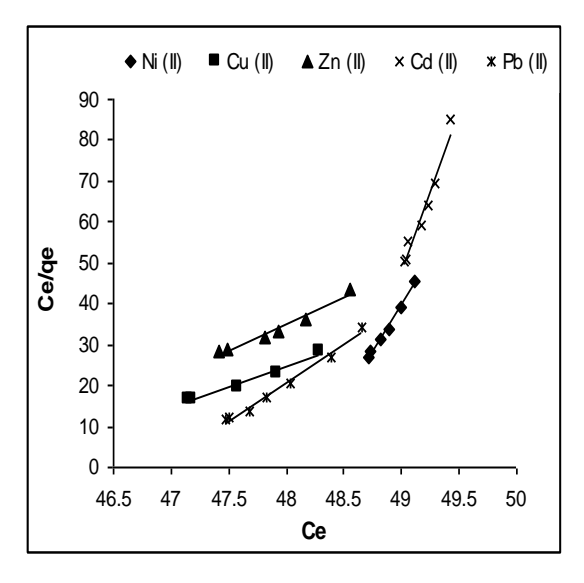
where C_e is the equilibrium constratin (mmol/L), Qe is the amount of adsorbed at equilibrium (mmol/g) and Q^o and b are Langmuir constants related to adsorption capacity and energy of adsorption respectively. The liner plot (Fig. 12) C_e/Q_e versus C_e shows that adsorption obeys Langmuir model. These constant were calculated as 101.32, 352.46, 211.24, 119.41 and 249.19 mg/g as maximum capacity for Ni(II), Cu(II), Zn(II), Cd(II) and Pb(II) respectively. The results were comparable with commercial resin Duolite GT-73. The Q_{max} of Duolite GT-73 for Cu(II), Cd(II) and Pb(II) were 62, 106 and 122 mg/g respectively. Prasad et al [28] reported Q_{max} values for synthetic resin (methacrylic acid-co-ethyleneglycol dimethacrylate) were 416.67 and 588.24 mg/g for Cu(II) and Ni(II) respectively. Sorption energy constant for Ni(II), Cu(II), Zn(II), Cd(II) and Pb(II) are 0.0714 L/mg, 0.1131 L/mg, 0.0912 L/mg, 0.0883 L/mg and 0.1081 L/mg respectively. The essential characteristics of Langmuir equation can be expressed in terms of a dimensionless separation factor or equilibrium parameter, R_L [32]. The values indicates the isotherm to be either unfavourable (R_L <1), linear (R_L =1), favourable ($0 < R_L$ <1) or irreversible (R_L =0). The values of R_L obtained for the metal-resin system are shown in Table 3. The R_L value for all the metals under study are lying between 0 and 1 indicate favourable adsorption.

This adsorption was confirmed by Freundlich model (eq. 6):

$$\log q_e = \log K_f + (1/n) \log C_e \tag{6}$$

where C_e is the equilibrium concentration (M) and q_e is the amount adsorbed (mmol/g). A linear plot (Figure 13) of log qe versus log C_e shows the applicability of Freundlich isotherm. The adsorption capacity (K_f) and the adsorption intensity (1/n) are directly obtained from the slope and the intercepts of the linear plot respectively and data are given in Table 3. The determined value of 1/n is of the same magnitude as those reported by Vaughan et al [33] for a commercial macrorecticular chelating resin Duolite GT-73. The higher fractional values of 1/n signify that strong

adsorption forces are operative on the system. The magnitude of 1/n also gives indication of the favourability and capacity of the adsorbent/adsorbate system. Treybal [34] has reported that 'n' values between 1 to 10 represents favourable adsorption. For all the systems reprted here, the exponent is 1 < n < 2 showing beneficial adsorption. Freundlich constants K_f were calculated as 83.34, 236.71, 172.39, 150.67, 209.11 and 1/n were calculated as 0.5213, 0.8731, 0.6543, 0.6376, 0.8044 for Ni(II), Cu(II), Zn(II), Cd(II) and Pb(II) respectively. The values of Freundlich constant are given in Table 3.



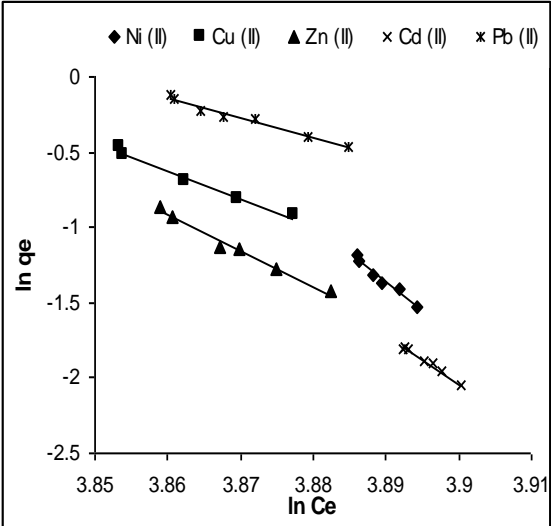


Fig. 12. Langmuir isotherm for the adsorption of metal ions on pHFR resin

Fig. 13. Freundlich isotherm for the adsorption of metal ions on pHFR resin

Metal	Langmuir constant				Freundlich constant		
ion	b (L mg ⁻¹)	Q° (mg g ⁻¹)	R_{L}	\mathbb{R}^2	K_{f}	1/n	R^2
Ni(II)	0.0714	101.32	0.327	0.9917	83.34	0.5213	0.9686
Cu(II)	0.1131	352.46	0.235	0.9797	236.71	0.8731	0.9834
Zn(II)	0.0913	211.24	0.208	0.9681	172.39	0.6543	0.9862
Cd(II)	0.0883	119.41	0.198	0.9644	150.67	0.6376	0.9912
Pb(II)	0.1081	249.19	0.216	0.9863	209.11	0.8044	0.9725

Table 3. Langmuir and Freundlich constants for metal ions.

Kinetic model (Langargren equation)

It is well established fact that the ion-exchange phenomenon follows reversible first order kinetics, when a single species is considered on a heterogenous surface [20]. The specific rate constant K_r for the sorbent was determined by Lagergren equation (7) [28].

$$Log (q_e - q) = log q_e - (K_r \times t) / 2.303$$
(7)

where q_e and q (mg/g) are the amounts of metal ions adsorbed at equilibrium and time, t (min) respectively. The straight line plot (Figure 13) of the log (q_e -q) versus time, t (at $30 \pm 2~^{\circ}C$) indicates the validity of the Lagergran equation for the system and explains that process follows first order kinetics. The values of K_r were calculated from the slop of the plot (Fig. 14) and found to be 4.145×10^{-3} , 4.606×10^{-3} , 4.375×10^{-3} , 8.290×10^{-3} and 5.987×10^{-3} min⁻¹ for Ni(II), Cu(II), Zn(II), Cd(II) and Pb(II) respectively. Anand et al [28] reported similar K_r values viz. 11.3×10^{-3} min⁻¹ for Cu(II) and 9.9×10^{-3} min⁻¹ for Ni(II) with synthetic resin (methacrylic acid-co-ethyleneglycol dimethacrylate).

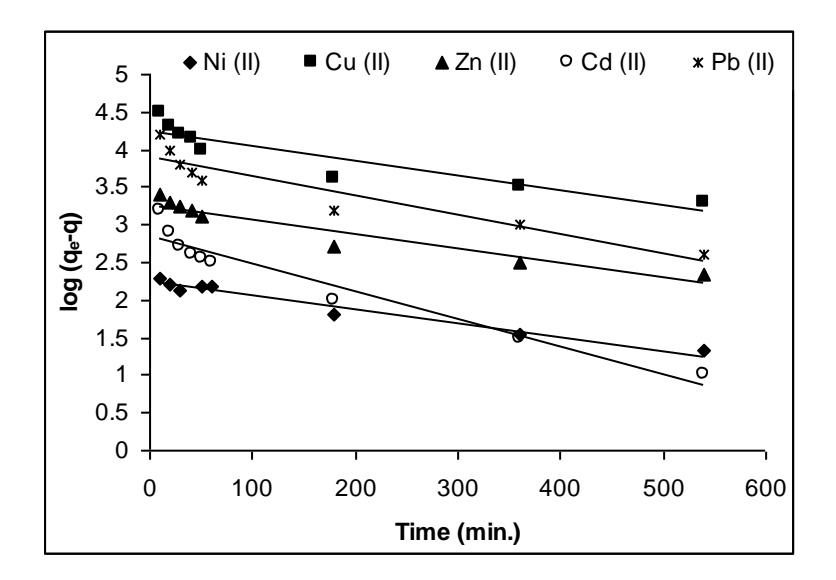


Fig. 14. Langergan plot for specific rate constant of metal ions on pHFR resin

Diffusion models

Sorption kinetics are usually controlled by various factors including, (i) Solute transfer from the solution to the boundry film of the particle (bulk diffusion) (ii) diffusion from the film to the surface of the sorbent (external diffusion) (iii) diffusion from the surface to the intraparticular sites (intraparticle diffusion) (iv) Solute adsorption by complexation or physico-chemical sorption or ion exchange.

By providing sufficient agitation to avoid particle and solute gradients in the batch reactor makes it possible to ignore bulk diffusion [28]. The process of intraparticle diffusion and external diffusion are the possible rate controlling steps. Several models have been used to described the effect of external diffusion and intraparticle diffusion of solute on adsorbent. In the present work Spah and Schlunder model [35] and Weber and Morris model [36] have been chosen to describe the external diffusion and intraparticle diffusion respectively on the resin.

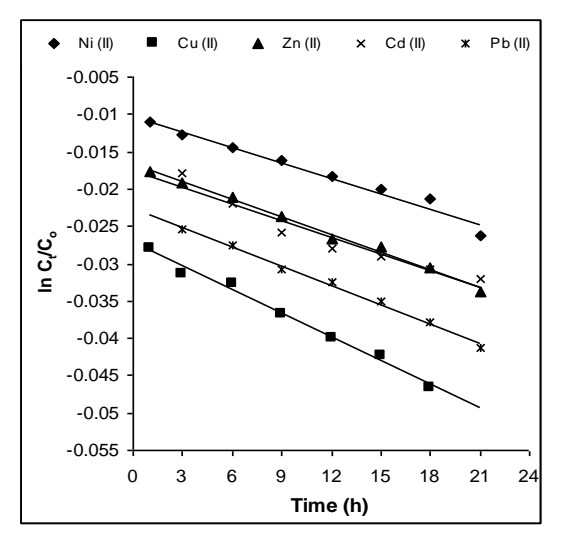
Spahn and Schlunder model

If external diffusion of metal cations (within the diffuse layers outside the sorbent) is the rate limiting step then the sorption data can be fitted into the following equation [35].

$$\ln\left(C_{t}/C_{o}\right) = -K_{s}\left(A/V\right) \times t \tag{8}$$

where K_s is external diffusion coefficient, C_o is initial metal ion concentration, C_t is concentration at time t, A/V is external sorption area to the total solution volume, t is sorption time. The external diffusion coefficient can be calculated from the slope of the straight line obtained from the plot of $\ln (C_t/C_o)$ versus t (Fig 15).

The external diffusion model shows excellent correlation with the sorption data, with high correlation coefficients obtained. This would indicate that the sorption of metal ions under study is a probably a surface process occurring on the exterior of the sorbent particle. The external diffusion coefficient (K_s) values of Ni(II), Cu(II), Zn(II), Cd(II) and Pb(II) for pHFR was calculated, the values are given in the Table 4. The value for external diffusion coefficient (K_s) for pHFR is in the range of 0.00193-0.00276 mmol/h. Similar type of results were reported by Prasad et al [28], while studying uptake behaviour of copper and nickel on methacrylic acid-co-ethylene glycol dimethacrylate polymer.



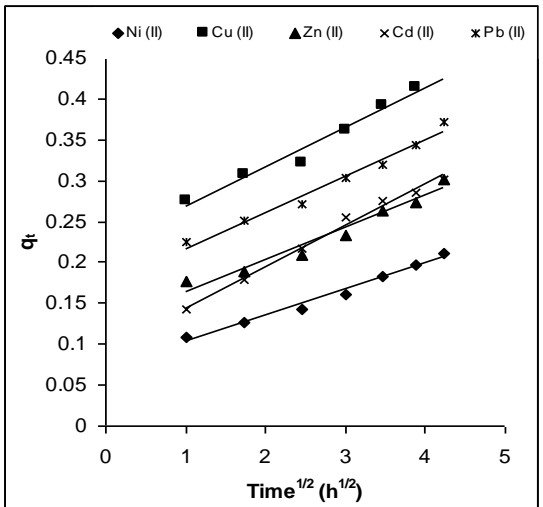


Figure 15. External diffusion plot for the sorption of metal ion exchange of pHFR resin

Figure 16. Intra-particle diffusion plot for the sorption of metal ion exchange of pHFR resin

Weber and Morris model

An empirically found functional relationship, common to the most sorption processes, is that the uptake varies almost proportionally with $t^{1/2}$, the Weber and Morris plot [36], rather than with the contact time, t.

$$q_t = k_{id} t^{1/2} + I$$
 (9)

where, q_t is amount of sorbate retained at time t, k_{id} is intra-particle diffusion rate constant, I is thickness of the boundary layer.

According to above equation (9), a plot of q_t versus $t^{1/2}$ should be a straight line (Fig 16) with a slope k_{id} and intercept I when sorption mechanism follows the intraparticle diffusion process. Values of intercept give an idea about the thickness of boundary layer, i.e., larger the intercept the greater is the boundary layer effect [27].

The plot of q_t versus $t^{1/2}$ is presented in Fig. 16. The values of I for pHFR for various metal ions under study are found in the range of 0.071-0.222 mmol/L $h^{1/2}$, Weber and Morris [36] pointed out that a functional relation common to the majority of the intraparticle diffusion treatment is that the uptake varies almost proportionately with the half power of the time. The values intraparticle coefficient (K_{id}) and I are given in Table 4. From the external diffusion and intraparticle diffusion data, it can be concluded that diffusion process is mainly controlled by intraparticle diffusion.

Metal	External Diffusion		Intra-particle diffusion		
ions	K _s	R^2	K _{id}	I	\mathbb{R}^2
Ni (II)	0.00193	0.912	0.0319	0.071	0.983
Cu (II)	0.00276	0.921	0.0477	0.222	0.969
Zn (II)	0.00220	0.914	0.0390	0.125	0.963
Cd (II)	0.00193	0.938	0.0504	0.094	0.992
Pb (II)	0.00249	0.903	0.0443	0.173	0.979

Table 4. Data of external and intra-particle diffusion rate constant

Conclusion

The elemental analysis, FTIR and 1H-NMR confirmed the assumed structure of terpolymeric resin mentioned in scheme-I. No sharp peaks are observed in the difractogram of the resin confirms the amorphous nature of the pHFR resin. Thermogravimetric analysis suggests that the decomposition reaction is first order, exothermic and slower one. The pH titration study of the resin was carried and results are studied. The pH titration study of the resin was carried and results are studied. General trend of chelating ability of resin is Pb(II) > Zn(II) > Cd(II) > Cu(II) > Ni(II). Thus, resin can be used for removal of heavy toxic metals. From the result of rate of exchange it is observed that the time required for 50 % exchange ($t_{1/2}$) for zinc(II) and lead(II) is about 55 min., for cadmium(II) and nickel(II) is 2.5 h, for copper(II) is 48 min. respectively. The data obtained from Langmuir and Freundlich equations indicating beneficial adsorption occurring through monolayer mechanism involving chemisorption (ion-exchange/chelation). Thermodynamic parameters shows that adsorption process is exothermic and spontaneous, which implies increased sorption at higher temperature. From the results of various diffusion models, it can be concluded that diffusion process is mainly controlled by intra-particle diffusion.

Acknowledgement

The authors are grateful to The Head, Dept. of Chemistry, Veer Narmad South Gujarat University, Surat for providing laboratory facility. We are also thankful to Mr. Ankur Raval, Sahjanand Medical Technologies Pvt. Ltd. (Surat) for providing optical photograph facility.

References

- 1. R. C. DeGeiso, L. Donaruma, E. A. Tomic. 1962. Chelation ion-exchange properties of a salicylic acid-formaldehyde polymer. Anal. Chem, 34(7): 845-847.
- 2. M. M. Patel, Manavalan R (1983) Indian J Chem 22A: 117-119.
- 3. M. M. Patel and R. Manavalan. 1984. Synthesis and characterization of p-hydroxybenzoic acid –thiourea-trioxane copolymer J Indian Chem Soc, 61: 490-494.
- 4. P. M. Shah, A. V. Shahl and B. A. Shah. 2008. Metal ions uptake by chelating resin derived from o-substituted benzoic acid and its synthesis, characterization and properties. Macromolecular Symposia. 274 (1), 81-90.
- 5. B. A. Shah1, A. V. Shah, and N. B. Patel. 2008. Benign Approach of Microwave Assisted synthesis of Copolymeric Resin with Improved Thermal, spectral and Ion-exchange Properties. Iranian Polymer Journal. 17(1), 3-17.
- 6. F. Vernon, H. Eccles. 1974. Chelating ion-exchangers containing salicylic acid. Anal Chim Acta, 72, 331-338.

- 7. M. V. Vyas, R. N. Kapadia. 1980. Synthesis and physico-chemical studies of some new amphoteric ion-exchangers. Indian J Technol, 18, 411-415.
- M. V. Vyas, R. N. Kapadia. 1981. Synthesis and evaluation of chelating amphoteric ion exchanger. Indian J Technol, 19, 491-492.
- S. Amin and R. N. Kapadia. 1997. Synthesis and characterization of amphoteric ion-exchangers. Journal of Scientific and Industrial Research, 56, 540-544.
- 10. M. Mubarak, F. Rimawi and F. Khalili. 2004. Chelating properties of some phenolic formaldehyde polymers towards some lanthanide ions. Solvent Extraction and Ion Exchange, 22, 721-725.
- 11. S. Samal, R. Das and Day R. 2000. Synthesis, characterisation and metal on uptake of chelating resin derived from formaldehyde-condensed azodyes of aniline and 4,4'-diaminophenyl methane coupled with phenol/resorcinl. J Appl Polym Sci, 77, 3128-3132.
- 12. I. Burgeson, B. Cook, D. Blandchard and D. Weier. 2006. Evaluation of elution parameters for cesium ion-exchange resin. Sep Sci Technol, 41, 2373-2390.
- 13. S. Fiskum, D. Blandchard, K Thomas K, T. Trang-Le. 2006. Sep Sci Technol 41: 2461-2467.
- 14. B. A. Shah, A. V. Shah and R. R Bhatt. 2007. Studies of chelation ion-exchange properties of copolymer resin derived from salicylic acid and its analytical application. Iranian polymer Journal, 16(3), 173-182.
- 15. B. A. Shah, A. V. Shah and P. M. Shah. 2006. Synthesis, Characterization and analytical applications of osubstituted benzoic acid chelatiang resin. Iranian polymer Journal, 15(10), 809-819.
- 16. A. I. Vogel. 1989. Quantitative Inorganic Analysis, 5th Ed., Longaman, London.
- 17. A. Helfferich. 1962. Ion exchange, McGraw-Hills, NewYork.
- 18. R. Kunnin. 1958. Ion exchange resin, Wiley, London.
- 19. R. M. Silverstain, G. C. Bassler. 1991. Spectrometric Identification of Organic Compound. John Wiley and Sons Inc., New York.
- 20. E. Pehlivan and T. Altum. 2006. The sstudy of various parameters affecting the ion-exchange of Cu²⁺, Zn²⁺, Ni²⁺, Cd²⁺ and Pb²⁺ from aqueous solution on Dowex 50W synthetic resin. J Hazard Mater, B134, 149-156.
- 21. A. Tager. 1978. Physical Chemistry of Polymer. Mir Publisher, Moscow.
- 22. S. A. Johnson, E. S. Brighan, T. E. Mollouk. 1997. Effect of micropore on the structure and properties of zeolite polymer replica. Chem Mater. 9, 2448-2458.
- 23. W. M. Jackson. 1964. Thermal degradation of resins. J Appl Polym Sci. 8, 2873-2879.
- 24. Charlls RG .1963. metal chelate polymers derived from tetraacetylethane J Poly Sci. A1(1), 267-276.
- 25. B. A. Shah, A. V. Shah, B. N. Bhandari and R. R. Bhatt. 2008. Synthesis, characterization and chelation ion-exchange studies of a resin copolymer derived from 8-hydroxyquinoline-formaldehyde-catechol. J Iranian Chem Soc, 5(2), 252-261.
- C. Peniche-Covas, L. W. Alvarez, W. Arguelles-Monal. 1992. The adsorption of mercuric ion by chitosan. J Appl Polym Sci, 46, 1147-1453.
- 27. G. Karthikeyan, K. Anbalagan, N. M. Andal. 2004. Adsorpion dynamics and equilibrium studies of Zn(II) onto chitosan. J Chem Sci, 116(2), 119-127.
- 28. H. H. Prasad, K M. Popat, P. S. Anand. 2002. Synthesis of crosslinked methacrylic acid-co ethyleneglycol dimethacrylate polymers for the removal of copper and nickel from water. Indian J Chem Technol, 9, 385-393.
- 29. A. Demirbas, E. Pehlivan. 2005. Adsorption of Cu(II), Zn(II), Ni(II), Pb(II) and Cd(II) from aqueous solution on Amberlite IR-120 synthetic resin. J Colloid Interf. Sci, 282, 20-26.
- 30. I. S. Lima, C. Airoldi. 2004. A thermodynamic investigation on chitosan-divalent cation interaction. Thermochim. Acta, 421, 133-139.
- 31. Baraka A, Hall PJ, Heslop MJ (2007) Melamine-formaldehyde-NTA chelating gel resin: synthesis, characterization and application for copper(II) ion removal from synthetic wastewater. J Hazard. Mater. 140: 86-94.
- 32. D. K. Singh, M. Srivastava, 2006. Synthesis, characterization and analytical applications of a new chelating resin containing p-bromophenylhydroxamic acid. J Liq Chrom Related Technol. 29: 1433-1445.
- 33. T. Vaughan, C. W. Seo, W. E. Marshall. 2001. Removal of selected metal ions from aqueous solution using modified corncobs. Biresor. Technol 78: 133-139.
- 34. R. E. Treyabl. 1980. Mass transfer operations, McGraw Hill, New York.

- 35. H. Spahn, U. Schlunder. 1975. The scale-up of the activated carbon column for water purification based on results from batch test-1: Theoretical and experimental determination of adsorption rates of single organic solutes in batch test. Chem Eng Sci, 30, 529-535.
- 36. J. C. Morris, W. J. Weber. 1962. Advance in Water Pollution Research, Pergamon Press, New York.



DETERMINATION OF ORGANIC AND INORGANIC MERCURY SPECIES IN SUNGAI KINTA, PERAK BY REVERSED-PHASE HIGH PERFORMANCE LIQUID CHROMATOGRAPHY (HPLC) ON-LINE COUPLED WITH ICP-MS

(Penentuan Kandungan Spesis Raksa Organik dan Bukan Organik di Sungai Kinta, Perak Melalui Kaedah HPLC-ICP-MS)

Norshidah Baharuddin 1* , Norashikin Saim 2 , Rozita Osman 2 , Sharifuddin Md. Zain 3 , Hafizan Juahir 4 , Siti Rafzah Saari 1

¹Sirim Berhad, 40911 Shah Alam, Selangor, Malaysia
²Faculty of Applied Sciences,
Universiti Teknologi MARA, 40450 Shah Alam, Selangor, Malaysia
³Department of Chemistry, Faculty of Science,
Universiti Malaya, 56000 Kuala Lumpur, Malaysia
⁴Department of Environmental Sciences, Faculty of Environmental Study,
Universiti Putra Malaysia, 43400 Serdang, Selangor, Malaysia

*Corresponding author: shidah@sirim.my

Abstract

This paper describes a simple method for mercury speciation in river water samples of Sungai Kinta, Perak. Separation and measurement were done by high-performance liquid chromatography on-line with inductively coupled plasma mass spectrometry (HPLC/ICP-MS). Separation of mercury species was accomplished within 6 minutes on an AQ C18 4.6mm i.d x 150mm, 5μ m reversed phase column with 0.1% (w/v) L-cysteine as mobile phase. Under the optimum instrumental conditions, recoveries of 101-104% for MeHg⁺ and 96-104% for Hg²⁺ were obtained with experimental detection limits of 1ngL⁻¹ for inorganic mercury and 1.5μ gL⁻¹ for organic mercury.

Keywords: HPLC/ICP-MS, reversed phase, L-cysteine, mobile phase

Abstrak

Kajian ini bertujuan untuk membangunkan satu kaedah untuk analisa spesies raksa dalam air sungai di Sungai Kinta, Perak. Penganalisaan kandungan spesies raksa telah dijalankan dengan menggunakan *high-performance liquid chromatography on-line with inductively coupled plasma mass spectrometry (HPLC/ICP-MS)*. Pemisahan spesies raksa dicapai dalam masa 6 minit dengan menggunakan turus fasa terbalik AQ C18 4.6mm i.d x 150mm, 5μm dengan 0.1% (w / v) L-sisteina sebagai fasa gerak. Di bawah keadaan instrumentasi yang optimum, pemerolehan semula 101-104% untuk MeHg⁺ dan 96 – 104% untuk Hg²⁺ telah diperolehi dengan had-had pengesanan 1ngL⁻¹ untuk raksa tak organik dan 1.5μgL⁻¹ untuk raksa organik.

Kata kunci: HPLC/ICP-MS, fasa terbalik, L-sisteina, fasa gerak

Introduction

Mercury is found throughout the ecosystem in trace amounts: in soil, air, water and living organisms [1]. The accumulation of monomethylmercury (MeHg) in fish and the subsequent poisoning of the Minamata inhabitants, was a turning point in the analysis of environmental levels of toxic metals, because it was apparent that to provide a clear picture of toxicity, biogeochemistry and bioaccumulation, it is necessary to measure all the different physicochemical forms [2]. MeHg and the other organomercury compounds are more toxic than Hg(II), because of their lipophilic nature, which allows them to permeate biological membranes and enter cells.

Norshidah Baharuddin et al: DETERMINATION OF ORGANIC AND INORGANIC MERCURY SPECIES IN SUNGAI KINTA, PERAK BY REVERSED-PHASE HIGH PERFORMANCE LIQUID CHROMATOGRAPHY (HPLC) ON-LINE COUPLED WITH ICP-MS

The most common methods currently in use for the speciation analysis of mercury species are Gas Chromatography (GC) and High Performance Liquid Chromatography (HPLC) coupled to an elemental specific detector such as inductively coupled plasma-mass spectrometry (ICPMS) [1]. GC coupled with ICP-MS currently has some of the lowest reported detection limits [2] for mercury species with detection limits of 0.027 pgg⁻¹ for methyl mercury (CH₃Hg) and 0.27 pgg⁻¹ for inorganic mercury (Hg²⁺) with solid phase microextraction (SPME) pre-concentration. Other detection methods such as atomic fluorescence spectroscopy with solid phase extraction [3] can reach detection limits as low as 0.01 ngL⁻¹ for CH₃Hg and is suitable for the analysis of mercury species in ocean water [4]. However, the drawback of GC is that the species have to be rendered volatile and this requires a derivatisation step with either Grignard reagents or more recently tetraalkyborate compounds [5]. This derivatisation step can be time consuming and can sometimes result in species transformations [6], thus alternative method is required. HPLC on the other hand requires no derivatisation step, as the species do not need to be volatile before injection [7], simplifying the sample preparation considerably. However, to reach the detection limits is necessary. Various preconcentration methods have been reviewed [8] including on-line [7], and off-line [9] pre-concentration on various materials such as C-18 micro-columns [10,11] and sulfhydryl cotton [12]. However, to successfully separate mercury species by HPLC, ion pairing agents such as L-cysteine [13,14] are required, which when coupled with vapour generation and ICP-MS gives detection limits of between 0.03 and 0.11 ngmL⁻¹. HPLC-ICP-MS with offline pre-concentration reached detection limits of 5.2 ngL⁻¹ for Hg²⁺ and 5.6 ngL⁻¹ for CH₃Hg, recently microbore HPLC-ICP-MS has been used for the speciation analysis of mercury [15]. ICP-MS offers extremely low detection limits ranging from sub part per billion (ppb) to trillion (ppt) for most elements. It has a rapid multi-element scanning capability over a wide range of masses with lower detection limits compared to GF-AAS and ICP-AES. Detection limits generally depend on the element, sample matrix, preparation, and the instrumental conditions used for analysis. The detection limits in ICP-MS particularly for elements which occur abundantly in nature, are often determined by blank values. Argon plasma in the HPLC-ICP-MS system able to decompose and ionize an element, irrespective of the chemical structure of the species.

For these reasons, the aim of this work was to develop a powerful speciation method applicable for trace analysis of mercury species in water samples from Sungai Kinta water in Malaysia with appropriate performance characteristics in order to identify and quantify each mercury species.

Materials and Methods

Chemical and Reagents

Mercury (Hg) standard, 1000mgL⁻¹ and 2-mercapthoethanol for electrophoresis (> 98%) were purchased from Merck, Germany. Methylmercury chloride (99.9%) and L-Cysteine (≥ 98.5%) were obtained from Fluka, Germany and Sigma, USA, respectively. The stock standard solutions were prepared by dissolving the standard in the solution of L-Cysteine hydrochloride (Fluka, Germany). Gold standard, 1000mgL⁻¹ from Perkin Elmer, USA was used to wash out the mercury species that retain in the column after each analysis.

Instrumental

Perkin Elmer High Performance Liquid Chromatography (HPLC) series 200 consisting essentially of series 200 quaternary pump, series 200 LC Peltier column oven, series 200 LC vacuum degasser and series 200 LC auto sampler (Perkin Elmer, USA). The separation of the mercury species was performed on an AQ C18 4.6 mm i.d x 150mm, 5μ m column and 50 μ L of the sample was injected into the chromatographic column. The operational conditions are shown in Table 1.

An Inductively Coupled Plasma-Mass Spectrometry (Perkin-Elmer SCIEX, Model ELAN DRC-e, USA) system consisted of S10 auto sampler (Perkin Elmer, USA) and equipped with concentric nebulizer, a cyclonic spray chamber, quartz torch with a quartz injector tube, was used. ELAN DRC-e was equipped with platinum sampler and skimmer cones. Nebulizer capillary tubing was used to connect the nebulizer and the peristaltic pump tubing. Sample introduction system components are cyclonic spray chamber (Glass Expansion, Inc., Australia) and a Meinhard® type A nebulizer. The effluent from the LC column was directly connected to the nebulizer with PEEK tubing (1.59 mm o.d.) and a low dead volume PEEK connector (Part No.: WE024375). Instrumental performance optimization, including nebulizer gas flow, ion lens voltage and torch alignment was carried out. Both mercury isotope, ²⁰²Hg and ²⁰⁰Hg for organic and inorganic mercury were monitored which were obtained by integrating

peak area, using the Chromera software (Perkin Elmer, version 3.4). The operational conditions as shown in Table 2.

Table 1. Operational parameters of the HPLC system

HPLC System	Perkin Elmer Model 200 (Quaternary pump, auto sampler, column oven, vacuum degasser)		
Column	AQ C18 4.6mm i.d x 150mm, 5μm		
Mobile phase	0.1% w/v L-cysteine		
Separation Scheme	Isocratic		
Flow rate of the mobile phase	1 ml/min		
Column temperature	25°C		
Auto sampler flush solvent	100% methanol HPLC grade		
Injection volume	50 μl		
Sample	River Water		

Table 2: Operational parameters of the ICP-MS system

ICP-MS System	ELAN DRC-e
Nebulizer	Meinhard® type A
Spray Chamber	cyclonic
Nebulizer gas flow	0.78 L/min
RF Power	1400W
Plasma gas flow	15 L/min
Reaction gas	Argon
Monitoring masses	Hg, $m/z = 202$ and 200
Analysis Time	6 minutes
CeO+/Ce+	<2%
Ba++/Ba	<2%
Rpq	0.05

Daily Optimizations and Performance Check is conducted for optimum performance of the instrument. The instrument was tuned using a Smart Tune Solution-Standard ELAN & DRC-e $10~\mu g L^{-1}$ Barium (137Ba), Beryllium (9Be), Cerium (140Ce), Cobalt (59Co), Indium (115In), Magnesium (24Mg), Plumbum (207Pb), Rhodium (103Rh) and Uranium (238U). The ratio of oxides (140Ce16O/140Ce) and doubly charged ions (140Ce2+/140Ce+) were maintained at a low level to minimize the potential interferences. The background for 220 should be less than 2 cps, but the result for background can be ignored if doubly charged and oxide criteria were achieved.

Sampling locations

Sungai Kinta is one of the important rivers in the state of Perak Darul Ridzwan and it is one of main tributaries of Sungai Perak. Sungai Kinta flows from Gunung Korbu at Ulu Kinta, Tanjung Rambutan to Sungai Perak. The tributes of Sungai Kinta are Sungai Pari,Sungai Buntong, Sungai Kledang, Sungai Raya, Sungai Pinji, Sungai Johan, Sungai Kampar and Sungai Chenderiang. Sungai Kinta flow through Tanjung Tualang, Batu Gajah, Papan, Pusing, Lahat , Ipoh, Tanjung Rambutan and Ulu Kinta. The size of river basin is 2500 km² and about 100km in length. Sungai Kinta's main function is for water supply. Therefore, there is a need to protect the river's water quality. The Sungai Kinta dam is at the last phase of the Greater Ipoh Water Supply II Scheme under implementation by Lembaga Air Perak (LAP). It is able to provide 639 million litres of water per day and is expected to be able to meet water demand in the Kinta Valley until 2020 [22].

Sungai Kinta is currently classified with an average Class III water quality and a water quality index of 51.9 – 76.5. The major causes of pollution in the Sungai Kinta Basin are industrial discharge, improper sewage treatment, residential discharge, wet markets, pig/chicken farms, sand-mining, land development, and soil erosion [22]. The sampling sites for this study are at Kampung Temiang, Tanjung Rambutan, Ulu Kinta, Kampung Paloh, Hutan lipur, and River Front as shown in Fig. 1 and Table 3.

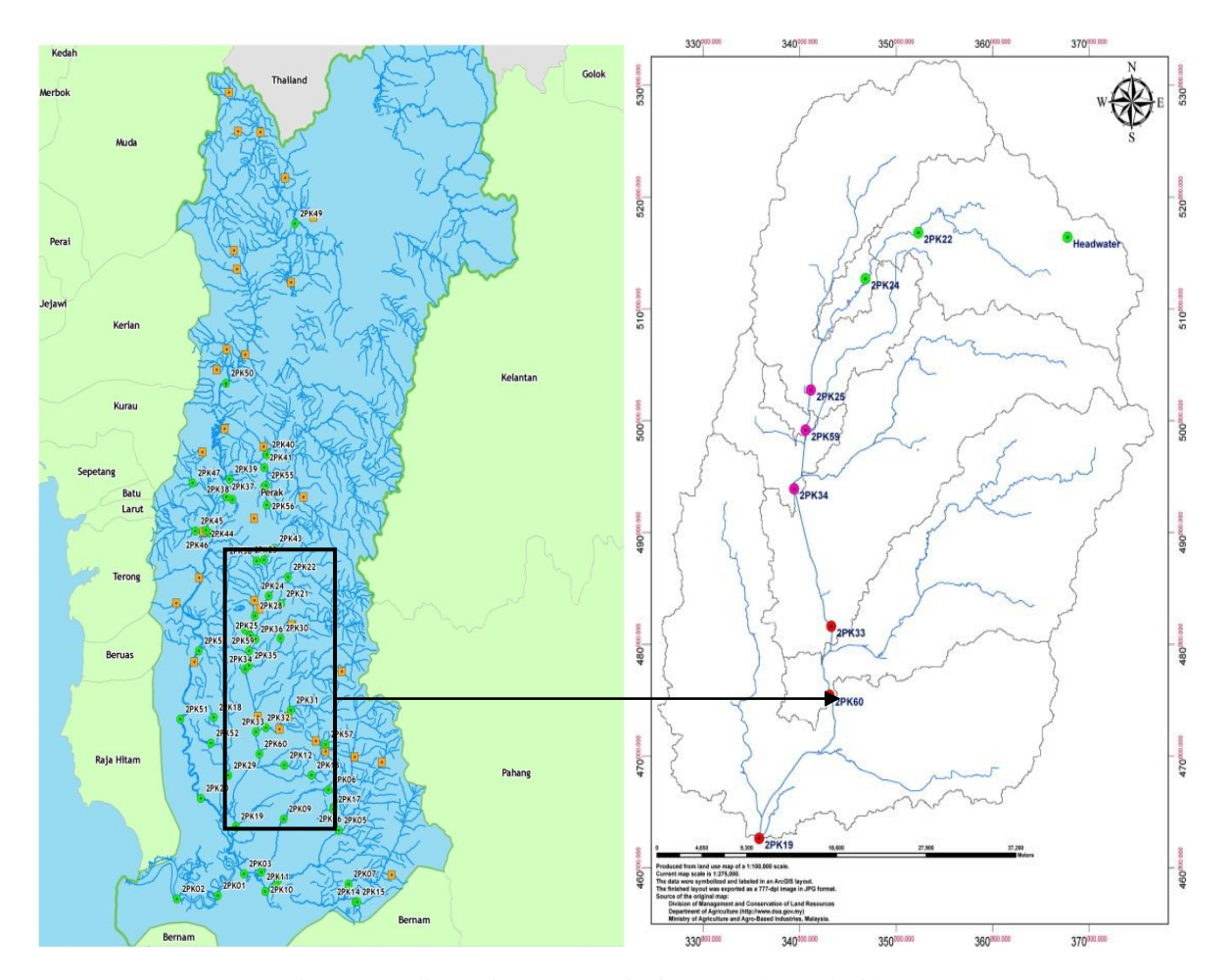


Fig. 1. Sampling points at Sungai Kinta, Perak Darul Ridzwan (Source: Alam Sekitar Malaysia)

Table 3. Sampling locations

Sampling Station	Coordinate		Location (Area description)	
	Longitude	Latitude	Location (Area description)	
2PK 19	E 101° 01.211'	N 04° 07.123'	Laksamana Bridge, Hilir Perak Border	
2PK 22	E 101° 09.372'	N 04° 40.119'	Tanjung Rambutan Mosque	
2PK 33	E 101° 04.359'	N 04° 19.595'	Corner before Tanjung Tualang town	
2PK 34	E 101° 02.681'	N 04° 27.883'	Kampung Pisang, batu Gajah (Car Wash)	
2PK 59	E 101° 03.300'	N 04° 30.355'	Jalan Kampung Pengkalan	
2PK 60	E 101° 04.950'	N 04° 16.679'	Kampung Baru Timah-Kampung Tronoh	

Sample and standard preparation

Inorganic mercury and methylmercury were used for the preparation of standard stock solution. 2 to 3 drops of 2-mercaptoethanol for electrophoresis were added to methyl mercury to aid in dissolving. The stock solutions were stored at 4 °C prior to the analysis. Analytical working solutions were prepared daily by diluting the stock solutions with calibration blank prior to analysis. Mixed standards of the following two species were made: 5, 10, 15, and 20 µgL⁻¹. These were prepared by mixing the individual stock species standards and prepared daily.

All samples were stored in sampling bottle at 4 °C without acidification to prevent changes in species distribution. Samples were filtered through Whatman 0.45 µm nylon filter membranes 30mm diameter directly into the auto sampler vial and injected in the chromatographic system, and analyzed in duplicate.

Results and Discussion

Method validation

The validity of methods and procedures used for mercury speciation are determined by linearity, limit of detection (LOD) and recovery. The linearity of the method was studied using deionised water spiked with mercury species i.e. Hg^{2+} and $MeHg^+$ at the levels 1, 1.5, 2, and 2.5 μgL^{-1} . Linear regression analysis was used to evaluate whether the mercury results were significantly different from the standard calibration curve. Good linearity was obtained for the mercury species with a determination coefficient (R^2) in the range 0.966 to 0.999 as shown in Table 4. The detection limits were found to be 1 ngL^{-1} and 1.5 μgL^{-1} for Hg^{2+} and $MeHg^+$, respectively. Under the optimized condition the limit of detection (LOD) and accuracy were calculated to ascertain the applicability of the proposed method. The recovery of the mercury species that were added to the deionised water was in the range 95 to 104% for Hg^{2+} and 101 to 111% for $MeHg^+$. Fig. 2 shows a chromatogram of a standard solution containing Hg^{2+} and $MeHg^+$ under optimized conditions. The calibration curves of the mercury species under optimized experimental conditions were drawn within the range of 1.0 μL^{-1} - 2.8 μgL^{-1} .

Mercury species	Linearity range (µgL ⁻¹)	\mathbb{R}^2	Retention time (min)	Instrumental LOD
Hg^{2+}	1-2.5	0.999	2.17	1.0 ngL ⁻¹
$MeHg^+$	1-2.5	0.966	4.20	1.5 μgL ⁻¹

Table 4. Study of the linearity range and detection limits

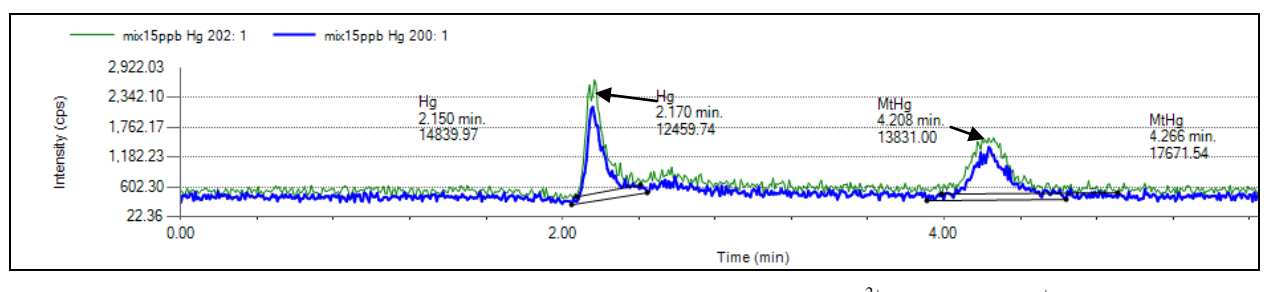


Fig. 2. HPLC-ICP-MS of two mixed Hg species standards in pure water: Hg²⁺ 2.17min, MeHg⁺ 4.20min

Possible matrix effects on the calibration were estimated by spiking representatives real river water samples. These samples were collected at various locations in order to have different matrix contents, e.g. high suspended solids. Samples collected were spiked with a standard mixture of mercury species giving an added mercury concentration

Norshidah Baharuddin et al: DETERMINATION OF ORGANIC AND INORGANIC MERCURY SPECIES IN SUNGAI KINTA, PERAK BY REVERSED-PHASE HIGH PERFORMANCE LIQUID CHROMATOGRAPHY (HPLC) ON-LINE COUPLED WITH ICP-MS

of 10 $\mu g L^{-1}$ each. When the LC-ICP-MS procedure was applied to the analysis of six spiked real river water samples, recoveries were satisfactorily with values ranging from 85% to 115%.

Analysis of samples

Table 5. Analysis of mercury species in Sungai Kinta (µgL⁻¹) and the pH value

Sampling Time	Station	Hg^{2+}	MeHg ⁺	pН
February 2011	SP1 (upstream)	0.20	<1.5	6.68
	SP1 (upstream)	0.20	<1.5	6.95
	SP2 (middlestream)	0.19	<1.5	7.06
	SP2 (middlestream)	0.20	<1.5	6.87
	SP3 (downstream)	0.18	<1.5	6.93
	SP3 (downstream)	0.23	<1.5	6.62
Mac 2011	SP1 (upstream)	0.21	<1.5	6.73
	SP1 (upstream)	0.22	<1.5	6.74
	SP2 (middlestream)	0.19	<1.5	7.41
	SP2 (middlestream)	0.20	<1.5	6.72
	SP3 (downstream)	0.19	<1.5	6.92
	SP3 (downstream)	0.23	<1.5	6.89
May 2011	SP1 (upstream)	0.22	<1.5	6.62
	SP1 (upstream)	0.20	<1.5	6.62
	SP2 (middlestream)	0.19	<1.5	7.31
	SP2 (middlestream)	0.22	<1.5	6.82
	SP3 (downstream)	0.17	<1.5	6.63
	SP3 (downstream)	0.22	<1.5	6.87

Results correspond to mean values, n=2 (standard deviation for Hg^{2+} and $MeHg^{+}$ are 0.01 and 0.08, respectively) For mercury in natural waters, the main species to be identified and determined are Hg^{2+} and $MeHg^{+}$. The results are shown in Table 5. It was observed that the Hg^{2+} was dominating the Sungai Kinta, the $MeHg^{+}$ was not detected or below the instrumental limit of detection. Therefore, it could not be considered as an important source of $MeHg^{-}$

to downstream waters. MeHg concentration is independent of total Hg levels provided that some Hg is available for methylation [24]. Methylmercury is formed from inorganic mercury by the action of anaerobic organisms that live in aquatic systems including lakes, rivers, wetlands, sediments, soils and the open ocean [23]. This methylation process converts inorganic mercury to methylmercury in the natural environment. It indicates that Hg methylation is a complex process and is affected by many factors such as temperature, pH, dissolved oxygen, organic matter, and so on [25]. It is noted that in natural waters MeHg⁺ levels are usually much lower than those of Hg⁺ [6]. Recent report [5] estimates a total mercury concentration in natural waters ranging from 0.2 to 100 ngL⁻¹, while MeHg⁺ levels are much lower i.e. 0.05 ngL⁻¹ [6]. According to the National Water Quality Standards For Malaysia, the limit for total mercury is classified according to the classes: Class I is absent, Class IIA/IIB is 0.001 mg/L, Class III is 0.0001 mg/L and Class IV is 0.002 mg/L and Class V level above IV.

Conclusion

HPLC-ICP-MS is appropriate for water samples analysis, even when the matrix in the water sample is high. One of the advantages of the HPLC-ICP-MS system is the ability of the argon plasma to decompose and ionize an element, irrespective of the chemical structure of the species. The detection limits for MeHg⁺ and Hg²⁺ are better than 10ngL^{-1} and meet the current regulatory requirements[17]. The detection limits obtained for MeHg⁺ and Hg²⁺ were 1.5 μ L⁻¹ and 1 ngL⁻¹, respectively.

References

- 1. Lan-Fang C., Shiuh-Jen J., and Sahayam A.C. (2007). "Speciation analysis of mercury and lead in fish samples using liquid chromatography—inductively coupled plasma mass spectrometry." *Journal of Chromatography A.* **1176.** 143–148.
- Jianguo, C., Hengwu C., Xianzhong J., and Haiting C. (2009). "Determination of ultra-trace amount methyl-, phenyl- and inorganic mercury in environmental and biological samples by liquid chromatography with inductively coupled plasma mass spectrometry after cloud point extraction preconcentration." *Talanta.* 77. 1381–1387.
- 3. Castillo, A., Roig-Navarro A.F., and Pozo O.J. (2006). "Method optimization for the determination of four mercury species by micro-liquid chromatography-inductively coupled plasma mass spectrometry coupling in environmental water samples." *Analytica Chimica Acta.* **577**. 18–25.
- 4. Cairns, W.R.L., Ranaldo M., Hennebelle R., Turetta C., Capodaglio G., Ferrari C.F., Aur'elien D., Cescon P., and Barbante C. (2008). "Speciation analysis of mercury in seawater from the lagoon of Venice by on-line preconcentration HPLC–ICP-MS." *Analytica Chimica Acta*. **622**. 62–69.
- 5. Susan, C. Hight, and John C. (2006). "Determination of methylmercury and estimation of total mercury in seafood using high performance liquid chromatography (HPLC) and inductively coupled plasma-mass spectrometry (ICP-MS): Method development and validation." *Analytica Chimica Acta.* **567**. 160–172.
- 6. Roberto, M.B., Margarita T.V., Jose E.S.U, and Alfredo S.M. (2000). "Field sampling, preconcentration and determination of mercury species in river waters." *Analytica Chimica Acta.* **419**. 137–144.
- José, S.D.S., Miguel de la G., Augustin, P., Maria, L. PD.S. (2009). "Determination of organic and inorganic mercury species in water and sediment samples by HPLC on-line coupled with ICP-MS." *Talanta*. 80. 207– 211.
- 8. Wang, M.F., Weiyue, S. J, Zhang, F., Wang B., Zhu M., Li B. Z. Y., Chai, Z. (2007). "Development of a mild mercaptoethanol extraction method for determination of mercury species in biological samples by HPLC–ICP–MS." *Talanta.* **71**. 2034–2039.
- 9. Cattani, I., Spalla, S., Beone, G.M., Del Re., A.A.M., Boccelli, R., Trevisan, M. (2008). "Characterization of mercury species in soils by HPLC–ICP-MS and measurement of fraction removed by diffusive gradient in thin films." *Talanta*. **74**. 1520–1526.
- 10. María, M.S., Julio, A.L. (2009). "Analytical speciation of mercury in fish tissues by reversed phase liquid chromatography-inductively coupled plasma mass spectrometry with Bi³⁺ as internal standard." Talanta. **79**. 706–711.
- 11. Isabel, L., Susana, C., Carmen, C., Yolanda M. (2010). "Approach for rapid extraction and speciation of mercury using a microtip ultrasonic probe followed by LC-ICP-MS." *Talanta*, **82.** 594–599.

Norshidah Baharuddin et al: DETERMINATION OF ORGANIC AND INORGANIC MERCURY SPECIES IN SUNGAI KINTA, PERAK BY REVERSED-PHASE HIGH PERFORMANCE LIQUID CHROMATOGRAPHY (HPLC) ON-LINE COUPLED WITH ICP-MS

- 12. Chwei-Sheng, C., Shiuh-Jen, J., Danadurai K. S.K. (2001). "Determination of mercury compounds in fish by microwave-assisted extraction and liquid chromatography-vapor generation-inductively coupled plasma mass spectrometry." *Spectrochimica Acta Part B.* **56**. 1133-1142.
- 13. Haiting, C., Jianguo, C., Xianzhong, J., Danyi, W. (2009). "Determination of trace mercury species by high performance liquid chromatography-inductively coupled plasma mass spectrometry after cloud point extraction." *Journal of Hazardous Materials.* **172**. 1282–1287.
- 14. Yong-guang, Y., Ming, C., Jin-feng, P., Jing-fu, L., Gui-bin, J. (2010). "Dithizone-functionalized solid phase extraction—displacement elution-high performance liquid chromatography—inductively coupled plasma mass spectrometry for mercury speciation in water samples." *Talanta.* 81. 1788–1792.
- 15. Jairo, L. R., Samuel, S. de. S., Vanessa, C. de. O.S., Fernando, B. Jr. (2010). "Methylmercury and inorganic mercury determination in blood by using liquid chromatography with inductively coupled plasma mass spectrometry and a fast sample preparation procedure." *Talanta.* **80**. 1158–1163.
- 16. Xiaoyu, J, Yi H., Xinli L., Taicheng, D. H.Chen. (2010). "Speciation of mercury in water samples by dispersive liquid-liquid microextraction combined with high performance liquid chromatography-inductively coupled plasma mass spectrometry." *Spectrochimica Acta Part B: Atomic Spectroscopy*.
- 17. Dengyun, C., Miao, J., Xiaoru, W. (2005). "Determination of Methyl Mercury in Water and Soil by HPLC-ICP-MS." Agilent Technologies.
- 18. Martine, L., Willy, B. P. Q., Milena, H. (2005). "Mercury in environmental samples: Speciation, artifacts and validation." *Trends in Analytical Chemistry.* **24**. No. 5.
- 19. Yao-Chin, W. and Chen-Wen, W. (1993). "High-performance liquid chromatography of inorganic mercury and organomercury with 2-mercaptobenzothiazole." *Journal of Chromatography*. **28**. 133-137.
- 20. Kerstin, L.d, Michael, F., Paul, W. (2010). "Methods for the determination and speciation of mercury in natural waters—A review." *Analytica Chimica Acta*. **663**. 127–138.
- 21. L. –P. Yu., X. –P. Yan (2003). "Factors affecting the stability of inorganic and methylmercury during sample storage." *Trends in Analytical Chemistry.* **22**. 245-253.
- 22. Quarterly DOE Update on Environment, Development & Sustainability, Issue 3/2006. Available from http://www.doe.gov.my.
- 23. Ullrich, S., Tanton, T. and Abdrashitova, S. (2001). "Mercury in the Aquatic Environment: A Review of Factors Affecting Methylation". Critical Reviews in Environmental Science and Technolog.y 31. (3): 241.
- 24. Winch, S., Praharaj, T., Fortin, D. and Lean, D.R.S. (2008). "Factors affecting methylmercury distribution in surficial, acidic, base-metal mine tailings." Science of the Total Environment. **392**. 242-251.
- 25. Ebinghaus, R., Wilken, R.D. and Gisder, P. (1994). "Investigations on the formation of monomethylmercury (II) in the Elbe." Vom Wasser. **82**. 19-25.



STABILITY OF THE ABSORBED DOSE TO WATER CALIBRATION COEFFICIENT, $N_{D,w}$ FOR THERAPY LEVEL IONIZATION CHAMBERS BELONGING TO LOCAL RADIOTHERAPY CENTRES: ANALYSIS OF RESULTS OBTAINED DURING 2004 -2010

(Kestabilan Pekali Kalibrasi Dos Terserap Terhadap Air, $N_{D,w}$ Untuk Kebuk Pengionan Tahap Terapi Kepunyaan Pusat Radioterapi Tempatan: Analisis Keputusan Yang Diperoleh Sepanjang 2004-2010)

S. B. Samal^{1*}, W. Priharti¹, S. S. Chong¹, T. Kadni² and M.T. Dolah²

¹School of Applied Physics, Faculty of Science and Technology, Universiti Kebangsaan Malaysia 43600 UKM Bangi, Selangor

> ²Secondary Standard Dosimetry Laboratory (SSDL) Malaysian Nuclear Agency (Nuclear Malaysia) 43000 Kajang, Selangor

*Corresponding author: sbsamat@ukm.my

Abstract

According to the IAEA, the calibration of therapy level ionization chambers in terms of absorbed dose to water calibration coefficient, $N_{D,w}$ must be within \pm 1.5% acceptance limit. This is for the purpose of getting accurate absorbed dose for the patient undergoing radiotherapy treatment. The objective of this work is to evaluate the deviation of $N_{D,w}$ for 29 chambers belonging to 16 local radiotherapy centres. Eight types of chambers have been calibrated at the SSDL Laboratory of Malaysian Nuclear Agency for the period of seven years. The mean μ of the $N_{D,w}$ deviation together with its standard error (SE) and standard deviation σ_{N-1} were calculated. It is found that out of 29 chambers, 26 chambers yielded μ ± SE within the permitted value of \pm 1.5%. For the other three chambers, despite their values of μ ± SE lie slightly outside the range of \pm 1.5%, they are still within the 95% confident interval of the \pm 1.5%. It is concluded that the $N_{D,w}$ of the chambers belonging to the local radiotherapy chambers are stable in their performance the dose to the patients measurement.

Keywords: absorbed dose to water calibration coefficient $N_{D,w}$, local radiotherapy centres, percentage deviation, SSDL Malaysia, stability of $N_{D,w}$

Abstrak

Menurut IAEA, julat penerimaan pekali kalibrasi dos terserap terhadap air, $N_{D,w}$ untuk kebuk pengionan tahap terapi mesti berada antara \pm 1.5%. Hal ini bertujuan untuk mendapatkan dos terserap yang tepat bagi pesakit yang menjalani rawatan radioterapi. Objektif kerja ini adalah untuk menilai sisihan $N_{D,w}$ bagi 29 kebuk pengionan kepunyaan 16 pusat radioterapi tempatan. Lapan jenis kebuk telah dikalibrasi di makmal SSDL Agensi Nuklear Malaysia dalam tempoh tujuh tahun. Nilai purata μ untuk sisihan $N_{D,w}$ bersama dengan nilai ketidakpastian standard (SE) dan juga sisihan standard σ_{N-1} dikira. Didapati bahawa 26 daripada 29 kebuk menunjukkan nilai μ \pm SE berada dalam julat yang dibenarkan iaitu \pm 1.5%. Walaupun nilai μ \pm SE untuk tiga kebuk yang lain berada di luar julat \pm 1.5%, namun ianya masih berada dalam aras keyakinan 95% daripada \pm 1.5%. Dapat disimpulkan bahawa nilai $N_{D,w}$ untuk kebuk pengionan kepunyaan pusat radioterapi tempatan adalah stabil bagi pengukuran dos kepada pesakit.

Kata kunci: Pekali kalibrasi dos terserap terhadap air, $N_{D,w}$, pusat radioterapi tempatan, peratus sisihan, SSDL Malaysia, kestabilan $N_{D,w}$

Introduction

It has been well documented that accuracy in the beam calibration of the radiotherapy machines would contribute to the accurate dose delivery to the patients [1,2]. Therapy level ionization chamber (IC) is the important tool for the calibration, therefore its accurate absorbed dose to water calibration coefficient, $N_{D,w}$ certainly would contribute to the accurate dose delivery [3]. It is anticipated that the $N_{D,w}$ of an IC would change with time, therefore the IAEA has recommended that an IC should be calibrated every year for its $N_{D,w}$ [4].

For the determination of $N_{D,w}$, SSDL Malaysia of Malaysian Nuclear Agency (Nuclear Malaysia) has participated in the postal IC intercomparison programmes [5]. Some of the results are shown in Table 1, which shows that the laboratory has provided therapy-level $N_{D,w}$ values within the internationally accepted standards i.e. within the \pm 1.5%. For this reason, Nuclear Malaysia is capable for providing the $N_{D,w}$ values for IC belonging to the local radiotherapy centres (RC).

The purpose of this work is to study the $N_{D,w}$ values of 29 ICs belonging to the 16 RC, from the year 2004 to 2010. These $N_{D,w}$ values were determined by Nuclear Malaysia. The objective is to find out how the $N_{D,w}$ values vary with time i.e. its stability.

Table 1. The intercomparison results of $N_{D,w}$ between Nuclear Malaysia (NM) and IAE	A

CALIBRATION	ICM: 1.1	$N_{D,w}$ (m0	Deviation	
YEAR	IC Model	NM	IAEA	(%)
1995	NE 2581	57.20	56.79	0.72
1997	NE 2581	57.08	57.07	0.02
1998	NE 2571	45.33	45.39	- 0.13
2002	M 30001	52.46	52.35	0.21
2004	M 30001	52.52	52.35	0.32

Experimental

Figure 1 shows the experimental set-up for the determination of $N_{D,w}$. The method follows the procedures of substitution method recommended by the IAEA [6]. The PMMA water phantom is of size 30 cm \times 30 cm \times 30 cm. A waterproof sleeve is used to place the IC at its reference point at a depth 5 g/cm² in the water phantom. In this work a reference standard chamber of 0.6 cm³ NE2571(#1028) is used.

Table 2 lists the type of the 29 ICs belonging to the 16 RCs. The table also shows the $N_{D,w}$ calibration frequency for a period of seven years from the year 2004 to 2010. The IAEA requires each IC to be calibrated every year for purpose of getting the most recent value of $N_{D,w}$. However in this work, the determination of RC's $N_{D,w}$ is based on the request by the RC themselves not the request by the SSDL Malaysia. Whenever SSDL Malaysia receives the IC, the calibration work will be done immediately. In other words, the frequency of each IC calibration is determined by the radiotherapy centres themselves.

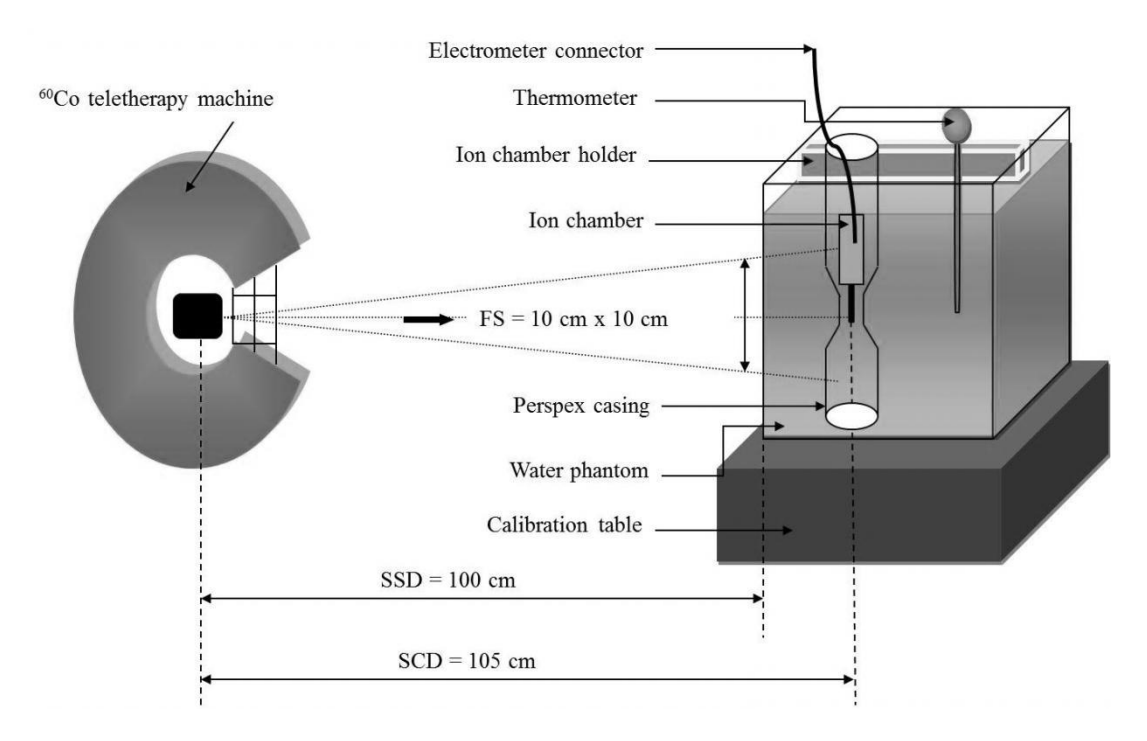


Figure 1. Experimental setup of $N_{D,w}$ calibration

Table 2. $N_{D,w}$ calibration frequency for chambers belonging to local radiotherapy centres

IC Model	IC No RC No	DC No	Гиол	$N_{D,w}$ calibration frequency						
ic wiodei		RC No	Freq.	2004	2005	2006	2007	2008	2009	2010
CC 13#7063	1	4	3				√	√	√	_
FC 65-G#1328	2	3	3				\checkmark	√	√	
FC 65-G#1371	3	5	4	√	√	√	\checkmark			
FC 65-G#367	4	7	7	√	√	√	\checkmark	√	√	√
FC 65-G#368	5	4	6	√		√	\checkmark	√	√	√
FC 65-G#369	6	4	4			√	√	✓	✓	
FC 65-G#371	7	5	3					√	√	√
FC 65-G#744	8	14	6	√		√	√	√	✓	√
FC 65-G#WD 362	9	11	3	√	√		√			
FC 65-G#WD 445	10	13	6	√	√	√	√	√	✓	
FC 65-G#WD 878	11	11	5		√	√	√	√	√	
FC 65- G#WD1219	12	6	5			√	V	√	√	√
FC 65-P#1437	13	8	3				√	√		√

Samat, S. B. et al: STABILITY OF THE ABSORBED DOSE TO WATER CALIBRATION COEFFICIENT, $N_{D,w}$ FOR THERAPY LEVEL IONIZATION CHAMBERS BELONGING TO LOCAL RADIOTHERAPY CENTRES: ANALYSIS OF RESULTS OBTAINED DURING 2004 -2010

FC 65-P#742	14	14	5	√		√		\checkmark	\checkmark	✓
NE 2571#2257	15	8	4	√	√	✓	✓			
NE 2571#2798	16	15	5	√		✓	✓	✓	✓	
NE 2581#1180	17	12	6		√	V	✓	V	✓	✓
NE 2581#621	18	3	7	√	√	V	✓	V	✓	✓
PPC 40#310	19	13	4			✓	✓	✓	✓	
PPC 40#314	20	9	3				✓	✓	✓	
TM 30013#1745	21	10	4			V	✓	V	✓	
TM 31010#0426	22	5	4			V	✓		✓	✓
TW 30001#2120	23	15	5			✓	✓	✓	✓	✓
TW 30013#1646	24	1	4			✓	✓	✓	✓	
TW 30013#1681	25	16	5			V	✓	V	✓	✓
TW 30013#2139	26	16	4			V	✓	V	✓	
TW 31010#1005	27	16	4			✓	✓	✓	✓	
W 30001#1210	28	15	5	√	√		✓	✓	✓	
WDIC 70#062	29	2	5	√	√		√	√	√	

Table 3 shows an example of $N_{D,w}$ calibration results for IC=4 and RC=7. Since there are seven values of $N_{D,w}$, there are only six deviations $\Delta(\%)$ that can be calculated, as the first $N_{D,w}$ was taken as the standard. These six deviations were then used to get the mean μ , standard error SE and standard deviation σ_{N-1} . The SE and σ_{N-1} are calculated at 68.26% confident interval (CI). The same calculation was repeated for the other ICs.

In this work, the results of $\mu \pm SE$ and $\mu \pm \sigma_{N-1}$ were compared with the deviation limit of $\pm 1.5\%$ accepted by the IAEA [7]. If $\mu \pm SE$ is within the limit, it is said that the chamber is stable in maintaining its $N_{D,w}$.

Table 3. The results of $N_{D,w}$ for chamber FC 65-G#367 calibrated each year from 2004-2010

IC No RC	RC No	Calibration	$N_{D,w}$ (1	Deviation	
	KC NO	Year	First	Consequent	(%)
4	7	2004	48.69	-	
		2005		47.87	-1.68
		2006		48.24	-0.92
		2007		47.81	-1.81
		2008		48.45	-0.49
		2009		48.20	-1.01
		2010		48.33	-0.74

Results and Discussion

The results of $\mu \pm SE$ and $\mu \pm \sigma_{N-1}$ for the Δ (%) are given in Figures 2 and 3 respectively. In general it can be seen that (a) all μ for the 29 ICs lie within the limit of \pm 1.5%, which shows that the 29 ICs are stable in providing their $N_{D,w}$, (b) the value of $\mu \pm SE$ (Figure 2) is smaller than $\mu \pm \sigma_{N-1}$ (Figure 3) by a factor of square root of N, where N

is the number of the deviations, as expected. For the results of IC=4 and RC=7 mentioned above, the $\mu \pm SE$ and $\mu \pm \sigma_{N-1}$ are indicated by the arrows in the two figures.

We shall now examined $\mu \pm SE$ only (Figure 2) for all the ICs as SE is in actual fact is the uncertainty in the mean. It can be seen that there are three ICs (IC no 7, 20 and 24) that give the values slightly higher than \pm 1.5%. If we examine carefully the values of the SE for three ICs that lie outside acceptable limit of \pm 1.5%, we found that their values are acceptable as they are less than 95% confidence interval of the limit, i.e. 79.6% or 1.27 standard deviation (SD) for IC no. 7 (1.91=1.27×1.5), 94.4% or 1.91 SD for IC no. 20 (2.86=1.91×1.5) and 75% or 1.15 SD for IC no. 24 (1.72=1.15×1.5).

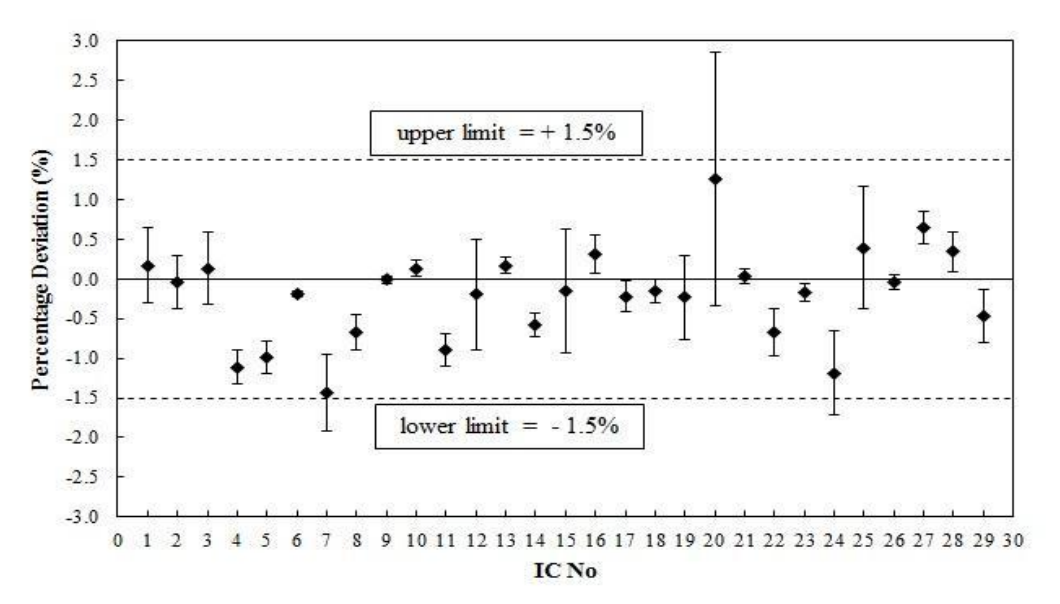


Figure 2. Deviation of $\mu \pm SE$

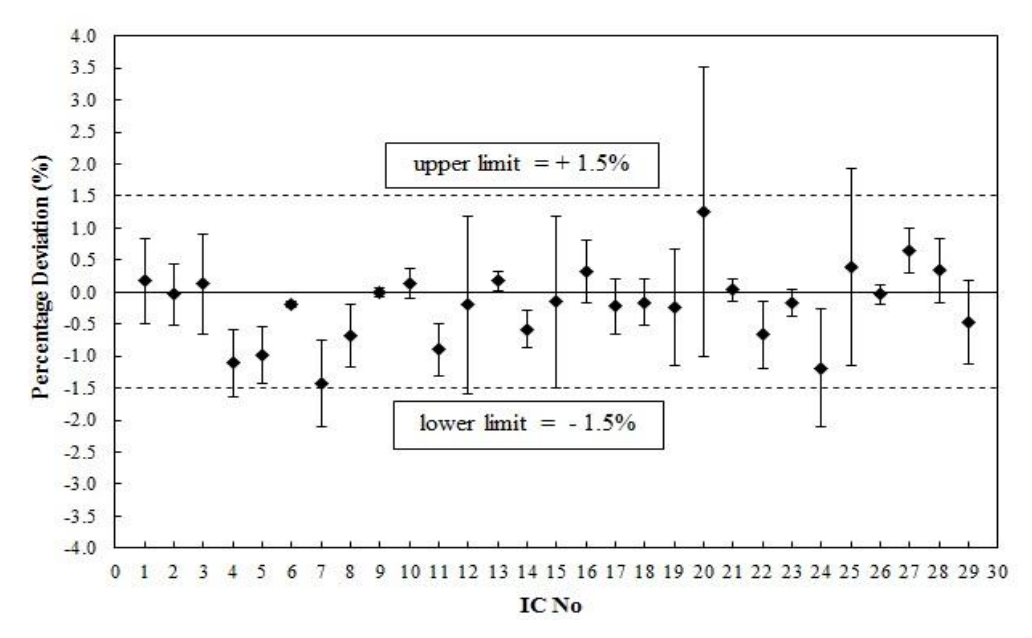


Figure 3. Deviation of $\mu \pm \sigma_{N-1}$

Samat, S. B. et al: STABILITY OF THE ABSORBED DOSE TO WATER CALIBRATION COEFFICIENT, $N_{D,w}$ FOR THERAPY LEVEL IONIZATION CHAMBERS BELONGING TO LOCAL RADIOTHERAPY CENTRES: ANALYSIS OF RESULTS OBTAINED DURING 2004 -2010

Conclusion

As the $N_{D,w}$ calibration coefficient are stable with time, it is concluded that the chambers being studied are in their good performance for the purpose patients dose measurement.

Acknowledgement

We gratefully acknowledge Universiti Kebangsaan Malaysia for a research grant, Project code UKM-ST-07-FRGS0154-2010.

References

- 1. IAEA, 1998. Building a better future: Contributions of nuclear science and technology. Vienna,
- 2. IAEA. 2004. Radiation, people and the environment. Vienna.
- 3. Samat, S.B., Evans, C.J., Kadni, T. Ooi, A.S. & Dollah, M.T. 2003. The -10% and 13% errors arising from misinterpretation of the two IAEA protocols TRS-277 and TRS-398: Causes and prevention. *SSDL Newsletter* 48: 16-18.
- 4. IAEA. 2000. Absorbed Dose Determination in External Beam Radiotherapy: An International Code of Practice for Dosimetry Based on Standards of Absorbed Dose to Water, TRS 398, Vienna.
- Samat, S.B., Evans, C.J., Kadni, T. & Dollah, M.T. 2009. Malaysian participation in the IAEA/WHO postal TLD and postal ionization chamber intercomparison programme: Analysis of results obtained during 1985-2008. Rad. Prot. Dos. 133(3): 186-191.
- 6. IAEA. 1994. Calibration of dosimeters used in radiotherapy: A manual sponsored by the IAEA and WHO. TRS 374. Vienna
- 7. IAEA. 2003. Results of comparison of therapy level ionization chamber calibration coefficient (Reference:MAL/02/01). IAEA/WHO Network of Secondary Standard Laboratories.



EFFECTS OF VARIOUS PARAMETERS ON IN-HOUSE COCKTAIL DEVELOPED FOR THE MEASUREMENT OF GROSS ALPHA AND BETA IN AQUEOUS ENVIRONMENTAL SAMPLES USING LIQUID SCINTILATION COUNTING TECHNIQUE

(Kesan Pelbagai Parameter Ke Atas Koktil yang Dibangunkan Sendiri bagi Pengukuran Gros Alfa dan Beta Di Dalam Sampel Air Persekitaran Menggunakan Teknik Pembilang Sintilasi Cecair)

Zaini Hamzah¹, Masitah Alias¹*, Ahmad Saat², Abdul Kadir Ishak³ and Zaharudin Ahmad³

¹Faculty of Applied Sciences, Universiti Teknologi MARA, 40450 Shah Alam, Selangor ²International Education Centre (INTEC), Universiti Teknologi MARA, 40200 Shah Alam, Selangor ³Radiochemistry and Environmental Laboratory, Malaysian Nuclear Agency, 43000 Bangi, Selangor

*Corresponding author: ellyaa@yahoo.com

Abstract

Liquid scintillation counting (LSC) is a versatile technique for measuring beta emitters in organic liquid samples. When this technique is applied to the aqueous environmental samples, the limitation is to incorporate the aqueous phase which contains the radionuclides of interest into an organic phase which can readily mix with a scintillator that is responsible for the detection of photon through excitation processes. The in-house cocktail was developed by mixing the organic solvent which contains primary and secondary solutes with a specific emulsifier (Triton-N101) which is capable of linking the aqueous phase to the organic phase through its hydrophilic and hydrophobic tails. The best proportion for water: toluene: Triton-N101 is 2: 4: 4, respectively. Since the aqueous environmental samples are analyzed, there is a need to study various effects such as pH, buffer and salts on the cocktail to ensure the stability of the cocktail being used. ³H and ²³²U tracers were used throughout this study. pH value shows an optimal condition for both tracers, while acid, base, buffer and salts all show decreased in counting efficiency when the their concentrations increased.

Keywords: liquid scintillation counting, cocktail, emulsifier, Triton N101, tritium

Abstrak

Pembilang sintilasi cecair (PSC) adalah merupakan teknik yang terbaik untuk mengukur pemancar beta di dalam sampel cecair. Apabila teknik ini digunakan untuk sampel air sekitaran, keterbatasannya adalah dari segi menggabungkan fasa akuas yang mengandungi radionuklida yang ingin dikaji ke dalam fasa organik yang mengandungi sintilator yang bertanggungjawab ke atas pengesanan foton melalui proses pengujaan. Koktil yang dibangunkan di makmal mengandungi pelarut organik yang mengandungi bahan larut primer dan sekunder dengan emulsifier khusus yang mampu menghubungkan fasa akuas dengan fasa organik melalui ekor hidroforbik dan hidrofiliknya. Nisbah terbaik untuk setiap bahagian air:toluen:Triton-N101 ialah 2:4:4 masing-masing. Disebabkan sampel yang dikaji adalah sampel persekitaran, adalah perlu untuk mengkaji kesan pelbagai keadaan seperti pH, asid, bes, buffer dan garam ke atas koktil. Penyurih ³H dan ²³²U telah digunakan di sepanjang kajian ini. pH menunjukkan keadaan optima untuk kedua-dua penyurih, manakala asid, bes, buffer dan garam semua menunjukkan penurunan efisiensi pembilangan apabila kepekatannya meningkat.

Kata kunci: Pembilang sintilasi cecair, koktil, emulsifier, Triton N101, tritium

Zaini Hamzah et al: EFFECTS OF VARIOUS PARAMETERS ON IN-HOUSE COCKTAIL DEVELOPED FOR THE MEASUREMENT OF GROSS ALPHA AND BETA IN AQUEOUS ENVIRONMENTAL SAMPLES USING LIQUID SCINTILATION COUNTING

TECHNIQUE

Introduction

The sample preparation procedures for liquid scintillation counting (LSC) is obtain a homogeneous solution for efficient energy transfer from the sample to the liquid scintillation cocktail. Aqueous solutions are some of the simplest and most commonly found in liquid scintillation analysis. In general, they provide the environment necessary for many assays and separations, including the most encountered solvent media for the numerous radioisotopes used in LSC [1]. The main methods for producing aqueous samples are by dissolution, extraction, and distillation. Dissolution simply involves dissolving the sample in water. Extraction can be either extraction of the sample from a solid matrix by water (solid/liquid extraction), or extraction of the sample from a liquid matrix by water (liquid/liquid extraction). Distillation involves separation of the aqueous component evaporation [1].

Measurement of environmental beta emitter in aqueous solution is not an easy task since the common method of liquid scintillation counting has its own limitations. Apart from Cerenkov counting method, one needs to incorporate the aqueous phase into the organic phase where the energy transfer from beta particles to the solvent and later scintillator occurs. The use of commercial cocktail to serve this purpose does not always give desired result. For example, the use of emulsifying cocktails, such as ULTIMA Gold AB, contains phosphate esters and is buffered to a slightly acidic. The addition of the sodium carbonate solution to the cocktail results in a reaction between the slightly acidic phosphate ester and the sample of interest. Carbon dioxide, a by-product of this reaction, is released into the air. Unfortunately, the radioactive carbon from the sample becomes involved with the reaction, resulting in the release of $^{14}CO_2$ [2].

Commercial cocktails, despite convenience, are always expensive and pose some degree of limitation for their use. To overcome this little problem, one can develop one's own cocktail using the Van der Laarse method to reduce the cost and localize the application [3]. The main focus for this cocktail development is to get the best proportion between water, solvent and emulsifier to produce a solution which can incorporate more volume of water, clear and stable solution, giving the best count rate and the best merit value. The choice of emulsifier is quite crucial for it is responsible for the formation of micelle. The smaller the micelle, the more likely is the emission from the isotope located in the aqueous layer to promote a scintillation event from the adjacent scintillation solution. The presence of any hydrophilic quenching agent is localized in the aqueous part of the micelle so it cannot compete with the scintillation process, hence quench effects are reduced or absent (obviously hydrophobic impurities may still become an impurity quench). The formation of micelles is time dependent and any sample should be allowed to stabilize before counting. This depends upon the nature of the sample (and detergent) and should be determined by repeated counts over a period of time until stable counts are observed [4].

This cocktail is used for the measurement of gross alpha and beta activity in aqueous environmental solutions. Gross alpha and beta analyses are widely used as the first step of the radiological characterization of drinking waters and it makes it possible to screen samples for relative levels of radioactivity there on [5]. Natural waters contain both alpha (e.g. ²³⁸U) and beta (e.g. ⁴⁰K) emitters in widely varying concentrations which are responsible for a generally small fraction of the total dose received from natural and artificial radioactivity [6, 7]. Radium isotopes formed as a result of radioactive decay of ²³⁸U and ²³²Th, both of which occur naturally in the environment. ²²⁶Ra is an alpha emitter. Radium, which has similar chemical properties to calcium, is one of the major sources of the radioactivity found in water. ²²⁶Ra may internally radiate the human body for a long time, since its half-life of 1620 years [8]. Therefore, the harmfulness of ²²⁶Ra dissolved in water is said to be about 40 times that of ⁹⁰Sr [9].

The aim of this study is to develop the best cocktail mixture for the measurement of aqueous environmental sample using liquid scintillation counting technique. The effects of pH, acid, base buffer and salt were also studied to ensure the best counting efficiency for the measurement of environmental samples. The cocktail was then tested for the measurement of a few environmental samples for its applicability.

Materials and Methods

The preparation of in-house cocktail was done according to the method explained by Zaini [3]. The effects of pH, acid, base, buffer and salts were dealt here individually to see their effects on the in-house cocktail developed for this investigation.

Effect of pH on the stability and detection efficiency of the mixture

Acetic acid was prepared in 250 mL volumetric flask by diluting concentrated acetic acid 95% pure purchased from Merck with water. In another 250 mL volumetric flask, 20.5 g of sodium acetate 95% pure (Merck) was dissolved in water together with tritium and uranium-232 solutions with specific activity 25.5 Bq/mL and 23.05 Bq/mL respectively was added and made up to 250 mL. Twelve buffer mixtures were prepared in twelve different small flasks, according to the Table 1. Respective mixtures of 2.0 mL were transferred into a counting vial and mixed with 8.0 mL of toluene-Triton N-101 (both were purchase from Merck) mixtures to obtain the right proportions. Every vial was shaken well for a few minutes and left for one day to stabilize the mixture. All of these vials were then counted for the activity of tritium and the appearance recorded.

Acetic acid	Sodium acetate	Tritium Uranium-232					2
0.2M	0.2M	pН	% Detection	Appearance	pН	% Detection	Appearance
(x ml)	(y ml)	Value	Efficiency		Value	Efficiency	
9.5	0.5	4.0	45.53	Clear	3.9	22.24	Clear
9.0	1.0	4.2	40.39	Clear	4.3	18.62	Clear
8.0	2.0	4.6	37.14	Clear	4.7	16.31	Clear
7.0	3.0	4.8	33.25	Clear	4.9	15.42	Clear
6.0	4.0	5.0	29.67	Clear	5.1	12.63	Clear
5.0	5.0	5.2	28.70	Cloudy	5.3	10.61	Cloudy
4.0	6.0	5.4	27.66	Cloudy	5.5	9.24	Cloudy
3.0	7.0	5.6	26.97	Cloudy	5.7	9.28	Milky
2.0	8.0	5.8	26.01	Milky	5.9	8.53	Milky
1.0	9.0	6.1	25.1	Milky	6.3	7.03	Milky
0.5	9.5	6.5	25.28	Milky	6.6	6.25	Milky

Table 1. pH of acetic acid – sodium acetate buffer mixture

Effects of acids and bases on the stability and detection efficiency of the mixture

a. The effect of hydrochloric acid on the stability and detection efficiency of tritium

A series of 50 ml of 0.0, 0.1, 0.2, 0.3, 0.4, 0.5, 0.6, 0.7, 0.8, 0.9 and 1.0 M of hydrochloric acid solutions were prepared by dilution of the concentrated stock. These acid solutions were made radioactivity by adding a standard amount of tritium and uranium-232 solutions with specific activity 25.25 Bq/mL and and 11.51 Bq/mL respectively. These solutions which are 4.0 mL were transferred into a set of counting vials, each containing 8.0 mL of toluene-Triton N-101 with PPO and POPOP as scintillator. All vials were shaken well and left for one day before they were counted.

b. The effect of sodium hydroxide on the stability and detection efficiency of tritium

This experiment was carried out in the same way as in section (a) except that sodium hydroxide was used in the place of hydrochloric acid.

c. The effect of hydrochloric acid and ammonium acetate (Buffer) on the stability and detection efficiency of tritium

The experiment similar to the one done on hydrochloric acid on the stability and detection efficiency, but instead ammonium acetate was added as buffer. Ammonium acetate of 0.25 g and 0.5 g were added into two sets of mixtures respectively.

d. The effect of Sodium Hydroxide and Ammonium acetate (Buffer) on the stability and detection Efficiency of Tritium

This experiment was done in the same manner as above but substituting hydrochloric acid with sodium hydroxide.

Zaini Hamzah et al: EFFECTS OF VARIOUS PARAMETERS ON IN-HOUSE COCKTAIL DEVELOPED FOR THE MEASUREMENT OF GROSS ALPHA AND BETA IN AQUEOUS ENVIRONMENTAL SAMPLES USING LIQUID SCINTILATION COUNTING

TECHNIQUE

Effect of buffers on the stability and detection efficiency of the mixture

The aim of the experiments was to study the effect of buffer alone on the cocktail and to determine the optimum concentration of this buffer in order to obtain the best counting value. Ammonium acetate was chosen as the buffer for this analysis. The effect of ammonium acetate on the stability and detection efficiency of the mixture was studied. A series of 0.0, 0.2, 0.4, 0.6, 0.8 and 1.0 g of ammonium acetate were transferred into six counting vials. The aqueous solution containing 2 mL of tritium and uranium-232 solutions with specific activity 25.25 Bq/mL and and 11.51 Bq/mL respectively and the vials were shaken well. When all the ammonium acetate has dissolved, 8.0 mL of toluene-Triton N 101 was added to make up the total volume of 10 mL. All vials were shaken well, left for one day before being counted. The optimum concentration of ammonium acetate in the mixture was determined by repeating the above experiment in the range of 0.0 to 0.2 g of ammonium acetate.

Effects of salts on the stability and detection efficiency of the mixture

Eight clean counting vials were prepared followed by addition of 0.0, 0.2, 0.4, 0.6, 0.8, 1.0, 1.2 and 1.4 g of Analar sodium chloride (Merck) were weighted into each of counting vial in sequence. The water including 4.0 mL tritium and uranium-232 solutions with specific activity 25.25 Bq/mL and and 11.51 Bq/mL respectively was added and vials were shaken well to dissolve the sodium chloride. The 8.0 mL toluene—Triton N-101 with the scintillator was added into each vial and shaken well. After one day, all the vials were counted to measure the detection efficiency of tritium and uranium-232.

Results and Discussion

Effect of pH on the stability and detection efficiency of the mixture

As indicated by Figures 1a and 1b, the counting efficiency is decreasing with increasing of pH (Figures 1a and 1b). pH value is important since the solubility of the radionuclide is dependent on pH, in which radionuclides are more soluble in the acidic region. Aqueous environmental samples are normally present in the pH range of 6 - 8 [10]. Hence, preserved environmental water samples at pH less 2 will give better results as compared to the unpreserved one.

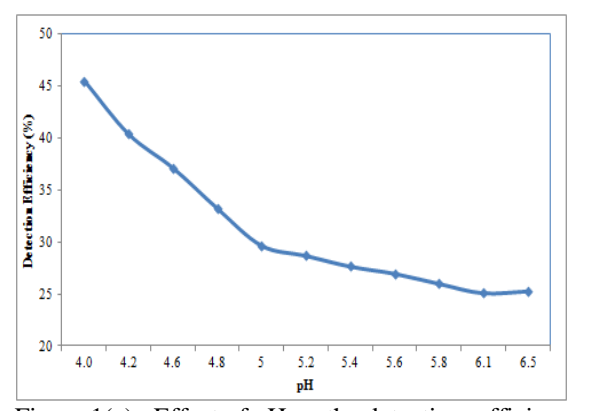


Figure 1(a). Effect of pH on the detection efficiency of aqueous tritium in the mixture

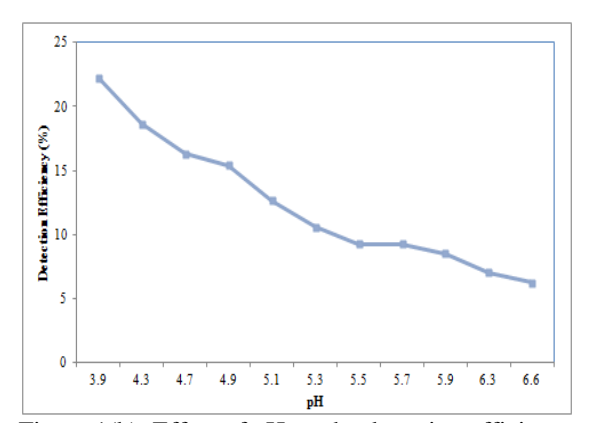


Figure 1(b). Effect of pH on the detection efficiency of aqueous uranium-232 in the mixture

Effect of Acids and Bases on the stability and detection efficiency of the mixture

The effect of acid and base on the stability and detection efficiency of the mixture is shown in Figures 2(a & b) where the efficiency seems to increase with the increasing molarity of the acid. Figures 3(a & b) show the decreasing detection efficiency with the increasing molarity of base. Since the molarity of the acid and base has a direct relationship with pH, therefore a slight increase in the amount of acid and base in the water samples and cocktail will inadvertently the efficiency of radionuclides detection efficiency.

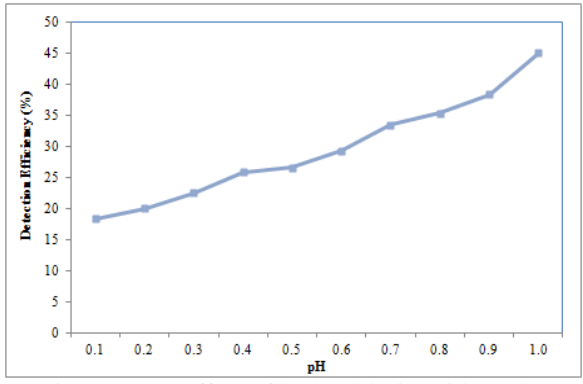


Figure 2(a). Effect of hydrochloric acid on the detection efficiency of tritium

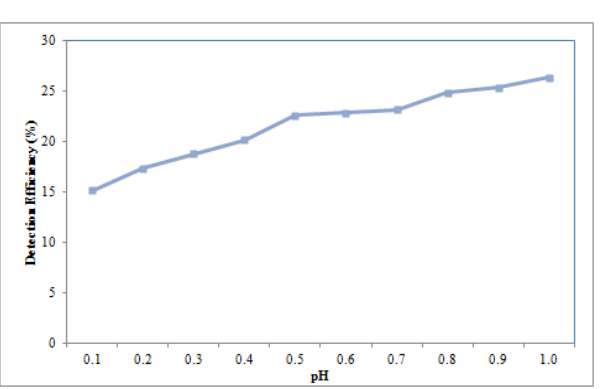


Figure 2(b). Effect of hydrochloric acid on the detection efficiency of uranium -232

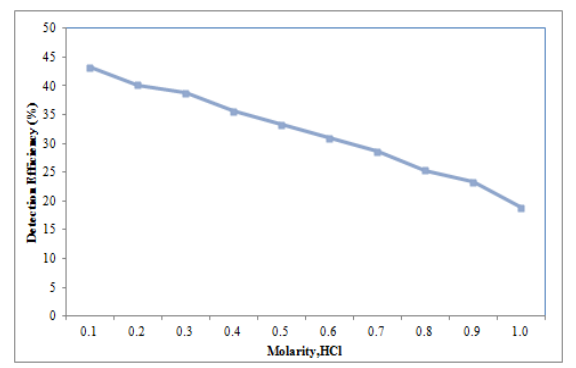


Figure 3(a). The effect of sodium hydroxide on the detection efficiency of tritium

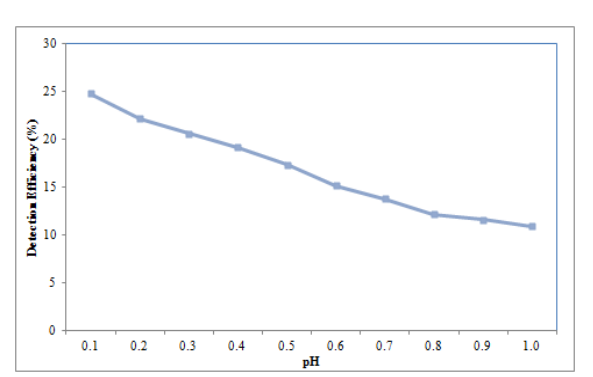


Figure 3(b). The effect of sodium hydroxide on the detection efficiency of uranium -232

Effects of buffers on the stability and detection efficiency of the mixture

Similarly, with the addition of buffer into the system, the effect remains the same. Buffer will stabilize the system and produce smooth graphs at reasonable concentration interval (see Fig 4a and 4b).

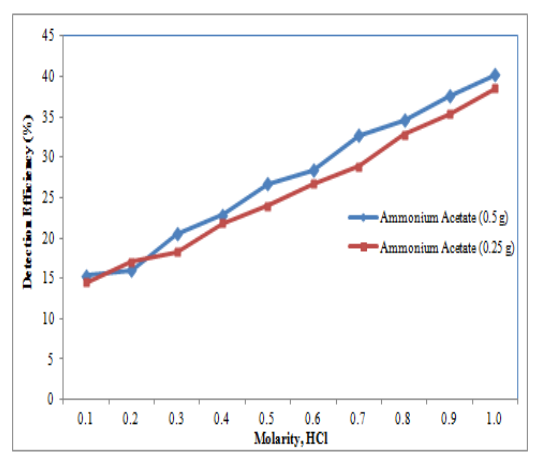


Figure 4(a). The effect of buffer –acid on the detection efficiency of tritium

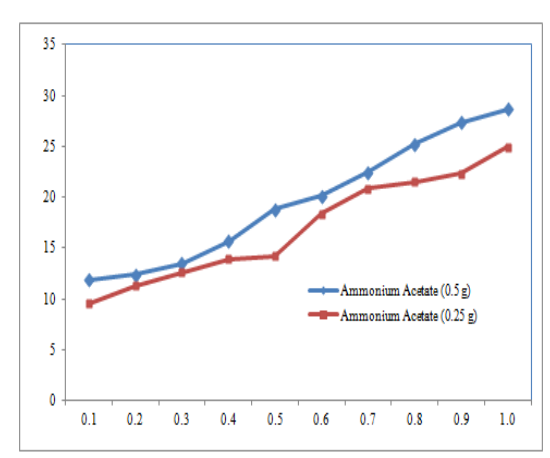
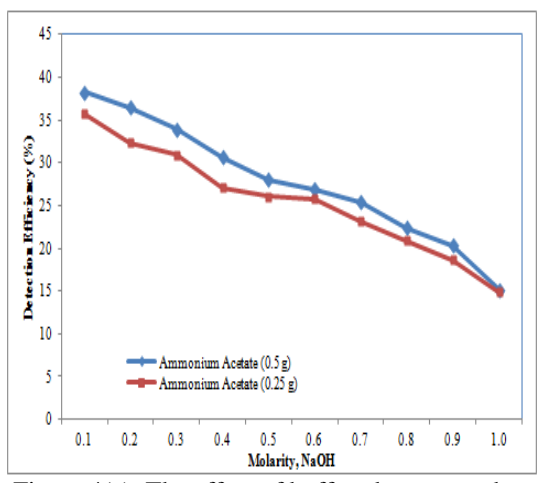


Figure 4(b). The effect of buffer-acid on the detection efficiency of uranium -232

Zaini Hamzah et al: EFFECTS OF VARIOUS PARAMETERS ON IN-HOUSE COCKTAIL DEVELOPED FOR THE MEASUREMENT OF GROSS ALPHA AND BETA IN AQUEOUS ENVIRONMENTAL SAMPLES USING LIQUID SCINTILATION COUNTING TECHNIQUE



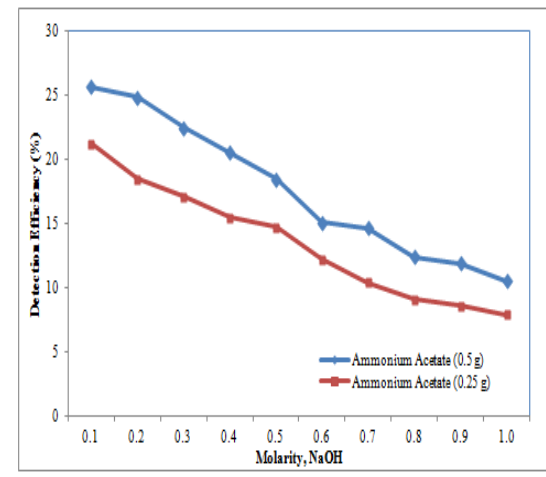


Figure 4(c). The effect of buffer –bases on the detection efficiency of tritium

Figure 4(d). The effect of buffer-base on the detection efficiency of uranium -232

Addition of ammonium acetate to cocktail system will stabilize the effect on the efficiency, where the counting efficiency is increase and after reaching optimum efficiency will decrease as the amount of ammonium acetate increased as shown in Figure 5. The optimum amount of ammonium acetate is 0.25 g.

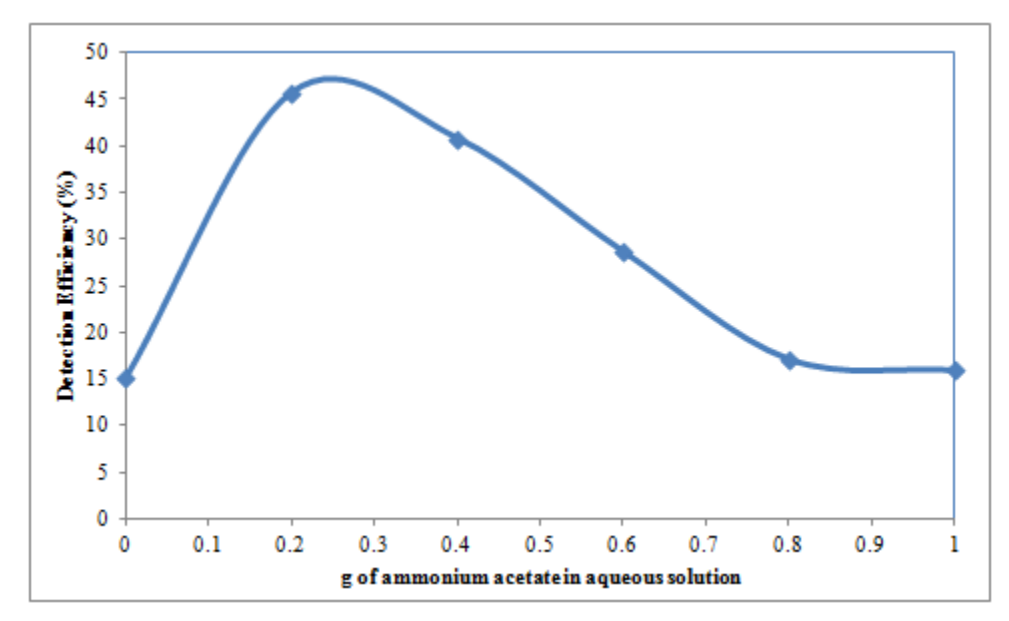


Figure 5. The effect of ammonium acetate (buffer) on the detection efficiency of tritium

Effects of salts on the stability and detection efficiency of the mixture

Addition of more than 0.2 g of salt (sodium chloride) will cause the efficiency to decrease rapidly as shown in Figure 6.

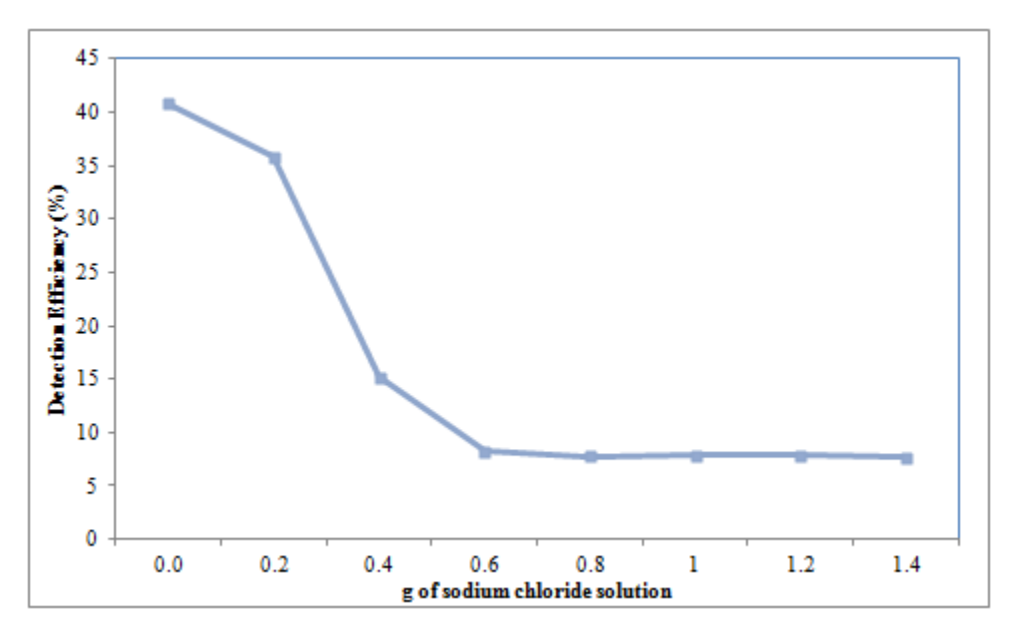


Figure 6. The effect of sodium chloride on the detection efficiency of tritium

Overall, the results show some effect of these parameters to the stability and efficiency of the cocktail-water system. One needs to study these effects to set the optimum condition for the counting of specific radionuclides. More over with the latest LSC equipment incorporating the alpha beta counting mode, one could explore more in term of analyzing specific radionuclides in the environmental samples. Therefore, one can move away from counting gross alpha and gross beta only but with the help of alpha and beta spectra we can calculate the activity of each radionuclide present in the sample. These optimum conditions help to reduce the background counts and provide improved spectra for subsequence analyses.

Analysis of water samples

Using the optimum condition above, different types of water samples were collected, prepared and measured using the alpha/beta counting mode of LSC and the results are shown in Table 2. The results show that hot spring water contains relatively high alpha compared to river water. Khazanah River in Cameron Highlands has a slightly higher alpha because it is located not far from the entrance to the Sultan Abu Bakar Dam. Samples from Lata Rek dam and Former tin mining lake (SK2) have slightly high alpha content due to its geological background. Lata Rek is situated on the granite rocks and former tin mining lake has the accumulation of heavy minerals which contains natural radiaonuclides in it. Other river waters show low alpha activity concentration.

Gross beta is from beta emitter in the uranium and thorium decay series such as ²¹⁸Po, ²¹⁴Pb and ²¹⁴Bi, ²¹²Pb, ²¹²Bi and ⁴⁰K which dissolved in water. Among the radionuclides ⁴⁰K and ²²⁸Ra are sufficiently soluble and abundant to contribute beta activities to some ground water. The energy of beta particle emitted by ⁴⁰K is high enough to be measured by the gross-beta technique. In contrast, ²²⁸Ra emits a relatively weak beta particle that may not be detected by gross-beta measurements. Although it is not expected to be present at the time of sampling, ingrowth of ²²⁸Ac from ²²⁸Ra approaches 95% of secular equilibrium with ²²⁸Ra within about a day. Although not well studied, Ac probably is sparingly soluble in most ground water [11]. Thus, gross-beta activity from these two radionuclides is approximately equal to the activity of ²²⁸Ra in ground water at the time of sampling.

Zaini Hamzah et al: EFFECTS OF VARIOUS PARAMETERS ON IN-HOUSE COCKTAIL DEVELOPED FOR THE MEASUREMENT OF GROSS ALPHA AND BETA IN AQUEOUS ENVIRONMENTAL SAMPLES USING LIQUID SCINTILATION COUNTING TECHNIQUE

Table 2.	Gross al	nha and	gross	beta i	n different	type's water

Sample Code	Types of water	Activity Concer	tration (mBq/L)
		Gross Beta	Gross Alpha
HS-Labok	Hot Spring	650 ± 46	568 ± 22
HS-Sungkai	Hot Spring	958 ± 71	856 ± 48
Bertam river	River Water	930 ± 68	304 ± 29
Khazanah river	River Water	912 ± 66	282 ± 28
Lata Rek Dam	River Water	2193 ± 159	577 ± 52
Lata Rek (DS)	River Water	1096 ± 79	291 ± 29
Kuala Tahan	River Water	1053 ± 77	347 ± 33
Jeti K. Keniam	River Water	1184 ± 87	217 ± 21
SK2	Lake Water	6080 ± 20	517 ± 92
LT2	Lake Water	9223 ± 14	328 ± 50

MDA Gross Alpha 50 mBq/L; Gross Beta 220 mBq/L

Figures 7 (a and b) show the spectra of alpha and beta from the sample measured. The spectrum here contain mixed radionuclides and difficult to analyze, unless the radiochemical separation was applied prior to the analysis. The circle indicates the possible radionuclides present in the samples.

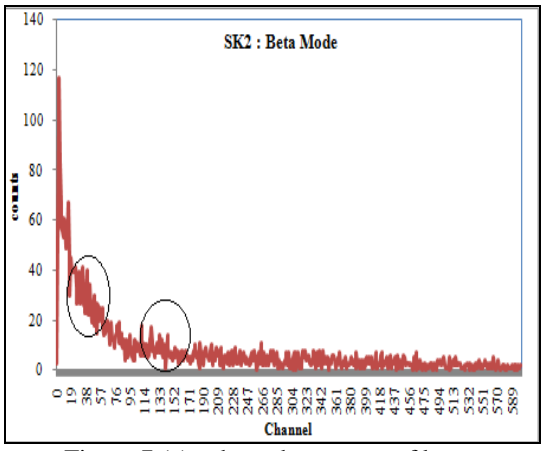


Figure 7 (a). show the spectra of beta

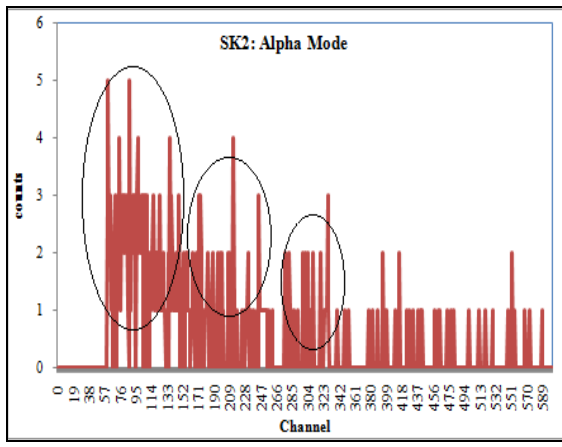


Figure 7 (b). show the spectra of alpha

Conclusion

In-house cocktail can be used for measuring of gross alpha and gross beta in the environmental aqueous samples. There is a need to consider various effects such as pH, acid and base, buffer and salt for optimization purpose. In general, when the amount of acid, base, buffer and salt are increased, the efficiency will decreased and the effect of pH is reduced if we chose the optimum pH. The gross alpha and gross beta measurement is important for screening purpose and radiochemical separation is needed to get the individual radionuclide which can be confirmed from the spectrum analysis.

Acknowledgement

The authors would like to thank Malaysian Nuclear Agency for allowing the project to be carried out at Malaysian Nuclear Agency (NM) laboratory in Bangi.

References

- 1. LSC Technical Tips from Packard (SC-005) (1997). Counting Solutions
- Perkin Elmer Application Note (2007). LSC in Practice Counting ¹⁴C in High Activity Sodium Carbonate Solution.
- 3. Zaini Hamzah, Masitah Alias, Zaharudin Ahmad, 2011. Discriminator setting cocktail preparation for analysis of alpha and beta emitters in aqueous solution using liquid scintillation counter. The Malaysian Journal of Analytical Sciences, 15(1), 27-36
- 4. A. Dyer (1980). Liquid Scintillation Counting Practice, publisher (pg 30)
- 5. Victor Jobbagy, Norbert Kavasi, Janos Somlai, Peter Dombavari, Csaba Gyongvosi, Tibor Kovacs. (2011). Gross alpha and beta activity concentrations in spring waters in Balaton Upland, Hungary. *Radiation Measurement*, 46: 159-163.
- 6. Gursel Karahan, Neset Ozturk and Ahmet Bayulken (2000). Natural radioactivity in various surface waters in Istanbul, Turkey. *Water Resources*, 34(18), 4360-4370.
- 7. UNSCEAR, United Nations Scientific Committee on Exposure to Atomic Radiation Report 1993.
- 8. H. Ozmen, F. Kulaher, A. Cukurovah, M. Dogru (2004). Concentration of heavy metal and radioactivity in surface water and sediment of Hazar Lake (Elazig, Turkey). *Chemosphere*, 55, 401-408.
- 9. Higuchi, H. (1981). The analysis of radium in the environmental samples. *Radioisotopes*, 30, 618.
- 10. United Nation, Guidance on Transformation/Dissolution of Metals and metal Compounds in Aqueous Media Report 2007.
- 11. Alan H. Welch, Zoltan Szabo, David L.Parkhurst, Peter C. Van Metre (1995). Gross beta activity in ground water: natural sources and artifacts of sampling and laboratory analysis. *Applied Geiochemistry*, 10, 491-503.



SORPTION COEFFICIENTS OF ¹³⁷Cs ONTO VARIOUS MALAYSIAN SOIL SERIES

(Pekali Serapan ¹³⁷Cs ke atas Pelbagai Siri Tanih Malaysia)

Zidan Mohamed M.Houmani¹, Amran Ab.Majid¹, Shahidan Radiman¹, Zaharudin Ahmad²

¹Faculty of Science and Technology, Universiti Kebangsaan Malaysia, 43600 UKM Bangi, Selangor, Malaysia ²Nuclear Malaysia , 43000 Bangi, Selangor D.E, Malaysia

*Corresponding author: houmani67@yahoo.com

Abstract

The ratio of equilibrium radionuclide concentration in the solid phase to the concentration in soil solution i.e. the distribution coefficient (K_d) can be used for quantification of a radionuclide's migration potential in the subsurface. K_d is one of the main parameter that describes soil absorbability for any radionuclide. In this study, distribution coefficients (K_d 's) of ¹³⁷Cs were measured by a batch technique for five Malaysian soil series samples to evaluate the absorbability of ¹³⁷Cs. The five Malaysian soils series samples i.e. Durian, Rengam, Holyrood, Segamat and Selangor were collected systematically at different depths (0-20 cm, 20-40 cm and 40-60 cm), at five different sites in Malaysia. The calculated K_d values for Durian, Holyrood, Rengam, Segamat and Selangor soil series were in the range of 958 to 3231 ml g⁻¹, 273 to 1349 ml g⁻¹ (mean: 853 ± 444 ml g⁻¹), 202 to 1739 ml g⁻¹ (mean: 754 ± 724 ml g⁻¹), 216 to 546 ml g⁻¹ (mean: 388 ± 113 ml g⁻¹) and 3389 to 5919 ml.g⁻¹ (mean: 4657 ± 918 ml g⁻¹), respectively. Thus this study indicated that the ¹³⁷Cs K_d values of the soils varies with type and depth of the soil and can be used as a good backfill choice for final disposal sites for retarding migration of ¹³⁷Cs.

Keywords: K_d – values, ¹³⁷Cs, Malaysian Soil Series

Abstrak

Nisbah kepekatan radionuklid seimbang dalam fasa pepejal larutan tanih iaitu pekali taburan (K_d) boleh digunakan untuk mengkuantitikan potensi pemindahan radionuklid di dalam sub permukaan. K_d merupakan salah satu parameter utama yang menerangkan keupayaan penyerapan tanih untuk pelbagai radionuklid. Dalam kajian ini, pekali taburan (K_d) ¹³⁷Cs diukur menggunakan teknik kelompok untuk sampel lima siri tanih Malaysia bagi menilai penyerapan ¹³⁷Cs. Lima sampel siri tanih i.e Durin, Rengam, Holyrood, Segamat dan Selangor dikumpulkan secara sistematik pada kedalaman yang berbeza (0-20 cm, 20-40 cm dan 40-60 cm) pada lima tapak yang berbeza di Malaysia. Keputusan pengiraan nilai K_d untuk masing-masing siri tanih Durian, Holyrood, Rengam, Segamat dan Selangor berada dalam julat 958 hingga 3231 ml g⁻¹, 273 hingga 1349 ml g⁻¹ (min: 853 \pm 444 ml g⁻¹), 202 hingga 1739 ml g⁻¹ (min: 754 \pm 724 ml g⁻¹), 216 hingga 546 ml g⁻¹ (min: 388 \pm 113 ml g⁻¹) dan 3389 hingga 5919 ml g⁻¹ (min: 4657 \pm 918 ml g⁻¹). Oleh itu, kajian ini menunjukkan bahawa nilai K_d ¹³⁷Cs untuk tanih yang berbeza jenis dan kedalaman boleh digunakan sebagai pilihan yang baik untuk pengambusan (backfill) tapak pelupusan akhir bagi merencat permindahan keluar ¹³⁷Cs.

Kata kunci: Nilai K_4 , ¹³⁷Cs, siri tanih Malaysia

Introduction

One of the hazardous radionuclides is 137 Cs because of its long half-life ($T_{1/2} = 30.2$ yr) and high transfer factor by inhalation and ingestion. Knowledge of the mobility of 137 Cs in the natural environment is needed for the assessment of the impact of accidental 137 Cs releases to the environment. This study focused on improving knowledge on the physical and chemical properties of the soil and the mechanisms by which the 137 Cs is uptaken from soil to the food chain or the means that lead to the contamination of the water supplies [1]. The parameter known as (K_d -value) is defined as the distribution of a radionuclide in soil divided by the concentration in the soil

pore water. The value of the K_d depends on the type of radionuclide, the physical, chemical and mineralogical properties of the soil, and the temperature. The K_{d} -value of the radionuclides needs to be determined in order for the analyst to assess its contribution to the dose to the public. Mollah and Ullah have studied the sorption coefficients (K_d) of ¹³⁷Cs on soil matrices collected from locations in and around the proposed site for shallow land disposal of low-level radioactive wastes at the Atomic Energy Research Establishment (AERE) campus, Savar, Bangladesh. They found that the K_d for ¹³⁷Cs ranged from 1278 to 2156 mL g⁻¹[2]. Elejalde et al (1973) have determined the distribution coefficients of ¹³⁷Cs in 58 soils from 12 points in Biscay (Spain). The highest mean percentages of ¹³⁷Cs sorption were found in the residual category (69.93%), exchangeable (13.17%) and organic matter (12.54%) fractions. The study also included calculation of the partial K_d's for chemical species as well as the relationships of the coefficients both between themselves and with the soil parameters. The treatment with ¹³⁷Cs leads to the sorption of most of the activity, with distribution coefficients K_d in the range from 484 to 42724 cm³ g⁻¹ [3]. Soil distribution coefficients (K_d 's) of ¹³⁷Cs were measured by Nakamaru et al. (2007) for 87 Japanese agricultural soils to evaluate the adsorbability of ¹³⁷Cs [4]. Soil organic matter (SOM) may affect ¹³⁷Cs mobility because OM is a reactive colloid. Therefore, tracer studies were carried out to clarify the effect of SOM on ¹³⁷Cs mobility in different soils. The 137 Cs K_d 's ranged from 215 to 43400 L kg $^{-1}$ with a geometric mean of 2210 L kg $^{-1}$. These results suggest that dissolved organic matter (DOM) increases the mobility of ¹³⁷Cs but that SOM can decrease the mobility of ¹³⁷Cs in soil by holding it in exchangeable and SOM-bound forms.

Materials and Methods

Soil sampling and preparation

Undisturbed soil samples were taken from the designated sampling stations shown in Table 1. and Figure 1. First, the detritus (grass and litter) at each sampling station were cleared from the ground surface and the soil was dug with a spade. Soil samples were collected from depths of 0-20 cm, 20-40 cm and 40-60 cm. About 500 g soil samples were collected from each depth. The samples were sealed in plastic bags and taken to the laboratory for further analysis. In the laboratory, the samples were air dried at room temperature, disaggregated using a wooden mortar and pestle and sieved through a 2 mm mesh for further use and analysis. In addition, soil cores (7.6 cm diameter and 4 cm long) were also taken from each depth for bulk density determination.

Station No.	Soil series names	Grid References	Locations
1	Durian	03 ⁰ 28′02.9″ N 102°06′31.8″ E	93 km from Kuala Lumpur to Kuantan , 167 Kuantan to Kuala Lumpur – Kuantan Old Road
2	Holyrood	03°09 [′] 45.8 [″] N 101°34 [′] 02.4 [″] E	Located at Mature Rubber tree in Rubber Research Institute, Sungai Buloh. 15 km to Batu Tiga, 5 km to Sungai Buloh from Batu Tiga
3	Rengam	03°25′02.4″ N 101°53′42.3″ E	Kuala Lumpur to Bentong old roar, 16 km to Bentong, 60 km to Kuala Lumpur
4	Segamat	03°30′15.9″ N 102°32′58.8″ E	$110\ \mathrm{km}$ to Kuantan – Chenor road , near to the AtTaqwa Mosque
5	Selangor	03°20′56.3″ N 101°18′29.8″ E	Located at Indian Cemetery , Kuantan Village to Bukit Rotan Road

Table 1. Locations of soil sampling stations

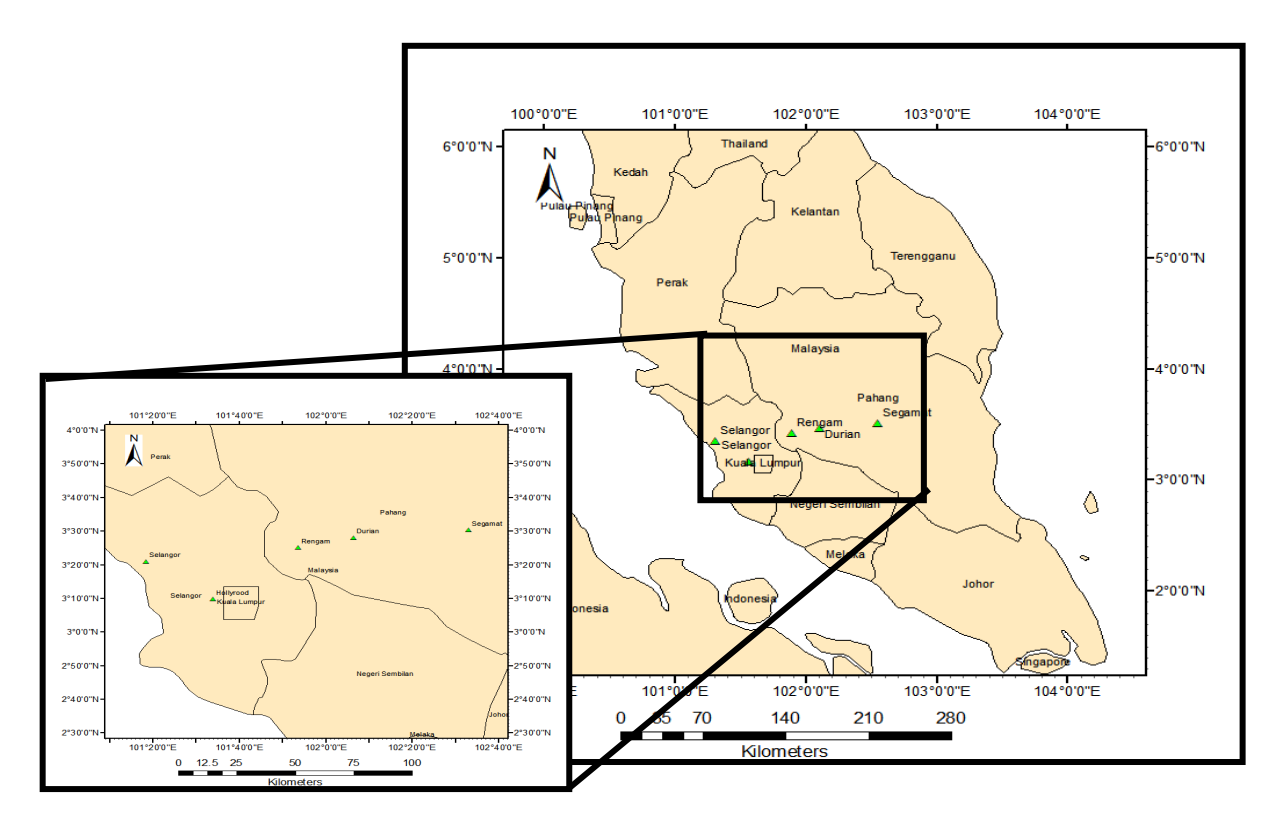


Figure 1. Location of soil sampling stations of five Malaysian soil series

Laboratory sorption experiments

The sorption of 137 Cs on five Malaysian soil series was studied using the batch technique on at least three replicates. The solution-soil ratio was maintained as 20:1 throughout the experiments in accordance with ASTM D4319-93 [5]. Twenty ml of 1788 Bq ml⁻¹ 137 Cs tracer was spiked into deionised water. This solution was then mixed with 1.0 \pm 0.1 g of each soil in 50 cm³ polyethylene centrifuge tube with screw caps and septum sealed. Suspensions were initially preconditioned, using deionised water with on 137 Cs spike by shaking for 24 h at 23 \pm 2 0 C using an end-over-end shaker. The spiked slurries were shaken for 7 days to achieve the equilibrium of 137 Cs adsorption, the solution phase was separated by centrifugation at 3000 rpm, and the supernatant was filtered though a 0.45- μ m micropore filter. The 5 cm³ of the supernatant was pipetted into small glass vials. The activity concentration measurements of 137 Cs in the vials was performed with a Canberra p-type HPGe well detector (GCW 2523) with active volume of 155 cm³, a relative photopeak efficiency of 25%, and a resolution at the 1332 keV energy of 60 Co of 2.3 keV (FWHM).

 $K_{\rm d}$ (ml g⁻¹) was then calculated using equation 1:-

$$K_d(ml/g) = \frac{(C_i - C_f)}{C_f} \cdot \frac{V}{M}$$
 (1)

where C_i (Bq ml⁻¹) is initial activity of the radiotracer in the aqueous phase, C_f (Bq ml⁻¹) is activity of radiotracer in the final supernatant, V is solution volume (20 ml), and M is soil dry weight (1.0 ± 0.01 g).

Treatment of the raw counting data was performed with the GENIE 2000 program. The activity (cps) of the ¹³⁷Cs photopeak (661.6 keV) was determined. Based on the background and blank counts, the minimum detectable activity (MDA) for this geometry was derived using Currie's Method formula [6]:

$$MDA = \frac{\sigma\sqrt{B}}{\varepsilon PTW} (Bq.kg^{-1}), \tag{2}$$

Where, σ is statistical coverage factor (= 1.645) (P \leq 0.05), B is background radiation of the radionuclide of interest, ε is counting efficiency of the detector, P is absolute transition probability of γ -decay, W is dried sample weight in g, and T is counting time in seconds. The MDA for ¹³⁷Cs determined was 2.087 Bq kg⁻¹.

Results and Discussion

The results of the experiments regarding distribution coefficients of 137 Cs in the five Malaysian soil types are shown in Table.2 and Figure.2. The calculated K_d values for Durian, Holyrood, Rengam, Segamat and Selangor soil series (all three depths included) were in the mean of $(2126.22 \pm 887.91 \text{ ml g}^{-1})$, $(853.36 \pm 444.98 \text{ ml g}^{-1})$, $(754.98 \pm 724 \text{ ml g}^{-1})$, $(388.88 \pm 113.99 \text{ ml g}^{-1})$ and $(4657 \pm 918 \text{ ml g}^{-1})$, respectively. The results also showed that the K_d -values depend on the depths of the soil. The K_d -values increase with depth except for Segamat and Selangor soil series. The results of this study indicated that 97.96 - 99.39%, 93.19 - 98.54%, 91.00 - 98.86%, 91.57 - 96.47% and 99.41 - 99.66% of added 137 Cs tracer was strongly adsorbed by the Durian, Holyrood, Rengam, Segamat and Selangor soil series, respectively. The soil series in this study showed higher K_d -value in upper layer.

Table 2. Mean distribution coefficients (K_d -value) for ¹³⁷Cs in five of Malaysian soil series

Depths			Soil series		
(cm)	Durian	Holyrood	Rengam	Segamat	Selangor
		$K_{ m d}$ -val	ue in (ml g ⁻¹) \pm S.	D [*]	
0-20	1061.91 ± 137.16	292.54 ± 17.32	206.61 ± 4.26	517.03 ± 35.39	5345.99 ± 499.67
20-40	2293.49 ± 389.84	975.29 ± 28.54	341.54 ± 22.90	386.94 ± 18.73	5099.78 ± 426.56
40-60	3023.26 ± 186.09	1292.25 ± 88.89	1716.79±35.23	262.68 ± 42.89	3526.39 ± 125.52

*S.D: Standard deviation

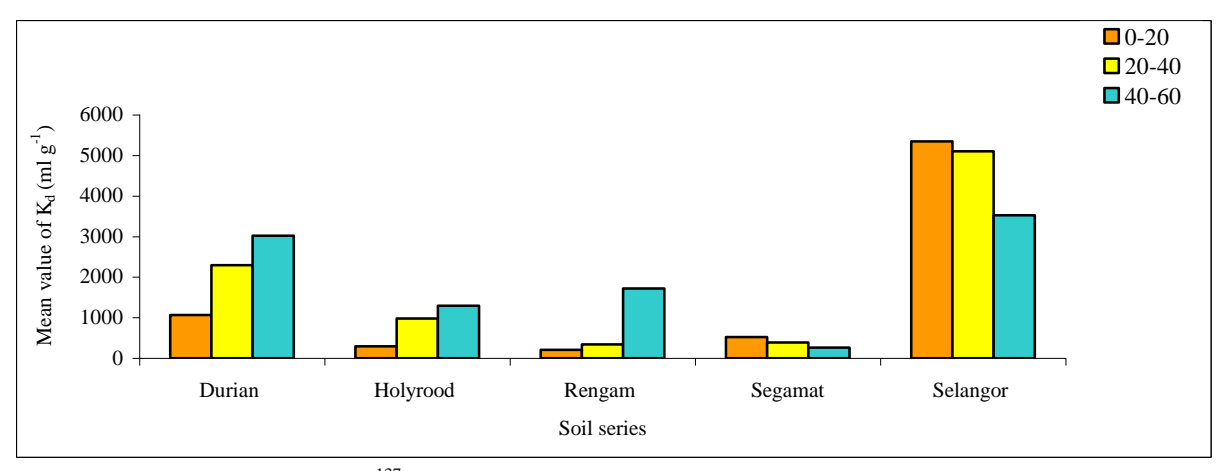


Fig 2. ¹³⁷Cs adsorption onto five of Malaysian soils series.

Given the above results, it can be concluded that further investigation is required in order for a better relationship between K_d-value and physico-chemical soil properties to be established. Soils have the tendency to absorb and distribute the ¹³⁷Cs depending upon the texture and physicochemical properties. The investigation was made to measure the absorption capacity of the soil in batch method to accommodate 137Cs. Selangor soil exhibits the maximum sorption coefficient value with a steep decrease towards depth, which might be attributed to the decrease in porosity. Other soils did not exhibit the remarkable sorption except Durian soil, and Segamat soil was found with minimum sorption coefficient value. The behaviour of the different soils was presenting different trends with respect to their depth. Selangor and Segamat soils show that the K_d values decrease with the increase in depth, however other three soils presents more sorption coefficient with the depth. The variability in the values of sorption coefficients can be attributed to the type of soil and its composition. Zidan et al (2010) have reported the texture of Selangor soil as a clayey one with concentration of clay mainly combination of Kaolinite, illite and monmorillonite ranging from 65%, 74% and 76% at the depths of up to 20, 40 and 60 cm respectively [7]. ¹³⁷Cs distribution or sorption coefficients may need some type of interactions to clayey nature of the specific particles. It was also observed that Durian soil's composition is clayey too but with less concentration as compared to the Selangor soil. The nature of the other soils including Holyrood and Rengam is not Clayey but sandy which did not allow the Cs to incorporate properly for channelling to migration [8]. In case of Segamat soil, minimum sorption of ¹³⁷Cs was observed even the texture of soil was not sandy but clayey [9]. The lack of sorption capacity of the clay towards Cs incorporation can be attributed to the type or concentration of the clay contents. Instead of being Calyey in texture, the Segamat soil was not able to allow Cs for remarkable sorpion and migration values which might be attributed to different nature and composition of the clay than Selangor soil. Bachhuber et al. (1982) have reported the rates of distribution, migration and retardation factors of the distribution coefficients of ¹³⁷Cs in the various horizons using batch method. They have made their findings of the distribution coefficients based on the accumulated organic matter in the soil [10]. Chang and Hsu have reported the adsorption of ¹³⁷Cs on bentonite clay which is an evidence regarding existence of some interactions between clay and ¹³⁷Cs [11].

Conclusion

The distribution and migration of ¹³⁷Cs in the soil depends in particular on its adsorption properties and the movement of soil water. The movement of water carrying the subject matter in the soil is determined by the amount of precipitation and other soil properties including texture, porosity and organic contaminants. The adsorption properties are also determined by the proportion, type and composition of the clay mineral content of the soil. This study has revealed some trends of sorption in relation to the nature or type of clay. The sorption was not supported by soil containing sandy texture but enhanced sorption was observed with the soil containing a combination of clay including kaolinite, illite and montmorillonite i.e Selangor soil. The obtained results indicate that these types of soil could be considered as good backfill choices for final disposal sites for retarding migration of ¹³⁷Cs.

Acknowledgement

The authors would like to thank Mr. Yii from the Malaysian Nuclear Agency for his invaluable guidance and assistance during the experimental work of ¹³⁷Cs measurements by the well-type HPGe detector, We are also grateful to Dr. Sahibin Abd. Rahim from the School of Environmental and Natural Resource Sciences, FST, UKM, for his advice on the physico-chemical properties of Selangor soil series.

References

- 1. Eisenbud, M. (1973). *Environmental radioactivity*. 2nd ed, *Environmental sciences*. New York,: Academic Press.
- 2. Mollah, A. S., & Ullah, S. M. (1998). Determination of distribution coefficient of ¹³⁷Cs and ⁹⁰Sr in soil from AERE,Savar. *Waste Management* 18:287-291.
- 3. Elejalde, C., Herranz, M., Legarda, F., &Romero, F. (2000). Determination and analysis of distribution coefficients of ¹³⁷Cs in soils from Biscay (Spain). *Environmental Pollution* 110 (1):157-164.
- 4. Nakamaru, Y., Ishikawa, N., Tagami, K., &Uchida, S. (2007). Role of soil organic matter in the mobility of radiocesium in agricultural soils common in Japan. *Colloids and Surfaces A: Physicochemical and Engineering Aspects* 306 (1-3):111-117.
- 5. ASTM. (1984). Standard Test Method for Distribution Ratios by the Short-Term Batch Method. In *Annual Book of ASTM Standards*: American Society for Testing and Materials.

Zidan Mohamed M. Houmani et al: SORPTION COEFFICIENTS OF ¹³⁷Cs ONTO VARIOUS MALAYSIAN SOIL SERIES

- 6. Currie, L. A. (1968). Limits for qualitative detection and quantitative determination *Anal Chem* 40:586-593.
- 7. Houmani, Z. M., Ab.Majid, A., Radiman, S., & Ahmad, Z. (2010). Influence of the physico-chemical properties of Selangor soil series on the distribution coefficient (*K*_d-value) of ²²⁶Ra. *Journal of Radioanalytical and Nuclear Chemistry* 285:271-277.
- 8. Ikram, A., Mahmud, A., &Napi, D. (1987). Effects of P-fertilization and inoculation by two vesicular-arbuscular mycorrhizal fungi on growth and nodulation of Calopogonium caeruleum. *Plant and Soil* 104 (2):195-207.
- 9. Alias, M., Hamzah, Z., Saat, A., Omar, M., Tajuddin, Z., Kadir, W. M. W. A., &Solleh, M. R. M. Level of Naturally Occurring Radioactive Material, K-40 in soil Oil Palm's Cultivated Soil.
- 10. Bachhuber, H., Bunzl, K., &Schimmack, W. (1982). The Migration of ¹³⁷Cs and ⁹⁰Sr in Multilayered Soils: Results From Batch, Column and Fallout Investigations. *Nuclear Technology* 59 (2):291-301.
- 11. Chang, K.-P., Hsu, C.-N., &Tamaki, H. (1993). Basic study of ¹³⁷Cs sorption on soil. *Journal of Nuclear Science and Technology* 30 (12):1243-1247.



SEASONAL INFLUENCE ON WATER QUALITY STATUS OF TEMENGGOR LAKE, PERAK

(Pengaruh Musim Terhadap Kualiti Air Tasik Temenggor, Perak)

Wan Mohd Afiq Wan Mohd Khalik¹ and Md. Pauzi Abdullah^{1,2}

¹School of Chemical Science and Food Technology, ²Centre for Water Research and Analysis (ALIR), Faculty of Science and Technology, Universiti Kebangsaan Malaysia, 43600 Bangi, Selangor, Malaysia

*Corresponding author: mpauzi@ukm.my

Abstract

A study of the water quality in Temenggor Lake was conducted within two different seasons, namely wet season (November – January 2009) and dry season (March – July 2010). Thirteen sampling stations were selected representing open water body of the lake particularly surrounding Banding Island. Three depths layered sampling (surface, middle and bottom of lake) was performed at each sampling stations except in zone B. An average WQI for Temenggor Lake in wet season (90.49) is slightly higher than the average for dry season (88.87). This study indicates quite significant seasonal influence of rainfalls on environmental lake ecosystems by improving the quality through dilution effect on several parameters. Statistical analysis of two-way ANOVA test indicates that all measured parameters are affected by seasonal changes except for pH, turbidity, DO, BOD, oil and grease. Biochemical Oxygen Demand (BOD) and water hardness showed significant relationship with local community activities. Considering future development as ecotourism destination, the water quality of Temenggor Lake should be maintained thus some sort of integrated lake management system model on the integrated water resource management concept should be implemented.

Keywords: Temenggor Lake, Water Quality, Seasonal Variation

Abstrak

Satu kajian kualiti air di Tasik Temengor telah dijalankan dalam tempoh dua musim yang berbeza iaitu, musim basah (November – Januari 2009) dan musim kering (Mac – Julai 2010). Tiga belas stesen persampelan telah dipilih mewakili sistem air terbuka tasik terutamanya sekitar Pulau Banding. Persampelan pada tiga kedalaman (permukaan, tengah dan dasar tasik) telah dijalankan di semua stesen persampelan kecuali zon B. Nilai purata IKA untuk Tasik Temengor pada musim basah (90.49) adalah lebih tinggi berbanding daripada musim kering (88.87). Kajian semasa menunjukkan pengaruh yang cukup besar oleh hujan semasa musim basah ke atas ekosistem tasik dengan cara meningkatkan kualiti melalui kesan pencairan terhadap beberapa parameter. Analisis statistik ANOVA dua hala menunjukkan bahawa kesemua parameter yang diukur terjejas oleh perubahan bermusim kecuali pH, kekeruhan, oksigen terlarut, BOD serta minyak dan gris. Permintaan oksigen biokimia dan keliatan air menunjukkan hubungan yang signifikan dengan aktiviti masyarakat setempat. Memandangkan pembangunan sekitar tasik dimasa hadapan sebagai destinasi eko pelancongan, kualiti air Tasik Temenggor perlu dikekalkan. Oleh itu suatu model sistem pengurusan bersepadu tasik bersandarkan konsep pengurusan sumber air bersepadu (IWRM) perlu dilaksanakan.

Kata kunci: Tasik Temenggor, Kualiti Air, Perubahan Musim

Introduction

Temenggor Lake is the largest man-made lake in Perak, and the second largest in Peninsular Malaysia. This catchment area of 152 km² formed as a result of hydroelectric dam established in 1974 and completed in 1977. The dam water is also used as a drinking water supply for northern peninsular of Malaysia populations [1]. Temenggor Lake is divided into three zones namely Conservation Zone, Recreational Fishing Zone and Commercial Zone. Conservation Zone includes upstream of Temenggor Lake such as Kejar River, Tiang River and Gadong River.

Increased in human population has resulted in new human settlements around lakes which served as water resources or tourism area which resulted in the deterioration of water quality [2,3]. Having mega diversity of flora and fauna as partly within the Royal Belum Temenggor Conservation area, Temenggor Lake was noted as a popular freshwater ecosystem as well developed in line with the concept of ecotourism. However no proper study on the water quality of the lake was performed. It is imperative that a study be carried out to evaluate the status of lake's water quality. This study was carried out for the purpose as well as to identify any possible pollution sources and to assess the impact of Orang Asli settlement on the lake's water quality.

Materials and Methods

Sampling Activity

Field sampling was conducted within wet season (November – January 2009) and dry season (March – July 2010). A total of 13 sampling stations were divided into 2 main zones namely zone A: Banding Island which is considered as part of commercial area and zone B: Royal Belum Temenggor which is noted as conservation area. Portable GPS was used to determine the coordinate each sampling station on location as presented in Table 1. Water samples were collected at three depths from each sampling station except for zone B in which depth measurement less than 5 m. Van Dorn water sampler was used to collected sample before transfer into 1000 mL HDPE and glass bottle prior for laboratory analysis.

Table 1. Sampling Station, Coordinate and Depth Measurement for Temenggor Lake Study

Station	Location	Coo	rdinate	Depth (meter)	
		Latitude	Longitude	Wet	Dry
	Zone A: Banding Island				
SS01	Banding Fisheries Centre	05° 33.138 N	101° 21.180 E	10.32	8.12
SS02	Banding Island Public Jetty	05° 33.097 N	101° 20.887 E	7.80	5.66
SS03	Mohd Shah Resort	05° 32.928 N	101° 21.190 E	21.20	20.07
SS04	Banding Island Southern Region	05° 31.748 N	101° 20.845 E	13.00	11.45
SS05	Banding Island Resort	05° 33.522 N	101° 20.481 E	11.05	10.03
SS06	Banding Island Resort (discharge point)	05° 32.559 N	101° 20.404 E	4.30	4.20
SS07	Banding Island Northern Region	05° 33.951 N	101° 20.103 E	11.00	8.77
	Zone B: Royal Belum Temenggor				
SS08	Orang Asli Settlement Tiang River	05° 33.950 N	101° 20.105 E	4.30	2.10
SS09	Orang Asli Settlement Tiang River Middle Pathway	05° 41.659 N	101° 26.515 E	3.50	2.55
SS10	Orang Asli Settlement Kejar River	05° 47.447 N	101° 24.502 E	3.50	3.01
SS11	Base Camp Kejar River	05° 47.437 N	101° 24.504 E	2.70	2.50
SS12	Perak River Upstream	05° 48.592 N	101° 25.286 E	2.90	1.49
SS13	Mess Estuary (Kejar River)	05° 48.056 N	101° 24.896 E	5.20	3.84

Samples were stored in a cool box containing ice cube at temperature of approximately 4 °C before transferring to Pulau Banding Rainforest Research Center (PBRRC) for further analysis. All sampling, preservative and samples handling technique were in accordance with APHA 1998 for Examination of Water and Wastewater (20th Edition) [4].

In situ Measurement

Physical water quality was measured *in situ* using YSI model 550 multi sensor probe for pH, temperature, turbidity, conductivity and dissolved oxygen. Depth level of each sampling station was measured using an echo sounder[®] model speedtech. Calibration of every YSI model 550 probes was conducted in the laboratory prior before field sampling and once again after sampling progress work was done.

Laboratory Analysis

All samples collected from the field were kept in a refrigerator at a temperature below 4°C to reduce all the activities and metabolism of the organisms in the water. Preliminary analysis for various chemical parameters such as suspended solid, oil and grease were performed at the Pulau Banding Rainforest Research Centre. Further analysis (COD, nitrate, phosphate, and metals) were performed at chemistry laboratory, UKM.

List of method used were Ammoniacal-Nitrogen (Salicylate Method), Water Hardness (EDTA Titration Determination), Suspended Solids (Gravimetric Method), Biochemical Oxygen Demand (Incubation Method as BOD₅), Chemical Oxygen Demand (Reactor Digestion and Colorimetric Determination), Oil & Grease (Extraction-Gravimetric Method), Nitrate (Cadmium Reduction Method) and Phosphate (Ascorbic Acid Method). Ammonia-N, Chemical Oxygen Demand, Nitrate and Phosphate were determined by using a spectrophotometer Model HACH DR 2000 at a specified wavelength (APHA 1998; HACH 2003).

Results and Discussion

The range, mean and standard deviation of *in situ* measurement parameters within seasonal change are as shown in Table 2. Statistical analysis shows that only temperature and turbidity as *in situ* parameters measured in this study have significant differences (P<0.05) between seasonal change. In term of spatial variation only dissolved oxygen have significant differences (P<0.05). Correlation analysis was also conducted to examine the relationship between different variables.

Parameter	Wet S	eason	Dry Season		
	Range	Mean (SD)	Range	Mean (SD)	
Temperature (°C)	23.35 – 29.34	27.53 ± (1.85)	26.52 – 30.23	28.68 ± (1.24)	
pH	6.72 - 8.32	$7.29 \pm (0.49)$	6.89 - 7.71	$7.35 \pm (0.25)$	
Conductivity (µScm ⁻¹)	30 - 50	$37.74 \pm (5.06)$	37 - 52	$42.63 \pm (4.16)$	
Turbidity (NTU)	2 - 7	$2.85 \pm (1.41)$	3 - 26	$6.31 \pm (6.33)$	
Dissolved Oxygen (mgL ⁻¹)	4.15 - 9.03	$6.79 \pm (1.85)$	3.32 - 8.73	$6.67 \pm (1.47)$	

Table 2. Range, mean and standard deviation for *in situ* parameters

Rainfall

The rainfall data through the sampling period was provided by Malaysia Meteorological Centre. From November 2009 to July 2010, 49.60-174.30 mm of rainfall was recorded in Temenggor Lake. Total number of raining days was 13 days as the start of raining season approximately in October till December every year. The monthly rainfall has shown significant relationship with parameters such as COD (r=0.673), oil and grease (r=0.793) and suspended solids (r=0.978).

Ammoniacal Nitrogen

The ammoniacal nitrogen concentrations was recorded to be in range of 0.02 - 0.05 (mean 0.03 ± 0.01) and 0.13 - 0.52 (mean 0.21 ± 0.09) mgL⁻¹ respectively for wet and dry seasons. These findings showed that highest concentration for ammoniacal nitrogen was recorded at Mohd Shah Resort (SS03) with values of 0.05 mgL⁻¹ (wet season) and at Base Camp Kejar River (SS11) with values of 0.52 mgL⁻¹ (dry season).

Ammoniacal nitrogen is commonly produce from decomposition of urea and protein by products, thus it is normally abundance as domestic waste in hydrological ecosystem [5]. Hence previous study partially claimed that major contribution of ammonium pollution may come from septic systems, although decomposition of ammonium may occur in the drain field pathways [6]. Human activity is well known to play important role as contributor to ammoniacal nitrogen abundance in the lake ecosystems in which concentrations could be higher than 5 mgL⁻¹[7]. Low level of ammoniacal nitrogen concentrations recorded in this present study indicates that sources of pollution from septic systems namely at Mohd Shah Resort or the Base Camp at Kejar River were not yet significant for Temenggor Lake ecosystems.

Several previous studies related to agricultural field impact reported that an application of fertilizers used inorganic nitrate content could be a significant source for high concentrations of ammonium nitrate in lake ecosystems [7]. Otherwise less usage of phosphorus content in non-agricultural areas often associated with low levels of ammonium content [6]. Since there was no large scale agricultural activities around Temenggor Lake area, except for small plots around Orang Asli settlement, agricultural activities will not be the significant source of ammoniacal nitrogen in the Temenggor lake ecosystems.

Statistical analysis using two ways ANOVA test indicates that ammoniacal nitrogen has no significant differences between sampling stations (P>0.05) but significantly different on seasonal period (P<0.05) in which wet season recorded significantly higher than the dry season. Ammoniacal nitrogen has shown positive correlation with conductivity (r = 0.664) and turbidity (r = 0.794).

Water Hardness

The concentration of water hardness were recorded to be in the range of 2.00 - 13.20 (mean 5.35 ± 2.92) and 2 - 16 (mean 8.98 ± 4.01) mgL⁻¹ respectively for wet and dry seasons. This study has shown that highest concentrations for hardness was recorded at Base Camp Kejar River (SS11) with values of 13.20 mgL^{-1} (wet season) and Orang Asli Settlement Tiang River (SS08) with values of 16 mgL^{-1} (dry season). This may be related to natural conditions at the stations and the impact of human activities particularly at Orang Asli settlement (SS08) and at Kejar River Base Camp (SS11). Moreover, the level of water hardness in dry season is probably enhanced by increasing evaporation rate in hydrological lake ecosystems [8].

The lowest concentration of water hardness was recorded at Banding Island Southern Region (SS04) with values of 2 mgL⁻¹ for both seasons. This may be due to its location away from any human activities. Statistical analysis using two ways ANOVA test indicates that water hardness has no significant different between seasons but is significantly different between stations (P<0.05).

Total Suspended Solids (TSS)

The concentration of suspended solids were recorded to be in the range of $1.02-9.00~\text{mgL}^{-1}$ (mean 3.71 ± 1.87) and $2.33-17.80~\text{mgL}^{-1}$ (mean 7.03 ± 4.85) respectively for wet and dry seasons. This study has shown that highest concentrations for TSS was recorded at Orang Asli Settlement Tiang River (SS08) with values of 9 and 17.80 mgL^{-1} respectively for both wet and dry seasons. Overall low levels of suspended solids in Temenggor Lake indicates a remarkably good sign for lake's water quality.

The Orang Asli Settlement Tiang River (SS08) as expected recorded higher level of suspended solids compared to other stations, since it is at Orang Asli communities settlements which is major population in Royal Belum Temenggor, where activities of their daily works specifically of water usage for cleaning as well as disposal of domestic waste contribute to the increase in suspended solids. Furthermore, the use of boat as main transport around the settlement area where the depth of lake can be considered as low (which is less than 5 meter during dry season),

allow resuspension of sediments to occurs [9] thus promotes an increase in suspended solids concentrations in the lake ecosystems.

According to Ooshaksaraie et al. [10] rate of soil erosion will increase when the cover of vegetation was disturbed or removed. Consequently, it will cause a drastically increase in the amount of surface runoff and velocity entering the lake. In this present study, low level of suspended solids concentration recorded during wet season indicates that most of the lake's riparian areas are still highly vegetated.

The lowest suspended solids concentrations were recorded at Perak River upstream (SS12) with value of 1.02 mgL⁻¹ (wet season) and at Banding Island Public Jetty (SS02) with value of 2.33 mgL⁻¹ (dry season). Perak River upstream was highly expected to be very clean (very low in suspended solids) since factors such as far away from human disturbance and high water flow make it cleaner than other areas. The low levels of suspended solids recorded at Banding Island Public Jetty (SS02) during dry season may be due to the low tourist activities at the time of sampling. Statistical analysis using two ways ANOVA test indicates that suspended solids has no significant differences between sampling stations (P>0.05) but has shown significant differences on seasonal period with (P<0.05). Suspended solids has shown positive correlation with temperature (r = 0.651) at P<0.05.

Biochemical Oxygen Demand (BOD)

The concentration of biochemical oxygen demand (BOD) was recorded to be in range of 0.26 - 2.19 (mean 1.25 ± 0.57) and 0.24 - 3.26 (mean 1.42 ± 0.80) mgL⁻¹ respectively for wet and dry seasons. This study has shown that highest value for BOD was recorded at Banding Fisheries Centre (SS01) with values of 2.19 mgL^{-1} (wet season) and at Orang Asli Settlement Tiang River (SS08) with values of 3.26 mgL^{-1} (dry season).

Since an availability of oxygen to living organism decreases with increasing BOD value, high BOD values obtained indicate maximum oxygen consumption and probably pollution load on the aquatic system [11] like what happen at station SS08. In this present study, the recorded BOD values were slightly higher in dry season but overall it can still be considered low and very much similar to those reported by Shuhaimi et al. [12] for Kenyir Lake $(0.61 - 2.87 \text{ mgL}^{-1})$.

The lowest BOD concentrations were recorded at Base Camp Kejar River (SS11) with values of 0.26 mgL⁻¹ (wet season) and also at Orang Asli Settlement Middle River Pathway (SS09) with values of 0.24 mgL⁻¹ (dry season). The BOD value at station SS11 tend to be decline during wet rather than dry season possibly due to current changes that increase speed of water overflow after receiving input from station SS12.

Statistical analysis using two ways ANOVA test indicates that BOD has significant differences between sampling stations (P<0.05) but no significant differences on seasonal period (P>0.05). Low levels of biochemical oxygen demand recorded in this present study indicates that organic pollution is not yet significant for the lake ecosystems. Biochemical Oxygen Demand (BOD) has shown positive correlation with temperature (r = 0.693) COD (r = 0.663) and negative correlation with pH (r = -0.584) at P<0.05.

Chemical Oxygen Demand (COD)

The concentration of chemical oxygen demand (COD) was recorded to be in range of 9.00 - 34.67 (mean 17.47 ± 7.28) and 7.00 - 28.00 (mean 15.21 ± 5.95) mgL⁻¹ respectively for wet and dry seasons. This study has shown that highest concentrations for COD was recorded at Banding Fisheries Centre (SS01) with values of 34.67 mgL⁻¹ (wet season) and 28.00 mgL⁻¹ (dry season). Activities at the centre may introduce some organic or chemical pollutions into the lake.

Higher concentrations of COD recorded in dry season may be due to less dilution of pollutant as noted for other parameters and by other study [11]. Statistical analysis using two ways ANOVA test indicates that COD has significant differences between sampling stations and seasonal periods (P<0.05). COD has also shown positive correlation with BOD (r = 0.663) also oil and grease (r = 0.693) at P<0.05. Despite some variations among stations, overall the level of COD, as of BOD, is still low indicating low level of organic and chemical pollution.

Oil and Grease

The concentration of oil and grease of Temenggor Lake was recorded to be in range of 0.667 - 104 (mean 24 ± 23.27) and 11.73 - 62.20 (mean 31 ± 16.63) mgL⁻¹ respectively for wet and dry seasons. This study has shown that highest concentrations for oil and grease was recorded at Banding Fisheries Centre (SS01) with values of 104 mgL^{-1} (wet season) and also at Orang Asli Settlement Tiang River (SS08) with values of 62.20 mgL^{-1} (dry season).

The highest value of oil and grease recorded at SS01 may be contributed local activities such as restaurant, boating, washing as well as water recreation from nearby Banding Island Public Jetty. In this present study, surprisingly the Banding Island Public Jetty (SS02) did not record high value of oil and grease as expected. This may be due to the low boating activities at the time of sampling. Higher values recorded at SS01 and SS08 may be due to local activities namely boating and related activities.

Statistical analysis using two ways ANOVA test indicates that oil and grease has significant differences between sampling stations and seasonal period (P<0.05). In this present study, at the moment boating activities have not significantly impact on the overall level of oil grease in the lake water. This may be due to the rapid mixing of water and low tourism activities at least during the sampling period. There were a positive correlation between oil grease and COD (r = 0.693) but having negative relationships with pH (r = -0.585) at P<0.05.

Nitrate

The concentration of nitrate was recorded to be in the range of 0.01 - 0.03 (mean 0.016 ± 0.01) and 0.03 - 0.05 (mean 0.042 ± 0.012) mgL⁻¹ respectively for wet and dry seasons. This study has shown that the overall level of nitrate is very low. Highest concentrations of nitrate of 0.05 mgL⁻¹ was recorded at SS05 (Island Resort near discharge point) in dry season.

The lowest concentration was obtained at Orang Asli Settlement Tiang River Middle Pathway (SS09) with values of 0.03 and 0.02 mgL⁻¹ respectively for wet and dry seasons. Statistical analysis using two ways ANOVA test indicates that nitrate has not differ significantly between sampling stations and but differ significantly on seasonal period (P<0.05). The lower levels of nitrate recorded in this study indicates that sources of pollution from agriculture is not yet significant for the lake aquatic environment especially in term of spatial measurement. There were a positive correlation between nitrate content and phosphate (r = 0.555) at P<0.05.

Phosphate

The concentration of phosphate was recorded to be in range of 0.39 - 0.84 (mean 0.621 ± 0.14) and 0.13 - 0.63 (mean 0.33 ± 0.19) mgL⁻¹ respectively for wet and dry season. The highest concentrations for phosphate was recorded at Mohd Shah Resort (SS03) with values of 0.84 mgL⁻¹ (wet season) and at Banding Island Southern Region (SS04) with values of 0.63 mgL⁻¹ (dry season).

As with nitrate, the low level of phosphate recorded overall in the lake water indicates that the lake did not yet expose to eutrophication. Similarly the lake seems not to receive high input of domestic waste water effluent since high concentrations of reactive phosphate is largely due to domestic waste water effluent enriched with phosphorus compounds [13].

Statistical analysis using two ways ANOVA test indicates that nitrate has no significant differences between sampling stations but differ significantly on seasonal period (P<0.05). There were a positive correlation at P<0.05 between phosphate and nitrate (r=0.555), phosphate and conductivity (r=0.590) and negative relationship with respect to DO value (r=-0.55).

Water Quality Index (WQI)

Water quality index (WQI) commonly used to aggregate data on water quality parameters at different times and in different places and to translate this information into a single value that determines the duration and spatial units involved [14]. The values of WQI at all sampling stations for wet and dry seasons were determined by using an

expression adopted by Malaysia Department of Environment based on six parameters as give by the following expression [15]:

$$WQI = 0.22*S_{I}DO + 0.19*S_{I}BOD + 0.16*S_{I}COD + 0.15*S_{I}AN + 0.16*S_{I}SS + 0.12*S_{I}PH$$

This study has shown that WQI ranges from 83.00-95.67 (wet season) and 76.67-94.01 (dry season), slightly better for wet season particularly for Mohd Shah Resort (SS03). Contrary to usual observation, the average water quality index in wet season with values of 90.49 was slightly higher than an average water quality index for dry season with values of 88.87. This implies that meteorological compartment such as total rainfall doesn't have negative influenced on water quality but instead improve environmental aquatic through dilution of several pollutants. It also indicates the absence of dirty runoff entering the lake during rain as shown by the levels of TSS. Water Quality Index classification was based on Interim National Water Quality Standard Malaysia which categorized water quality into five classes namely class I (WQI > 92.7), class II (WQI 76.6 – 92.7), class III (WQI 51.9 – 76.5), class IV (WQI 31.0 – 51.9) and class V (WQI < 31.0) based on beneficial use of the water. The calculated values of WQI for all sampling stations (an average of 3 depths) and their classes are shown in Table 3 for both seasons.

Table 3. Mean WQI status in Temenggor Lake

Station	Wet Season		Dr	y Season
-	WQI	INWQS CLASS	WQI	INWQS CLASS
SS01	83.00	II	87.41	II
SS02	91.18	II	92.36	I
SS03	83.59	II	76.67	II
SS04	86.04	II	84.03	II
SS05	88.55	II	91.18	II
SS06	91.72	II	91.43	II
SS07	87.50	II	85.44	II
SS08	91.90	II	86.81	II
SS09	93.73	I	91.49	II
SS10	93.88	I	90.95	II
SS11	95.67	I	90.96	II
SS12	95.48	I	94.01	I
SS13	94.12	I	92.59	II
Mean WQI	90.49	II	88.87	II

Table 3 shows that the overall class for Temenggor Lake is class II at both seasons. However with the WQI values very much close to class I, the water quality of the lake can be considered as very clean. Moreover there are stations that already registered as class I in both wet and dry seasons.

As shown in Table 4, the WQI of the lake water seems to change with depths particularly in wet season. While no appreciable change of class recorded in dry season, the water quality changes from class I for surface water to class II for middle level and eventually to class III for bottom layer. This may be due to turbulence cause by heavy rain and its effect on some parameters such as COD and BOD which plat a significant role in the calculation of WQI.

Table 4. Mean	WQI values	according to depth
---------------	------------	--------------------

Depth	Wet Season		Dry Season		
	WQI	INWQS CLASS	WQI	INWQS CLASS	
Surface	93.71	Ι	91.24	II	
Middle	90.63	II	87.57	II	
Bottom	75.93	III	81.36	II	

Conclusion

The water quality of Temenggor Lake can be considered as clean, in the order of Class II with some stations showing better quality of Class I. This study indicates quite significant seasonal influence of rainfalls on the lake aquatic ecosystems by improving the water quality through dilution effect on to several parameters namely suspended solid, ammoniacal nitrogen, nitrate and phosphate. The study has also shown that the present ecotourism activities (maybe because the intensity is not yet heavy) have minimal impact on water quality except for certain parameters namely ammoniacal nitrogen (mainly from sewage) and oil & grease (from restaurant and boating activities). Surprisingly, no significant increase in oil and grease level was recorded at transport jetty indicating less boating activities during the study. Considering future development of the lake as popular ecotourism destination, the water quality of the lake should be maintained or improved further. An effective management of domestic waste, sewage treatment (namely at Orang Asli settlements, resorts and food outlets), oil & grease (from boating activities), possible soil erosion from open-up of land and logging activities in the vicinity of the lake and organic pollutants (from aquaculture activities namely fish cages) should be planned and enforced. However for the sustainability of the lake, a more integrated approach to the management of the Temenggor Lake based on model of integrated water resource management concept, IWRM should be implemented by all stake holders.

Acknowledgement

This study has been funded by Research University Grants UKM-GUP-NBT-08-27-114 and UKM-OUP-NBT-29-152/2010. Authors are also thankful to Centre for Water Research and Analysis, FST, UKM (ALIR) and to Pulau Banding Rainforest Research Centre for valuable assistance during sampling and analysis.

References

- 1. Northern Malaysia Heritage Portal (2007). Belum Temenggor Rainforest Complex. Website Article http://northern.malaysianaturalheritage.com/?p=112 Online [29 Mei 2009].
- 2. Kawnsar-Ul-Yaqoob, Pandit, A. K., and Wani, A. S. (2008). Comparative Physicochemical Limnology of three lakes of Kashmir Himalaya. Proceedings of Taal 2007: *The 12th World Lake Conference*: 1922 1927.
- 3. Mathur, P., Agarwal, S. and Nag, M. (2008). Assessment of Physico-Chemical Characteristics and Suggested Restoration Measures for Pushkar Lake, Ajmer Rajasthan (India). Proceedings of Taal 2007: *The 12th World Lake Conference*: 1518 1529.
- 4. APHA (1998). Standard methods for the examination of water and wastewater (Edition 20th). Washington, DC: American Public Health Association.
- 5. Shafiul C., and Karen G. (2006). The Impact of Land use on Surface Water Quality in Queens County, New York. *Journal of Environmental Hydrology* 14 (15): 1 7.
- 6. McGinley, P and Turyk, N. (2003). Assessment of Water Quality, Sediment, Groundwater, and Tributaries of Easton Lake, Adams County, Wisconsin. Draft Report to the DNR: 1 40.

- 7. Cane, F., Hoxha, B., and Avdolli, M. (2010). Water Quality in Carstic Lake, Albania. *Natura Montenegrina Podgorica* 9 (3): 349 355.
- 8. Sisodia, R. and Moundiotiya, C. (2006). Assessment of the Water Quality Index of Wetland Kalakho Lake, Rajasthan, India. *Journal of Environmental Hydrology* 14 (23): 1 11.
- 9. Strauss, E. A. (2000). The Effects Of Organic Carbon And Nitrogen Availability On Nitrification Rates In Stream Sediments. Department of Biological Sciences. University Notre Dame, Indiana
- 10. Ooshaksaraie, L., Basri, N. E. A., Bakar, A. A., and Maulud, K. N. A. (2009). Erosion and Sediment Control Plan to Minimize Impact of Hosuing Construction Activities on Water Resource in Malaysia. *European Journal of Scientific Research* 33 (3): 461 470.
- 11. Sharma, R., and Capoor, A. (2010). Seasonal Variations in Physical, Chemical and Biological Parameters of Lake Water of Patna Bird Sanctuary in Relation to Fish Productivity. *World Applied Sciences Journal* 8 (1): 129 132.
- 12. Shuhaimi-Othman, M., Ahmad, A., Mushrifah, I., and Lim, E. C (2007). Seasonal Influence on Water Quality and Heavy Metals Concentration in Tasik Chini, Peninsular Malaysia. Proceedings of Taal 12th World Lake Conference: 300 303.
- 13. Puri, P. J., Yenkie, M. K. N., Battalwar, D. G., Gandhare, N. V., and Dhanorkar, D. B. (2010). Study and Interpretation of Physico-Chemical Characteristic of Lake Water Quality in Nagpur City (India). *Rasayan J. Chemistry* 3 (4): 800 810.
- 14. Jawad Alobaidy, A, H, Abid, H. S., and Maulood, B. K. (2010). Application of Water Quality Index for Assessment of Dokan Lake Ecosystem, Kurdistan Region, Iraq. *Journal of Water Resource and Protection* (2): 792 798.
- 15. Norhayati,M. (1981). Indices for Water Quality Assessment in a River, MSc Thesis, Asian Institute of Technology, Bangkok, Thailand.



ANALISIS KROMATOGRAFI GAS x KROMATOGRAFI GAS– SPEKTROMETRI JISIM MASA-PENERBANGAN MINYAK PATI *GLOBBA PATENS* VAR. *PATENS*

(Analysis of Gas Chromatography x Gas Chromatography–Time-of-Flight Mass Spectrometry of Essential Oils from *Globba patens* var. *patens*)

A. Masila¹, W.A. Yaacob^{1*}, I. Nazlina²

¹Pusat Pengajian Sains Kimia dan Teknologi Makanan, ²Pusat Pengajian Biosains dan Bioteknologi, Fakulti Sains dan Teknologi, Universiti Kebangsaan Malaysia, 43600 Bangi, Selangor, Malaysia

*Corresponding author:wanyaa@ukm.my

Abstrak

Minyak pati daun, batang, dan rizom *Globba patens* var. *patens* (Zingiberaceae) yang diperolehi dengan penyulingan-air adalah 0.0021%, sedikit, dan juga sedikit. Komponen kimia mereka dan peratus masing-masing ditentukan dari analisis dengan kromatografi gas-spektrometri jisim masa-penerbangan (KGxKG-SJMP). Terpena adalah penyumbang utama minyak dengan rizom memberikan amaun terendah 30.56%. Sebatian utama dalam minyak daun adalah β-tujena (11.45%, 1), β-selinena (7.82%, 2), dan α-pinena (5.27%, 3); batang, β-pinena (2.77%, 4), mirtenol (2.30%, 5), dan β-elemena/ledena oksida (2.23%, 6/7); rizom, kariofilena oksida (2.74%, 8), *D*-limonena (2.71%, 9), dan 7-(1-metiletilidena)-bisiklo[4.1.0]heptana (1.93%, 10).

Kata kunci: Globba patens var. patens, minyak pati, KGxKG-SJMP

Abstract

Leaf, stem, and rhizome essential oils of *Globba patens* var. *patens* (Zingiberaceae) were obtained by hydrodistillation at 0.0021%, in small quantity, and also small quantity. Their chemical components and each percentage were determined from analysis by using gas chromatographyxgas chromatography—time-of-flight mass spectrometry (GCxGC-TOFMS). Terpenes were the oils major contributor with the rhizome gave the lowest amount of 30.56%. Major compounds in the leaf oil were β -thujene (11.45%, 1), β -selinene (7.82%, 2), and α -pinene (5.27%, 3); the stem, β -pinene (2.77%, 4), myrtenol (2.30%, 5), and β -elemene/ledene oxide (2.23%, 6/7); the rhizome, caryophyllene oxide (2.74%, 8), *D*-limonene (2.71%, 9), and 7-(1-methylethylidene)-bicyclo[4.1.0]heptane (1.93%, 10).

Keywords: Globba patens var. patens, essential oil, GCxGC-TOFMS

Pengenalan

Wilayah Indo-Malaya merupakan pusat kepelbagaian Zingiberaceae. Dari 50 genus dan 1500 spesies dunia, sekurang-kurangnya 20 genus dan 300 spesies terdapat di Malaysia [1]. Zingiberaceae merupakan keluarga terbesar order Zingiberales yang pada amnya terdiri dari sub-famili Zingiberoideae dan Costoideae. Sub-famili Zingiberoideae mengandungi kumpulan Alpinae, Hedychieae, dan Globbeae. Globbeae berbeza dari Alpinae dan Hedychieae dari segi ia hanya mengandungi genus tunggal *Globba* [2]. Kebanyakan *Globba* tumbuh bertaburan di kawasan hutan tropika dan sub-tropika terutamanya di kawasan lembah dan lereng bukit hutan tanah pamah yang gembur [3]. Kini terdapat 100 spesies *Globba* dunia [4] dan 33 spesies telah direkodkan di Malaysia [3]. Tumbuhan *Globba* berguna bagi merawat tekanan darah tinggi, gonorea, reumatism, cacing, sakit perut, diarea, disenteri, dan demam, serta dalam pembuatan losyen [5]. *Globba patens* var. *patens* mempunyai bunga yang sangat menarik dan yang menjadi penyebar tumbuhan ini ke kawasan yang lebih jauh. Bila bunga *Globba patens* var. *patens* mencecah

Masila et al: ANALISIS KROMATOGRAFI GASxKROMATOGRAFI GAS-SPEKTROMETRI JISIM MASA-PENERBANGAN MINYAK PATI GLOBBA PATENS VAR. PATENS

bumi, rumpun baru akan muncul pada jarak sehingga 120 cm dari rumpun induk. *Globba* merupakan tumbuhan herba bersaiz kecil, tinggi rata-rata melebihi 50 cm, dengan bunga muncul dari pucuk. Kajian ini bertujuan menganalisis komposisi kimia minyak pati *Globba patens* var. *patens* dari bahagian daun, batang, dan rizom menggunakan kromatografi gasxkromatografi gas-spektrometri jisim masa-penerbangan.

Bahan dan Kaedah

Bahan tumbuhan

Daun, batang, dan rizom segar *Globba patens* var. *patens* diambil dari Sungai Tekala, Semenyih, Selangor. Nama spesies tumbuhan disahkan oleh En. Shamsul Khamis dari Institut Biosains, Universiti Putra Malaysia.

Penyulingan-air minyak pati

Bahagian daun (657 g), batang (855 g), dan rizom (450 g) tumbuhan *Globba patens* var. *patens* dipotong, dimasukkan air, dan dikisar. Buburan disuling 5-6 jam dengan alat-radas jenis-Clevenger. Hasil penyulingan dikering dengan natrium sulfat kontang memberikan 14 mg minyak daun (0.0021%) serta amaun sangat sedikit minyak batang dan rizom sehingga tidak boleh disedut keluar dengan pipet. Minyak yang terjerap pada garam pengering dibilas dengan diklorometana dan larutannya disimpan dalam botol kecil tertutup pada -18°C sebelum dianalisis.

Kromatografi gas×kromatografi gas-spektrometri jisim masa-penerbangan (KGxKG-SJMP)

Minyak pati dianalisis dengan alat KG×KG Agilent 6890N yang dilengkapi pengmodulasi terma LECO. Dua turus yang diguna adalah Rtx-5MS (30 m, diameter dalam 0.25 mm, ketebalan filem 0.1 μm) dan Rtx-17 (1 m, diameter dalam 0.1 mm, ketebalan filem 0.1 μm). Program suhu ketuhar yang diguna: bagi Rtx-5MS suhu mula 50°C selama 2 min, kemudian ditingkat pada 5°C/min ke 240°C, dan kekal selama 5 min manakala bagi Rtx-17 suhu mula 55°C selama 2 min, kemudian ditingkat pada 5°C/min ke 245°C, dan kekal selama 5 min. Suhu suntikan 200°C; saiz suntikan 1 μl dengan nisbah pemecahan 50:1; gas pembawa He pada kadar aliran 1 ml/min dan tekanan 20 psi; suhu pengmodulasi 30°C luar-set dari oven utama; frekuensi modulasi 4 saat dengan masa denyut panas 0.8 saat.

Analisis spektrometri jisim (SJ) dijalankan dengan pergandingan kepada SJ LECO Pegasus 4D–Masa-Penerbangan. Parameter operasi: hentaman elektron pada 70 eV; suhu sumber 200°C; julat imbasan jisim 50-500 U; kadar perolehan 200 spektrum/s. Komponen minyak dikenalpasti menerusi perbandingan spektrum jisim mereka dengan spektrum jisim dari pengkalan data perisian NIST versi 2.0. Spektrum dengan kesamaan, kebalikan, dan kebarangkalian melebihi 800, 800, dan 1000 dianggap mempunyai padanan yang baik [6].

Hasil dan Perbincangan

Peratus hasil minyak pati

Peratus minyak dari daun *Globba patens* var. *patens* adalah 0.0021% manakala amaun minyak batang dan rizom adalah terlalu sedikit yang hanya terjerap pada natrium sulfat kontang tanpa boleh dipipet keluar.

Analisis komposisi minyak pati

Sebanyak 108 sebatian berbeza telah dikesan dari ketiga-tiga minyak seperti yang tersenarai dalam Jadual 1. Terpena menyumbang sejumlah 103 sebatian manakala selebihnya bukan terpena. Daun adalah penyumbang utama terpena (55.30%) diikuti batang (40.36%) dan rizom (30.56%). Jumlah peratus kesemua sebatian dalam minyak daun adalah paling tinggi (55.49%) diikuti batang (40.50%) dan rizom (32.53%). Komposisi hidrokarbon monoterpena minyak daun, batang, dan rizom adalah 18.76, 8.12, dan 9.51%; monoterpena beroksigen 6.68, 12.07, dan 8.92%; hidrokarbon seskuiterpena 25.55, 13.32, dan 5.75%; seskuiterpena beroksigen 4.31, 6.83, dan 6.23%; hidrokarbon diterpena 0.00, 0.00, dan 0.15%; diterpena beroksigen 0.00, 0.02, dan 0.003%; serta bukan terpena 0.19, 0.14, dan 1.97% (Rajah 1). Hanya daun yang didominasi seskuiterpena (jumlah 29.86%) berbanding monoterpena 25.44% (tiada diterpena dan ada 0.19% bukan terpena).

Jadual 1. Komposisi terpena dan bukan terpena yang terdapat dalam minyak pati daun, batang, dan rizom segar $Globba\ patens$ var. patens

Bil	Nama	Nombor Daftar CAS	Masa Penahanan ^a (s)	Minyak Daun (%)	Minyak Batang (%)	Minyak Rizom (%)
Hidro	karbon monoterpena		(5)	(/0/	(/0/	(/0/
1	<i>p</i> -Simenena	1195-32-0	715, 0.760	_	0.07	0.69
2	Tuja-2,4(10)-diena	36262-09-6	432, 1.064	-	0.09	_
3	β-Tujena	28634-89-1	455, 1.184	11.45	-	_
4	Terpinolena	586-62-9	435, 1.952	-	-	1.46
5	α-Felandrena	99-83-2	540, 1.416	0.21	-	_
6	β-cis-Osimena	3338-55-4	525, 1.328	0.28	-	1.79
7	Limonena	138-86-3	505, 1.264	1.30	0.69	-
8	β-Pinena	127-91-3	450, 1.192	-	2.77	1.62
9	α-Pinena	80-56-8	415, 1.008	5.27	_	_
10	Kamfena	79-92-5	430, 1.016	0.25	0.59	-
11	D-Limonena	5989-27-5	405, 0.840	-	-	2.71
12	γ-Terpinena	99-85-4	420, 0.832	-	-	0.40
13	β-Mirsena	123-35-3	465, 1.136	-	0.65	0.84
14	α-Terpinena	99-86-5	495, 1.208	-	0.03	-
15	α-Osimena	502-99-8	525, 1.336	-	0.55	-
16	Tujena	58037-87-9	410, 1.000	-	0.59	-
17	β-trans-Osimena	3779-61-1	515, 1.296	-	0.74	-
18	2,7-Dimetil-(3Z)-3-Okten-5-una	28935-76-4	415, 1.032	-	1.35	-
		Pera	tus sub-jumlah	18.76	8.12	9.51
Mono	terpena beroksigen					
19	Pinokarvon	30460-92-5	470, 2.064 705, 2.768	-	0.43	1.14
20	Karvon	99-49-0	510, 2.040	-	-	0.15
21	Mirtenal	564-94-3	770, 2.624	0.59	2.19	-
22	Karvakrol	499-75-2	935, 1.888	0.44	-	-
23	Perilal	2111-75-3	895, 2.040	-	0.06	-
24	<i>p</i> -Simen-8-ol	1197-01-9	750, 2.600	-	0.07	-
25	3(10)-Karena-4-ol	1753-35-1	460, 2.016	-	-	0.54
26	β-Siklositral	432-25-7	815, 2.216	-	0.07	-
27	trans-Karveol	1197-07-5	500, 2.024	-	-	0.52
28	Mirtenol	515-00-4	770, 2.336	1.65	2.30	1.20
29	3-Pinanon	18358-53-7	730, 2.624	1.41	0.38	-
30	l-Pinokarveol	547-61-5	665, 2.224	0.30	1.06	-
31	cis-Karveol	1197-06-4	810, 2.136	-	0.02	-
32	3-Pinanon	15358-88-0	730, 2.728	-	1.33	-

Masila et al: ANALISIS KROMATOGRAFI GASxKROMATOGRAFI GAS–SPEKTROMETRI JISIM MASA-PENERBANGAN MINYAK PATI *GLOBBA PATENS* VAR. *PATENS*

33						
	α-Sitral	141-27-5	890, 1.832	-	0.04	-
34	(S)-cis-Verbenol	18881-04-4	675, 2.192	-	0.08	-
35	<i>l</i> -Kamfor	464-48-2	675, 2.496	-	0.06	-
36	Mirtanal	4764-14-1	745, 2.456	-	0.05	-
37	Borneol	507-70-0	475, 2.168	-	-	1.75
38	D-Fenchol	2217-02-9	455, 1.976	-	-	0.91
39	Linalol	78-70-6	595, 1.688	1.63	-	-
40	α-Terpineol	98-55-5	760, 2.232 490, 2.024	0.66	1.35	1.20
41	Eukaliptol	470-82-6	510, 1.376	_	0.27	1.31
42	cis-4-Tujanol	15537-55-0	555, 1.488	_	0.04	-
43	trans-β-Terpineol	7299-41-4	635, 1.984	_	0.05	_
44	l-Borneol	464-45-9	695, 2.304	_	0.13	_
45	ekso-Fenchol	22627-95-8	620, 1.864	_	0.35	_
46	Lavandulol	498-16-8	710, 2.248	_	0.03	_
47	Mirtanol	514-99-8	870, 1.928	_	0.12	_
48	trans-Geraniol	106-24-1	865, 1.800	_	0.06	_
49	Kamfena hidrat	465-31-6	680, 2.272	_	0.15	_
50	cis-Geraniol	106-25-2	825, 1.896	_	0.03	_
51	Bingpian	10385-78-1	715, 2.496	_	0.87	0.2
52	4-Terpineol	562-74-3	735, 2.248	_	0.48	-
32	4 Terpineor		us sub-jumlah	6.68	12.07	8.92
Hidro	karbon seskuiterpena	Terac	us sub-juman	0.00	12.07	0.72
53	α-Kalakorena	21391-99-1	1190, 1.472	_	0.02	_
54	Kalamenena	483-77-2	1170, 1.464	_	0.14	-
55	α-Panasinsena	56633-28-4	615, 2.184	_	-	0.77
56	Helmintogermakrena	75023-40-4	1155, 1.408	0.54	-	_
57	<i>cis</i> -β-Farnesena	28973-97-9	1105, 1.344	-	1.11	-
51	cis p i ainesena		1105, 1.544			
	•			_	0.32	1.64
58 59	α-Kopaena	3856-25-5	1025, 1.320	-	0.32	1.64 0.63
58	α-Kopaena Chamigrena		1025, 1.320 670, 2.520			
58 59	α-Kopaena	3856-25-5 18431-82-8	1025, 1.320 670, 2.520 560, 1.976	-		0.63
58 59 60	α-Kopaena Chamigrena β-Elemena Farnesena 2-Isopropenil-4a,8-dimetil- 1,2,3,4,4a,5,6,7-	3856-25-5 18431-82-8 33880-83-0	1025, 1.320 670, 2.520	-		0.63
58 59 60 61 62	α-Kopaena Chamigrena β-Elemena Farnesena 2-Isopropenil-4a,8-dimetil- 1,2,3,4,4a,5,6,7- oktahidronaftalena	3856-25-5 18431-82-8 33880-83-0 502-61-4 103827-22-1	1025, 1.320 670, 2.520 560, 1.976 115, 1.296 1125, 1.368	- - 3.82 0.99	- - 0.95	0.63 0.44
58 59 60 61 62	α-Kopaena Chamigrena β-Elemena Farnesena 2-Isopropenil-4a,8-dimetil- 1,2,3,4,4a,5,6,7- oktahidronaftalena cis,trans-α-Farnesena	3856-25-5 18431-82-8 33880-83-0 502-61-4 103827-22-1 26560-14-5	1025, 1.320 670, 2.520 560, 1.976 115, 1.296 1125, 1.368	3.82 0.99	- - 0.95	0.63 0.44
58 59 60 61 62 63 64	α-Kopaena Chamigrena β-Elemena Farnesena 2-Isopropenil-4a,8-dimetil-1,2,3,4,4a,5,6,7- oktahidronaftalena cis,trans-α-Farnesena β-Selinena	3856-25-5 18431-82-8 33880-83-0 502-61-4 103827-22-1 26560-14-5 17066-67-0	1025, 1.320 670, 2.520 560, 1.976 115, 1.296 1125, 1.368 1140, 1.328 1145, 1.448	3.82 0.99 2.87 7.82	- - 0.95 0.83	0.63 0.44 -
58 59 60 61 62 63 64 65	α-Kopaena Chamigrena β-Elemena Farnesena 2-Isopropenil-4a,8-dimetil- 1,2,3,4,4a,5,6,7- oktahidronaftalena cis,trans-α-Farnesena β-Selinena Humulena	3856-25-5 18431-82-8 33880-83-0 502-61-4 103827-22-1 26560-14-5 17066-67-0 6753-98-6	1025, 1.320 670, 2.520 560, 1.976 115, 1.296 1125, 1.368 1140, 1.328 1145, 1.448 1105, 1.424	3.82 0.99 2.87 7.82 0.80	- - 0.95	0.63 0.44 -
58 59 60 61 62 63 64 65 66	α-Kopaena Chamigrena β-Elemena Farnesena 2-Isopropenil-4a,8-dimetil-1,2,3,4,4a,5,6,7- oktahidronaftalena cis,trans-α-Farnesena β-Selinena Humulena β-Farnesena	3856-25-5 18431-82-8 33880-83-0 502-61-4 103827-22-1 26560-14-5 17066-67-0 6753-98-6 18794-84-8	1025, 1.320 670, 2.520 560, 1.976 115, 1.296 1125, 1.368 1140, 1.328 1145, 1.448 1105, 1.424 1105, 1.312	3.82 0.99 2.87 7.82 0.80 2.52	- - 0.95 0.83 - 0.81	0.63 0.44 -
58 59 60 61 62 63 64 65 66 67	α-Kopaena Chamigrena β-Elemena Farnesena 2-Isopropenil-4a,8-dimetil-1,2,3,4,4a,5,6,7- oktahidronaftalena cis,trans-α-Farnesena β-Selinena Humulena β-Farnesena 1-Etenil-1-metil-2,4-bis(1-metiletilidena)sikloheks-ana	3856-25-5 18431-82-8 33880-83-0 502-61-4 103827-22-1 26560-14-5 17066-67-0 6753-98-6 18794-84-8 339154-91-5	1025, 1.320 670, 2.520 560, 1.976 115, 1.296 1125, 1.368 1140, 1.328 1145, 1.448 1105, 1.424 1105, 1.312 1200, 1.440	3.82 0.99 2.87 7.82 0.80 2.52 1.13	- - 0.95 0.83 - 0.81 - 0.37	0.63 0.44 - 0.63
58 59 60 61 62 63 64 65 66 67 68	α-Kopaena Chamigrena β-Elemena Farnesena 2-Isopropenil-4a,8-dimetil-1,2,3,4,4a,5,6,7- oktahidronaftalena cis,trans-α-Farnesena β-Selinena Humulena β-Farnesena 1-Etenil-1-metil-2,4-bis(1- metiletilidena)sikloheks-ana Kariofilena	3856-25-5 18431-82-8 33880-83-0 502-61-4 103827-22-1 26560-14-5 17066-67-0 6753-98-6 18794-84-8 339154-91-5 87-44-5	1025, 1.320 670, 2.520 560, 1.976 115, 1.296 1125, 1.368 1140, 1.328 1145, 1.448 1105, 1.424 1105, 1.312 1200, 1.440	3.82 0.99 2.87 7.82 0.80 2.52 1.13 2.95	- - 0.95 0.83 - 0.81	0.63 0.44 - 0.63 - - - - 0.37
58 59 60 61 62 63 64 65 66 67 68 69	α-Kopaena Chamigrena β-Elemena Farnesena 2-Isopropenil-4a,8-dimetil- 1,2,3,4,4a,5,6,7- oktahidronaftalena cis,trans-α-Farnesena β-Selinena Humulena β-Farnesena 1-Etenil-1-metil-2,4-bis(1- metiletilidena)sikloheks-ana Kariofilena Viridiflorena	3856-25-5 18431-82-8 33880-83-0 502-61-4 103827-22-1 26560-14-5 17066-67-0 6753-98-6 18794-84-8 339154-91-5 87-44-5 21747-46-6	1025, 1.320 670, 2.520 560, 1.976 115, 1.296 1125, 1.368 1140, 1.328 1145, 1.448 1105, 1.424 1105, 1.312 1200, 1.440 1070, 1.408 690, 2.560	3.82 0.99 2.87 7.82 0.80 2.52 1.13	- - 0.95 0.83 - 0.81 - 0.37	0.63 0.44 - 0.63
58 59 60 61 62 63 64 65 66 67 68 69 70	α-Kopaena Chamigrena β-Elemena Farnesena 2-Isopropenil-4a,8-dimetil- 1,2,3,4,4a,5,6,7- oktahidronaftalena cis,trans-α-Farnesena β-Selinena Humulena β-Farnesena 1-Etenil-1-metil-2,4-bis(1- metiletilidena)sikloheks-ana Kariofilena Viridiflorena α-Kubebena	3856-25-5 18431-82-8 33880-83-0 502-61-4 103827-22-1 26560-14-5 17066-67-0 6753-98-6 18794-84-8 339154-91-5 87-44-5 21747-46-6 17699-14-8	1025, 1.320 670, 2.520 560, 1.976 115, 1.296 1125, 1.368 1140, 1.328 1145, 1.448 1105, 1.424 1105, 1.312 1200, 1.440 1070, 1.408 690, 2.560 990, 1.304	3.82 0.99 2.87 7.82 0.80 2.52 1.13 2.95	- - 0.95 0.83 - 0.81 - 0.37	0.63 0.44 - 0.63 - - - - 0.37 0.27
58 59 60 61 62 63 64 65 66 67 68 69	α-Kopaena Chamigrena β-Elemena Farnesena 2-Isopropenil-4a,8-dimetil- 1,2,3,4,4a,5,6,7- oktahidronaftalena cis,trans-α-Farnesena β-Selinena Humulena β-Farnesena 1-Etenil-1-metil-2,4-bis(1- metiletilidena)sikloheks-ana Kariofilena Viridiflorena	3856-25-5 18431-82-8 33880-83-0 502-61-4 103827-22-1 26560-14-5 17066-67-0 6753-98-6 18794-84-8 339154-91-5 87-44-5 21747-46-6	1025, 1.320 670, 2.520 560, 1.976 115, 1.296 1125, 1.368 1140, 1.328 1145, 1.448 1105, 1.424 1105, 1.312 1200, 1.440 1070, 1.408 690, 2.560	3.82 0.99 2.87 7.82 0.80 2.52 1.13 2.95	- - 0.95 0.83 - 0.81 - 0.37	0.63 0.44 - 0.63 - - - - 0.37

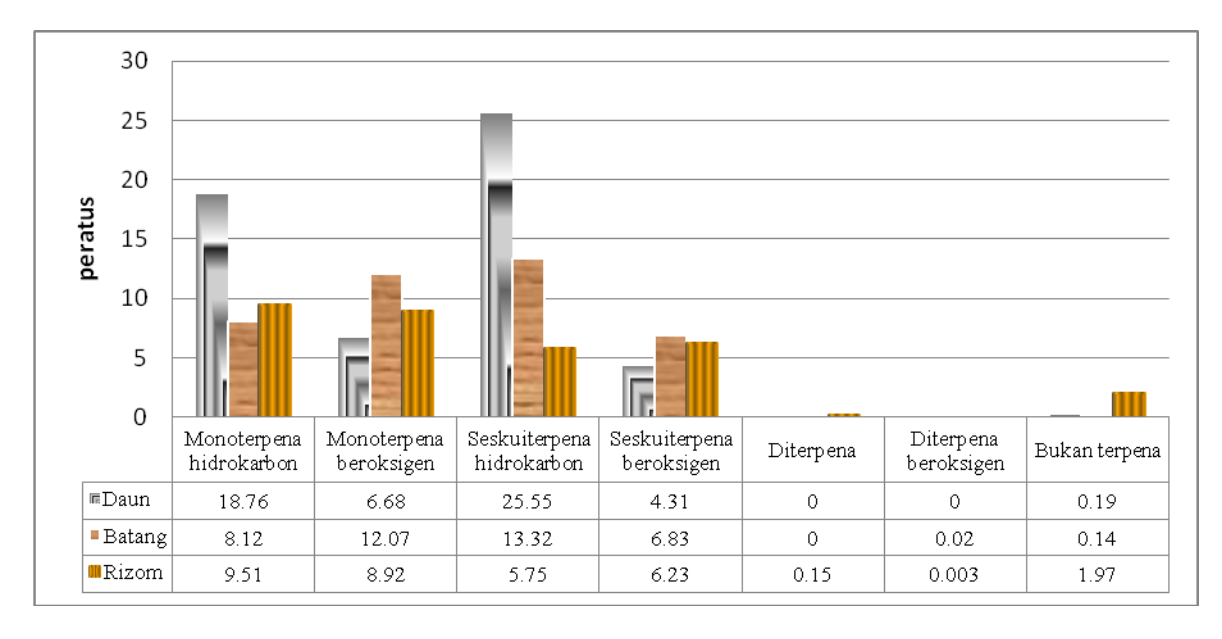
73	Sativena	3650-28-0	1095, 1.344	-	0.24	-
74	Aloaromadendrena	25246-27-9	1180, 1.368	-	0.12	-
75	Santalena	512-61-8	1070, 1.296	-	0.06	-
76	1-Etenil-1-metil-2,4-bis(1-metiletenil)sikloheksana	110823-68-2	1150, 1.040	-	0.13	-
77	β-Elemena	515-13-9	1040, 1.368	2.11	2.23	-
78	α-Gurjunena	489-40-7	1185, 1.352	-	1.54	-
79	γ-Murolena	30021-74-0	1135, 1.384	-	0.95	-
80	δ-Elemena	20307-84-0	975, 1.344	-	0.10	-
81	Aromadendrena	489-39-4	1115, 1.352	-	1.08	-
82	γ-Elemena	30824-67-0	1200, 1.464	-	0.44	-
83	Dekahidro-1,1,7-trimetil-4- metilena-1H-	109119-91-7	1095, 1.304	-	0.43	-
84	sikliprop[e]azulena Isokariofilena	118-65-0	1060, 1.344	_	0.20	_
85	Farnesana	3891-98-3	1110, 1.016	_	0.20	-
65	Particsana		atus sub-jumlah	25.55	13.32	5.75
Secknit	erpena beroksigen	1 (1)	atus sub-juman	23.33	13.32	3.73
86	Spatulenol	6750-60-3	1255, 1.472	_	0.58	_
87	6-Isopropenil-4,8a-dimetil-	726134-57-2	1325, 1.536	_	0.34	_
	1,2,3,5,6,7,8,8a- oktahidronaftalen-2-ol				0.54	
88	Kariofilena oksida	1139-30-6	640, 2.336	0.86	-	2.74
89	Humulena oksida II	19888-34-7	650, 2.360	-	-	0.58
90	Ledena oksida	882187-44-2	1220, 1.512	-	2.23	1.07
91	trans,trans-Farnesal	502-67-0	1330, 1.408	-	0.02	0.01
92	Farneson	19317-11-4	1315, 1.392	-	0.01	-
93	β-Spatulenol	77171-55-2	1265, 1.528	-	0.78	-
94	Dehidronerolidol	2387-68-0	1185, 1.392	-	0.18	-
95	d-Ledol	577-27-5	1240, 1.416	-	0.54	-
96	Kubenol	21284-22-0	1255, 1.432	-	0.08	-
97	trans-Nerolidol	40716-66-3	1205, 1.344	1.95	1.64	-
98	(±)-Globulol	51371-47-2	675, 2.568	1.50	-	1.81
99	<i>d</i> -Nerolidol	142-50-7	735, 2.632	-	-	0.02
100	τ-Murolol	19912-62-0	1265, 1.464	-	0.37	-
101	(±)-Nerolidol	7212-44-4	1505, 1.536	-	0.06	-
		Pera	atus sub-jumlah	4.31	6.83	6.23
Hidrok	arbon diterpena					
102	Fitan	638-36-8	620, 1.968	-	-	0.15
		Pera	atus sub-jumlah	0.00	0.00	0.15
Diterpe	ena beroksigen					
103	Isofitol	505-32-8	1450, 1.184	-	0.02	0.003
		Per	atus sub-jumlah	0.00	0.02	0.003

Masila et al: ANALISIS KROMATOGRAFI GASxKROMATOGRAFI GAS-SPEKTROMETRI JISIM MASA-PENERBANGAN MINYAK PATI GLOBBA PATENS VAR. PATENS

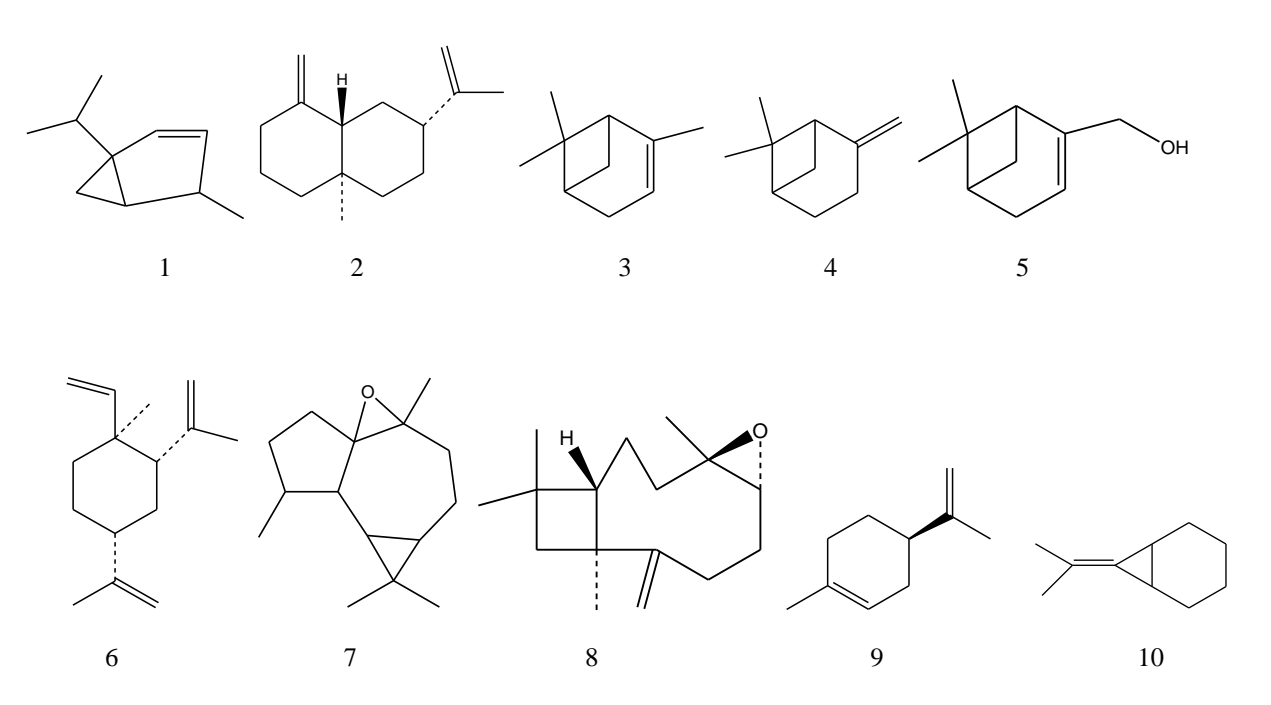
Bukan terpena									
104	o-Simena	527-84-4	505, 1.368	0.19	0.03	-			
105	7-(1-Metiletilidena)- bisiklo[4.1.0]heptana	53282-47-6	365, 0.832	-	-	1.97			
106	o-Menta-2(8),3-diena	99805-90-0	580, 1.568	-	0.07	-			
107	α-Kamfolenal	4501-58-0	640, 2.048	-	0.03	-			
108	cis-4-Dekenal	21662-09-9	760, 2.096	-	0.01	-			
		Peratus sub-jumlah		0.19	0.14	1.97			
			Peratus jumlah	55.49	40.50	32.53			

a = Masa penahanan pertama dan kedua adalah bagi turus primer dan sekunder

Struktur 10 sebatian utama *Globba patens* var. *patens* ditunjukkan dalam Rajah 2. Tiga sebatian utama dalam daun seperti yang dapat dilihat dalam Jadual 1 adalah β-tujena (1) (11.45%) diikuti β-selinena (2) (7.82%) dan α-pinena (3) (5.27%); batang, β-pinena (4) (2.77%), mirtenol (5) (2.30%), β-elemena (6) (2.23%), dan ledena oksida (7) (2.23%); rizom, kariofilena oksida (8) (2.74%), *D*-limonena (9) (2.71%), dan 7-(1-metiletilidena)-bisiklo[4.1.0]heptana (10) (1.93%). Kariofilena oksida (8) yang merupakan sebatian paling utama dalam rizom *G. patens* var. *patens* juga adalah sebatian paling utama (21.8%) dalam seluruh tumbuhan *G. ophioglossa* dan kedua utama (10.3%; paling utama kariofilena 31.7%) dalam seluruh tumbuhan *G. schomburgkii* [7]. Kariofilena juga didapati paling utama (19.3-24.2%) dalam *G. ophioglossa*, *G. cenua*, dan *G. marantina* [8].



Rajah 1. Perbandingan peratusan setiap kumpulan terpena dan bukan terpena dalam minyak daun, batang, dan rizom segar *Globba patens* var. *patens*



Rajah 2. Sepuluh sebatian dari tiga sebatian berperatus tertinggi dalam masing-masing daun, batang, dan rizom *Globba patens* var. *patens*

Analisis mendapati bahawa tiga sebatian utama dalam daun, batang, dan rizom *Globba patens* var. *patens* adalah masing-masing berbeza. Seperti yang dapat dilihat dalam Jadual 1, ketiga-tiga sebatian utama yang terdapat dalam daun iaitu β-tujena (1), β-selinena (2), dan α-pinena (3) langsung tidak wujud dalam batang dan rizom. β-Pinena (4) dan ledena oksida (7) sebagai dua sebatian utama batang wujud dalam rizom pada kedudukan ke-8 (1.62%) dan ke-14 (1.07%) tetapi tidak wujud dalam daun; mirtenol (5) pula wujud dalam daun dan rizom pada kedudukan ke-10 dan ke-11 (1.65 dan 1.20%); β-elemena (6) didapati wujud dalam daun pada kedudukan ke-10 (2.11%) tetapi tidak wujud dalam rizom. Bagi tiga sebatian utama rizom pula, kariofilena oksida (8) didapati wujud dalam daun pada kedudukan ke-16 (0.86%) tetapi tidak wujud dalam batang; *D*-limonena (9) dan 7-(1-metiletilidena)-bisiklo[4.1.0]heptana (10) tidak wujud dalam daun dan batang.

Kesimpulan

Hidrokarbon monoterpena dan seskuiterpena (18.95%) adalah terpena utama dalam minyak pati daun segar *Globba* patens var. patens. Sebatian utama dalam minyak daun adalah β -tujena (1), β -selinena (2), dan α -pinena (3). β -Pinena (4) adalah sebatian utama dalam batang diikuti mirtenol (5) dan kemudian β -elemena/ledena oksida (6/7). Dalam rizom pula kariofilena oksida (8) adalah komponen utama diikuti *D*-limonena (9), dan kemudian 7-(1-metiletilidena)-bisiklo[4.1.0]heptana (10).

Penghargaan

Pengarang pertama ingin mengucapkan terima kasih kepada Bahagian Tajaan dan Biasiswa, Kementerian Pelajaran Malaysia kerana memberi peluang bagi mengikuti pengajian Sarjana Sains dalam Kimia di Universiti Kebangsaan Malaysia. Kami juga ingin merakamkan penghargaan dan ucapan terima kasih kepada Kementerian Pengajian Tinggi Malaysia dan Universiti Kebangsaan Malaysia kerana pemberian peruntukan bagi membiayai kajian ini di bawah Skim Geran Penyelidikan Fundamental UKM-ST-06-FRGS0110-2009 dan Dana Operasi Universiti Penyelidikan UKM-OUP-KPB-31-156/2011.

Masila et al: ANALISIS KROMATOGRAFI GASxKROMATOGRAFI GAS-SPEKTROMETRI JISIM MASA-PENERBANGAN MINYAK PATI GLOBBA PATENS VAR. PATENS

Rujukan

- 1. Habsah, M., Ali, A.M., Lajis, N.H., Sukari, M.A., Yap, Y.H., Kikuzaki, H., Nakatani, N. 2005. Antitumor promoting and cytotoxic constituents of *Etlingera elatior*. *Malaysian Journal of Medical Sciences*. 12(1): 6-12.
- 2. Zakaria, M.B. & Ibrahim, H. 1986. Phytochemical screening of some Malaysian species of Zingiberaceae. *Malaysian Journal of Science* 8: 125-128.
- 3. Takano, A., Hernawati & Tamin, R. 2001. Notes on *Globba* Linnaeus in Sumatra, W. Malaysia & Borneo: a new record of *Globba brachyanthera* var. *rubra* in Sumatra. *Folia Malaysiana* 2(1): 25-34.
- 4. Larsen, K., Ibrahim, H., Khaw, S.H. & Saw, L.G. 1999. *Gingers of Peninsular Malaysia and Singapore*. Kota Kinabalu: Natural History Publications (Borneo) Sdn. Bhd.
- 5. Ibrahim, H. & Rahman, A.A. 1988. Several ginger plants (Zingiberaceae) of potential value. *Proceeding of the Seminar on Malaysian Traditional Medicine*, hlm. 159-161. Kuala Lumpur: IPT, University Malaya.
- Dallüge, J., van Stee, L.L.P., Xu, X., Williams, J., Beens, J., Vreuls, R.J.J. & Brinkman, U.A.T. 2002. Unravelling the composition of very complex samples by comprehensive gas chromatography coupled to time-of-flight mass spectrometry. cigarette smoke. *Journal of Chromatography*, A 974(1-2): 169-184.
- 7. Raj, G., George, V., Dan, M. & Sethuraman, M.G. 2010. Essential oil composition of *Globba schomburgkii* Hook. f. and *Globba ophioglossa* Wight. *Journal of Essential Oil Research* 22(3), 220-222.
- 8. Menon, A.N. & Dan, M. 2009. Chemical composition of essential oils of *Globba* species from south India. *Journal of Essential Oil Research* 21(1), 59-60.



SPECTROPHOTOMETRIC DETERMINATION OF ORGANOPHOSPHATE INSECTICIDE (CHLORPYRIFOS) BASED ON DIAZOTISATION WITH ANTHRANILIC ACID

(Penentuan Spektrofotometri Racun Serangga Organofosfat (Chlorpyrifos) Berdasarkan Pendiazoan dengan Asid Antranilik)

N.V.S. Venugopal*, B. Sumalatha, Srinivasa Rao Bonthula and G. Veeribabu

Department of Chemistry, G.I.T, GITAM UNIVERSITY, Visakhapatnam-530045, A.P, India

*Corresponding author: venu7000@gmail.com

Abstract

New reaction system was found for spectrophotometric determination of chlorpyrifos pesticide. This is based on reaction of chlorpyrifos with diazotized anthranilic acid in alkaline medium to form an orange-red color. The solution containing 200ppm chlorpyrifos pesticide and 2 ml of decinormal sodium hydroxide is colorless and with the addition of diazotized anthranilic acid, an immediate orange-red dye is formed. The method is rapid, simple and easy to carry out. The absorbance maximum was observed at 450nm. The Beers law is obeyed up to 8.18 ppm for chlorpyrifos standard solution. Water and vegetable samples were collected in different areas of Visakhapatnam district, Andhra Pradesh, India to determine the chlorpyrifos and found low levels in the range up to 0.04ppm. Interference study was carried for other pesticides and ions.

Keywords: chlorpyrifos, anthranilic acid, diazotization, water and vegetables

Abstrak

Suatu sistem tindak balas baru telah ditemui bagi penentuan spektrofotometri racun perosak chlorpyrifos. Ia berasaskan tindakbalas pendiazoan dengan asid antranilik dengan pembentukan larutan berwarna oren-merah. Larutan yang mengandungi 200 ppm racun perosak chlorpyrifos dan 2 ml natrium hidroksida desinormal adalah tidak berwarna dan dengan penambahan asid antranilik akan membentuk larutan berwarna oren-merah. Kaedah yang digunapakai adalah pantas, ringkas dan mudah untuk dijalankan. Nilai serapan maksimum diperhatikan pada 440 nm. Hukum Beers dipatuhi sehingga 8 ppm terhadap larutan piawai chlorpyrifos. Sampel air dan sayuran telah dikumpul dari kawasan yang berbeza di daerah Visakhapatnam, Andhra Pradesh, India dalam penentuan kandungan chloropyrifos dan mendapati kandungannya rendah dan berjulat sehingga 0.04 ppm. Kajian gangguan oleh racun perosak dan ion lain telah dijalankan.

Kata kunci: chlorpyrifos, asid antranilik, pendiazoan, air dan sayuran

Introduction

Chlorpyrifos is a crystalline organophosphate insecticide. The IUPAC name of chlorpyrifos is O, O-diethyl O-3,5,6-trichloro-2-pyridyl phosphorothioate and with molecular formula $C_9H_{11}Cl_3NO_3PS$. Chlorpyrifos is moderately toxic and chronic exposure has been linked to neurological effects, developmental disorders, and autoimmune disorders. Chlorpyrifos is manufactured by reacting 3,5,6-trichloro-2-pyridinol with diethylthiophosphoryl chloride[1]. Chlorpyrifos is registered only for agricultural use, where it is "one of the most widely used organophosphate insecticides", according to the United States Environmental Protection Agency (EPA). The crops with the most intense chlorpyrifos use are cotton, corn, almonds and fruit trees including oranges and apples. It is produced via a multistep synthesis from 3-methylpyridine. An example of the consumption pattern of the pesticide is given in Figure 1 [2].

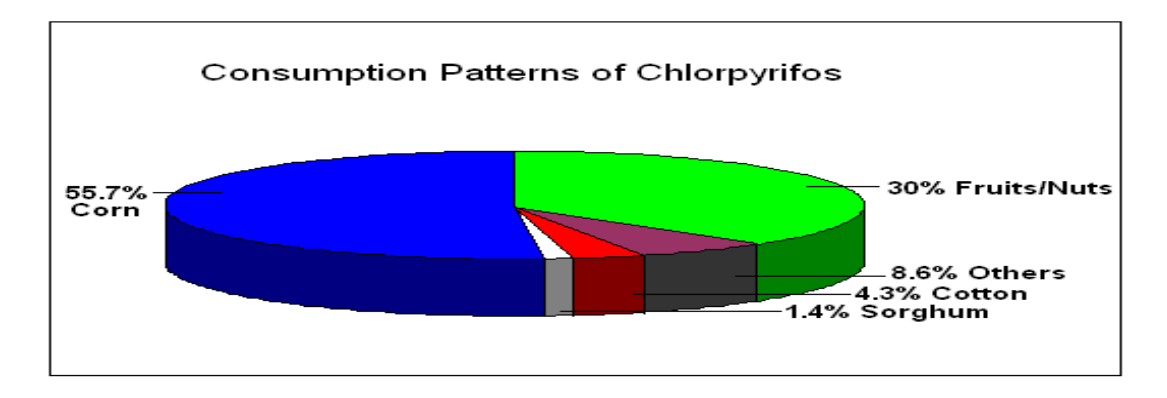


Figure 1. Consumption pattern of pesticides

Chlorpyrifos is an organophosphate, with potential for both acute toxicity at larger amounts and neurological effects in fetuses and children even at very small amounts. Recent research indicates that children exposed to chlorpyrifos while in the womb have an increased risk of delays in mental and motor development at age 3 and an increased occurrence of pervasive developmental disorders such as ADHD [3]. An earlier study demonstrated a correlation between prenatal chlorpyrifos exposure and lower weight and smaller head circumference at birth [4]. A study of the effects of chlorpyrifos on humans exposed over time showed that people exposed to high levels have autoimmune antibodies that are common in people with autoimmune disorders. There is a strong correlation to chronic illness associated with autoimmune disorders after exposure to chlorpyrifos [5].

The immediate health hazard from air born chlorpyrifos in the examined houses was negligible, but the findings suggest that it is necessary to monitor chemicals which may contaminate indoor air and to assess the risk of prolonged exposure to such chemicals. The measuring of urinary metabolite TCP of chlorpyrifos via biological monitoring would be useful, allowing comprehensive evaluation of the exposure to chlorpyrifos in indoor air [6].Chlorpyrifos is used for termite control in construction, forestry and field crops.

Numerous instrumental methods have been described for the detection of chloropyrifos generally analyzed by spectrophotometry [7-8], thin layer chromatography (TLC) [9] and GC-MS [10], liquid chromatography-mass spectrometry[11], and gas chromatography[12]. In this paper the author developed a spectrophotometric method based on diazotization with anthranilic acid and determined after extraction of chloropyrifos pesticide in water and vegetables.

Materials and Methods

Chemical and reagents

A JASCO (Model UVIDEC-610) UV-VIS Spectrophotometer with 1cm matched quartz cuvettes was used for all absorbance measurements. Systronics pH Meter (Model 331) is used. All chemicals and reagents used are AnalR grade. The organic solvents like dichloromethane, ethyl acetate and hexane used were HPLC grade and purchased from E Merck. Technical grade pesticide standards were used for standardizations. Anhydrous sodium sulphate (AR) from E Merck used for residue extraction.

Extraction and clean up

Each vegetable was chopped into small pieces. All vegetables and fruits were collected from agricultural fields near Sabbavaram area, Visakhapatnam district, India. A representative sample (50 gm) was taken with 5-10 gm anhydrous sodium sulphate in blending machine to make fine paste. The sample was extracted with 100 ml of ethyl acetate hexane or dichloromethane on mechanical shaker for one hour, extract was filtered, concentrated up to 5 ml on rotary evaporator. The clean-up of chlorpyrifos was performed out by using column chromatography, packed

with Florisil. The extract was eluted with ethyl acetate, hexane or dichloromethane. Elute was concentrated to 5-10 ml on rotary evaporator.

Sampling

Several samples of water and vegetables were collected from agricultural fields in Sabbavaram, Visakhapatnam district. Samples of one kilogram of carrot, cabbage (vegetables) were procured and kept in refrigerator till analysis.

Spectrophotomeric Method

2 mL of decimolar sodium hydroxide was added to an aliquot of working standard of chloropyrifos (0.5-8.0 $\mu g/mL$). To this colorless solution, 1ml of diazotized anthranilic acid is added to give orange-red color. The solution was kept aside for 5 min before taking absorbance and absorbance was measured at 450 nm against reagent blank. The absorbance corresponding to the bleached color which in turn corresponds to the analyte chloropyrifos concentration was obtained by subtracting the absorbance of the colorless blank solution from that of test solution. The method was applied to various samples collected in different areas in Visakhapatnam district.

Results and Discussion

The method is based on the reaction of chlorpyrifos with diazotized anthranilic acid in presence of sodium hydroxide forms an orange red color and measured at 450 nm. The absorption maximum is shown in Figure 2. The decrease tendency in absorbance is proportional to chlorpyrifos. The Beer's law is obeyed in the range of 0.5-8.18 μ g/mL.

CHLOROPYRIFOS-ANA 1.0 8.0 **ABSORBANCE** 0.6 0.4 0.2 0.0 350 400 600 450 500 550 650 **WAVELENGTH (nm)**

Figure 2. Absorption maxima of chlorpyrifos

The reaction scheme involved is as given below:

Step 1:

Step 2:

Diazotization of Anthranilic acid

Step 3:

Presence of pesticide residues in water and vegetables has become global phenomenon. For the development of solid phase extraction conditions, a volatile solvent system must be used, as rapid evaporation of a large volume would be required in sample preparation without causing loss of volatile pesticides. The solvent system must be sufficiently polar to extract most polar pesticides. A flow rate of 0.5rnL/min was sufficient to recover all the pesticides except hexaconazole. It was noted that the solid phase extraction should not be left dry after conditioning. This could result in a significant loss of pesticides. It was observed that increasing the polarity of solvent gives lower recoveries. Twelve samples of water and vegetables were collected from agricultural fields in Sabbavaram, Visakhapatnam district for the determination of chlorpyrifos are tabulated and the optical characteristics are given in Table 1 and Table 2 respectively. Very low concentrations were observed in few samples.

Table 1. Optical characters, precision and accuracy

Parameter	Values
Maximum absorption	450nm
Color	Orange-red
Relative standard deviation (RSD)	0.74%
% range of error (confideny limit) at 95% confidence level	10±0.025

Table 2. Chlorpyrifos in	water and	vegetables	collected in	Sabbavaram,	Visakhapatham

S. No.		Name of the item	Pesticide residue, mg/Kg
1	Water	Rice field	0.30, 0.29, 0.27
		Banana field	5.12, 5.06, 4.08
2	Vegetables	Carrot	8.18, 6.11, 8.17
	-	Cabbage	5.60, 7.76, 8.14

Conclusion

The present method was tailor-made in view of the previous information about the most prevalent pesticides in the area. The method is rapid, simple and easy to carry out. Application of the method for analysis of chlorpyrifos in water and vegetables from Sabbavaram show the presence of chlorpyrifos in the range of 0.27 - 8.18 mg/kg.

Acknowledgement

The author thanks the head of Department of Chemistry, G.I.T, GITAM University for their support and encouragement.

References

- 1. Muller, Franz, ed., (2000), Agrochemicals: Composition, Production, Toxicology, Applications. Toronto: Wiley-VCH. p. 541.
- 2. Source: http://www.speclab.com/compound.htm
- 3. Rauh VA, et al., Pediatrics, (2006), 118, e1845-e1859, Pediatrics.aappublications.org. http://pediatrics.aappublications.org/cgi/content/abstract/peds.2006-0338.
- 4. Whyatt RM, et al., Environmental Health Perspectives, (2004), 112, 1125–32, Ehponline.org. http://www.ehponline.org/docs/2004/6641/abstract.html. Retrieved November 20, 2011.
- Thrasher, PhD, Jack D.(2002) Gunnar Heuser, M.D., PhD, Alan Broughton, M.D., PhD, Immunological Abnormalities in Humans Chronically Exposed to Chlorpyrifos, Archives of Environmental Health, 57:181– 187
- 6. Dai H, Asakawa F, Suna S, Hirao T, Karita T, Fukunaga I, Jitsunari F,(2003) Investigation of Indoor Air Pollution by Chlorpyrifos: Determination of Chlorpyrifos in Indoor Air and 3,5,6-Trichloro-2-pyridinol in Residents' Urine as an Exposure Index, Environ Health Prev. Med. 8(4), 139–145.
- 7. Elosa D. Caldas, Maria Hosana conceicao, Maria Clara C. Miranda, Luiz cesar K. R. de Souza and Joaq., (2001), Determination of dithiocarbamate fungicide residue in food by spectrophotometric method using a vertical disulfide reaction system, J. Agric. Food Chem., 49,10, 4521-4525.
- 8. E. K. Janghel, J.K. Rai, M.K. Rai, V.K. Gupta, (2007), New sensitive spectrophtometric determination of cypermethrin insecticide in environmental and biological samples, J. Braz. Chem. Soc., Vol. No.18 No.3. 590-594.
- 9. Patil V.B. and Shingare M.S.,(1994) Thin layer chromatographic spray reagent for the screening of biological material for the presence of carbaryl, Analyst, 119, 415-416.
- Thanh D. N., Ji E. Y., Dae M. L., Gae H. L.(2008) A multiresidue method for the determination of 107 pesticides in cabbage and radish using QuEChERS sample preparation method and gas chromatography mass spectrometry, Food Chemistry, 110, 1, 207-213.

- 11. Blasco.C.,M.Fernadez, Y. Pico and Font, (2004), Comparison of solid-phase microextraction and stir bar sorptive extraction for determining six organophosphorus insecticides in honey by liquid chromatography–mass spectrometry, J.of.Chromatography, 1030,77-85.
- 12. Martinez.R.C., Roman F.J.S, Gonzalaz, E.R, E.H.Hernandez E.H and Prado Flores, M, (2001), Determination of herbicides and metabolites by solid-phase extraction and liquid chromatography: Evaluation of pollution due to herbicides in surface and groundwaters, Journal of Chromatography A, 950,157-166.



RADIOLOGICAL IMPACT OF DRINKS INTAKES OF NATURALLY OCCURRING RADIONUCLIDES ON ADULTS OF CENTRAL ZONE OF MALAYSIA

(Impak Radiologi Radionuklid Tabii dalam Air Minuman ke atas Orang Dewasa di Kawasan Tengah Semenanjung Malaysia)

A.A. Tawalbeh^{1*}, S.B. Samat¹, M.S. Yasir¹, M.Omar²

¹School of Applied Physics, Faculty of Science and Technology, Universiti Kebangsaan Malaysia 43600 UKM Bangi, Selangor, Malaysia. ²Malaysian Nuclear Agency (Nuclear Malaysia), 43000 Bangi, Selangor, Malaysia.

*Corresponding author: flower77alaa@yahoo.com

Abstract

Fifty three samples of different types of imported and locally produced drinks consumed in central zone of Malaysia were analyzed using gamma-ray spectrometry system. The measurement was conducted for 12 hours using a Canberra p-type high purity germanium (HPGe) gamma spectrometer with 30% relative efficiency resolution of 1.8 keV at 1.33 MeV. The detector was connected to a computer with MCA card (Accuspec B) and Genie-2000 Analysis software of Canberra Industries, USA. The geometric means of daily intakes of 238 U, 232 Th and 40 K were 0.05, 0.08 and 27.23 respectively. Also the values give annual committed effective doses of 0.8, 6.5 and 61.53 μ Sv yr⁻¹ for 238 U, 232 Th and 40 K, respectively for population in central zone of Malaysia. The net radiological impact of these radionuclides is 68.83 μ Sv yr⁻¹. This value gives cancer risk factor of 1.72 ×10⁻⁷. Also the value of net radiological impact gives loss of life expectancy of 0.43 days only. Whereas ICRP cancer risk factor for general public is 2.5 ×10⁻³ and total risk involve from the all natural radiation sources based on global average annual radiation dose of 2.4 mSv yr⁻¹ is 6.0 ×10⁻³. The estimated cancer risk shows that probability of increase of cancer risk from daily Malaysian drinks is only a minor fraction of ICRP values. Therefore the drink samples investigated here does not pose any significant health hazard and is considered radiologically safe for human consumption.

Keywords: ²³⁸U, ²³²Th and ⁴⁰K, naturally occurring radionuclides (NORM), drinks, dietary intake, radiation dose, cancer risk

Abstrak

Lima puluh tiga sampel daripada pelbagai jenis minuman tempatan import yang terdapat di zon tengah Malaysia dianalisis menggunakan sistem spektroskopi sinar gama. Pengukuran ini dijalankan selama 12 jam menggunakan gamma spektrometer Canberra jenis-p germanium berketulinan tinggi (HPGe) dengan resolusi kecekapan 30% relatif sebanyak 1.8 keV di 1.33 MeV. Pengesan dihubungkan ke komputer dengan MCA kad (Accuspec B) dan Genie-2000 Analisis perisian Canberra Industries, Amerika Syarikat. Cara geometri pengambilan harian ²³⁸U, ²³²Th dan ⁴⁰K 0.05, 0.08 dan 27.23 masing-masing. Nilai ini juga memberikan dos komited berkesan tahunan 0.8, 6.5 dan 61.53 μSv yr⁻¹ untuk ²³⁸U, ²³²Th dan ⁴⁰K, masing-masing untuk penduduk di zon tengah Malaysia. Impak bersih radiologi dari radionuklid ini adalah 68.83 μSv yr⁻¹. Nilai ini memberikan faktor risiko kanser 1.72 ×10⁻⁷. Juga nilai impak radiologi bersih memberikan kerugian jangka hayat 0.43 hari sahaja. Manakala faktor risiko kanser ICRP bagi orang awam ialah 2.5 ×10⁻³ dan risiko jumlah yang terlibat dari semua sumber radiasi semulajadi berdasarkan purata dos sinaran tahunan global 2.4 mSv yr⁻¹ adalah 6.0 × 10⁻³. Anggaran risiko kanser menunjukkan kebarangkalian peningkatan risiko kanser dari minuman harian di Malaysia hanyalah sebahagian kecil nilai ICRP. Oleh itu, sampel minuman yang dikaji di sini tidak menimbulkan sebarang bahaya kesihatan yang ketara dan dianggap selamat secara radiologi untuk kegunaan manusia

Kata kunci: ²³⁸U, ²³²Th dan ⁴⁰K, radionuklida semulajadi (NORM), minuman, ambilan diet, dos radiasi, risiko kanser

Tawalbeh et al: RADIOLOGICAL IMPACT OF DRINKS INTAKES OF NATURALLY OCCURRING RADIONUCLIDES ON ADULTS OF CENTRAL ZONE OF MALAYSIA

Introduction

²³⁸U, ²³²Th and ⁴⁰K are three long-lived naturally occurring radionuclides present in the earth crust. Radionuclides such as 40 K, 226 Ra that occur naturally in soil are incorporated metabolically into plants and ultimately find their way into food and water [1]. Generally, there are two sources of environmental radionuclide, natural (mainly from the ²³⁸U, ²³²Th series) and artificial (i.e ¹³⁷Cs) sources. These radionuclides can be released into the environment as a result of human activities including energy production and military operations such as nuclear weapons testing or caused by nuclear accidents (e.g 1986 Chernobyl Disaster and 2011 Fukushima Earthquake). Ionizing Radiation is dangerous to the health, especially the charged particles and the high energy photon [2]. The main natural radioactive sources of ionizing radiation are the long lived ²³⁸U, ²³²Th and their decay series and the ⁴⁰K. The radiological hazard can be the consequence of external or internal exposure. Radionuclides can enter human body through inhalation and ingestion. The ingested radionuclides could be concentrated in certain parts of the body. For examples, ²³⁸U accumulated in human lungs and kidney, ²³²Th in lungs, liver and skeleton tissues and ⁴⁰K in muscles. Depositions of large quantities of these radionuclides in particular organs will affect the health condition of the human such as weakening the immune system, induce various types of diseases, and finally increase in mortality rate. The environmental radionuclides present the most risk to human health, so it is important for us to understand the transport, fate and effects of radionuclides moving through the drinks and food. There are many types of drink in Malaysia. The main component of daily serving are such as water, tea, coffee, and chocolate drink. Generally, central zone of Malaysia consumes a large amount of different type of drinks as shown in Table1 [3]. Since naturally occurring radioactive materials (NORM) are present in all type of drinks commodities, the levels in some type of drinks consumed in central zone of Malaysia need to be established in order to forecast any possible radiological risk associated with the consumption of the drinks. Thus, the main objectives of this research are to quantify the presence of natural radionuclides in some important drinks consumed in central zone of Malaysia, and to determine impact of these radionuclides on human in normal and natural background conditions. Finally, to estimate the health detriment in terms of cancer risk.

Table 1. Drinks consumption statistics for central zone of Malaysia.

Type of drink	$EMI^1 \pm SE^2 (g/day)$
Drinking water	1,565.07±19.27
Mineral water	1,565.07±19.27
Tea	278.65 ± 7.96
Coffee	172.91 ± 6.58
Chocolate drink	129.98 ± 5.17
Herbs drink	90.53 ± 5.05
Carbonated drink	64.96±3.64
Fruit juices	57.95 ± 2.60
Soybean drink	54.85 ± 2.12
Energy drink	44.14 ± 2.23
Fresh milk	37.94 ± 4.10
Sweetened condensed milk	34.11 ± 1.10
Yoghurt	16.86±1.86
Wine	8.62 ± 1.56
Water melon	8.3 ± 0.39

¹Estimated mean intake, ² Standard error of mean,

Source: Ministry of Health Malaysia (MHO) and Food Safety Quality. 2006.

Materials and Methods

Materials

Fifty three types of drinks were taken as the sample. All samples used were both local and imported drinks and were obtained from local markets. The name of the samples and their number are as follows: drinking water (3), mineral water (3), tea (6), coffee (3), chocolate drink(3), herbs drink (3), carbonated drink (3), fruit juices(4), soybean drink (3), energy drink (3), frish milk (3), sweetened condensed milk (3), yoghurt (3), wine(3) and water melon(3). This makes the total number of samples collected as fifty three.

Sample Preparation

The samples were prepared for the natural radioactivity measurement. Each liquid sample was weighted and sealed in 500 ml marinelli bottles and kept at room temperature (25 °C) for at least 30 days before counting in to allow reaching the secular equilibrium of ²³²Th and ²³⁸U with their respective decay products, in which the activities of all radionuclide within each series are nearly equal. The amount of samples counted is calculated by weightless the bottle without and with samples.

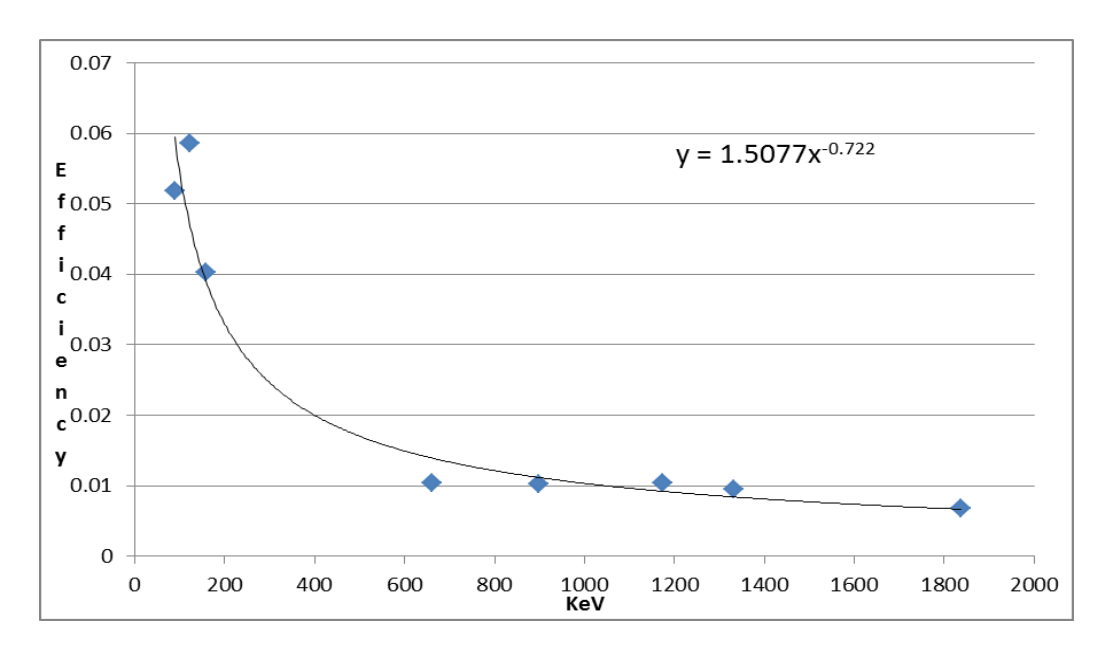


Figure 1. Efficiency graph for standard water on 12/04/2011 for software PCA.

Natural radioactivity measurement

The measurement was conducted for 12 hours using a Canberra p-type High Purity Germanium (HPGe) Gamma Spectrometer with 30% relative efficiency resolution of 1.8 keV at 1.33 MeV. The detector was connected to a computer with MCA card (Accuspec B) and Genie-2000 Analysis software of Canberra Industries, USA. A10-cm thick lead bricks shielded the detector from the background radiation from the radionuclides in the environment and cosmic rays. The system was calibrated using ²⁴¹Am, ¹⁰⁹Cd, ⁵⁷Co, ¹²³Te, ⁵¹Cr, ¹¹³Sn, ⁸⁵Sr, ¹³⁷Cs, ⁸⁸Y, ⁶⁰Co, for their known energy (which covers the energy range from 60 keV to 1333 keV) and peak width of gamma-ray emission. The counting efficiency was determined previously for all of its counting geometry. Figure 1 shows the Efficiency graph for standard water. The redionuclides were identified according to their individual photopeak, which are 609 keV (²¹⁴Bi) and 351.9 keV(²¹⁴Pb) for ²³⁸U, 238 keV (²¹²Pb), 583.191, 510.80 keV (²⁰⁸Tl) and 911keV(²²⁸Ac) for ²³²Th. And 1460 keV for ⁴⁰K. The activity of ²²⁶Ra during the equilibrium was assumed to be the same as its parent, ²³⁸U. The specific activity for each radionuclide was calculated using this equation [4]:

Tawalbeh et al: RADIOLOGICAL IMPACT OF DRINKS INTAKES OF NATURALLY OCCURRING RADIONUCLIDES ON ADULTS OF CENTRAL ZONE OF MALAYSIA

$$A_S = \frac{(C_s - C_b)}{t E_Y P_Y M_s} \tag{1}$$

where A_S is the specific activity of each radionuclide in Bq/kg, C_s the count rate in cps for sample, C_b the count rate in cps for background, E_{Υ} and P_{Υ} are detection efficiency and emission probability of γ -ray, t is counting time and M_S is the mass of the sample in kg.

Results and Discussion

Contribution of radioactivity due to ²³⁸U, ²³²Th and ⁴⁰K to internal radiation doses on adult population in Malaysia was estimated using their published mass fractions in daily drinks. Geometric mean (GM) on these estimated daily intakes in terms of elemental concentration and activity are reported in Table2. Radioactivities levels of ²³⁸U, ²³²Th and ⁴⁰K in daily drinks are calculated by using conversion rate for uranium = 0.64 Bq/kg, thorium = 1.02 Bq/kg and potassium = 340.38 Bq/kg. Detailed discussion on the estimated radiation doses due to ingestion these radionuclides are given below.

Uranium-238

The estimated GM activity is 0.05 Bq/d. The Annual Committed effective dose (ACED) is calculated using the observed annual intake of 238 U activity of 18.25 Bq and ICRP dose coefficient of 4.4×10^{-8} Sv/Bq for adult members of the public [5]. It is estimated as 0.8 μ Sv yr⁻¹. Details are listed in Table 3.

Table 2. Daily intakes of uranium, thorium and potassium concentrations and their activities from the Malaysian diet

Analysis parameter	<u>Ura</u>	nium	Thor	ium_	Potas	ssium
	Conc. (kg/d)	Activity (Bq/d)	Conc. (kg/d)	Activity (Bq/d)	Conc. (k g/d)	Activity (Bq/d)
Geometric mean (GM)	0.08	0.05	0.08	0.08	0.08	27.23

Table 3. Annual committed effective dose of adult population of Malaysian from intake of 238 U, 232 Th and 40 K

Radionuclide	Daily intake (Bq)	Annual intake (Bq)	Dose coefficient (Sv/Bq)	Annual committed dose (μSv)
²³⁸ U	0.05	18.25	4.4×10^{-8}	0.8
²³² Th	0.08	29.78	2.2×10^{-7}	6.5
40 K	27.23	99.39×10^4	6.2×10^{-9}	61.53
otal contribution				68.83

Comparison with other countries of the world was also made by calculating committed effective doses of their populations using published estimates for 238 U intake and presented in Table 4. The table shows that population of UK receives lowest annual radiation dose 0.01 μ Sv yr⁻¹ [6]. While population of China receives highest annual radiation dose 1 μ Sv yr⁻¹ [7]. Whereas population of Malaysia receives second highest annual radiation dose 0.8 μ Sv yr⁻¹. The radiation doses due to ingestion of 238 U activity determined in the present work (0.8 μ Sv yr⁻¹) lie well within the observed range (i.e. 0.01- 1 μ Sv yr⁻¹) of other countries listed in Table 4.

Table 4. Annual committed effective dose of adult population of world from intake of ²³⁸U.

adionuclides	Dose (µSv yr ⁻¹)	Reference
UK	0.01	UNSCEAR (2000)
Philippine	0.11	Akhter et al. (2007)
India	0.11	Akhter et al. (2007)
Japan	0.13	Akhter et al. (2007)
World average	0.25	UNSCEAR (2000)
USA	0.26	UNSCEAR (2000)
S.Korea	0.75	Akhter et al. (2007)
Malaysia	0.8	Present study
China	1.00	Akhter et al. (2007)

Thorium-232

The estimated GM activity is 0.08 Bq/d. The ACED due to the ingestion of 232 Th was estimated using the observed annual intake of 29.78 Bq and ICRP dose coefficient of 2.2×10^{-7} Sv/Bq (Table 3) for adult members of the public [5]. It is 0.08 μ Sv yr⁻¹. ACED of adult population of other countries are also calculated using the available data in literature and listed in Table 5. The table shows that population of Philippine receives lowest radiation dose 0.05 μ Sv yr⁻¹ while population of Malaysia receives highest dose 6.5 μ Sv yr⁻¹. The second and third highest are Bangladesh and China countries. The radiation doses due to ingestion of 232 Th activity determined in the present work is larger than radiation doses due to ingestion of 232 Th activity of other countries. This is due to high concentration of 228 Ra in Malaysian soil compared to the concentration of 228 Ra in others countries soil [8].

Table 5. Annual committed effective dose of adult population of world from intake of ²³²Th.

Radionuclides	Dose (μSv yr ⁻¹)	Reference
Philippine	0.05	Akhter et al. (2007)
Japan	0.10	Akhter et al. (2007)
India	0.21	Akhter et al. (2007)
USA	0.33	Akhter et al. (2007)
S.Korea	0.33	Akhter et al. (2007)
World average	0.37	UNSCEAR (2000)
Pakistan	0.8	Akhter et al. (2000)
China	1.02	Akhter et al. (2007)
Bangladesh	1.15	Akhter et al. (2007)
Malaysia	6.5	Present study

Potassium-40

The estimated GM activity is 27.23 Bq/d. The ACED due to the ingestion of 40 K was estimated using the observed annual intake of 99.39×10^4 Bq and ICRP dose coefficient of 6.2×10^{-9} Sv/Bq for general puplic [5] as presented in Table 3. The ACED is calculated to be $61.53~\mu Sv$. Comparison was also made with the available Potassium ingestion data of other countries of the world, by calculating committed effective doses of various populations and presented in Table 6. The results shows that population of Malaysia receives lowest annual dose ($61.53~\mu Sv$) while population of China receives $164~\mu Sv$ annual dose [9]. While Iran receives high est annual dose ($262~\mu Sv$). The

Tawalbeh et al: RADIOLOGICAL IMPACT OF DRINKS INTAKES OF NATURALLY OCCURRING RADIONUCLIDES ON ADULTS OF CENTRAL ZONE OF MALAYSIA

total estimated value of annual effective dose from ^{40}K (61.53 μSv) is less than annual effective dose world reference value which is 178 μSv [10].

Table 6.	Annual committed	effective dose	e of adult po	opulation of	world from	intake of ⁴⁰ K.
racic o.	I minadi Committeed	cricetive dose	or address by	opaiation or	WOLLG ILOIN	munic or ix.

Radionuclides	Dose ($\mu Sv yr^{-1}$)	Reference
Malaysia	61.53	Present study
Indonesia	74	Akhter et al. (2007)
Philippine	74	Akhter et al. (2007)
India	106	Akhter et al. (2007)
Japan	128	Akhter et al. (2007)
Turkey	160	Akhter et al. (2007)
China	164	Quan et al. (2008)
World average	178	UNSCEAR (2000)
USA	178	UNSCEAR (2000)
Pakistan	178.75	Akhter et al.(2007)
S.Korea	192	Akhter et al. (2007)
Canada	197	IAEA (1992)
UK	215	UNSCEAR (2000)
Spain	242	IAEA (1992)
Iran	262	IAEA (1992)

Cumulative radiological impact of these three naturally occurring radionuclides i.e. 238 U (0.8 μ Sv), 232 Th (6.5 μ Sv) and 40 K (61.53 μ Sv) in terms of annual committed effective dose is 68.83 μ Sv yr⁻¹, in which 40 K has major contribution. The net radiological impact of drinks from these radionuclides is significantly less than the ICRP dose limit of 223.29 μ Sv yr⁻¹.

Cancer risk

The risk incurred by a population is estimated by assuming linear dose-effect relationship with no threshold as per ICRP practice. For low doses ICRP fatal cancer risk factor is $0.05~{\rm Sv}^{-1}$ [11]. The risk factor states the probability of a person dying of cancer increases by 5% for a total dose of 1 Sv received during his lifetime. The estimated cumulative annual dose of $68.83~\mu Sv$ is used to estimate cancer risk for an adult person using the following relationship [7].

$$Risk = Dose(Sv) \times risk factor(Sv^{-1})$$
(2)

The estimated cumulative annual dose of $68.83~\mu Sv$ to Malaysian adults is used and life-time (50 yr) exposure is estimated as $3.44~\mu Sv$, which gives a risk factor of 1.72×10^{-7} . This value is a negligible fraction of the total risk involve (6.0×10^{-3}) from all natural radiation sources based on global average annual radiation dose of 2.4~m Sv/yr to man. The estimated values are significantly less than ICRP cancer risk factor of 2.5×10^{-3} based on annual dose limit of 1 mSv for general public, which gives annual death probability of 10^{-5} , i.e. 1 in 100, 000 [12]. The risk of cancer from measured radiation is also compared with other kinds of health risks using Cohen and Lee estimates [7]. The authors estimated an average loss of 15 days from occupational exposure of 3 mSv/yr from age 18 to 65. Based on their estimates the calculated health risk from the measured average radiation dose 0.068~m Sv/yr from present study is only 0.43days .

It is therefore concluded that 0.068~mSv/yr annual radiation dose attributable to drinks intake of three naturally occurring radionuclides ^{238}U , ^{232}Th and ^{40}K in Malaysia would not pose any significant radiological impact on health and cancer risk to population . The drinks are considered safe for human consumption.

Conclusion

The annual committed effective doses to Malaysian population from the drinks intake of naturally occurring radionuclides 238 U, 232 Th and 40 K have been determined and cancer risk is estimated. These estimated committed effective doses are 0.8, 6.5 and 61.53 μ Sv yr⁻¹ respectively. The net radiological impact of these radionuclides is 68.83 μ Sv yr⁻¹. This gives a cancer risk factor of 1.72×10^{-7} and loss of life expectancy of 0.43 days only. The estimated risk has no significant health hazared and malaysian drinks is radiologically safe, as per international standards.

Acknowledgement

The authors wish to thank Universiti Kebangsaan Malaysia UKM for funding this work. Special thanks to staff members of gama ray spectroscopy laboratory for their help and support during the undertaking of this project.

References

- 1. Eisenbud, M. & Gesell, T. 1997. Environmental Radioactivity from Natural Industrial and Military Sources. 4th ed., Academic Press An Imprint of Elsevier
- 2. Turner, J.E., 1995. Atoms, Radiation, and Radiation Protection. 2nd ed., John Wiley &Sons.
- 3. Ministry of Health Malaysia (MHO) and Food Safety Quality. 2006. Food consumption statistics for central zone for adult population aged 18-59 years.
- 4. Jabbar, T., Akhter, P., Khan, K., Jabbar, A. & Saleem, K. 2009. Radiological impact of composite food served at PINSTECH. Food and Chemical Toxicology 47:1205-1208.
- 5. International Commission on Radiological Protection (ICRP), 1997. Individual Monitoring for Internal Exposur of Workers. Pergamon Press, Oxford, Publication No. 78.
- 6. UNSCEAR, 2000. Sources and Effects of Ionizing radiation. Report to General Assembly, With Scientific Annexes, United Nation, New York.
- 7. Akhter, P., Rahman, K., Orfi, S.D., Ahmad, N. 2007. Radiological impact of dietary intakes of naturally occurring radionuclides on Pakistani adults. Food and Chemical Toxicology 45:272-277.
- 8. Omar, M., 1993. Radium activity in the steel in Malaysia. Malaysian Nuclear Science Journal 11:181 183.
- 9. Quan, W., Hongada, Z., Tiqiang, F. & Qingfen, L. 2008. Re- Estimation of internal dose from natural radionuclides for Chinese adult men. Radiation Protection Dosimetry 130: 434-441.
- 10. International Atomic Energy Agency (IAEA), 1992. Human dietary intakes of trace elements. IAEA/NAHRES-12, Vienna.
- 11. International Atomic Energy Agency (IAEA), 2004. Radiation, people and the environment. Division of Radiation and Waste Safety, IAEA Vienna.
- 12. International Commission on Radiological Protection (ICRP), 1991.1990 Recommendation of International Commission of Radiological protection. Pergamon Press, Oxfored, UK, ICRP Publication 60.



DEVELOPMENT OF A METHOD FOR THE SPECIATION OF MERCURY IN ENVIRONMENTAL SAMPLE ANALYSIS

(Pembangunan Kaedah Bagi Analisis Penspesian Merkuri Dalam Sampel Sekitaran)

M. M. Rahman^{1*}, M. Awang¹, A. M. Yusof², A. K. H. Wood³, S. Hamzah³ and A. Shamsiah³

¹Department of Pharmaceutical Chemistry, Faculty of Pharmacy,
International Islamic University Malaysia, Indera Mahakota, 25200 Kuatan, Pahang, Malaysia.

²Department of Chemistry, Faculty of Science,
Universiti Teknologi Malaysia, Skudai, Johor Bahru, 81310 Malaysia.

³Malaysia Nuclear Agency,
Bangi, Kajang, 43000 Malaysia

*Corresponding author: mdrahman@iium.edu.my

Abstract

Trace concentrations of mercury in water samples were determined by a method involving a simple and rapid procedure connecting the flow-injection inductively coupled plasma mass spectrometry (FI-ICP-MS) and graphite furnace atomic absorption spectrometry (GFAAS) techniques. Mercury vapor, generated by sodium borohydride as the reductant, was stabilized by potassium dichromate ($K_2Cr_2O_7$), then released by controlled heating and detected by FI-ICP-MS. A flow injection sample introduction system with time based injection was used and the sensitivity was found to be proportional to the mass of mercury introduced. Methyl mercury(II) was preconcentrated using the ammonium pyrrolidine dithiocarbamate (APDTC)-chloroform extraction procedure and the chloroform extract was introduced into the graphite tube. A linear calibration graph was obtained for 5-150 ng mercury in 2.5 ml of chloroform extract. Because of the high stability of MeHg(II)-APDTC complexes, it is possible to evaporate the extract in order to obtain a crystalline powder to be dissolved with a few micro liters of chloroform enacting MeHg(II) and Hg(II) can be detected at sub-nanogram levels.

Keywords: Methyl mercury, Flow Injection-Inductively Coupled Plasma Mass Spectrometry, Graphite Furnace Atomic Spectrometry and ammonium pyrrolidine dithiocarbamate

Abstrak

Kepekatan surih merkuri di dalam sampel air diuji melalui prosedur yang mudah dan pantas yang menghubungkan Penyuntikan Aliran Spektrometer Jisim Plasma Gandingan Teraruh (FI-ICP-MS) dan teknik Spektrometri Penyerapan Atom Relau Grafit (GFAAS). Wap merkuri, dihasilkan oleh natrium borohidrida yang bertindak sebagai bahan penurun, telah distabilkan oleh kalium dikromat ($K_2Cr_2O_7$), dan kemudiannya dibebaskan dengan pemanasan terkawal dan dikesan oleh FI-ICP-MS. Sistem pengenalan sampel penyuntikan aliran dengan penyuntikan merkuri berdasarkan masa telah digunakan dan didapati kepekaannya berkadar terus dengan kadar merkuri yang diuji. Merkuri(II) metil dipekatkan terlebih dahulu melalui prosedur pengekstrakan amonium pirolidina ditiokarbamat (APDTC)-kloroform dan ekstrak kloroform tersebut dipindahkan ke dalam tiub grafit. Graf kalibrasi yang linear telah diperolehi bagi 5-150 ng merkuri di dalam 2.5 ml ekstrak kloroform. Dengan kestabilan kompleks MeHg(II)-APDTC yang tinggi, ekstrak dapat disejatkan bagi memperoleh serbuk kristal untuk dilarutkan bersama-sama dengan beberapa mikro liter kloroform agar MeHg(II) dan Hg(II) dapat dikesan pada paras sub-nanogram.

Kata kunci: Merkuri metil, Penyuntikan Aliran Spektrometer Jisim Plasma Gandingan Teraruh, Spektrometri Penyerapan Atom Relau Grafit dan amonium pirolidina ditiokarbamat

Introduction

Mercury is an element that can exist in the environment in both the inorganic and organic forms. Both forms are toxic, but it is the organic form that exhibits extreme biological toxicity [1]. In humans, toxicity due to mercury intake is characterized by gastric pain, vomiting and possible renal failure. With chronic poisoning, mercury can cause injury to the central nervous system and renal damage. A level of 0.5 ppb [2] has also been set as the standard

Rahman et al: DEVELOPMENT OF A METHOD FOR THE SPECIATION OF MERCURY IN ENVIRONMENTAL SAMPLE ANALYSIS

for mercury in water for human consumption. So the trace elements play an important role in establishing the processes affecting these interactions. As the results detailed studies became available, there is a growing need for reliable measurements of very low concentrations of this element in a variety of samples, especially drinking water that is very important and directly related to human health.

Mercury contamination arises mainly from its industrial uses, such as in the manufacture of Hg cells batteries and Hg discharge lamps. It is also used as a catalyst in converting acetylene to vinyl chloride and acetate. Therefore analytically sensitive techniques are required to detect Hg at very low levels. A number of existing techniques are capable of detecting Hg at very low (ppb) levels but these have associated problems, either because of prohibitive cost or the unusual physical properties of the elements, namely, high vapour pressure and high volatility. Conventional flame atomic absorption spectrometry (FAAS) is relatively insensitive for determining Hg as it is extremely volatile and its residence time in the flame is very short. Mercury has a more sensitive line at 184.9 nm but this line cannot easily be utilized because flame gases and oxygen in the atmosphere interfere strongly at this wavelength and hence the less sensitive 253.7 nm line was to be used [1-3].

The high sensitivity and freedom from spectral interferences exhibited for most elements determined by inductively coupled plasma mass spectrometry (ICP-MS), compared with other atomic spectrometric techniques, makes it a very attractive choice for trace element analysis. Although most elements in the periodic table are ionized with an efficiency of more than 90% in the argon plasma, Hg, with an ionization potential of 10.43 eV is ionized with only 32.31% efficiency [4]. This results in a decrease in the detection power for Hg. In samples containing very low concentrations or samples, which have to be diluted in order to diminish matrix effects, detection capabilities became restricted, making analysis difficult. Preconcentration procedures improve sensitivity, and usually the detection limits are achievable. Flow injection (FI) sample preconcentration methods reduce the risk of contamination since FI systems are closed. This is especially important for the determination of ngL⁻¹ concentrations where high blank signals could lead to deterioration in precision of the signal to background ratio and degradation in the detection limit [5]. Thus, a suitable analytical method for measuring trace element speciation is necessary. The atomic spectroscopic methods that are usually used for elemental analysis generally do not distinguish the various species present for each element. However, speciation information can be obtained by solvent extraction separations with element selective detection by atomic spectroscopy [6,7]. Graphite furnace atomic absorption spectrometry (GFAAS) is one of the most attractive detection systems for elemental speciation, because of its excellent detection limits [3].

In a study on drinking water pollution from water treatment plants, Hg determination is performed by a preconcentration step with ammonium tetramethylenedithiocarbamate (ammonium phyrolidinedithio carbamate, APDTC) in chloroform, followed by determination by graphite furnace atomic absorption spectrophotometry (GFAAS). In this work a method for determining low levels of Hg by GFAAS with preliminary pre-concentration using the APDTC-chloroform system is described. Previous works have shown that losses of analyte occurred during the thermal cycle before atomization, but these losses can be reduced by matrix modification [6]. For example, absorbance values can be increased by the addition of sulfide ions to the analyte solution; this effect has been attributed to the formation of stable mercury (II) sulfide at the ashing temperature. The objective of this present work was to develop simple methods for the accurate FI-ICP-MS and GFAAS determinations and the speciation of mercury in aqueous samples at concentrations of ng L⁻¹.

Materials and Methods

In this work, a continuous-flow in situ nebulizer/Hg sample introduction system was coupled with ICP-MS for Hg determination with flow injection (FI) analysis. In this study, a solution containing 1 ng mL $^{-1}$ Hg(II) in 0.5% $K_2Cr_2O_7$ and 0.1 M HNO $_3$ was selected as the model to optimize the operating conditions of the hydride generation (HG) system. This solution was loaded in the injection loop and injected into the hydride generation (HG) system. Several operating parameters could affect the efficiency of hydride formation. The concentrations of $K_2Cr_2O_7$ and HNO $_3$ in the injected sample and carrier solution, the concentration of NaBH $_4$, and the volume of the mixing coil were studied to obtain the optimal conditions for the simultaneous determination of these four elements.

Reagents for FI-ICP-MS and GFAAS

All chemicals were of analytical grade. The reducing solution consisting of the following reagents (0.2%, 0.5%, 1.0% and 2%) NaBH₄ in 0.05% NaOH (2 g NaBH₄ + 2g NaOH pellets/l solution). These solutions were freshly prepared; the 0.5% K₂Cr₂O₇ solution was prepared by dissolving 0.5g K₂Cr₂O₇ (Fluka) in 100 mL of 1:1(v/v) HNO₃ (65%) (Merck). A 1M hydrochloric acid was used as a carrier solution and it was prepared by diluting concentrated (32%) HCl 1:9 (v/v) with deionized water. A primary standard stock solution 1000 mg L-1 was used; secondary stock solution of 10 mg L⁻¹ was prepared by dilution and working solutions of 5, 10, 15 and 20 µg L⁻¹ was used. Sub-boiling distilled HNO₃ was prepared in a PTFE still. Chloroform (Fluka) of analytical reagent grade (1000 ml) was extracted three times with 50 mL of 1 M nitric acid and stored in a pre-cleaned brown-glass bottle. A 1% (m/v) aqueous solution (100 mL) of APDTC (Fluka Chemicals Co) was extracted with six successive 5 mL portions of purified chloroform, and then stored in a pre-cleaned 100 ml PTFE bottle. Mercury (II) chloride stock solution (1000 mg L⁻¹) was prepared by dissolving (0.1354g) mercury (II) chloride in 10 mL of nitric acid and diluted to 100 mL with water. Methyl mercury(II) chloride stock solution (1000 ng L⁻¹) was prepared by dissolving (0.1252 g) of methyl mercury(II) chloride (OCO - China) in 10 mL of 1:9 (v/v) HCl and diluted to 100 ml with deionized water. The solution was stored in a refrigerator at 4-10 °C. Mercury working standard solutions (1 mg L⁻¹) of methyl mercury(II) compounds were freshly prepared daily by appropriate dilution of the stock solutions with deionized water.

Sampling

The polyethylene sampling vessel of 1.5 L capacity was acid-cleaned, rinsed with deionised water and then dried. The samples was preserved in acids such as 1% HNO₃ and refrigerated until ready for analysis. Water samples were analysed immediately after acidification and filtration by FI-ICP-MS. Drinking water samples were taken from the Negeri Sembilan and Melaka water treatment plants as shown in Figure 1. Water samples collected from four treatment plants at three different points and a total of 12 samples were collected at different intervals. The samples were filtered through a 0.45 μm Millipore membrane (Whatman) in a laminar flow hood and the filtrate was kept under suitable conditions.

Separation and Determination Procedure of Methyl Mercury Compounds by GFAAS

The water samples collected thought to contain inorganic and organic mercury (mainly methyl mercury) species [8]. A 500 mL portion of filtered water sample was transferred into a separating funnel and 1 M HNO₃ was added in order to adjust the pH to 1.7±0.1. A portion (5 x 500 ng of methyl mercury(II) standard solution in 500 mL water) was added, followed by 2 mL of 1% APDTC solution and 10 mL of purified chloroform. After shaking for 30 s then equilibrating the mixture, the phases were allowed to separate for 5 min. The aqueous phase contains inorganic mercury(II) while the organic phase contains organic mercury Hg(II). About 5.0 mL of the clear extract was transferred into a pre-cleaned glass cylinder. The calibration graph was prepared by plotting the peak height against the amount of mercury added to 500 mL of distilled water. The optimized experimental conditions of GFAAS was achieved with a lamp current of 3 mA, wave length of 253.7 nm, drying temperature of 100 °C, ashing temperature of 200 °C, atomizing temperature of 2000 °C, a period of 3 seconds before the purge gas flow stopped.

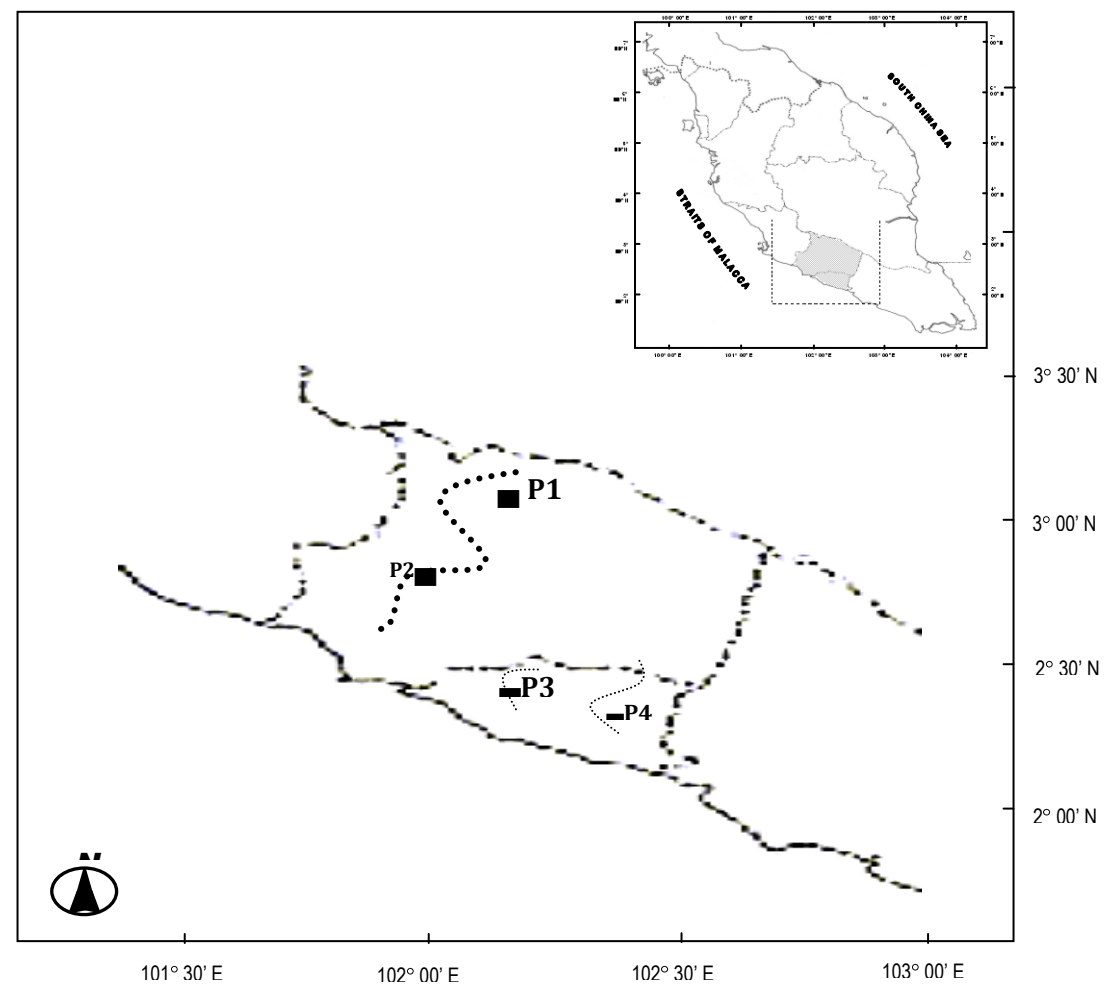


Figure 1. Location of Sampling

P1: Old treatment plant in Negeri Sembilan, P2: New treatment plant in Negeri Sembilan, P3: Old treatment plant in Negeri Melaka, P4: New treatment plant in Negeri Melaka

Results and Discussion

It is well known that the control of accuracy of the results for trace elements in water samples at sub-nanogram levels is extremely difficult. This is not only related to difficulties in the final measurement, but also even more to sampling and handling protocols. Important improvements in sampling and measurement techniques have been achieved, which have resulted in a dramatic increase in the confirmed Hg levels in surface water over the past few years [9]. Samples were kept in the laboratory in PTFE bottles, after they were sampled according to ultra clean protocol. The accuracy of Hg determination in water depends very much on the control of the blanks. These include blanks of the sampling device and sampling handling (storage, preservation, filtration and transportation). However, for this study we could only control blanks from the laboratory processing. Blank values for MeHg were very stable over the period of this study. The instrument detection limit (IDL) was also affected by the reproducibility of blank values. IDL is defined as two standard deviations of the blank. Particularly when low MeHg values were measured, many blanks were run. Another means of confirming the accuracy of the results was to analyze a known concentration standard solution (QCSS). For total Hg determination (0, 5, 10, 15 and 20 ppb) and MeHg (0, 5 and 7ppb) standard solutions were prepared at two different labs, the Malaysia Nuclear Agency Laboratory and

Chemistry Laboratory of University of Technology Malaysia. The verified results from different methods and measured detection limits were shown in the Table 1.

Effect of NaBH₄ Concentration on Ion Signals

NaBH₄ concentration is critical in the determination of Hg by hydride generation (HG). The effect of the concentration of NaBH₄ on the ion signals was investigated first. Figure 2 and Table 2 showed the peak area of the flow injection (FI) peak as a function of NaBH₄ concentration. Although the signal of Hg reached a maximum when NaBH₄ was about 2%, the Hg signals increased with NaBH₄ concentration. For the determination of the Hg, 2% NaBH₄ was used in this experiments. In this study, a quite higher concentration of NaBH₄ together with lower concentration of NaOH and HCl acid was used for hydride generation (HG). The methyl mercury(II) - APDTC complexes of inorganic and organo-mercury salts are very stable and can be easily recovered in the crystalline form by evaporation of chloroform solutions since the melting points of methyl mercury(II) chloride is 321 °C. It is clear that under these circumstances the volume of solvent used determines the smallest amount of Hg detectable. In order to improve the limits of detection, 5 mL of the extract, from a series of aqueous solutions containing 10 ng of mercury as methyl mercury(II) chloride, were evaporated by means of a gentle flow of nitrogen and the residues dissolved with variable but known volumes of solvent. As a result, the absorbance values increase with decreasing solvent volume of 20 μ L having been used for the analysis in all examples. It is evident that by employing a preconcentration step a detection limit of less than 1 ng can be achieved.

Table 1. Detection limits obtained by FIMS instrument and GFAAS

			<u> </u>			
		Detec	tion limit obtained by FI-MS in	strument		
Analyte	QCSS	Peak	QC Calcul. Value µgL ⁻¹	%RSD	Recovery %	IDL
-	$\mu \mathrm{gL}^{ ext{-l}}$	Signal			-	μg L ^{-l}
	0.0	0.0014		High		
Hg(II)	5.0	0.0396	5.01±0.01	2.1	100.1	0.53
	10.0	0.0783	9.98 ± 0.01	2.4	99.8	
	15.0	0.1160	15.03±0.01	3.0	100.2	
	20.0	0.1472	19.99 ± 0.01	5.3	99.9	
		Detect	ion limit obtained by GFAAS in	nstrument		
Analyte	QCSS	Blank	QC calcul. Value µgL ⁻¹	%RSD	Recovery%	IDL
•	$\mu g L^{-1}$	Signal			·	$\mu g L^{-1}$
	0.00	0.009	0.15±0.01	17.4		
MeHg(II)	5.0	0.328	4.96 ± 0.02	0.61	99.2	
	5.0	0.329	4.97 ± 0.04	10.8	99.3	0.44
	5.0	0.330	4.97 ± 0.01	3.4	99.4	
	7.0	0.417	6.41 ± 0.06	14.3	91.6	

IDL: Instrument detection limit, QCSS: Quality Control Standard Sample, %RSD: Relative Standard Deviation

Rahman et al: DEVELOPMENT OF A METHOD FOR THE SPECIATION OF MERCURY IN ENVIRONMENTAL SAMPLE ANALYSIS

Results of Inorganic Mercury and Methyl mercury

The concentrations of the samples were determined from both the calibrations. The obtained values were reported in $\mu g L^{-1}$.

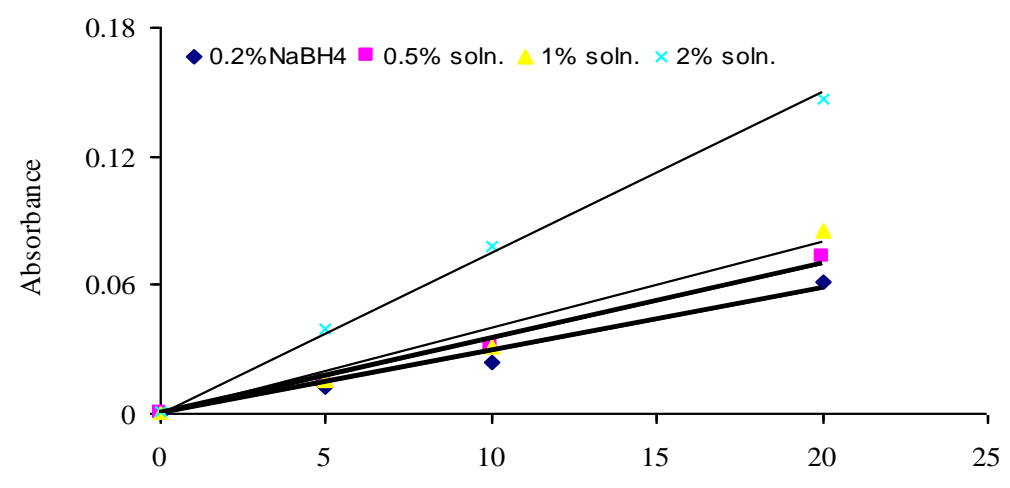


Figure 2. Calibration Curve for different concentrations of NaBH₄

			·	
Concentration	0.2% NaBH ₄ solution	0.5% NaBH ₄ solution.	1% NaBH ₄ solution.	2% NaBH ₄ solution.
$\mu \mathrm{gL}^{ ext{-}1}$	Absorbance	Absorbance	Absorbance	Absorbance
Blank	0.0001	0.0001	0.0001	0.0014
5	0.0129	0.0146	0.0153	0.04
10	0.0239	0.0315	0.0316	0.078
20	0.0617	0.0725	0.0858	0.147

Table 2. Obtained absorbance from different NaBH₄ solution

The QC data obtained during sample analyses provide an indication of the quality sample data and would be provided with sample results. The results shown in Table 3 show total mercury concentrations in the different water treatment plants in Negeri Sembilan and Melaka (P1 to P4) ranging from $0.60\pm0.04~\mu g~L^{-1}$ to 7.11 ± 0.12 , while methylmercury levels make up from 18% to 40% of the total mercury. In the raw water taken from the Negeri Sembilan water treatment plants, the total mercury determined were $7.11\pm0.12~\mu g~L^{-1}$ and $3.52\pm0.07~\mu g~L^{-1}$ from the old and new plant respectively and the methyl mercury ranged between $24.8~\mu g~L^{-1}$ to $22.7\mu g~L^{-1}$, $(23\sim25)\%$ of the total mercury recorded. In the raw water (RW) sample taken from the new water treatment plant of Melaka, the total Hg was $5.69\pm0.02~\mu g~L^{-1}$ and the methyl mercury recorded was $1.74\pm0.03~\mu g~L^{-1}$ representing 30.6% of the total mercury. While the total mercury concentrations were lower in the raw water in old water treatment plants in Melaka, $3.66\pm0.84~\mu g~L^{-1}$ (RW-3), the methyl mercury was 31.3% was similar $(0.11\pm0.01~\mu g~L^{-1})$ of the total mercury.

Table 3. Determination of mercury and speciation of methyl mercury by FIMS and GF-AAS respectively

SAMPLE	Result obtained by FIMS		Result obtained by GFAAS		Inor.
ID	total mercury (µg L ^{-l})		methyl mercury (μg L ^{-l})		mercury (µg L-1)
	Conc.	%RSD	Conc.	%RSD	Conc.
RW-1	7.11 ± 0.12	1.6	1.76 ± 0.015	3.52	5.35±0.12
PW-1	2.81 ± 0.01	0.4	0.58 ± 0.008	2.26	2.23 ± 0.01
FW-1	0.60 ± 0.04	high	> DL	3.42	0.57 ± 0.34
RW-2	3.52 ± 0.07	1.8	0.80 ± 0.01	2.24	2.73 ± 0.07
PW-2	2.21±0.01	0.5	0.78 ± 0.06	9.98	1.43 ± 0.01
FW-2	2.09 ± 0.08	3.7	0.57 ± 0.02	4.32	1.52 ± 0.08
RW-3	3.16 ± 0.84	2.6	0.99 ± 0.02	5.40	2.17±0.84
PW-3	2.14 ± 0.01	0.2	0.93 ± 0.02	3.83	1.21 ± 0.01
FW-3	1.48 ± 0.01	0.6	0.63 ± 0.02	6.02	0.85 ± 0.01
RW-4	5.69 ± 0.02	0.4	1.74 ± 0.03	6.14	3.96 ± 0.02
PW-4	2.69 ± 0.06	2.2	1.11 ± 0.01	1.39	1.58 ± 0.06
FW-4	1.26±0.10	8.0	0.52±0.01	0.87	0.74±0.10

(Total mercury - Methyl mercury = Inorganic mercury); DL: Detection Limit, RW: Raw Water, PW: Pretreatment Water, FW: Fresh Water

While it is premature to draw any conclusive remarks that the differences in the methyl mercury proportion to the total in the two raw water systems, the area could be related to erratic of climate factors, which also affect the characteristics of the biota. A total mercury concentration of $0.60\pm0.04~\mu g~L^{-1}$ and $2.09\pm0.08~\mu g~L^{-1}$ were found in fresh water at the old (FW-1) and new (FW-2) water treatment plants in Negeri Sembilan. These values compared with the mercury concentrations in the raw water seem to indicate a 91.6 % and 40.6 % of the total mercury removal in the old and new water treatment plants respectively. So it is clear that regarding Hg, the old water treatment plant in Negeri Sembilan was functioning better than the new one. On the other hand, a total mercury concentration of $1.48\pm0.01~\mu g~L^{-1}$ and $1.26\pm0.10~\mu g~L^{-1}$ were found in fresh water samples (FW-3 and FW-4) at the old and new water treatment plants in Melaka. These values compared with the mercury concentrations in the raw water seem to indicate a 53.2 % and 77.8 % of the total mercury removal in the old and new water treatment plants respectively. From these results, it is clear that the new water treatment plant in Melaka is more efficient than the old plant. Surprisingly the methyl mercury of $0.52\text{-}0.63~\mu g~L^{-1}$ is still present in the clean water samples taken at all the treatment plants, which is supposed to be easily decomposed by chlorine.

Precision and Accuracy

To check the precision of the method (GFAAS), 500-ml portions of distilled water were spiked with 5 x 500 ng of methyl mercury(II) chloride and extracted as already described. The results obtained were listed in Table 1. The difference between the mean mercury content of the drinking water and that of the distilled water represents the amount of mercury in 500 ml of drinking water. The relative standard deviation of seven repeated determinations of 500 mL of distilled water containing 5 ng L^{-1} of mercury (II), as methyl mercury(II) chloride was between 0.61 – 17.4 %.

Reproducibility was determined by using seven injections of a test mixture solution containing 5 μ g L⁻¹ of Hg. The relative standard deviations of the peak heights for these seven injections were in the range of 2.1 – 5.3 % for the element studied. Calibration curves based on peak heights were linear for the elements studied in the range tested (5 – 20) μ g L⁻¹. The detection limits were estimated from these calibration curves based on the usual definition as the amount (or concentration) of analyte necessary to yield a net signal equal to three times the standard deviation of the blank. The detection limit was 0.53 μ g L⁻¹ for inorganic mercury (Hg).

Rahman et al: DEVELOPMENT OF A METHOD FOR THE SPECIATION OF MERCURY IN ENVIRONMENTAL SAMPLE ANALYSIS

Conclusion

FI-ICP-MS provides a simple, rapid and accurate technique for the routine determination of trace amounts of Hg in water samples. This method yielded a large signal enhancement factor. Better detection limits would be expected if reagents of higher purity were used. GFAAS method described is extremely simple and allows nano-gram levels of methyl mercury(II) present as organo-mercury salts to be determined in water samples by direct injection of a portion of the chloroform extract. It was found that the chloroform extracts could be stored for more than one week without mercury losses. In order to determine mercury at the sub-nanogram levels it is necessary only to evaporate the chloroform from the extract and to redissolve the residue again with a few microliters of chloroform and to transfer the solution quantitatively into the graphite furnace.

References

- 1. Ellis L. A. and Roberts D. J., (1996). Novel method to determine mercury in sediment using a gold coated dual 'bent' tube trap. *J. Anal. At. Spectrom.*, 11, 1063-1066.
- 2. Bunce N., (1994). Environmental chemistry, Wuerz Pub. Ltd. Winnipeg, Canada, 2nd Edi., pp., 232-233.
- 3. Filippelli M., (1984). Determination of trace amounts mercury in sea water by graphite furnace atomic absorption spectrometry." *Analyst*, 109, 515-517.
- 4. Boomer, D. W. and Powell M. J., (1987). Determination of uranium in environmental samples using inductively coupled plasma mass spectrometry. *Anal. Chem.*, 59, 2810-2821.
- 5. Ebenzer D., Denoyer R. E., and Tyson F. J., (1996). Flow injection determination of mercury with preconcentration by amalgamation on a gold-platinum gauze by inductively coupled plasma mass spectrometry." *J. Anal. At. Spectrom.*, 11, 127-132.
- 6. Krull I. S., (1991). Trace metals analysis and Speciation. New York, USA; Elsevier.
- 7. Ebdon L., Hill S., and Ward R. W., (1987). Directly coupled liquid chromatography atomic spectroscopy. *Analyst*; 112, 1-16.
- 8. Schintu. M., T. Kaur and Kudo A., (1989). Inorganic and methyl mercury in inland waters. *Wat. Res.*, 6, 699-704
- 9. Wan C. C., Chen C. S. and Jiang S. J., (1997). Determination of mercury compounds in water samples by liquid chromatography- inductively coupled plasma mass spectrometry with an in situ nebulizer/ vapor generator. *J. Anal. At. Spectrom*, 12, 683-687.